Summer 8-2-2012

Design, Synthesis and Biological Evaluation of Novel Cannabinoid Antagonist

Abha Verma
University of New Orleans, averma2@uno.edu

Design, Synthesis and Biological Evaluation of novel cannabinoid antagonists

A Dissertation

Submitted to the Graduate Faculty of the
University of New Orleans
in partial fulfillment of the
requirements for the degree of

Doctor of Philosophy
in
Chemistry

by

Abha Verma

M.Sc. (Organic Chemistry Honors) Panjab University 2004
M.S. (Organic Chemistry) University of New Orleans 2010

August 2012

To my amazing parents - Mamma & Pappa

ACKNOWLEDGEMENT

Words are inadequate in offering my thanks to my advisor - Professor Mark Louis Trudell.

Dr. Trudell is a very brilliant, encouraging mentor and has a huge positive influence on both my academic research as well as personal life and has always motivated me towards excellence. Even though he is heavily involved with so many activities and research, he still found the time to answer all my queries and enlighten me. It's the discussions with him and his able guidance that has helped me learn valuable techniques of thinking and problem solving skills. He has always been my inspiration for hardwork and perfection in whatever he does. His mentorship was paramount in providing a well rounded experience consistent with my long-term career goals.

He encouraged me to not only grow as an experimentalist and a chemist but also as an instructor and an independent thinker. His faith in me and his invaluable suggestions have helped me going during the miserable failures. He has supported me throughout with his patience and knowledge whilst allowing me the room to work in my own way. I attribute the level of my degree to his encouragement and effort and without him; this thesis too, would not have been completed or written. I am really thankful to God for giving me the opportunity to work under his extraordinary guidance. One simply could not wish for a better supervisor. For everything you've done for me, Dr. Trudell, I thank you.

I also wish to thank my committee members- Dr. Gabriel Caruntu, Dr. Branco Jursic and Dr. Guijun Wang for their timely support and help throughout my graduate research. Many thanks to our collaborators Prof. Edwin Stevens, Prof. David Mobley at University of New Orleans, LA and Prof. Sari Izenwasser, Mr. Dean Wade of the University of Miami Miller School of Medicine, FL for helping us by doing specialized studies and providing all the complimentary data.

I wish to thank National Institute on Drug Abuse (DA23916) for the financial

support of this research, UNO's Student Government for travel awards, along websites Google Scholar and Scifinder for helping me.

I wish to thank all my past present group members - Dr. Xiaobo Gu, Dr. Lei Miao, Dr. Hong Shu, Dr. April Noble-Brooks, Dr. Andrea N. Forsyth, Alex, Kiran, Amber, Tushar, Maria & all the undergraduate research assistants and Post-docs in MLT-group especially Philip, Johnathan, Yiressy and Dr. Murali for providing amiable, cheerful and supportive environment, opportunities to try new cuisines and for some much needed humor and entertainment.

I would like to thank all my friends in the chemistry department especially Dr. Sarah Miller King; group members of Dr. Guijun Wang - Dr. J. R., Dr. Sherwin Cheuk, Dr. Kristopher Williams, Dr. Michael St. Martin, Sanjeeva, Hari for treating me like a family member; Dr.Alexis Lee, Dr. Hungtao Yu, Dr. Elisha Josepha, Dr. Srinivas, Dr. Girija, Dr. Chen, Mr. Harry Rees, Mr. Lionel, Dr. Corrinne and all the Chemistry Faculty for making my stay in the graduate school, a pleasant and memorable one.

I wish to thank Mr. Sean Hickey, Dr. Richard Cole and Dr. John Wiley for their support. I want to thank, past and present chemistry department chairpersons- Dr. Edwin Stevens and Dr.Matthew Tarr for allowing me to use all the instruments of the chemistry department whenever I needed them and providing the support and equipment I have needed to produce and complete my thesis. I also want to take this opportunity to thank Dr. Stacey Lomenzo and Dr. Trudell's wonderful children- Lindsay, Daniel and Ant Claire for showering me with their love and concern.

I would also like to thank all my teachers, friends and mentors who are now scattered all around the world and deserve my thanks - from my schools in Panchkula and Chandigarh; from Panjab University, Chandigarh; from Dr. Reddy

Pharmaceuticals, Hyderabad; from Indian Institute of Science, Bangalore and here at New Orleans, for always being so kind and generous to me. Without their wishes, moral support, coffee dates and silly fun activities, I would have been lost.

I will forever be thankful to my amazing parents, my mother, Shrimati Anjali Verma and my father, Late Shri Suresh Kumar Verma whose prayers, encouragement, unquestioning and unconditional love and support and innumerable sacrifices have inspired and enabled me to pursue all my dreams and decisions. Thank you mamma and pappa. I love you very much!

I would also like to extend my thanks to the rest of my family especially my in-laws, my father-in-law- Shri Ram Kumar Goyal, my mother-in-law- Late Shrimati Trishla Devi, for providing me with unending encouragement and wishes; my lovely and supportive sister- Suruchi Verma and my bright and spirited daughter- Nikita Goyal, for their unwavering love and being ever so patient with me and letting me away whenever they have needed me.

I have deep gratitude and respect for my wonderful husband and best friend, Dr. Navneet Goyal, for his constant motivation and help; for pushing me to become the best I could be and supporting me through every decision that I have made. He’s not only a smart and hardworking scientist; he is very lively, enthusiastic- the life of the party-kind-of-person who is a blessing for me.

Finally, and most importantly, I wish to thank God for everything and for being there for me.

TABLE OF CONTENTS

LIST OF FIGURES

LIST OF TABLES

LIST OF SCHEMES

ABSTRACT

This study was aimed at the development of novel CB1 cannabinoid receptor antagonists that may have clinical applications for the treatment of cannabinoid and psychostimulant addiction. The rationale for the design for our target was to incorporate a bioisosteric 1,2,3-triazole ring into the vicinal diaryl group revealed in the prototypical antagonist/inverse agonist SR141716 (Rimonabant) that was presumed to interact with a unique region in the CB1 receptors. Based on our preliminary results we identified a novel series of 1,2,3-triazole ester and keto derivatives as lead compounds for biological evaluation. Here in the design rationale, synthesis and CB1 receptor affinity for a series of 4,5-diaryl-1-substituted-1,2,3-triazoles of ester and ketones is described. These derivatives were synthesized via a one-pot regiospecific click/acylation reaction sequence from 1-azido-2,4-dichlorobenzene and commercially available arylacetylenes. From the structure-activity studies the 5-(4-chlorophenyl) congeners exhibited the most potent CB1 receptor affinities relative to other 5-(substituted-phenyl)

moieties. The 1-(2,4-dichlorophenyl)-5-(4-chlorophenyl)-4-propylcarbonyl-1,2,3-triazole (**31a**) was found to be the most potent (K_i = 4.6 nM) CB1 receptor ligand of the series and exhibited high CB1 selectivity (CB2/CB1 = 417).

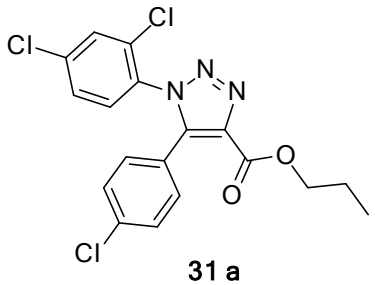

31 a

The triazole ester **31a** was further characterized as a cannabinoid antagonist in locomotor-activity studies by blocking the locomotor-reducing effects of cannabinoid agonist WIN55,212-2. In addition, unlike the prototypical cannabinoid antagonist **SR141716A** (Rimonabant), the triazole ester **31a** did not exhibit increased activity in locomotor activity studies, thus indicating the potential for a neutral antagonist profile.

Keywords: Cannabinoids; CB1-antagonist; Drug abuse therapeutics; Rimonabant; Click Reactions; 1,2,3-triazoles;

1. INTRODUCTION

Drug addiction is a complex illness. Drug abuse and addiction to various psychostimulants like morphine, cocaine marijuana etc. is a global problem. Marijuana and other psychostimulants, like cocaine and methamphetamine, are leading illicit drugs of abuse. The economic cost of illicit drug abuse and addiction is a tremendous burden to the United States health care system, costing billions of dollars annually. In addition, the devastating effect of drug addiction on individuals and families and society is equally significant. The problem is enhanced further by the fact that currently there is no effective pharmacotherapy available for the treatment of addiction to these illicit drugs. The development of new medications for the treatment of marijuana and psychostimulant abuse is extremely important to the welfare of the United States and rest of the world.[1]

To date, great advances have been made in understanding the biological and pharmacological mechanisms of illicit drugs. Approaches to the development of

pharmacotherapy have focused on the monoamine-regulated circuitry in the central nervous system. Exploration of dopaminergic and sertonergic transmission has revealed tremendous amounts of information important to understanding mechanisms of psychostimulants abuse. However, direct modulation of these neurological systems has been unsuccessful in producing sustainable therapeutic effects. Thus, no effective therapeutics is currently available to treat this complex illness.

Figure 1. Specific regions of brain govern specific functions. [1]

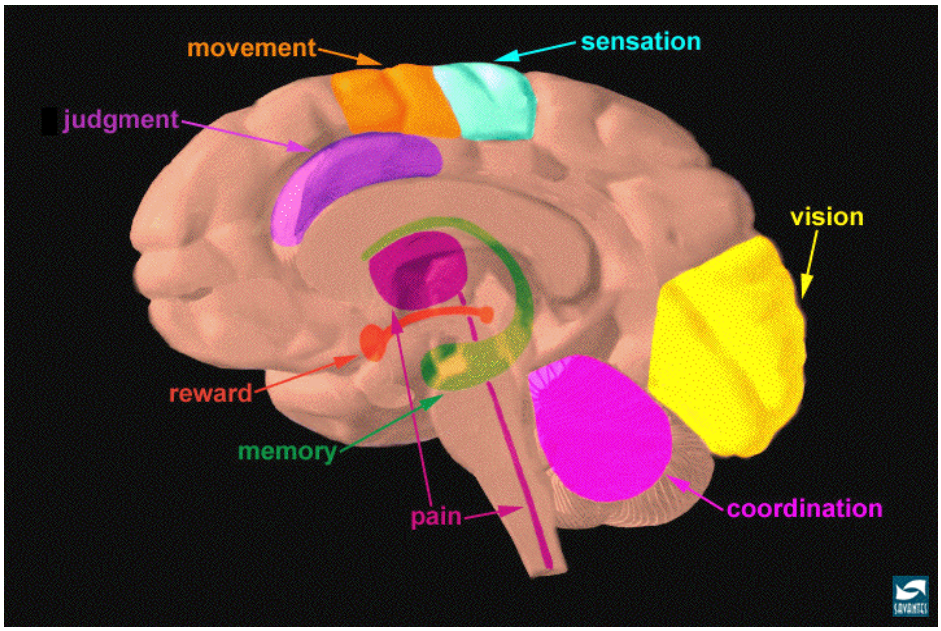

The path to drug addiction begins with the act of taking drugs. Over time, a person's ability to choose not to take drugs is compromised. As illustrated in Figure 1 certain

parts of the brain govern specific functions. Information is relayed from one area of the brain to other areas through complex circuits of interconnected neurons through a process called "neurotransmission." The Figure 1 also highlights the pathway connecting these structures.

Figure 2. The Reward Pathway.[1]

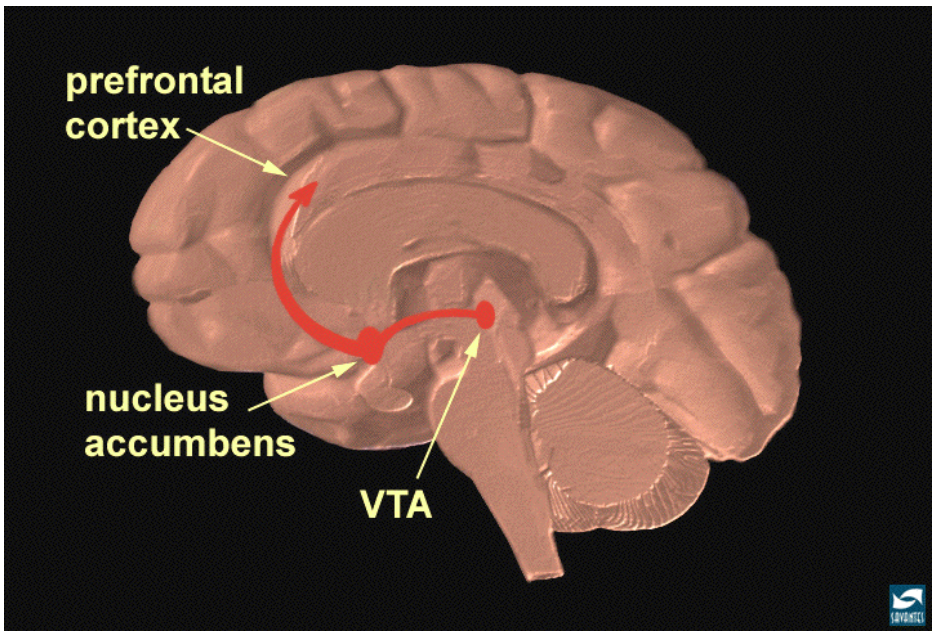

The reward pathway shown in Figure 2 is important for understanding the effects of drugs on the brain. This pathway is rich with monoamine regulated circuitries which gets activated by the rewarding stimulus like personal accomplishments, food, water, exercise etc.

When the reward pathway is activated by a rewarding stimulus, information travels from the Ventral Tegmental Area or VTA (in blue), to the nucleus accumbens (purple) and then up to the prefrontal cortex which is the area of judgement. Consequently, a person experiences a feeling of reward. This pathway is important for the survival of an organism as it provides motivation to repeat these processes.

Figure 3. Normal signaling communication.[1]

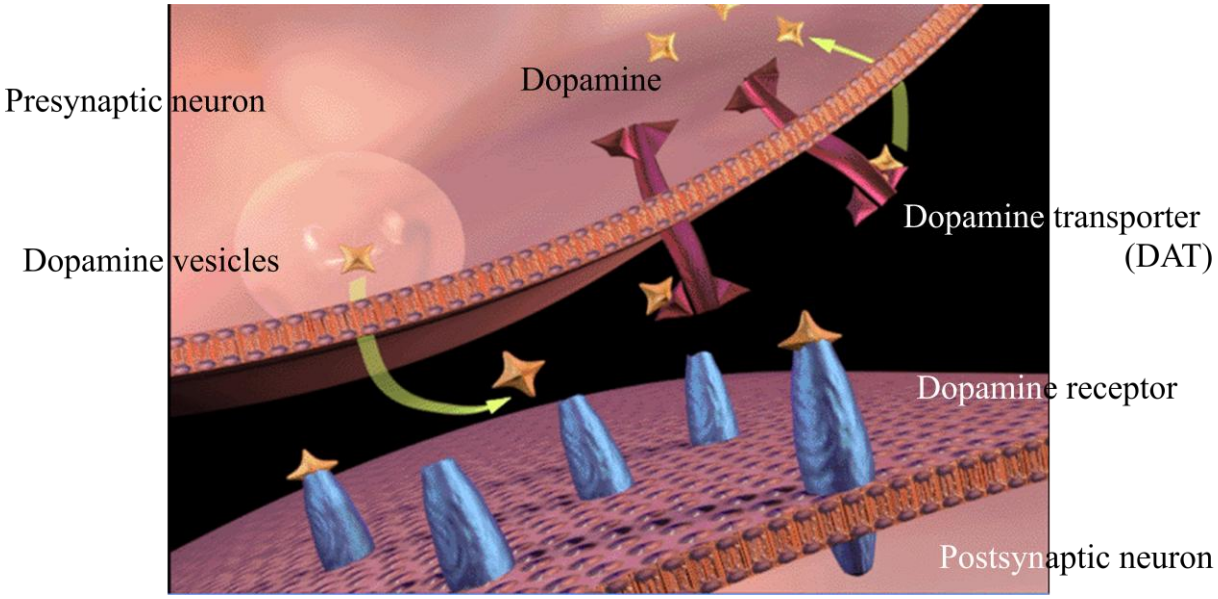

How this communication actually occurs can be seen in Figure 3. These brain regions talk among themselves by a process called neurotransmission involving a variety of chemical substances called neurotransmitters like dopamine, serotonin etc. When

presynaptic terminal receives a signal, dopamine is released by the presynaptic neuron into the gaps between two nerve cells called synapse. The dopamine then binds with specialized proteins called dopamine receptors on the post-synaptic neurons, thereby sending the signal forward.

After the electrical impulse has been propagated forward to the postsynaptic neuron causing the information in form of action impulse to travel further, dopamine is transported back to the presynaptic neuron by another specialized protein called dopamine transporter or DAT. This regulates the concentration level of dopamine in the synapse area.

However, drugs of abuse like cocaine can interfere in this normal communication. As illustrated in Figure 4, cocaine binds to the dopamine transporter and thus inhibits the reuptake of dopamine from the synapse, back to the presynaptic neuron resulting in buildup of dopamine concentration in the synapse.

This causes a continuous stimulation of the postsynaptic neuron which leads to increased number of impulses being received by the nucleus accumbens to activate the

reward system. With continued use of psychostimulants, the body relies on this drug to maintain the rewarding feelings and the person is no longer able to feel the positive reinforcement of natural rewards like food and water.

Figure 4. Inhibition of dopamine re-uptake.[1]

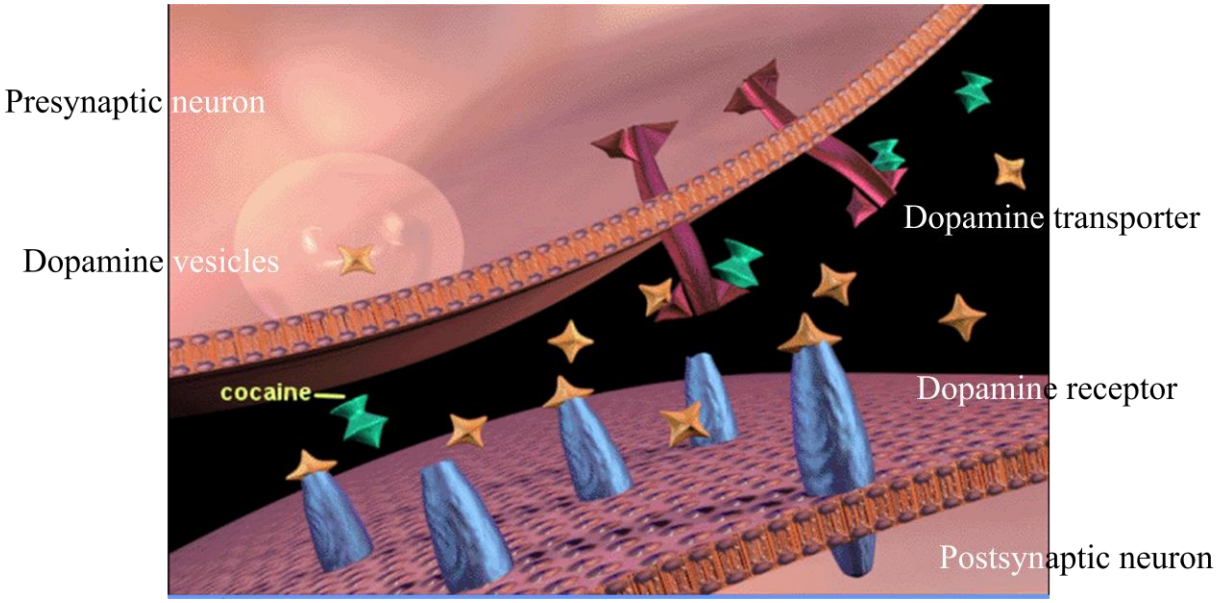

The reward feelings associated with marijuana are similar to the ones mediated by cocaine. The principle active chemical in marijuana is Δ^9- tetrahydrocannibol or **Δ^9-THC** (**3**). This psychoactive constituent has high lipid solubility and low water solubility. When someone smokes marijuana, **Δ^9-THC** rapidly passes from the lungs into the bloodstream, which carries the chemical to the brain. **Δ^9-THC** has analgetic and

neuroprotective properties with equal affinity for the two subtypes of the cannabinoid receptor. **Δ⁹-THC** acts upon specific sites in the brain, called cannabinoid receptors 1 (CB1), kicking off a series of cellular chain-reactions that ultimately increases dopamine concentration in the synapses and leads to the “high” that users experience when they smoke marijuana.

Figure 5. Δ⁹-THC Binding to CB-Receptors.[1]

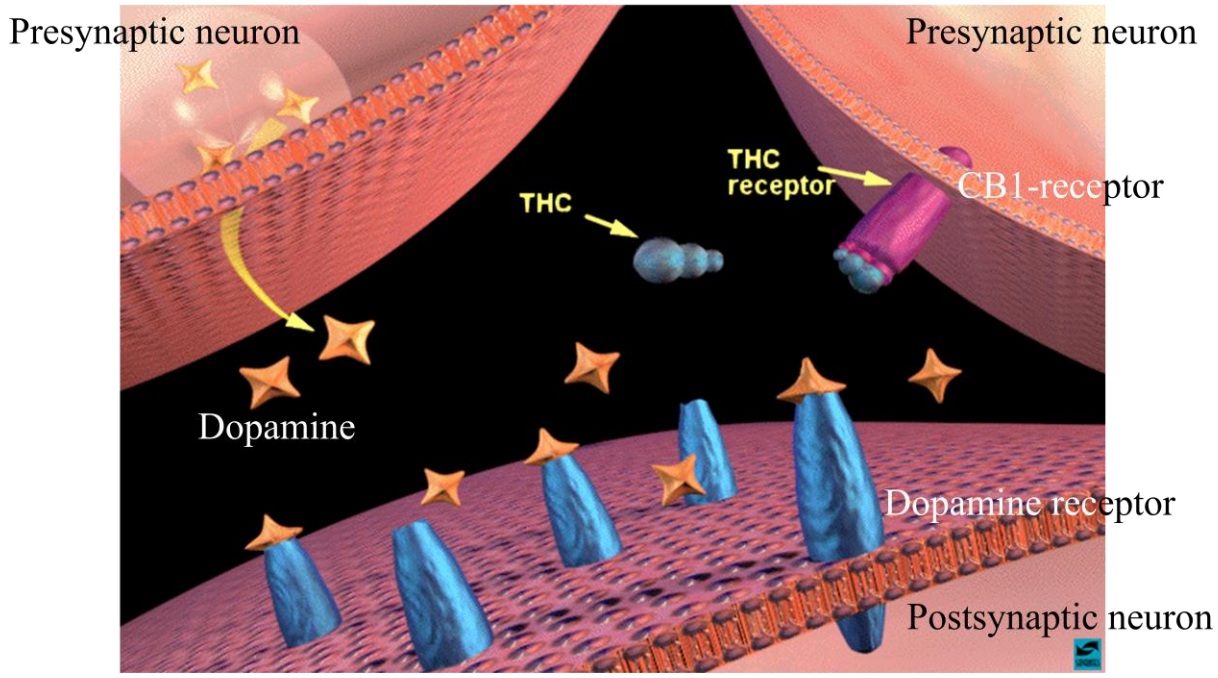

As shown in Figure 5, **Δ⁹-THC** binds to the CB receptors (magenta) on the neighboring terminal, which sends a signal to the presynaptic neuron and hence controls the release of dopamine. In 2010, approximately 29 million people aged 12 or

older were identified as illicit drug users according to the National Household Survey on Drug Use and Health.[1]

The three major illicit drugs derived from plants are, opium, coca and cannabis. Morphine has been isolated from opium early in the 19th century and structure elucidated in the 1920s by Robert Robinson. Cocaine was isolated from coca leaves in the middle of the 19th century and its structure was described by Richard Willstatter in the last decade of the 19th century. It is believe that the cannabinoids represent a medicinal treasure trove which waits to be discovered.

Now cocaine may be the most powerful psychostimulant but marijuana is the most popular and common drug of abuse in the world. It is made up of dried parts of the Indian hemp plant *Cannabis sativa* L. and its street names are hashish, bhang, pot, ganja, weed, grass, 420 and so on. Marijuana smoke has a pungent and distinctive, usually sweet-and-sour odor. It has a fast onset and the psychostimulant effects last for up to three hours.

Marijuana users represented 77% of those classified with illicit drug dependence or

abuse. Cannabis (marijuana) is one of the most commonly abused recreational drugs self- administered by smoking. For centuries marijuana have been used for medicinal and recreational purposes. Cannabis has been used by various civilizations as a therapeutic agent with advances as an analgesic, nausea, appetite stimulation and a host of other medical applications.

Historical evidence suggests that in 12,000 B.C. Emperor Shen Nung was the first to recognize that cannabis had potential medicinal properties, which was used as an analgesic. In India, the effects of smoking cannabis have been associated with faith (Bhaang) and were used as anesthetics and aphrodisiacs.[66] Marijuana is considered as therapeutic in several diseases and conditions like-Alzheimers, pain attenuation in AIDS and multiple sclerosis patients etc and 16 states including Washington DC have laws permitting the use of marijuana as treatment (Table 1). Cannabinoid-based medications include synthetic compounds, such as dronabinol (Marinol®) and nabilone (Cesamet®), which are FDA approved for treatment of vomiting and nausea. Sativex spray for relieving pain in cancer and Multiple sclerosis patients has been approved in several

countries.

Table 1. Timeline for Cannabinoids and Receptor System.

2,000 BC to 1,800 AD	Medicinal Cannabis used in Ancient China, Egypt, India, ancient Greeks.
800 AD to 1,800 AD	Medical Cannabis was used extensively in the medieval Islamic World
1800-1900	Medical Cannabis commonly used entire world as primary pain reliever until the invention of aspirin.
1925	England bans cannabis with Dangerous Drugs Act, and non-medicinal cannabis made illegal in Britain.
1927	Canada bans all forms of cannabis.
1937	Even though there are 28 cannabis pharmaceuticals on the American market, Cannabis banned in US with federal law, the 1937 Marijuana Tax Act.
1964	THC, tetra hydro cannabinol, the psycho-active component of cannabis, isolated by Raphael Mechoulam at Weizmann Institute in Israel
1970	Marijuana fully outlawed in US by Controlled Substances Act of 1970.
1975	Munson shows anti cancer effects of cannabis in Lewis Lung Tumors.
1980-2000	Cannabis research banned in US (de facto).
1985	FDA approves Marinol drug, a pure THC drug
1990	Endo-cannabinoid CB1 receptors cloned and found in brain
1992	First endo-cannabinoid isolated by Hanuš and Devane in Raphael Mechoulam's lab at the Hebrew University in Jerusalem. This new substance is named Anandamide.
	Table 1 Contd

1993	Endo-cannabinoid CB2 receptors cloned and found in the immune system.
1998	Di Marzo's in Naples Italy group found that cannabinoids (anandamide) inhibit breast cancer cell proliferation.
1999	Marinol (THC) was rescheduled from Schedule II to III of the Controlled Substances Act.
2000	Guzman's group in Spain found that cannabinoids inhibit the growth of C6 glioma cells.
2005	Sativex approved in Canada. Sativex is a whole cannabis plant extract, mouth spray approved for multiple sclerosis patients to alleviate neuropathic pain and muscle spasticity
2006	Cannabindiol found useful as anti-psychotic drug São Paulo, Brasil. SR141716A (Accomplia), approved by European Union as CB1 antagonist for obesity treatment.
2007	Sean D. McAllister - Cannabidiol inhibits aggressive breast cancer cells.
2008	Acomplia, Rimonabant (also known as SR141716) first CB1 receptor blocker suspended from the UK market because of adverse effects of suicidality, depression. This agent blocks the endo-cannabidiol receptors.
2009	Two components of cannabis plant identified. THC which is psychoactive, and the non-psychoactive Cannabidiol "CBD" represents up to 40% of extracts of the medical cannabis plant. Cannabidiol relieves convulsion, inflammation, anxiety, nausea, and inhibits cancer cell growth. Cannabidiol as effective as atypical antipsychotics in treating schizophrenia.
2010	10 million people arrested for marijuana since 1967. In the US, 16 states approved medical use of cannabis.

Moreover these cannabinoids seem to be unaffected by the mechanism of stubborn

bugs like methicillin-resistant *Staphylococcus aureus*.. Recently, in Jan 2012, Cannabis Science, a pioneering U.S. biotech company developing pharmaceutical cannabis products shared photographs from a cancer patient's tumors healing.[71] Although cannabis was a medicinal plant for thousands of years, its medical use was suppressed and banned throughout most of the 20th century. Banned in England, Canada and the US in the 1930's, medical cannabis represents the first casualty in a war against natural medicine waged by the pharmaceutical industry. While banned in the US, there have been major scientific breakthroughs in Israel, Spain, Italy and Brazil over the last two decades. These breakthroughs have made cannabis "the wonder drug of the 21st century".

The greatest cannabis researcher is unquestionably Raphael Mechoulam from Isreal, also known as the father of cannabis research. He discovered THC in 1964, the psycho-active component of cannabis. Mechoulam also discovered the first endogenous endo-cannabinoid in 1992, Anandamide, a sanskrit word translated as "bliss".

Even though marijuana has gone a full spectrum from being the scourge of the youth

to recreational and spiritual drug and then to medicinal properties, there is no doubt that marijuana abuse and its addiction and other cannabis related disorders are becoming a major public health issue. In 2006, 25% of Americans age 12 and over abused marijuana at least once prior to the year of being surveyed. According to 2010 statistics, 29 million people had taken marijuana and more than 15 million were new users in 2009. According to the NIDA, a study showed that 10.9% of 8th graders, 23.9% of 10th graders, and 32.4% of 12th graders had abused marijuana at least once in the year prior to being surveyed.

One of the major concerns is that most of the users are young adults for whom marijuana acts as a gateway drug for even harder drugs (39%, including methamphetamine and cocaine abuse). Today, there has been little deviation among these trends of marijuana and psychostimulant abuse. However, the development of effective medications for the treatment of illicit drug abuse has been elusive.

Hence, there a common pattern among the psychostimulants pathway. Unlike the normal circumstances where information flow is controlled[1], the cocaine and marijuana

intakers feel the high because of the constant stimulations being received by the nucleus accumbens to activate the reward system. This is depicted in Figure 6. With continued use of these psychostimulants the body starts to rely on them for maintaining the feelings of reward and the person is no longer able to feel the positive reinforcements of natural stimuli causing the craving and dependence problems also.

Figure 6. Comparison of normal (A) and abused neuron (B).[1]

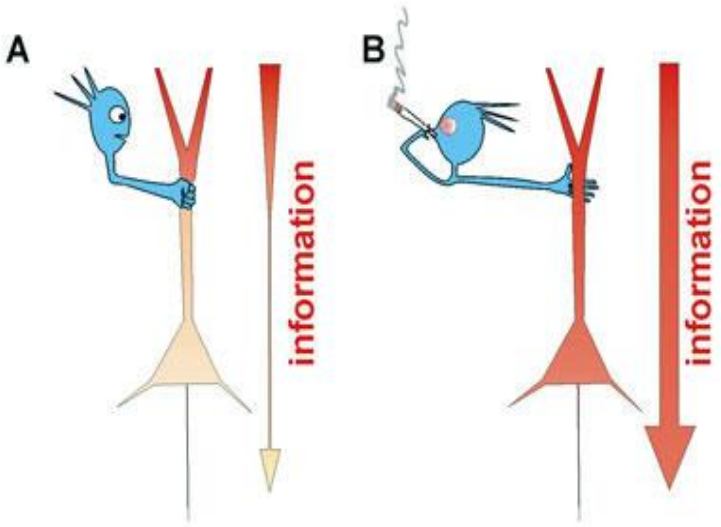

The psychoactive and physiological effects of marijuana intoxication include increased heart rate, lowered blood pressure, impairment of short term and working memory, impairment of coordination and perception, distortions of perception, Impairs coordination and balance, along increase in anxiety, paranoia and panic attacks.[1]

Research clearly demonstrates that marijuana has the potential to cause problems in daily life or make a person's existing problems worse. Long term abuses besides addiction are mental disorders like schizophrenia and depression, lung disorders as well as risk of cancer.

There is substantial evidence indicating that the cannabinoid system can modulate dopaminergic transmission indirectly and thus mediate the effects of cannabis and psychostimulants on the reward and pleasure circuitry of the brain.[2-5] Studies have shown that the prototypical cannabinoid antagonist **SR141716A** (**1**) attenuated the effects of Δ^9 - tetrahydrocannabinol (**3**, Δ^9 - **THC**) and cannabis in animals and human subjects.[6,7] The diarylpyrazoles **1** and **2** (AM251) have been shown to be potent and selective CB1 receptor ligands that inhibit the effects of typical cannabinoid agonists such as **3** and WIN55,212-2 (**4**) (Figure 7).[8,9] The pharmacological profile of **1** has been reported to include inverse agonist activity.[10]

The inverse agonist activity of **1** has been characterized by inhibition of [^{35}S]GTPγS binding, a decrease in K^+ ion currents and antagonism by CB1 agonists.[11] CB1

antagonists have been shown to block the effects of **Δ⁹-THC** (**3**)[8] and appear to be devoid of abuse liability.[9]

Figure 7. Cannabinoid Antagonists and Agonists.

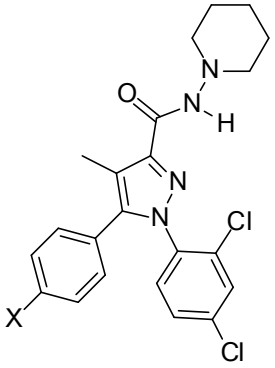

1 (X = Cl, SR141617A)
2 (X = I, AM251)

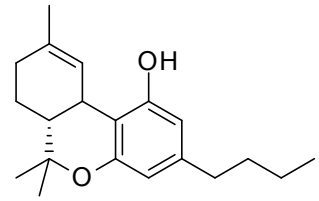

3 (THC)

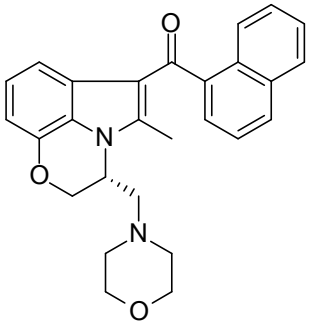

4 (WIN 55212-2)

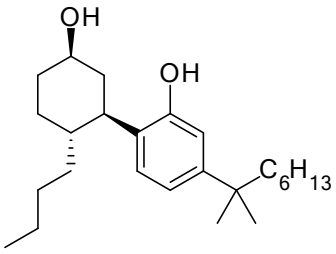

5 (CP 55,940)

The pyrazole **1** was the first compound reported to be both an antagonist *in vitro* and to be sufficiently potent *in vivo* to precipitate a withdrawal syndrome in cannabinoid-tolerant animals.[12,13]

In 1963, the structure and stereochemistry of cannabidiol (**CBD**) and **Δ⁹-THC** (**3**) were first determined. Unlike **Δ⁹-THC**, cannabidol (**CBD**) is not psychoactive and possess medical benefits such as relieving convulsion, inflammation, anxiety and nausea. It is an allosteric antagonist at the brain cannabinoid receptor that alters psychoactive effects of **Δ⁹-THC** and is selective for central nervous system (CNS) cannabinoid receptor subtype (CB1 subtype) over receptor subtypes found in the immune system (CB2 subtype).

Cannabinol (**CBN**) is the main product in the degradation of **Δ⁹-THC** and is found to be mildly psychoactive and has the same affinity at CB2 as cannabidol (**CBN**).[67] Currently, there are no effective treatments for marijuana abuse and development of new medications for treatment of marijuana abuse is essential. There is urgency for the development of pharmacotherapies to treat marijuana addiction while understanding the mechanism of marijuana action on the central nervous system (CNS). The physiological and behavioral effects of cannabinoids have been studied extensively and it has been suggested that a cannabinoid antagonist could be useful as treatment for marijuana

abuse.

The development of CB1 antagonists for psychostimulant addiction has been the subject of several studies with cocaine and methamphetamine.[14] This approach is based upon the fundamental mechanisms of psychostimulant neurobiology and neurochemistry. The mesocorticolimbic dopamine system, which includes neurons of the ventral tegmental area (VTA) and corresponding projections into the nucleus accumbens, amygdala, and prefrontal cortex, is believed to be the primary region of the brain that mediates the effects of psychostimulants (for e.g. cocaine and methamphetamine) and is closely associated with reward mechanisms.[15-17]

Cannabinoid receptors also are located in these regions, and cannabinoid agonists have been shown to elevate extracellular dopamine levels in these regions.[18] Drugs that elevate dopamine levels in the striatum, (e.g. cocaine, methamphetamine) typically exhibit potent abuse potential. As such, CB1 receptor antagonists are proposed to have potential utility as psychostimulant therapeutics in that they may mediate the abuse liability via inhibition of dopaminergic activity in the reward circuitry of the brain.[4,5] *In vivo*

characterization of CB1 antagonists/inverse agonists with psychostimulants has produced some promising results for future development as psychostimulant therapeutics.[14]

The antagonist **SR141716A (1)** has been shown to reduce rat cocaine-primed and cue-induced reinstatement of responding when reinforced by cocaine.[19] It was also found that **SR141716A** (**1**), reduced the motivational effects of cocaine in mice under progressive ratio conditions.

In 2006, European Union approved the use of **SR141716A** (**1**) for the purposes of weight control and treatment of obesity. At that time **SR141716A** (**1**), which was developed by Sanofi Aventis, blocked the same chemical receptors that trigger the munchies in marijuana smokers. Brand named as Acomplia, with its hydrochloride salt is called Rimonobant. It was launched in European market and at that time it was heralded as a possible new treatment for smoking cessation and metabolic disorders that can lead to heart attacks. The CB1 antagonist **AM251** (**2**) has been reported to reduce self-administration of methamphetamine in rats while both **1** and **2** have been

reported to be effective in reducing reinstatement of methamphetamine-seeking behavior.[20,21]

Despite these encouraging results, the inverse agonist activity exhibited by **SR141716A (1)** is thought to be deleterious for the development of drug abuse medication. Inverse agonists typically elicit pharmacological responses opposite to agonists and thus are not ideally suited for the treatment of drug addiction due to potential dysphoric side effects associated with these drugs. These include increased nociceptive sensitivity, decreased food intake and body weight, disruption of operant behavior and potential nausea in humans.[22-25] The side effects suggests that a CB1 antagonist with inverse agonist profiles may have limited use as a medication.[26,27] This was the case with the diet drug, Rimonabant® (a.k.a. Zimulti®, **SR141716A**, **1**). Although never approved by the FDA,[28] Rimonabant® was withdrawn from European markets due to concerns over suicidality and an increased risk of other psychiatric disorders.[29]

In lieu of these potential side effects, it is our aim to develop a novel CB1 receptor

antagonist that was devoid of any inverse agonist activity and that essentially acted as a neutral antagonist. Herein we describe the design, synthesis, structure and cannabinoid efficacy of a series of novel 4-alkoxycarbonyl-1,5-diaryl-1,2,3-triazoles which has led to the discovery of a new neutral CB1 antagonist.

2. THE ENDOCANNABINOID SYSTEM

The endocannabinoid system is a physiological system that is believed to regulate body weight, glucose and lipid metabolism, and tobacco dependence. The health implications of the endo-cannabinoid system are staggering. Cannabinoids act as a bioregulatory mechanism for most life processes. A few of the Medical Uses of Cannabinoids are, Relieves Chronic Pain; Reduces need for narcotics in chronic pain or Narcotics Addiction; Anti-Cancer (Breast, Colon, Pancreas, Brain-Glioma); Relieves Post Traumatic Stress Disorder, Phobias; Relieves Nausea and Vomiting associated with Chemotherapy; Improves Appetite in Wasting Syndromes; Relieves Migraine Headache; Relieves Glaucoma; Relieves Bladder incontinence; Used as Anti-convulsant; Used as Anti-depressant; Used as Atypical anti-psychotic; Used for Bi-Polar

Syndrome; Used for Multiple Sclerosis, ALS.

The endocannabinoid system consists of three components: cannabinoid receptors, their endogenous ligands (endocannabinoids), and the enzymes, proteins, and transporters involved in the synthesis and degradation of endocannabinoids.[30]

The research on cannabinoid receptors was stimulated by the identification of the chemical structure of Δ^9-tetrahydrocannabinol (**3**, **Δ^9-THC**), the major active component of marijuana. Although, the central and peripheral actions of marijuana have been studied for over half a century and marijuana has been used in medical and recreational applications throughout the ages, it has taken many years to understand the action mechanisms of cannabinoid receptors. The effects of **Δ^9-THC** have been assumed to be mediated by the binding of this drug to a certain type of receptors located throughout the body, defined as cannabinoid receptors. Endocannabinoids are endogenous compounds that bind to and functionally activate the same receptors **Δ^9-THC** binds to. A tremendous number of studies have contributed to the comprehension of the endocannabinoid regulation and function. Unlike many other neuromodulators or

hormones, endocannabinoids are not synthesized in advance or stored in vesicles. They are released “on demand” by Ca^{2+}-induced enzymatic cleavage from their phospholipid precursors in cell membranes.[31]

To date, five endocannabinoids have been identified. Anandamide (AEA, **6**) was the first endogenous ligand identified and reported in the early 1990’s. Anandamide together with 2-arachidonoyl glycerol (2-AG, **7**) are the two most studied endocannabinoids.[32] Anandamide and 2-arachidonoyl glycerol are biosynthesized “on demand” from their membrane lipid precursors, N-arachidonoyl-phosphatidylethanolamine (N-ArPE) and *sn*-1-acyl-2-arachidonoylglycerols (DAGs) respectively.[33]

Most of the proteins involved in the metabolism of Anandamide and 2-arachidonoyl glycerol have been fully characterized, especially the enzymes responsible for their biosynthesis and degradation. However, the route for the synthesis and inactivation of Virodhamine (**8**), *N*-arachidonoyldopanime (NADA, **9**), and noladin ether (**10**) still remains unclear. The cannabinoids have wide ranging effects on various systems

including mood, cognition and reward, immune, gastrointestinal and reproduction, sleep, neuroprotection, bone and cardiovascular function, in addition to apetite, lipid and carbohydrate metabolism.

Figure 8. Endocannabinoids.

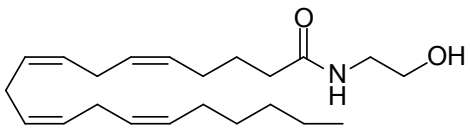

Anandamide **6**

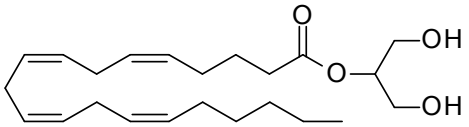

2-Arachidonoyl glycerol **7**

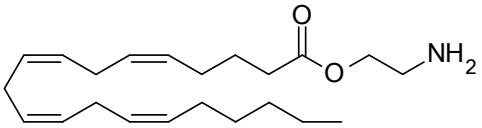

Virodhamine **8**

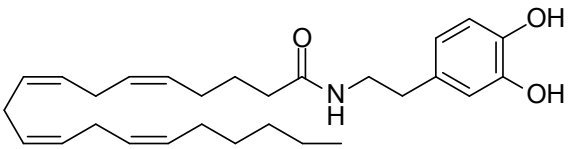

N-Arachidonyoyl-dopamine **9**

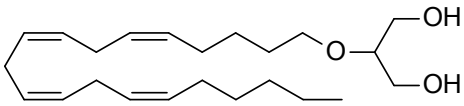

Noladin ether **10**

The orexigenic effect of the endocannabinoids is mediated via activation of AMP-activated protein kinase (AMPK). AMPK plays a central role in the control of energy homeostasis both at an individual cellular level and that of the whole body via its appetite stimulating effects in the hypothalamus. It seems that cannabinoids interact with a number of hormonal systems and possibly mediate their effects.

Initially, it was thought that the endocannabinoid system acted solely centrally through its effects on appetite and food intake. Widely prevalent presence of CB1 receptor centrally supports this. Also, central administration of anandamide into the nentromedial nucleus causes hyperphagia in rats. However, the endocannabinoids not only act centrally but also peripherally in the control of energy balance and metabolism. It has been suggested that cannabinoids increase weight by methods other than solely stimulating appetite.[31] A human study showed an increase in caloric intake and weight gain in volunteers who smoked cannabis when compared with controls. It was seen that, although the weight of participants continued to increase throughout the study, the increased food intake subsided after just a few days.

3. CANNABINOID RECEPTORS

The identification of the cannabinoid receptors was stimulated by the desire to understand the pharmacological and biochemical effects of the psychoactive effects of Δ^9-tetrahydrocannabinol (**Δ^9-THC**), the major psychoactive component of cannabis. It was believed that the effects of Δ^9-tetrahydrocannabinol (**Δ^9-THC**) are mediated by

occupation of receptors located throughout the body.

Two major types of Cannabinoid (CB) - receptors have been identified to date: CB1 and CB2. Though their crystal structures are still not known, they have been cloned and their amino acid sequences have been compared with each other and several other transmembrane proteins. Both the CB1 cannabinoid receptor and the CB2 cannabinoid receptors share the similar signaling sequence. The recreational effects of psychostimulants are primarily caused by CB1-receptors. Cannabinoid receptors (CB1, CB2) belong to the Class A, rhodospin-like family of G protein-coupled receptors (GPCRs).

The cannabinoid receptors signals primarily through the inhibitory G proteins G_i and G_o, to a less extend via G_s and $G_{q/11}$ with certain agonists. The CB2 receptors expressed by immune cells, including macrophages, are responsible for the anti-inflammatory and immunosuppressive effects of cannabinoids.[38] CB2 receptors are present in atherosclerotic lesions and exogenous cannabinoid compounds reduce the progression of atherosclerosis in ApoE-null mice by a mechanism that is sensitive to co-

administration of a CB2 receptorselective antagonist.[38] Although the existence of protein receptors for Δ^9-tetrahydrocannabinol (**Δ^9-THC**) had been indicated for a long time, Howlett *et al.*[32], for the first time, provided definitive evidence for a cannabinoid receptor. Upon the binding of cannabinoid ligands on cannabinoid receptors, the cannabinoid receptors were stimulated which leads to the activation of adenyl acyclase, the activation of mitogen-activated protein kinases, the inhibition of certain voltage-gated calcium channels and the activation of G protein-linked inwardly rectifying potassium channels.

A binding assay was developed and established that cannabinoid receptor CB1 inhibited adenylyl cyclase via a pertussin toxin protein and also to inhibit N-type Ca^{2+} channels facilitating activation of a G-protein-regulated voltage dependent K^+ channels. In contrast, the CB2R, while also inhibiting adenylate cyclase via a pertussin toxin $G_{i/o}$ protein, apparently do not regulate either Ca^{2+} or K^+ ion channels.[34] The modulation of ion channels by CB2 cannabinoid receptors is more variable than that of CB1 cannabinoid receptors.

4. CB1 RECEPTOR LIGANDS

Cannabis is obtained from the Indian hemp *Cannabis Sativa L*. and contains a variety of natural cannabinoids. Cannabinoids are terpenophenolic compounds with a structural relationship similar to (-)-trans-Δ^9-tetrahydrocannabinol (Δ^9-THC) **3** or compounds with the ability to bind to cannabinoid receptors. To date, at least 66 cannabinoids have been isolated from the cannabis plant. The most prevalent natural cannabinoids that have been studied extensively are Δ^9-THC (**3**), cannabidiol (CBD), and cannabinol (CBN) (Figure 9).[67]

Figure 9. Plant Cannabinoids.

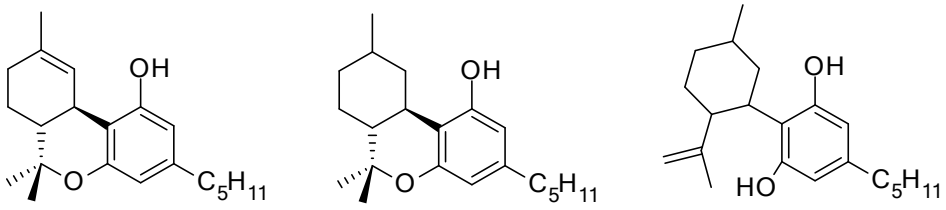

3 **CBN** **CBD**

The CB1 receptor is pharmacologically activated upon small molecule occupation of the binding sites. Based on structural features, cannabinoid receptor ligands fall into four classes[32]:

1. “Classical” Cannabinoids typified by tetrahydrocannabinol (**Δ⁹-THC**,);

2. “Non-classical” cannabinoids (e.g. CP55,940, **5**);

3. “Aminoalkylindoles” (e.g. WIN55212-2, **4**);

4. “Endocannabinoids” (e.g. anandamide, **6**).

Natural “classical” cannabinoids are dibenzopyran derivatives. Synthetic “nonclassical” cannabinoids are bicyclic and tricyclic analogs of **Δ⁹-THC** (**3**). However, eicosanoids “endocannabinoids” have a completely different structure. These ligands typically exhibit low nanomolar binding affinity for CB1 receptors and generally do not exhibit significant differential in binding affinity between the two subtypes of the cannabinoid receptors, CB1 and CB2. Of these ligands, anandamide (**6,** Figure 7) has been reported to exhibit selectivity for CB1 (K_i = 61 nM) over CB2 (K_i = 1930 nM).

CB1 receptor agonists inhibit cAMP production through inhibition of adenlyl cyclase, inhibit Ca^{+2} influx, activate K^+ channels and activate MAP kinase pathways. One of the many indications of CB1 receptor agonists is to increase intracellular dopamine levels in

brain (striatum) similar to cocaine. It is believed that CB1 agonist modulation of dopamine levels in the central nervous system is responsible partially for the abuse liability observed for cannabinoid agonists. CB1 receptors are associated with pleasure, appetite stimulation, learning & memory, thoughts, concentration, sensory and time perception, coordinated movement, bone formation and indirectly modulate dopaminergic transmission.

The CB1 cannabinoid receptor agonists have a great variety of potential pharmacological applications including nausea, glaucoma, cancer, stroke, pain, cachexia, and neuronal disorders such as multiple sclerosis and Parkinson's disease.[41] The role of CB1 receptors in these disease states and disorders, nature of the receptors active site, and the molecular interactions between the receptors and the ligands are not fully understood and are under intensive investigation.

Synthetic cannabinoids are useful in the determination of structure-activity relationships (SAR) of the endocannabinoid system. There was a need to find new synthetic cannabinoids with an increase in therapeutic activity and limited adverse side

effects. In the 1980's, Pfizer focused on these novel analgesic compounds. Early attempts at cannabinoid based analgesics and antiemetics led to the development of levonantradol (Figure 10). This cannabinoid compound was more potent than **THC**, easier to administer, but had too many side effects. From these early studies, CP 55-940 (**5,** Figure 7), a synthetic analog of **Δ^9-THC** was created and lead to the important discovery of CB1 receptor in 1988.

Figure 10. Synthetic cannabinoids.

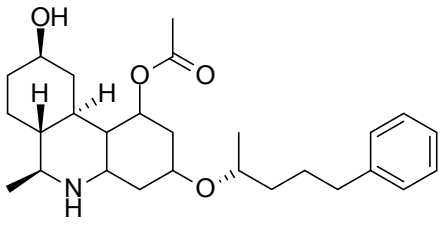

Levonantradol

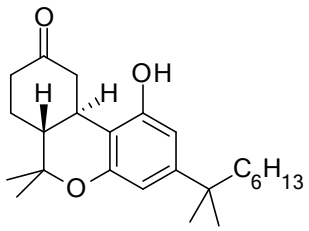

Nabilone

The aminoalkylindole derivative, WIN-55212-2 (**4**) is also a potent cannabinoid receptor agonist. This potent agonist has analgesic, anti-inflammatory and neuropathic properties. WIN-55212-2 (**4**) is a full agonist at the CB1 receptor with a higher affinity than **Δ^9-THC** for the CB1 receptor. The *in vitro* SARs of WIN-55212-2 (**4**) led to the development of new agonists. Nabilone is a synthetic analogue of **Δ^9-THC** and is

licensed for medical use. Nabilone mimics **Δ⁹-THC** (**3**) and is used therapeutically as an analgesic and antiemetic. This compound is not considered a narcotic by the World Health Organization (WHO) because it lacks the euphoric and recreational potential. In 1985, the U.S. Food and Drug Administration (FDA) approved nabilone for treating chemotherapy-induced nausea and vomiting, anorexia and as an appetite stimulant for AIDS patients.

CP 55,940 (**5**) mimics the effects of **Δ⁹-THC** (**3**) and is a full agonist at both CB1 and CB2 receptors. This synthetic analog allowed for radioligand binding assays that were not possible for **Δ⁹-THC** (**3**) due to the lipophilicity, which led to non-specific binding during *in vitro* experiments. The development of this analog led to further advancement in the cannabinoid field and also pushed for the need of selective agonists and antagonists for CB1 and CB2 receptors.

Among known cannabinoid receptor agonists there are several compounds exhibiting low efficacy agonist profiles *in vitro* and *in vivo*. Like the potent cannabinoid receptor ligand CP-55,940 (**5**) and WIN-55212-2 (**4**), they stimulated [^{35}S]GTPγS binding but were

significantly less potent and hence they have been designated as partial agonists.[4,18] The partial agonists include tetrahydrocannabinol (**Δ⁹-THC**), BAY59-3704 (**11**), CB-25 (**12**) and CB-52 (**13**).

Figure 11. Cannabinoid receptor partial agonists.

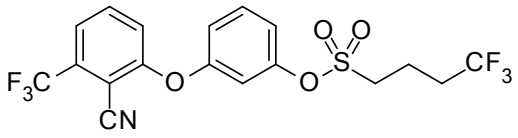

11 (BAY 59-3704)

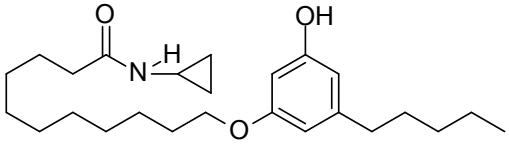

12 (CB-25)

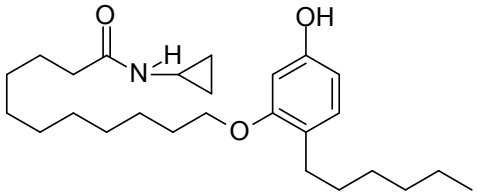

13 (CB-52)

CB2 is primarily involved in immune regulation- activation of this receptor results in suppression of immune system events like immune cell activation and proliferation, as well as production of some inflammatory mediators. It is not responsible for the psychoactive effects of THC. CB1 receptor agonists have been shown to increase intracellular dopamine levels in brain (striatum) similar to cocaine. It is believed that CB1

agonist modulation of dopamine levels in the CNS is responsible in part for the abuse liability observed for cannabinoids agonists.

5. CB1 RECEPTOR ANTAGONISTS

The CB1 cannabinoid receptor antagonists bind to CB1 receptors and block the effects of CB1 agonists. CB1 antagonists block stimulation of [^{35}S]GTPγS binding and block the inhibition of adenylate cyclase activity. The CB1 cannabinoid antagonists have potential applications in the treatment of obesity and nicotine dependence. The CB1 receptor antagonists known so far are diarylpyrazoles, or aminoalkylidoles or triazole drivatives.

Rimonabant was the first potent and selective antagonist (inverse agonist) of CB1 receptors. *In vivo* characterization of CB1 antagonists/Inverse agonists with psychostimulants has produced some promising results for future development as psychostimulant therapeutics.

While studies with the CB1 ligand **SR141716A** did not have an effect on cocaine and

amphetamine self-administration, it has been shown to reduce rat cocaine-primed and cue-induced reinstatement of responding when reinforced by cocaine. It was also found SR141716A reduced the motivational effects of cocaine in mice under progressive ratio conditions. These results suggest that CB1 antagonists have potential utility in reducing relapse among cocaine abusers. The CB1 antagonist AM251 (**2**) has been reported to reduce self-administration of methamphetamine in rats at doses that did not affect food-reinforced responding and also prevented reinstatement of extinguished methamphetamine seeking that was induced by re-exposure to a combination of methamphetamine and methamphetamine-associated cues.[44,45] Also SR141716A (**1**) has been reported to be effective in reducing reinstatement of methamphetamine-seeking behavior.

These results indicate that CB1 antagonists can effect psychostimulant induced behavior and clearly support further investigation of CB1 antagonists as target for the development of novel pharmacotherapies for drug abuse.[44] Although it has received less research attention, cannabinoid CB1 receptor antagonists have also been

proposed as treatments for methamphetamine. Cannabinoid CB1 receptor knockout mice are hyporesponsive to D-amphetamine on tests of locomotor activity, providing evidence for a role of CB1 receptors in amphetamine abuse.[45]

Accordingly, cannabinoid CB1 receptor antagonists have been proposed as potential medications for the treatment of drug abuse. The cannabinoid CB1 receptor antagonist/inverse agonist Rimonabant has gone through clinical trials for the treatment of nicotine dependence, and preclinical studies suggest that CB1 receptor antagonists may also have utility in treating opioid and alcohol abuse. Recent evidence suggests that the endocannabinoid system of the brain is involved in both the maintenance of drug taking behavior and relapse to drug taking after a period of abstinence.

In clinical trials, Rimonabant produced cardiovascular beneficial effects beyond that expected from weight loss alone and in one recent study employing intravascular ultrasonography, a reduction in the total volume of coronary atheromas. Rimonabant significantly reduces the development of atherosclerotic lesions in hyperlipidemic mice by exerting a number of anti-atherosclerotic effects including; reducing serum

cholesterol levels, reducing proinflammatory cytokines, inhibiting monocyte/macrophage proliferation and migration, and inducing reverse cholesterol transport in macrophages. However, the precise mechanisms by which Rimonabant exerts these anti-atherosclerotic effects remain to be determined. CB1 antagonists have been shown to block the effects of **Δ^9-THC** and appear to be devoid of abuse liability and CB1-receptors are viable targets.[5,45]

SR141716A or **Rimonabant** (**1**) was the first compound reported to be both and antagonist *in vitro* and to be sufficiently potent *in vivo* to precipitate a withdrawal syndrome in cannabinoid-tolerant animals. However currently available antagonist typically exhibit inverse agonist activity as well. Inverse agonists typically elicit pharmacological responses opposite to agonists and thus are not ideally suited for the treatment of drug addiction due to potential dysphoric effects associated with these drugs. These include increased nociceptive sensitivity, decreased food intake, decreased weight, disruption of operant behavior and potential nausea in humans. The side effects would undoubtly lead to low compliance and relapse among addicts.

Alternatively, neutral antagonists, since they possess no intrinsic activity, would be expected to exhibit diminished side effects and possess a better safety profile. As such neutral antagonists are good candidates for medication development. However, due to the limited availability of neutral antagonists, to our knowledge few studies have been performed with a neutral antagonist. The neutral antagonist LH21 (**15**) has been shown to demonstrate efficacy for the treatment of obesity.

Recently LH-21 was also determined as a neutral CB1 receptor antagonist with poor brain penetration, in diet-induced obese rats. These results support the hypothesis that treatment with the peripherally neutral acting CB1 receptor antagonist, LH-21, may promote weight loss through modulation of visceral adipose tissue.[27]

In lieu of lack of success with monoamine therapeutics, researchers have turned attention to alternative mechanisms to affect dopaminergic transmission and thus mediate the effects of psychostimulants on brain circuitry. To this end, it has been suggested that cannabinoid antagonists as potential medications for drug abuse have been subject of recent reviews and are discussed in more detail subsequently.

The development of CB1 antagonists for psychostimulant addiction is less straightforward and is rooted in the mechanisms of psychostimulant neurobiology and neurochemistry. Cannabinoid receptors are located in the regions along with mesocorticoloimbic dopamine system, the primary region of the brain that mediates the effects of psychostimulant (eg. cocaine and methamphetamine) and is closely associated with reward mechanisms.

Cannabinoid agonists have been shown to elevate extracellular dopamine levels in these regions. Drugs that elevate dopamine levels in the striatum, (eg. cocaine and methamphetamine) typically exhibit potent abuse potential. As such, CB1 receptor antagonists are proposed to have potential utility as psychostimulant therapeutics in that they may mediate the abuse liability via inhibition of dopaminergic activity.

6. CB1 ANTAGONIST AGAINST DRUG ABUSE

Molecular and neurobiological studies on the basis of the physiological and neurobehavioral effects of marijuana and cannabinoids have lagged behind other

natural addictive drugs such as cocaine, opium and tobacco. Behavioral pharmacologists are particularly interested in the roles of CB1 receptors because of their selective presence in the central nervous system and their association with brain-reward circuitry.[4]

The mesocorticolimbic dopamine system is believed to be the primary region of the brain mediating the effects of several drugs and is closely associated with brain-reward circuitry mechanisms. The mesocorticolimbic dopamine system includes neurons in the ventral tegmental area and corresponding projections into the forebrain regions.[18] Even though CB1 receptors do not reside on the mesencephalic dopaminergic neurons, they are located in these regions.[30] Studies further showed that CB1 receptor was present in certain brain regions with a high expression level. Furthermore, the cannabinoid receptor distribution was successfully mapped with the development of highly active cannabinoid receptor agonists.[35,36] The existence of cannabinoid receptor was ultimately proved by the cloning of a cannabinoid receptor in 1990 by Matsuda *et al.*[37] which was followed by the cloning of a second type of cannabinoid receptors three

years later in 1993.[38]

Figure 12 Localization of CB1 Receptors.[39]

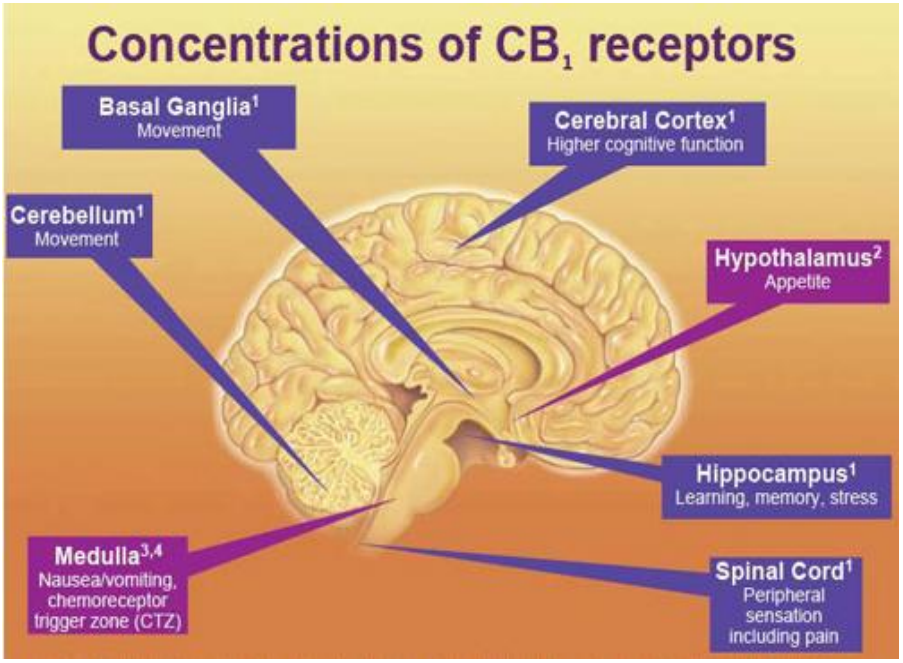

Much has been learned about the cannabinoid receptors by determining its localization. The localization of cannabinoid receptors was mainly determined using quantitative autoradiography, *in situ* hybridization and immunocytochemsitry.[39] Primates appear to have higher densities of cannabinoid receptors in cerebral cortex, hippocampus and cerebellar cortex than do rats. Thus CB receptor agonists and antagonists may act differently in rodents and primates for procedures highly dependent

on learning and memory. The autoradiographic studies performed by Herkenham *et al*. demonstrated significant results about CB1 receptors:

a) The CB1 cannabinoid receptors are mainly expressed in the central nervous system with high density in the cerebellum, hippocampus, and striatum. The CB1 cannabinoid receptors were highly abundant in the brain regions that are affected by psychoactive effects of Δ^9-tetrahydrocannabinol (**Δ^9-THC**);

b) The concentration was low in the brain regions unaffected by tetrahydrocannabinol (**Δ^9-THC**);

c) CB1 receptors were expressed abundantly on axon terminals.

The expression of CB1 receptors has also been described with high resolution from immunoctyochemical studies. It was revealed that CB1 receptors are expressed at very high levels in a subset of GABAergnic interneurones, the cholecystokinin (CCK) containing basket cells and at lower levels on many glutamatergic terminals throughout the brain. CB1 receptors are largely present on the preterminal axonal segment and

axons but very little on more proximal axons, dendrites, or the cell body. CB1 receptors are also found in fat, liver, pancreas, skeletal muscles, and a number of other peripheral tissues.[39] Conversely, the CB2 cannabinoid receptors are exclusively present in the immune system and modulate cytokine release. It has been found in the periphery of the spleen and cells associated with immune system like T-cells, B-cells, spleen, tonsils and monocytes. The presence of a third type of cannabinoid receptor has been indicated recently.[32]

CB1 receptor agonists elevate dopamine levels, while CB1 receptor antagonists or inverse agonists can attenuate the dopamine level elevations associated with drug abuse and diminish the stimulation of dopaminergic activity in the reward circuitry of the brain and attenuate the effects of drug abuse.

Therefore, the development of CB1 antagonists as potential therapeutic agents for drug abuse is straightforward. While the CB1 antagonist Rimonabant did not show to have an effect on cocaine and amphetamine self-administration, it has been reported to reduce rat cocaine-primed and cue-induced reinstatement studies with CB1 antagonist

CB1 antagonists have been shown to block the effects of **Δ^9-THC** and appear to be devoid of abuse liability.[15]

In a story very similar to the discovery of opiate receptors in the brain, cannabinoid receptors have been discovered along with their endogenous cannabinoids, representing the largest neurotransmitter system in the brain and immune system. This neurotransmitter system went undetected for decades because it involves an unheard of concept, retrograde transmission, or reversed flow of information from the post synapse to the pre-synapse.

At an inhibitory synapse, the presynaptic neuron provides an inhibitory input, decreasing the likelihood that the postynaptic neuron will fire (Figure 13). The neurotransmitters in the presynaptic vesicles and in the synapse are marked red while endocannabinoids are marked green. Now like in all synapses, information flows from the presynaptic neuron to the postsynaptic neuron via release of neurotransmitter and activation of postsynaptic receptors leading to changes in the activity of the postsynaptic neuron. However, the cannabinoid signaling mechanisms cause a pretty uncommon

event as they allow the postsynaptic neuron to modify the activity of the presynaptic neuron.

Figure 13. Model of Inhibitory Synapse.[46]

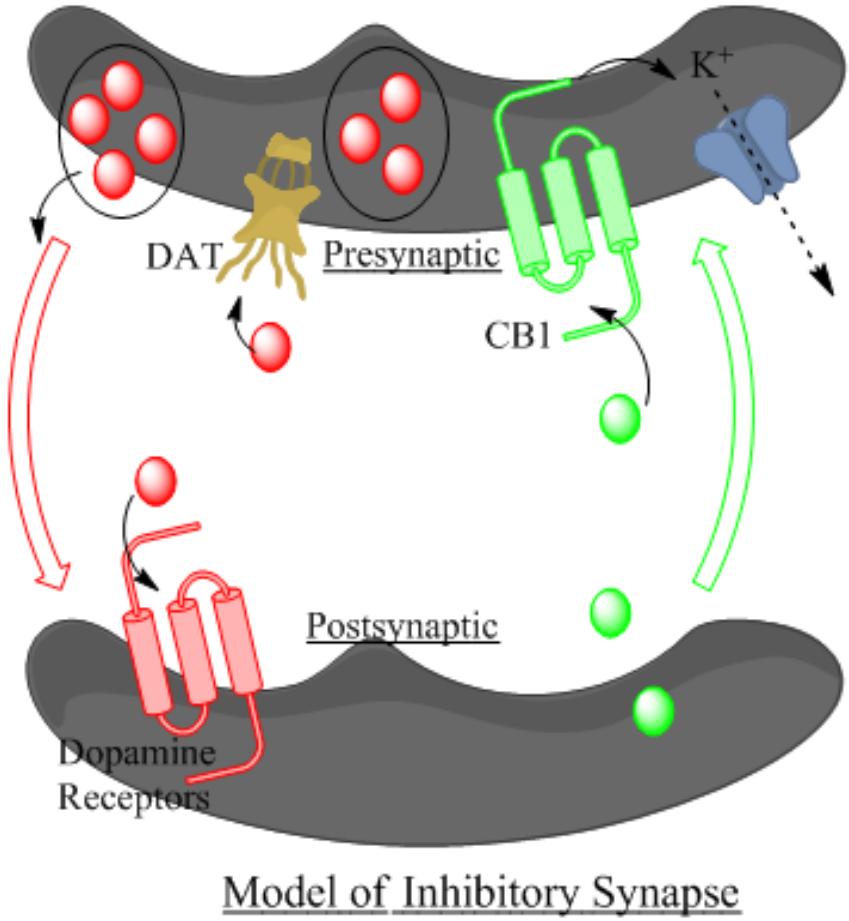

Hence, there is a two-way communication across the synapse, rather than the presynaptic neuron being the one-way communicator.

This is the “backward” or retrograde communication that goes on from postsynaptic

cell to presynaptic cell. The endocannabinoids are produced by the postsynaptic cell and are able to activate CB1 receptors located on presynaptic terminals. They are produced and released on demand, not stored in vesicles like many other neurotransmitters, so there are very specific triggers for endocannabinoid production.[32]

It was observed that when CB1 receptors are activated, there is a cumulative effect of complex signaling which controls release of neurotransmitters from the pre-synaptic neuron and hence further regulates the neuron firing. According to the proposed “Cannabinoid Hypothesis”, the endocannabinoid physiological control system (EPCS) has a potential role in the regulation of the rewarding effects of abused drugs through the neurobiological mechanisms.

These receptors use retrograde signaling, which is associated with the inhibition of transmission at the synapse by neurotransmitter suppression. Due to this abundant presence in the brain retrograde signaling of these cannabinoids are limitless and may explain the behavioral effects associated with cannabis. The retrograde messengers inhibit a host of neurotransmitters such as dopamine, serotonin, GABA, and

acetylcholine. The endocannabinoid transmission plays a significant role in the dependence/withdrawal to abused substances and drug seeking behavior through mediation of motivation.[63]

When CB1 receptors are activated, they signal through G-proteins to close calcium channels, preventing entry of calcium into the terminal. Calcium is needed for vesicles to fuse with the membrane and release inhibitory neurotransmitters into the synapse. So CB1 signaling stops inhibitory neurotransmitters from being released to the postsynaptic neuron.

CB1 receptor activation also results in opening of potassium channels. In a resting neuron, these channels are closed. Outflow of positively charged potassium ions leads to increase in the net negative charge across the membrane. This is called hyperpolarization, the opposite of depolarization. As can be imagined, since depolarization causes neurons to fire, hyperpolarization keeps a neuron from firing. This further decreases the chances that neurotransmitter will be released from the presynaptic terminal. The net result is that the postsynaptic neuron signals back to stop

neurotransmitter release from the presynaptic neuron.

Since endocannabinoid stimulation of CB1 receptors on presynaptic neurons can suppress neurotransmitter release from those neurons, so if we suppress inhibitory transmission from this circuit, we have more excitation and therefore more hunger. Throwing **Δ^9-THC** into this circuit, as someone might do when they have smoked marijuana, can lead to the same effect even if endocannabinoids are not being released by the presynaptic neuron. This is the reason, why marijuana smokers get the "munchies" (increased appetite), as they are losing suppression of hunger pathways.

CB1 was originally believed to be the "brain type" of receptors because it is among the most abundant G protein-coupled receptors in the central nervous system of mammalians. Now associating this with all the other circuits in brain, like reward, memory and motivation, for example, these are all circuits where CB1 receptors can be found and can be affected by **Δ^9-THC** and lead to alterations in behavior. **Δ^9-THC** interferes with the regulation of neuronal firing timing in the hippocampus, and a person cannot encode memories anymore. It relieves suppression upon dopaminergic neurons,

leading to dopamine release that gives a marijuana-intaker the “High”.

Figure 14 Comparison of endocannabinoids & exocannabinoids.[38]

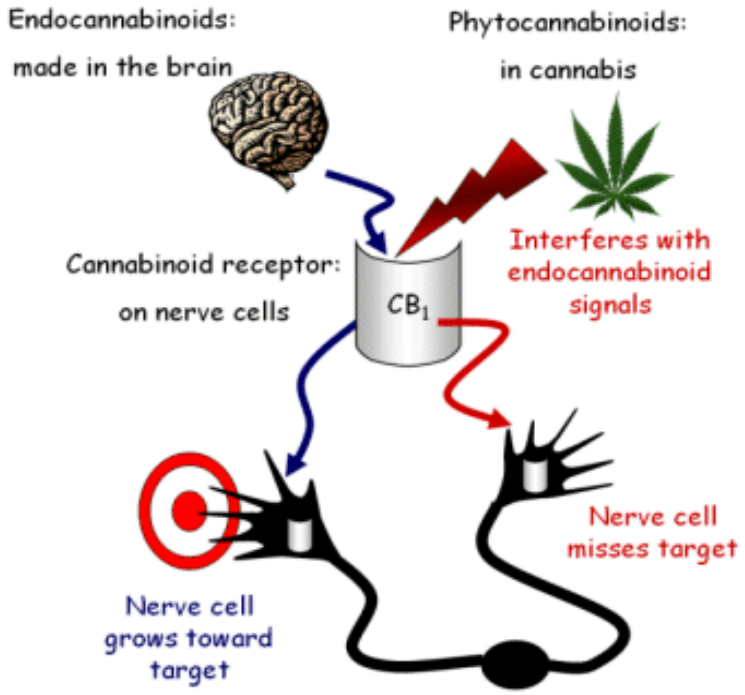

As can be seen, Figure 14 compares the effects of endocannabinoids and the sedating effects of natural as well as synthetic cannabinoids on CB1 receptors. It is seen that while endocannabinoids are necessasary for various physiological functions and development, on the other hand phytocannabinoids (obtained from plant source like hemp plant) and synthestic compounds interfere in the normal signaling process which further interferes in the physiological functions of the animal body. Now it is clear that

CB1 is predominantly expressed in the central nervous system but also, to a lesser extent, in various peripheral organs, while CB2 receptors are mostly expressed in the immune system. The endocannabinoid system appears to be involved in a rising number of pathological conditions and hence represents an exciting target for drug discovery.[40]

7. BINDING AFFINITY AND INHIBITION CONSTANT

The drugs are evaluated for their potency by the value of their binding affinity to a specific transporter. These values are typically expressed in terms of IC_{50} or K_i. The IC_{50} value is the concentration at which the compound is needed to displace 50% of the bound radio-labeled ligand.[38] Neurotransmitters, inhibitors, activators, and substrates are considered ligands since they have the ability to bind and form complexes with protein chains to initiate a cellular response that alters the chemical conformation of the receptor protein by an intermolecular force like ionic bonds, hydrogen bonds and van der Waals forces.

The radio-labeled ligands used, usually show high affinity for the targeted transporter or receptor. For example, ^{3}[H]WIN55,212-2 (**4**) and ^{3}[H]SR141716 (**1**) are used for CB1-receptors. K_i is the inhibition constant and is related to IC_{50} by the following equation:

$$K_i = \frac{IC_{50}}{1 + \left\{ \frac{[S]}{K_m} \right\}}$$

IC_{50} is the functional strength of the inhibitor i.e. the concentration at which the inhibitor is needed to displace 50% of bound radio-labeled ligand while [S] is concentration of radiolabeled ligand used and K_m is the affinity of the radiolabeled ligand for the specific protein receptor.[70]

If a ligand has a high affinity the receptor-ligand complex will be present for longer time interval as compared from low affinity. In addition, a high binding affinity implies a low concentration of a ligand to maximally occupy a receptor and trigger a physiological response. The above equation can also be expressed as:

$$K_i = \frac{IC_{50}}{\{ [S] / (K_d + 1) \}}$$

Where K_d is the dissociation constant of the radiolabeled ligand previously determined for the specific receptor. K_d is usually calculated by the following equation.

K_d = [R][L]/[RL]

Here, [R], [L] and [RL] represent molar concentrations of the protein, ligand and complex, respectively. Several factors can affect the IC_{50} values according to experimental conditions which include the type and amount of radio-labeled ligand, state of tissue (fresh or frozen), buffer, incubation time and protein content. Therefore K_i offers a better comparison of data since it takes into account the concentration and dissociation constant of the radio-labeled ligand and the IC_{50} value for the compound.

Binding assays are done by using a radioligand usually an agonist in a low concentration either at or below the dissociation constant, K_d. The binding specificity is determined in the presence of the range of the concentration competing non-radio- labeled compound usually an antagonist to measure the potency through binding competition at the radio labeled ligand.[70]

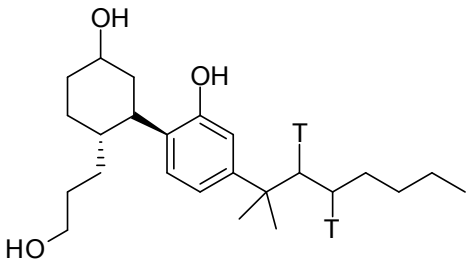

^{3}[H]CP 55,940

Full CB1 agonist, K_i = 3.4 nM

If an agonist can maximally stimulate the receptor it is considered a full agonist, for example WIN 55,940 (**4**) and CP 55,940 (**5**) are agonists for CB1 receptor. However, if an agonist can only partially activate the physiological response it is considered a partial agonist for example THC is a partial agonist for CB1 receptor (Figure 15).

An inverse agonist is an agent that binds to the same receptor as an agonist but induces a pharmacological response opposite to that agonist. A prerequisite for an inverse agonist response is that the receptor must have a constitutive (also known as intrinsic or basal) level activity in the absence of any ligand. An agonist increases the activity of a receptor above its basal level while an inverse agonist decreases the activity below the basal level. A neutral antagonist has no activity in the absence of an agonist or inverse agonist but can block the activity of either.

Figure 15. Dose response curves of an agonist, neutral antagonist, and inverse agonist[70]

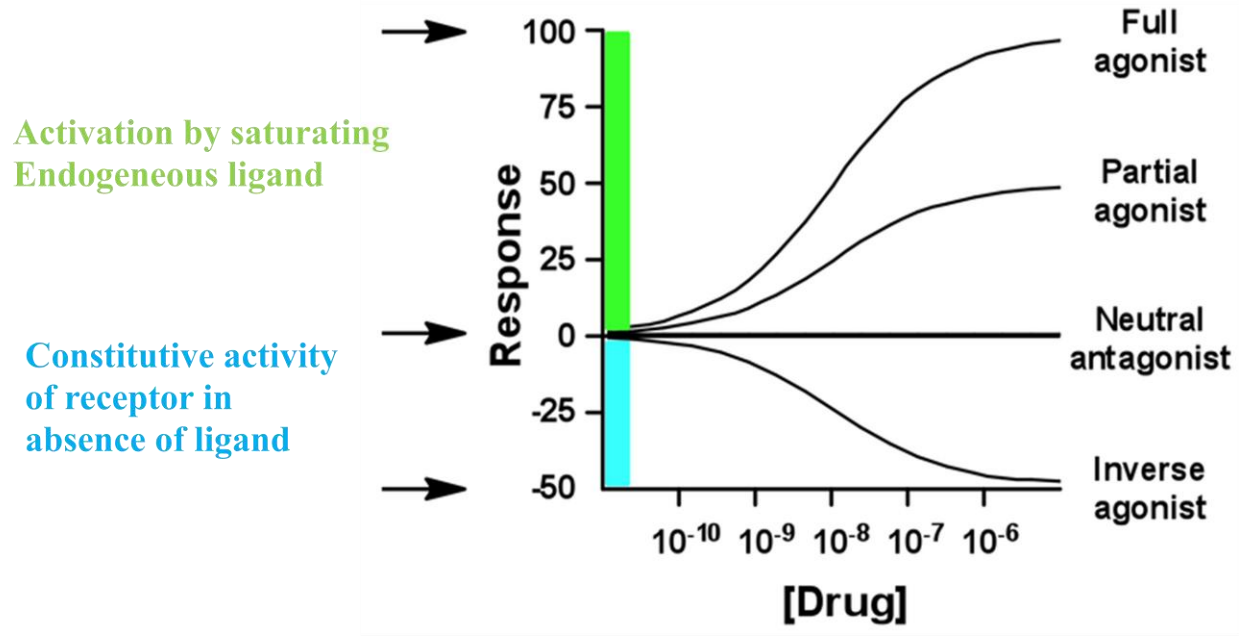

On the other hand if the physiologic response is not activated by binding of the ligand to the receptor it is then deemed an antagonist. Competitive antagonists (also known as surmountable antagonists) reversibly bind to receptors at the same binding site (active site) as the endogenous ligand or agonist, but without activating the receptor. Agonists and antagonists "compete" for the same binding site on the receptor. Once bound, an antagonist will block agonist binding. The term "non-competitive antagonism" (sometimes called non-surmountable antagonists) is used to describe two distinct phenomena: one in which the antagonist binds to the active site of the receptor irreversibly, and one in which the antagonist binds to an allosteric site of the receptor.

The efficacy of a full agonist is by definition 100%, a neutral antagonist has 0%, while an inverse agonist has < 0% (i.e., negative) efficacy.

8. PHARMACOPHORE FOR CB1 ANTAGONIST

To date characterization of CB1 and CB2 receptors has relied upon ligand-receptor interactions as the three dimensional structures and structures of binding sites have yet to be established. **SR141716A** (Rimonabant, **1**), the first CB1 receptor antagonist synthesized, was tested in humans and then approved as a drug for the treatment of obesity and related comorbidities.

Based on the structure of Rimonabant, numerous analogs have been synthesized to elucidate the structure-activity relationship information and the biological mechanisms. Most of those analogs were designed and synthesized based on the 1,5-diarylpyrazole ring as structural template, which was believed to be the molecular region binding to CB1 receptors. Various structural modifications of the prototype Rimonabant were undertaken and led to new series of cannabinoid compounds. Some of those

compounds turned out to be CB1 antagonists with good potency, CB1/CB2 selectivity and improved lipophilicity.

One of the most important structural modifications was focused on the changes of the C-3 acyl group. Analogs have been synthesized and evaluated to establish the influence of the presence of the carboxamide oxygen from the C-3 position on the binding affinity.[42] The carboxamide group was replaced by heterocyclic carboxamide bioisosteres, amino alcohols and even ketones. It was discovered that the potency was diminished relative to Rimonabant when the carboxamide oxygen was absent from the pyrazole ring. It was explained by the hypothesis that the carboxamide oxygen forms a hydrogen bond with the CB1 receptor binding region.

However, the functional assay results of those analogs suggested that the carboxamide group contributes to the inverse agonist property. Analogs without the carboxamide oxygen were identified as neutral antagonists in efficacy evaluations (Figure 19). Moreover, the analogs of Rimonabant consisting of long-chain alkyl amide have been synthesized and reported to exhibit good affinity for CB1 receptors.[43]

Analogs with alkyl chain longer than six carbons exhibited decreased binding affinity at CB1 receptors. Branched alkyl amides were generally more potent than the corresponding straight alkyl amides with same number of carbon atoms.[44]

Figure 16. Putative CB1-receptor amino acid side chains interaction with Rimonabant. (Modified from ref 46)

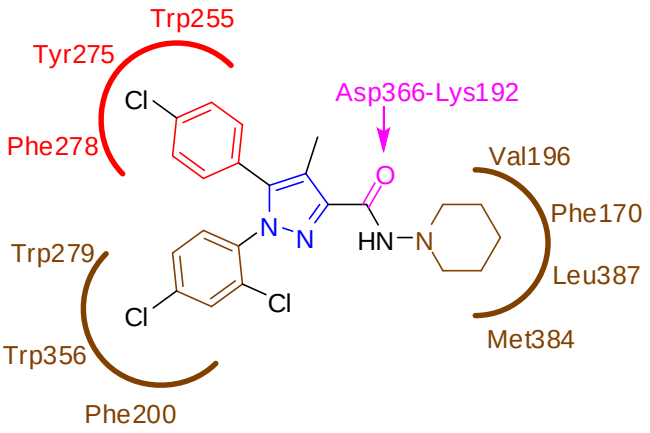

Based on the experimental and computational studies, the pharmacophoric requirements were concluded for the potency of the pyrazole analogs in CB1 binding: a *para*-substitute phenyl ring at the pyrazole C-5 position, a 2,4-dichlorophenyl ring at pyrazole N-1 position, and a carboxamide moiety at pyrazole C-3 position.[45] SAR studies revealed that the C-5 phenyl group was essential for the CB1 binding.

A general CB1 receptor inverse agonist pharmacophore model is shown in Figure 16

taking **Rimonabant** as a representative example.[46] Putative CB1 receptor amino acid side chain residues in receptor-ligand interaction are shown. Both vicinal aromatic rings are connected to a central core unit which is interconnected with a lipophilic moiety via a hydrogen bond acceptor unit (Figure 16). Substitution at the *p*-position of the phenyl with a halogen atom or an alkyl chain can effectively increase the binding affinity. In a recent study, pentyl chains with a variety of groups attached to the terminal carbon were used as the substituents at that position. The resulting analogs exhibited excellent binding affinity to CB1 receptors.

9. RATIONAL DRUG DESIGN

Bioisosterism is an important approach frequently used in medicinal chemistry to discover new lead compounds based on existing key ligands. It plays a significant role in attenuating toxicity, optimizing binding and altering pharmacokinetics of a lead compound. The three dimensional structures of thiazoles, triazoles, and imidazoles and the structure of pyrazole exhibit a high degree of similarity. Consequently, the pyrazole ring in Rimanabant can be replaced by such heterocyclic five-membered rings in order

to discover bioisosteres, compounds that have similar chemical or physical properties and therefore similar biological properties.

Based on Rimonabant as the prototype, ring bioisosterism has been the most widely used strategy to design and synthesize cannabinoid antagonists with optimal pharmacological properties. The first reported bioisosteric analogs of Rimonabant were 4,5-diarylimidazole-2-carboxamides synthesized by replacing the pyrazole core with an imidazole ring.[47] A series of 1,2-diarylimidazole-4-carboxamides were also described and structural modifications were conducted to established SAR information.[48]

The biological data clearly demonstrated that for both of those two isomeric series of imidazole analogs, the most potent ligands were those possessing substitution pattern very similar to that of **SR141716A**. In addition, most of those imidazole analogs showed antagonistic properties in functional assay studies. Some compounds displayed affinities for CB1 receptors comparative to that of **SR141716A** and had good oral bioavailability and brain penetration. The pyrazole core in **SR141716A** was also replaced by other five-membered bioisosteric rings (Figure 17). These included thiazole,

oxazole and 1,2,4-triazole derivatives. Those analogs were reported to be less potent than the methyl-diarylimidazoles discussed earlier.

Figure 17. Five-membered bioisosteric analogs of Rimonabant

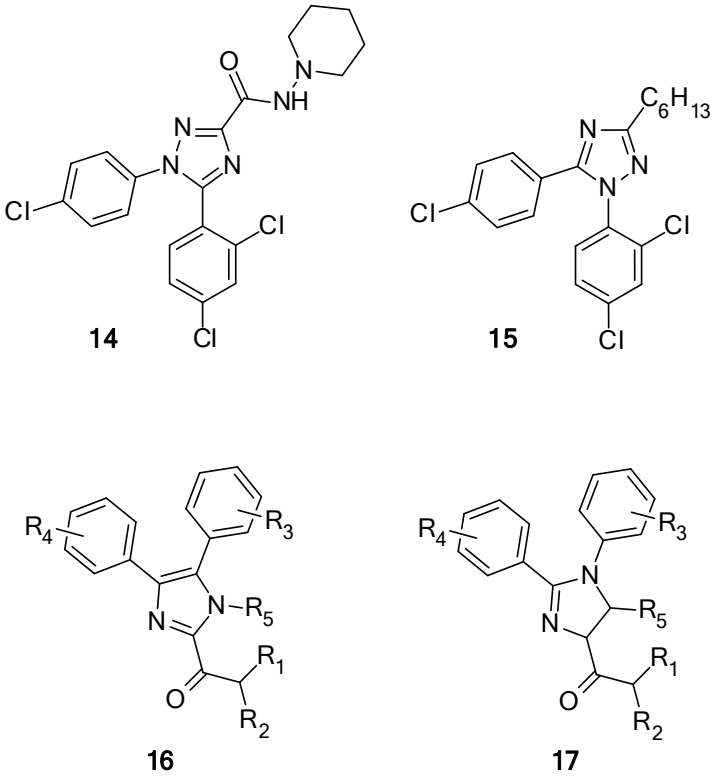

This difference in binding affinity may be attributed to the absence of methyl group which was believed to play a very important role in properly orienting the carbonyl group for molecular recognition at the CB1 binding pocket.

Despite the moderate binding affinity associated with the 1,2,4-triazole derivatives,

this series provided interesting compounds. The analogue bearing the same substituents as **SR141716A** was found to be an antagonist (**14**). Another 1,2,4-triazole derivative LH-21 (**15**) bearing a *n*-hexyl instead of a carboxamide was reported to be an antagonist both *in vitro* and *in vivo*. Also, it was one of the few known CB1 receptor antagonists without inverse agonistic properties.[27] Tremendous amount of work has also been done studying the structure-activity relationship of the imidazole bioisosteric analogue of **SR141716A** which are compound **16** and **17**.

In addition to the analogs with five-membered bioisosteric rings, six-membered ring replacement of the pyrazole ring in **SR141716A** has afforded a number of pyridine, pyrimidine and pyrazine derivatives (Figure 18). Diarylpyridine analogs with or without the carboxamide group were all synthesized and evaluated in binding assay studies. The ether **18**, a potent and selective CB1 agonist, demonstrated that the presence of amide moiety was not necessary for this category of compounds.

It could be replaced by other functional group combinations with the substituent at the pyridine C-5 position, such as the nitrile in **19**, to optimize pharmacological profiles.[24]

The introduction of a polar substituent to the pyrazine ring provided analogs **20** that were less lipophilic and more bioavailable.

Figure 18. Six-membered bioisosteric analogs of Rimonabant

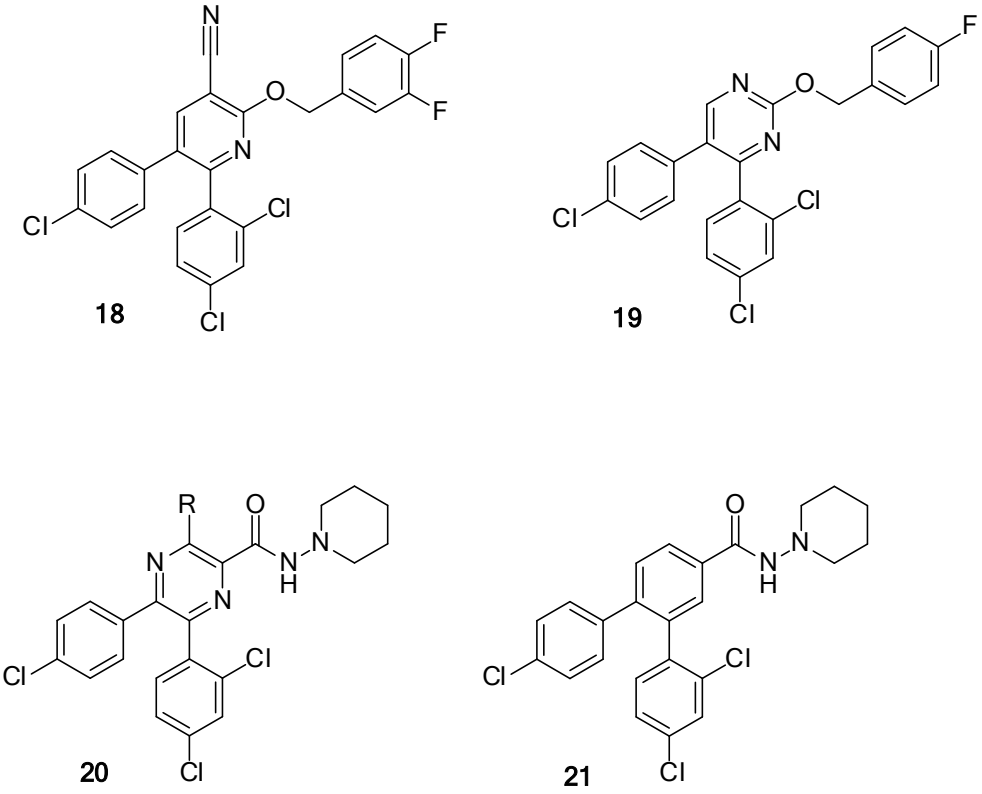

Compounds with phenyl group (**21)** as the central ring still exhibited good binding to CB1 receptor. It indicated that the presence of a heterocycle was not strictly required for a CB1 antagonist.[50] In 2002, Hurst *et al*, showed that **SR141716A** interaction with LYS 3.28(192) is crucial for its inverse agonism at the cannabinoid CB1 receptor.[42]

Figure 19. (a) Interaction of 3-carboxamide in **SR141716A** with LYS 3.28(192). (b) Absence of this interaction **VCHSR**.

(a)

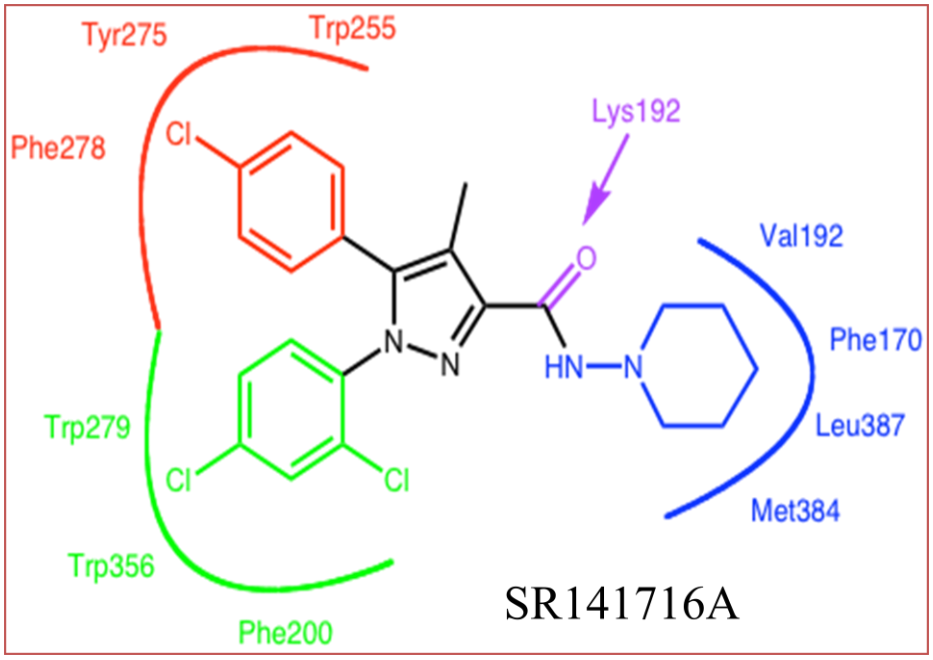

(b)

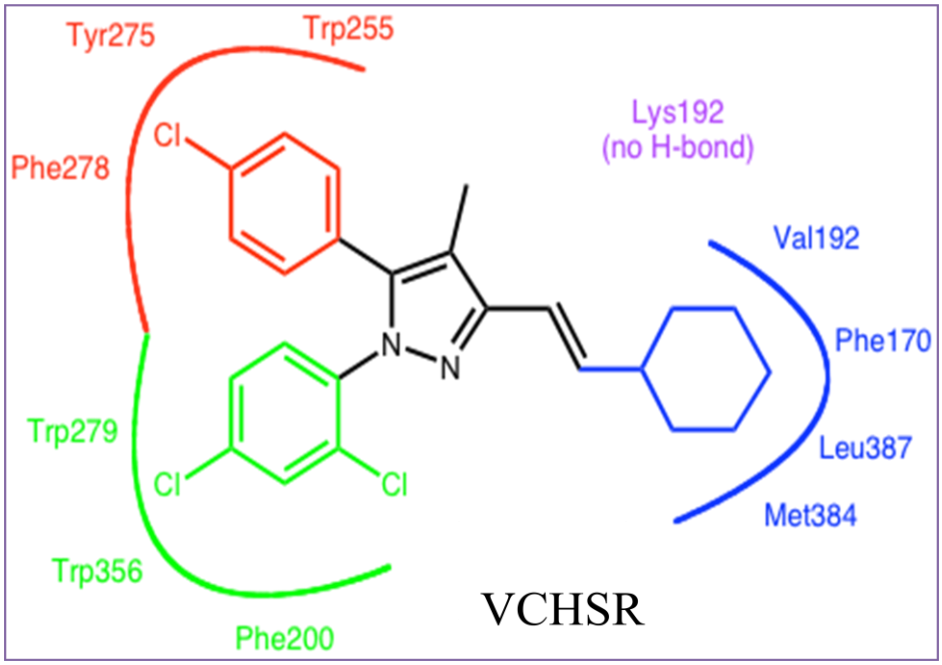

Later in 2006, the group modified to remove the hydrogen bonding capability in the C-3 substituent region, which removes the inverse agonist effect that rimonabant produces at high doses, so that VCHSR instead acts as a neutral antagonist, blocking the receptor but producing no physiological effect of its own.

Based on the structure of the 1,5 diarylpyrazole core template revealed in **Rimonobant (1)**, bioisosteric replacement was done to synthesize and identify a variety of potent bioisosteric analogs. In reviewing the literature, the 1,2,3-triazole ring systems which are one of the privileged structures were absent from the pool of derivatives as CB1-antagonists.[51]

Moreover the 1,2,4-triazole like **LH-21** derivatives have been reported to lack inverse agonist efficacy and elicit a neutral antagonist profile.The design rational was to incorporate the 1,2,3-triazole ring system into the vicinal diaryl groups which was presumed to interact with a unique region of the CB1 receptor. Despite the structural changes in these ligands, the pharmacological profiles of SR141716 based compounds have been fairly consistent.

10. PRELIMINARY STUDIES

CB1 antagonists have been shown to block the effects of Δ^9-THC and are also devoid of abuse liability. However, current antagonists exhibit inverse agonist activity eliciting the opposite response to an agonist.

The development of effective medications for the treatment of cannabinoid and psychostimulant abuse is of great importance to society. While many advances have been made in current understanding of drug addiction, there still remains a tremendous need for therapeutic agents capable of treating and maintaining sustained abstinence among cannabinoid and psychostimulant drug users. Addiction to the psychostimulant cocaine has proven to be extremely difficult to mediate.

Extensive studies directed toward the development of an agonist based pharmacotherapy in the form of dopamine reuptake inhibitors for the treatment of cocaine addiction have yet to identify a clinically useful therapeutic agent. In addition, the psychostimulant methamphetamine is rapidly becoming one of the most widely

abused drug in the United States. Currently there are no pharmacotherapeutic agents or strategies in place for the treatment of either cocaine or methamphetamine addiction.

As both cocaine and methamphetamine act as indirect agonists of dopamine systems, indirect attenuation of dopaminergic systems is believed to be a viable target for pharmacotherapy development. It has been suggested that the cannabinoid receptor system can indirectly modulate dopaminergic transmission and thus mediate the effects of psychostimulants on brain circuitry.

Moreover, in addition to their efficacy as treatments for stimulant abuse, cannabinoid antagonists would be useful in blocking the effects of cannabinoids and could therefore be useful for treating cannabinoid abuse as well. The studies proposed in this application are designed to provide novel, potent and selective cannabinoid receptor antagonists. Compounds identified in this study will then be made available to several research groups including National Institute of Drug Abuse Addiction (NIDA) Treatment Discovery Program, to evaluate the therapeutic potential by subsequent studies for the treatment of drug addiction.

Our strategy was to focus on the development of clinically useful cannabinoid application for the treatment of cannabinoid and/or psychostimulant addiction by the synthesis and development of new cannabinoid antagonist ligands based upon novel diaryl triazole scaffolds structures.

To explore this deficiency, we identified in our laboratories compound **22** (Figure 20) as our initial target for synthesis. With vicinal diaryl system retained and the pyrazole ring replaced by the 1,2,3-triazole ring system, it even had lower lipophilicity as compared to rimonabant. Another encouraging fact was that the 1,2,4-triazoles synthesized earlier (for example LH-21) did not show any inverse agonist activity which was a green signal for us to go ahead and synthesize 1,2,3-triazoles.

The construction of 1,2,3-triazole ring system exploits the 1,3-dipolar cycloaddition of an azide and a terminal alkyne, the click chemistry developed by Sharpless *et al.*[52] To achieve our goal, we wanted to not only synthesize novel compounds, we also wanted to characterize binding affinity at cannabinoid receptors. Ligand design rationale utilized developing structure activity relationship studies for each series, lead compounds in

literature and computational methods to optimize potency and lipophilicity. Potent and selective CB1 receptor antagonists inhibit the effects of typical cannabinoid agonists such as **Δ⁹-THC** and WIN 55,212-2 (**4**, Figure 7).

Figure 20. Initial target of synthesis.

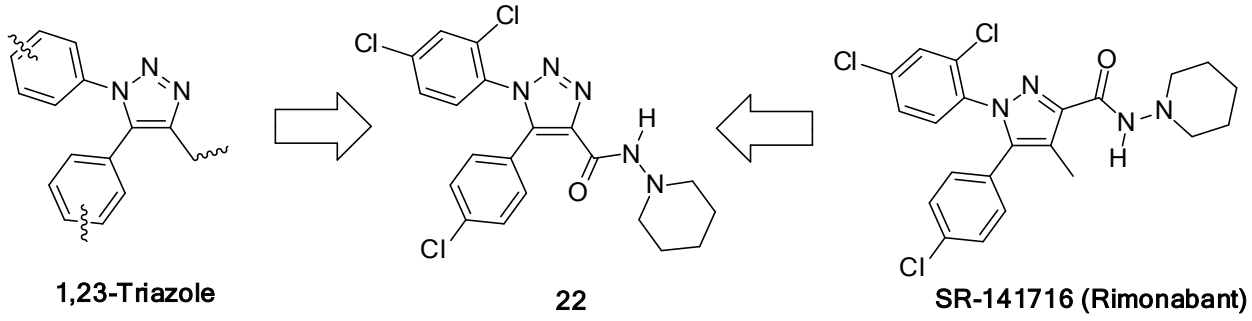

The program includes chemical synthesis, *in vitro* biological evaluation, and *in vivo* biological evaluation. Phase 1 of the study will consist of rational drug design and synthesis. Novel analogs will be designed based upon lead structures identified in our preliminary studies and supported by computational studies (Figure 21). In Phase 2, compounds will be evaluated *in vitro* studies to identify structural requirements for high affinity binding. The binding affinity results will be used to advance compounds to *in vitro* efficacy studies as well as provide feedback information for the optimization of compound structures to identify more potent ligands.

Figure 21. Flowscheme of CB1 receptor drug discovery program.

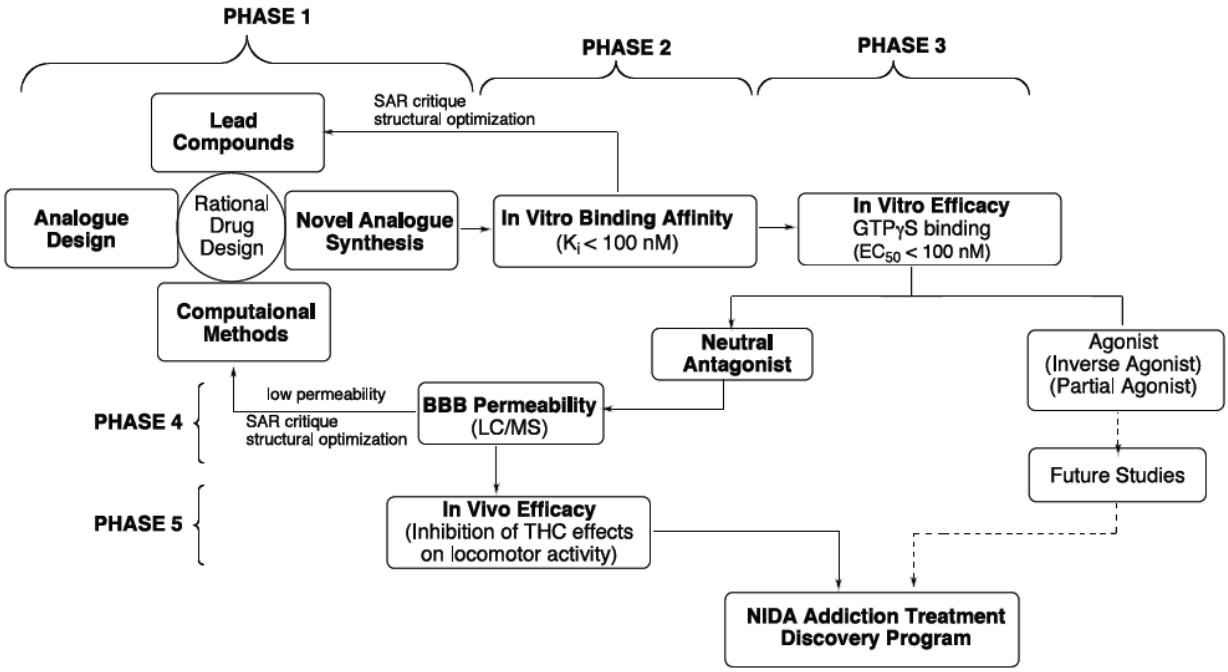

Phase 3 of the study will consist of *in vitro* characterization of compound efficacy and identify CB1 antagonists, agonists, or inverse agonists. As a result of their different action mechanisms and potential therapeutic values, inverse agonists and partial agonists will be directed to another program. Compounds that elicit neutral antagonist efficacy will be advanced to the blood-brain barrier permeability evaluations. Compounds that exhibit good blood-brain barrier permeability will be advanced to *in vivo* evaluation of antagonist efficacy. Compounds with poor blood-brain permeability

will be re-evaluated in the rational drug design process to improve their physical properties to improve permeability.

Finally, Phase 5 will establish *in vivo* antagonist activity for compounds that have met the goals of *in vitro* efficacy and blood brain permeability. Those compounds that exhibit good *in vivo* antagonist efficacy will be submitted to the National Institute of Drug Abuse and serve as a lead compounds in future studies aimed at developing them further as drug abuse medications. The various phases of the program all go simultaneously with each phase contributing to the refinement of the ligand structure.

After the novel triazole derivatives are synthesized and their binding affinities are determined, compounds that exhibit potent (K_i values < 100 nM) receptor affinity will be evaluated *in vitro* functional assays to identify compounds with antagonist activity. Antagonist efficacy will be determined by blockade of effects of **Δ^9-THC** on [^{35}S] GTP$_\gamma$S binding. CB1 receptor agonist inhibit cAMP production through inhibition of adenyly cyclase, inhibit Ca^{+2} influx, activate K+ channels and activate MAP kinase pathways. CB1 antagonists block stimulation of [^{35}S]GTP$_\gamma$S binding and block the inhibition of

adenlyl cyclase activity. A neutral CB1 antagonist will not exhibit inhibition of [^{35}S]GTP$_{\gamma}$S binding, while antagonizes the effects of CB1 agonists.

Compounds identified above that exhibit most promising pharmacological profiles as antagonists will be evaluated *in vivo* for the following:

(a) Blood Brain Barrier permeability, where the ability to cross the blood brain barrier will be determined in rats using LC/MS.

(b) Blockade of agonist effects, where the antagonist activity of the compound with good blood brain barrier permeability will be further established by evaluating for their ability to inhibit the effects of **Δ^9-THC** on locomotor stimulations in rats.

In reviewing the literature about CB1 receptor antagonists, it was noticed that the 1,2,3-triazole analogs were absent from the pool of **SR141716A** bioisosteric analogs. The initial design of the target compound in our laboratories was based upon prototypical structure of **SR141617A** and its related compounds discussed in the literature. The design rationale was to incorporate the 1,2,3-triazole ring with the vicinal diaryl system. This led to the compound **22** (Figure 20).[58]

Figure 22. Preliminary computational study

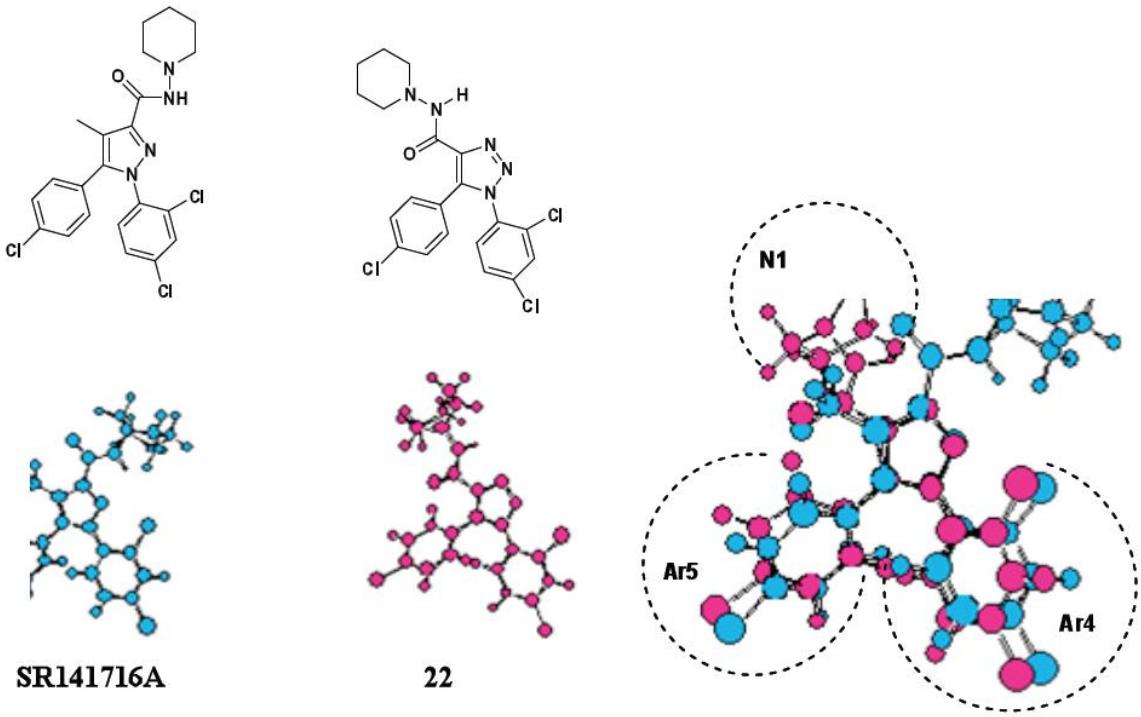

This design was supported by preliminary computational study. As illustrated in Figure 22, for the AM1 geometry optimized structures, a 1,2,3-triazole ring in **2** could replace the pyrazole ring and provide good overlap with **SR141716A** in the diaryl groups which was believed to be the molecular region binding to CB1 receptors. It was not clear at that time how the juxtaposition of the alignment of the carboxamide moieties of **22** relative to **SR141716A** would affect molecular recognition at CB1 receptors.

Molecular modeling studies reported for analogs of **SR141716A** had suggested that

increased steric bulk at C4 could be tolerated. This suggested that the carboxamide at C4 of **22** may not have detrimental effect on CB1 binding.

Scheme 1. Synthesis of azide by Cu(I)I.

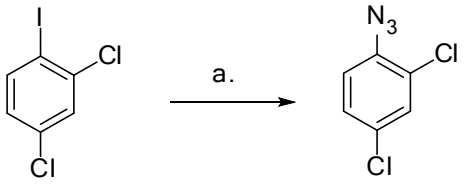

23a **24**

Reagents and conditions: a) NaN_3, Sodium ascorbate, CuI (10% mol), *trans*-1,2-di(aminomethyl)-cyclohexane ligand (15 mol%), DMSO/H_2O, 100 ºC, 2 h, 54% yield. [68]

The Ullmann-type of conversion iodobenzene catalyzed by CuI with *trans*-1,2-di(aminomethyl)-cyclohexane as ligand (Scheme 1) worked efficiently on 2,4-dichloroiodobenzend with a 54% yield from 2,4- dichloroiodobenzene.[58,68]

While the reaction can be performed using commercial sources of copper (I) such as cuprous bromide or iodide, the reaction works much better using a mixture of copper (II) (e.g. copper(II) sulfate) and a reducing agent (e.g. sodium ascorbate) to produce Cu(I) in situ.

As Cu (I) is unstable in aqueous solvents, stabilizing ligands are effective for

improving the reaction outcome, especially if tris-(benzyltriazolylmethyl)amine (TBTA) is used. The reaction can be run in a variety of solvents, and mixtures of water and a variety of (partially) miscible organic solvents including alcohols, DMSO, DMF, ^{t}BuOH and acetone.

Owing to the powerful coordinating ability of nitriles towards Cu(I), it is best to avoid acetonitrile as the solvent. The starting reagents need not be completely soluble for the reaction to be successful. In many cases, the product can simply be filtered from the solution as the only purification step required.

Furthermore important to the target selection was that computational logP (*C*log*P*) values for the 1,2,3-triazole derivatives typically exhibited a trend of improved lipophilicity over corresponding pyrazole or 1,2,4-triazole isomers of similar substitution and functionality.

Although the *C*log*P* values may vary from actual logP values, this trend of decreased lipophilicity was encouraging for us to move forward. Based on this analysis, the 1,5-diaryl-1,2,3-triazole was identified as an initial target for synthesis.

Scheme 2. Synthesis of initial target carboxamide analogue **22.** [68]

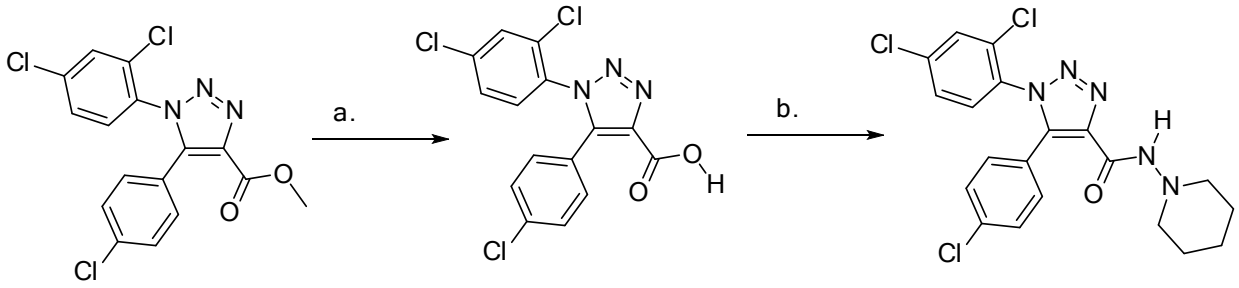

30a **22i** **22**

Reagents and conditions: a) KOH, MeOH, reflux; b) DIPEA, HBTU, CH_3CN, 1- aminopiperidine, 94% yield. [68]

To synthesize the target carboxamide analogue **22**, the carboxylic acid was proposed as an intermediate from which the carboxamide could be synthesized through a straightforward amidation (Scheme 2). The methyl ester **30** was synthesized by capuring the 4-magnesio-1,2,3-triazole with methyl chloroformate and concomitant hydrolysis gave the 1,5-disubstituted-1,2,3-triazole-4-carboxylic acid in a good yield.[68]

As shown in Figure 23, the X-ray crystallographic analysis of 4-methoxycarbonyl-1,5-diaryl-1,2,3-triazole served to confirm the regioselectivity of the cycloaddition reaction and unequivocally established the regiochemistry of the 1,2,3-triazole ring system.

After this confirmation the compounds were characterized further and submitted for binding affinity studies.

Figure 23. ORTEP Drawing of 4-methoxycarbonyl-1-(4-chlorophenyl)-5-(2,4-dichlorphenyl)- 1,2,3triazole **30a**.[55]

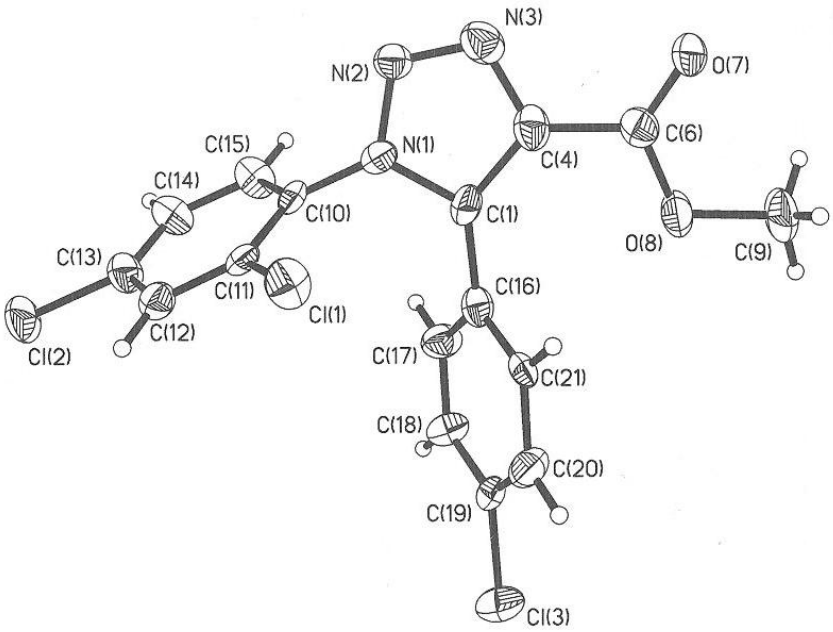

As illustrated in Table 2, the binding affinities for CB1 receptors of the three 1,5-diaryl-1,2,3-triazoles were determined *in vitro* by displacement of [^{3}H]**SR141716A** for CB1 receptors in rat brain. The K_i values summarized in Table 2 indicate that the initial **SR141716A** analogue carboxamide **22** exhibited only modest binding for CB1 receptors (K_i = 590 nM). The C4-unsubstituted analogue **36a** exhibited only micromolar affinity for CB1 receptors and was even less potent than the bulky carboxamide. It is suggested that substitution at the C-4 position of the 1,2,3-triazole ring is favorable for CB1 receptor binding and structural modification at this position may lead to compounds with

optimal pharmacological profiles.

Table 2. Preliminary Binding affinities.

Cpd	# K_i (CB1) nM	# K_i (CB2) nM	*$C\log P$	Mol. Wt.
1 (SR-141716)	11.5	1640.0	7.46	463.79
22	590 ± 170	-	5.99	450.75
30a	61 ± 1.1	-	6.26	382.63
31a	4.6 ± 0.012	1916 ± 247	6.21	410.68
36a	1,400 ± 270	-	5.01	324.59
Δ^9-THC	15.3	25.1	4.81	300.44
(6) Anandamide[41]	61.0	1930.0	6.18	347.53
(4) WIN 55,212-2	1.9	0.3	5.37	426.51

[a]All compounds were tested as the freebase.

[b]All values are the mean ±SEM of three experiments performed in triplicate.

[c]Percent inhibition at 10 μM. [d]Percent inhibition at 100 μM.

*The $C\log P$ values were calculated using CS ChemDrawOffice2010.

Inhibition at CB1 and CB2 receptors are determined by [^{3}H]**SR141716A** and WIN 55,212-2 respectively.

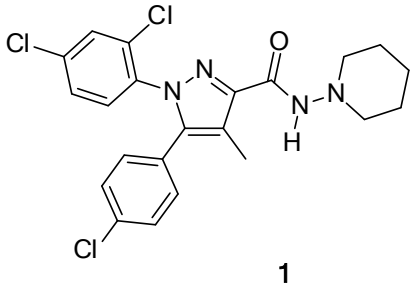

1

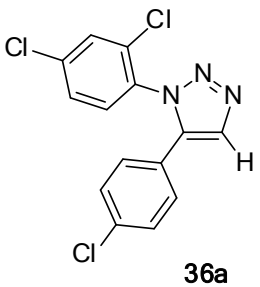

36a

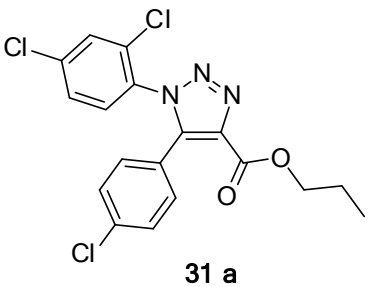

31 a

Anandamide (**6**) which is a strong CB1 agonist exhibits selectivity for CB1 over CB2 with K_i = 61 nM (CB1) and K_i = 1930 nM (CB2).[41] However, it was serendipitous to find that the simple ester analogue **30a** exhibited potent affinity for CB1 receptors. **30a** was roughly 50 times more potent than our originally designed compound **22** and about 6 times less potent than **Rimonabant**.

This prompted us to go on and study the Structure Activity Relationship of the triazole system to understand better the binding motifs of these drugs at CB receptor. And hence, we channeled our energies in synthesizing this new lead compound by substituting substituent with various other groups. With lower lipophilicity and lower molecular weight, we assume they will have better safety profiles.

11. RESULTS AND DISCUSSION

1,2,3-Triazoles are attractive constructs, which because of their unique chemical properties and structure should find many applications in organic, organometalic, and medicinal chemistry as well as in materials chemistry. Not present in natural products, these triazoles are remarkably stable to metabolic transformations, such as oxidation, reduction, and both basic and acidic hydrolysis. Furthermore, 1,2,3-triazole moieties are emerging as powerful pharmacophores in their own right. However, because of lack of convenient direct methods for their synthesis, these aromatic heterocycles have not received as much attention as they deserve.[52]

Known methods for the regioselective synthesis of 1,5-disubstituted- and 1,4,5-trisubstituted-1,2,3-triazoles include reactions of azides with active methylene compounds. Functional groups may also be introduced to the existing 1,2,3-triazole ring by lithiation of the heterocycle followed by reaction with an electrophile. One of the most attractive approaches to the synthesis of 1,2,3-triazoles are 1,3-dipolar cycloadditions of azides and alkynes. Although there are known examples of influencing the

regiochemistry of the addition by the electronic properties of the substrate, they are neither general nor reliable, usually requiring a strong electron-withdrawing substituent on the alkyne.

Metals, such as tin, germanium, or silicon, attached to the acetylenic carbon atom have been shown to give mainly 4-metalated 1,5-disubstituted triazoles. Reactions of sodium, lithium, or magnesium acetylides with organic azides have also been reported.[52] 1,5-Disubstituted 1,2,3-triazoles are the major products of these reactions and the scope of these transformations was investigated by Akimova *et al.* in the late 1960s.[52]

11.1. Synthetic approach for regioselective ring formation

To synthesize the target molecule, the key was to construct the 1,2,3-triazole ring with the right regiochemistry. One of the most attractive strategy for the synthesis of the 1,2,3-triazole ring system was to exploit the 1,3-dipolar cycloaddition reaction of an azide and a terminal alkyne (Scheme 3).[53] The reaction of azides and alkynes to form triazoles was first discovered by O. Dimroth over 100 years ago; however it was Rolf

Huisgen that really capitalized on the usefulness of the reaction. Since then it, along with other forms of click chemistry, have been promoted by K. Barry Sharpless.who has called it the “cream of the crop” of click reactions. The azide alkyne Huisgen cycloaddition combines simplicity with efficiency in a way that is unmatched by most other chemistries.

Finding the copper(I)-catalyzed route to 1,4-disubstituted-1,2,3-triazoles from azides and terminal alkynes highlighted the need for a direct way to achieve the complementary union of the same reactants, namely, one giving the regioisomeric 1,5-triazole analogs. Although Akimova *et al.* had studied such a process over 30 years ago, a citation search turned up no further uses of their nice one-step procedure, likely because of the poor to moderate yields they reported.[52]

A notable variant of the Huisgen 1,3-dipolar cycloaddition is the copper(I) catalyzed variant, no longer a true concerted cycloaddition, in which organic azides and terminal alkynes are united to afford 1,4-regioisomers of 1,2,3-triazoles as sole products (substitution at positions 1' and 4' as shown above). The copper(I)-catalyzed variant

was first reported in 2002 in independent publications by Meldal *et al*. at the Carlsberg Laboratory in Denmark and Fokin and Sharpless *et* a.l at the Scripps Research Institute. The copper(I) catalyzed variant which gives rise to a triazole from a terminal alkyne and an azide, is better termed the Copper(I)-catalyzed Azide-Alkyne Cycloaddition (CuAAC)

Scheme 3. The strategy to synthesize 1,2,3-triazoles

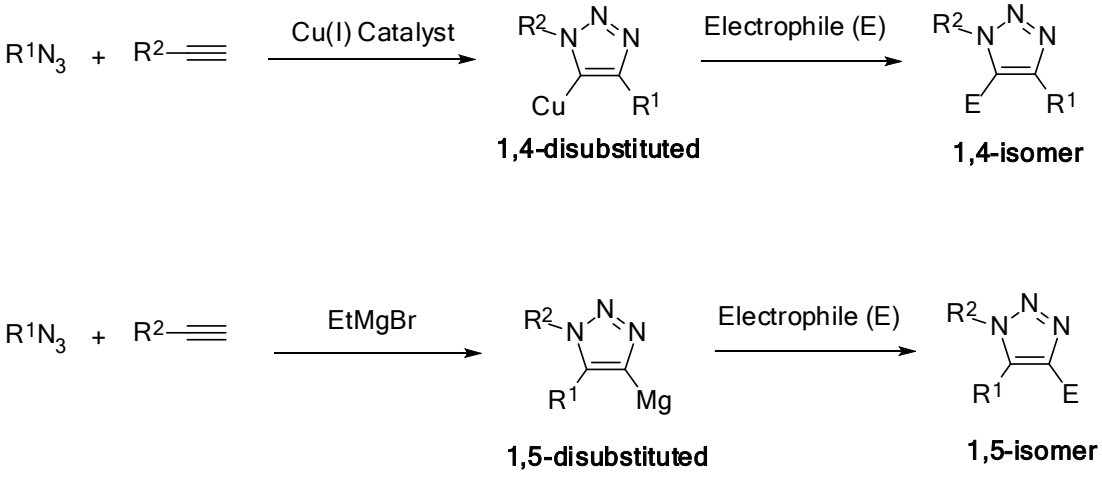

When Cu(I) salt was used as a catalyst for this reaction, the product was 1,4-disubstituted-1,2,3-triazole (Scheme 4). A mechanism for the reaction has been suggested based on density functional theory calculations. Copper is a first row transition metal with the electronic configuration [Ar] $3d^{10}$ $4s^{1}$. The copper (I) species generated in situ forms a pi complex with the triple bond of a terminal alkyne. In the

presence of a base, the terminal hydrogen, being the most acidic is deprotonated first to give a Cu-acetylide intermediate. Studies have shown that the reaction is second order with respect to Cu.[52]

Scheme 4. Copper catalyzed click reaction.

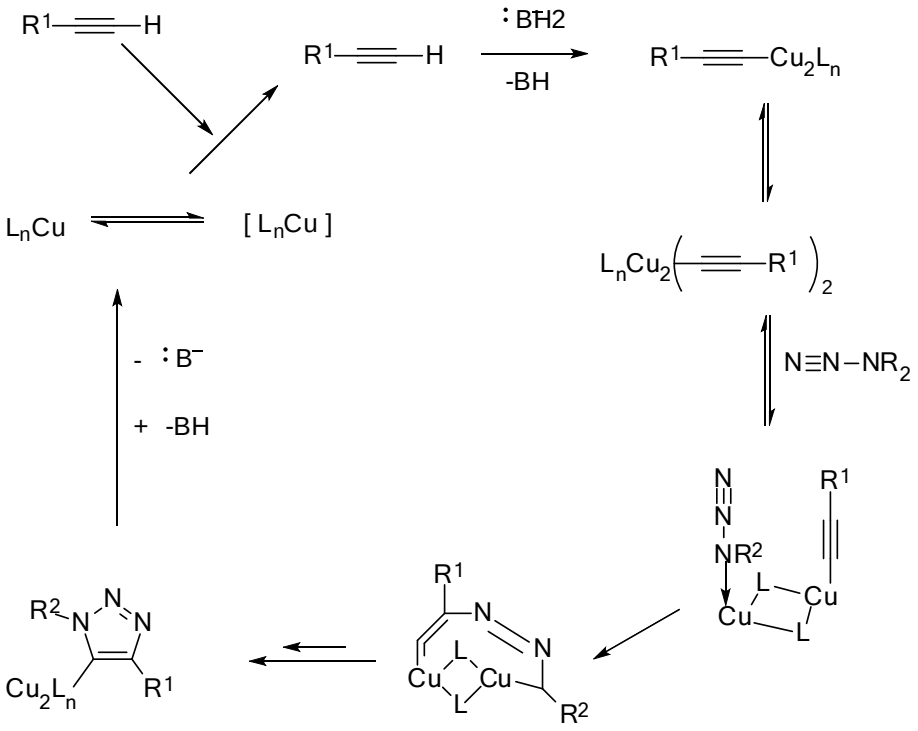

It has been suggested that the transition state involves two copper atoms. One copper atom is bonded to the acetylide while the other Cu atom serves to activate the azide. The metal center coordinates with the electrons on the nitrogen atom. The azide and the acetylide are not coordinated to the same Cu atom in this case. The ligands

employed are labile and are weakly coordinating. The azide displaces one ligand to generate a copper-azide-acetylide complex. At this point cyclization takes place. This is followed by protonation; the source of proton being the hydrogen which was pulled off from the terminal acetylene by the base. The product is formed by dissociation and the catalyst ligand complex is regenerated for further reaction cycles.

An important point to note is that in the uncatalyzed reaction the alkyne remains a poor electrophile and thus high energy barriers lead to slow reaction rates. The reaction is assisted by the copper which when coordinated with the acetylide lowers the pKa of the alkyne C-H by up to 9.8 units. Thus under certain conditions, the reaction may be carried out even in the absence of a base.

However the reaction of magnesium acetylide and a terminal alkyne gave the 1,5-disubstituted-1,2,3-triazole exclusively. This strategy would allow rapid regioselective ring construction of the target molecules and provide suitable intermediates for parallel synthesis of potential analogs.

Azides usually make fleeting appearances in organic synthesis. They serve as one of

the most reliable means to introduce a nitrogen substituent through the reaction. What makes azides unique for click chemistry purposes is their extraordinary stability toward H_2O, O_2, and the majority of organic synthesis conditions.

Despite the azidophobia due to hazards and dangers associated with azide, we have learned to work safely with azides because they are the most crucial functional group for click chemistry endeavors. The spring-loaded nature of the azide group remains invisible unless a good dipolarophile is favorably presented.

However, even then the desired triazole-forming cycloaddition may require elevated temperatures and, usually results in a mixture of the 1,4- and 1,5 regioisomers.

The principal source of the azide moiety is sodium azide. Sodium azide is made industrially by the reaction of nitrous oxide (N_2O), with sodium amide ($NaNH_2$), in liquid ammonia as solvent.

As one the building blocks for the cycloaddition reaction, 2,4-dichlorophenylazide **24** was required to be synthesized. Unlike the preparation of alkyl azides, there are only few effective methods available for the synthesis of aryl azides.

Scheme 5. Synthesis of azide.

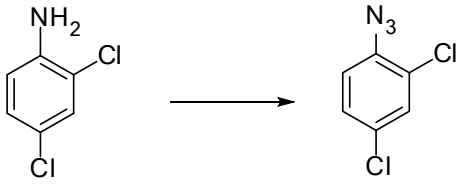

23b **24**

Reagents and conditions: $NaNO_2$, H_2O:HCl, NaN_3, 0 ºC; 2.5 h; 90% yield.

Aryl azides were generally synthesized by diazotization of aryl amine followed by the treatment of sodium azide (Scheme 5).[54] All the reagents required for the synthesis of azide in this reaction were commercially available and the reaction could be conducted on a gram-scale. This gave us yields more than 85% most of the times and the azide formed would be very pure based on thin layer chromatography analysis as well as based on proton NMR-spectra. We have to be careful while doing the synthesis of aryl azides. It is often preferred that the diazonium salt remains in solutions, but they do tend to supersaturate. Operators have been killed and injured by an unexpected crystallization of the salt followed by its detonation. The nucleophilic aromatic substitution reaction of azide synthesis proceeds with the usual diazotization method as shown in Scheme 6. This mechanism is a substitution reaction in organic chemistry in

which the nucleophile displaces a good leaving group, on an aromatic ring

Scheme 6. Synthesis of diazonium solution and the S_NAr (addition-elimination) mechanism for aryl azide synthesis.

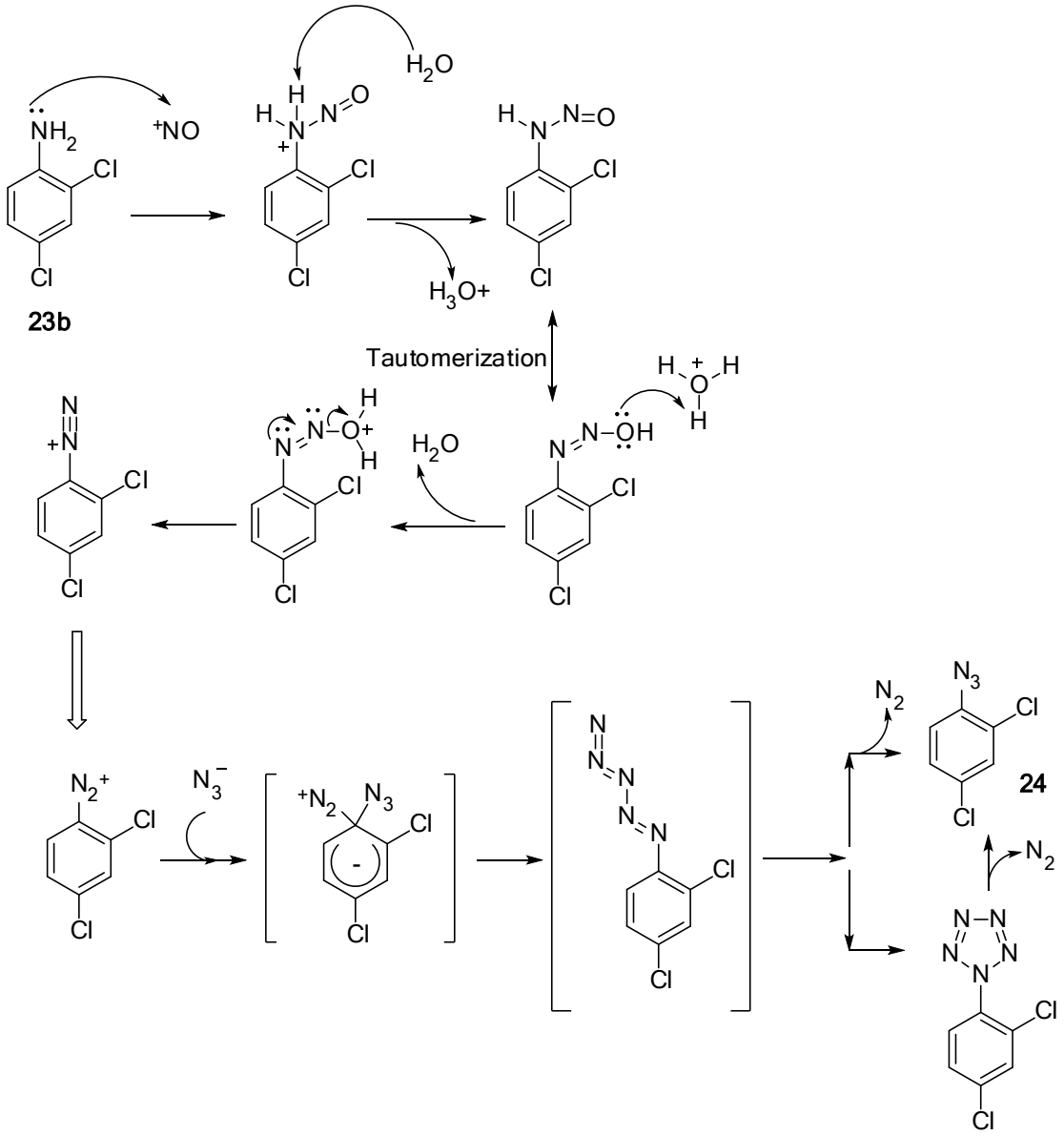

On basis of N-isotope labeling studies and kinetic studies of nitrogen evolution, Huisgen and Clusius proposed two probable mechanisms for azide formation.[55] Both of

these proposed mechanisms shown in Scheme 6 are second order rate reactions. Rate-determining step of the reaction is the attack of azide ion on the diazonium ion.

A careful observation led to the fact that this azide had to be prepared fresh for next reaction step to go well. A three day old azide would give lower yields while forming the 1,2,3-triazole as compared to the freshly made azide sample to synthesize the triazole ring which would result in better yields. The conformation of Grignard reagents in ethereal solutions is influenced by a dynamic equilibrium, the Schlenk Equilibrium between several species (Scheme 7). In diethylether and tetrahydrofuran all of these species are present, although the Grignard reagent R-MgX dominates.[55]

Scheme 7. Conformation of Grignard reagents in ethereal solutions.

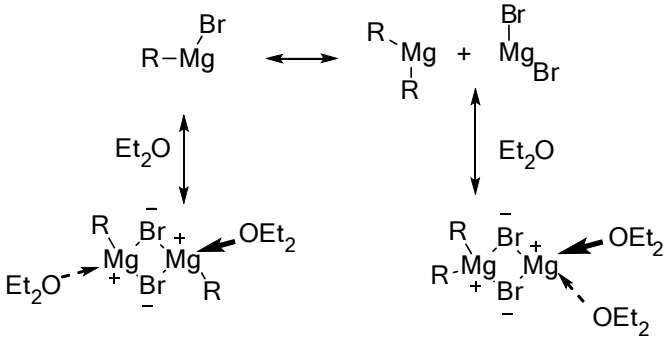

In 1,4-dioxane the equilibrium can shift towards the dialkyl-magnesium12 species because the magnesium-halides form insoluble complexes with 1,4-dioxane and are

removed from the equilibrium. In diethylether the Grignard reagents form monomers when the halogen is bromine or iodine, and dimers when the halogen is chlorine or fluoride. In THF all or these species are predominantly monomeric.The solid state structures of Grignard reagents are often monomeric or dimeric structures with a tetrahedral coordination of the magnesium, whereas solvent free Grignard reagents are often polymeric.

Grignard reagents are soluble in a number of aprotic solvents, using oxygen or nitrogen as donor-atoms to form complexes with the magnesium. Compared with alkyllithium compounds the Grignard reagents are less basic, and solutions in ethers are stable at room temperature or even higher. On the other hand a cooled solution of Grignard reagents tends to form precipitates which are very difficult to re-dissolve. A storage temperature around room temperature is suitable and recommended for most compounds

The proposed mechanism of the cycloaddition reaction is illustrated in Scheme.8.[52] The reaction begins with the nucleophilic attack of the acetylide on the terminal nitrogen

of the azide to form a linear intermediate which spontaneously closes to give the 4-metallotriazole species **25*Mg*** which leads to formation of 1,5-disubstituted-1,2,3-triazole **26*E*** when treated with an electrophile.

Scheme 8. Synthesis of triazole ring via an asynchronous transition state.

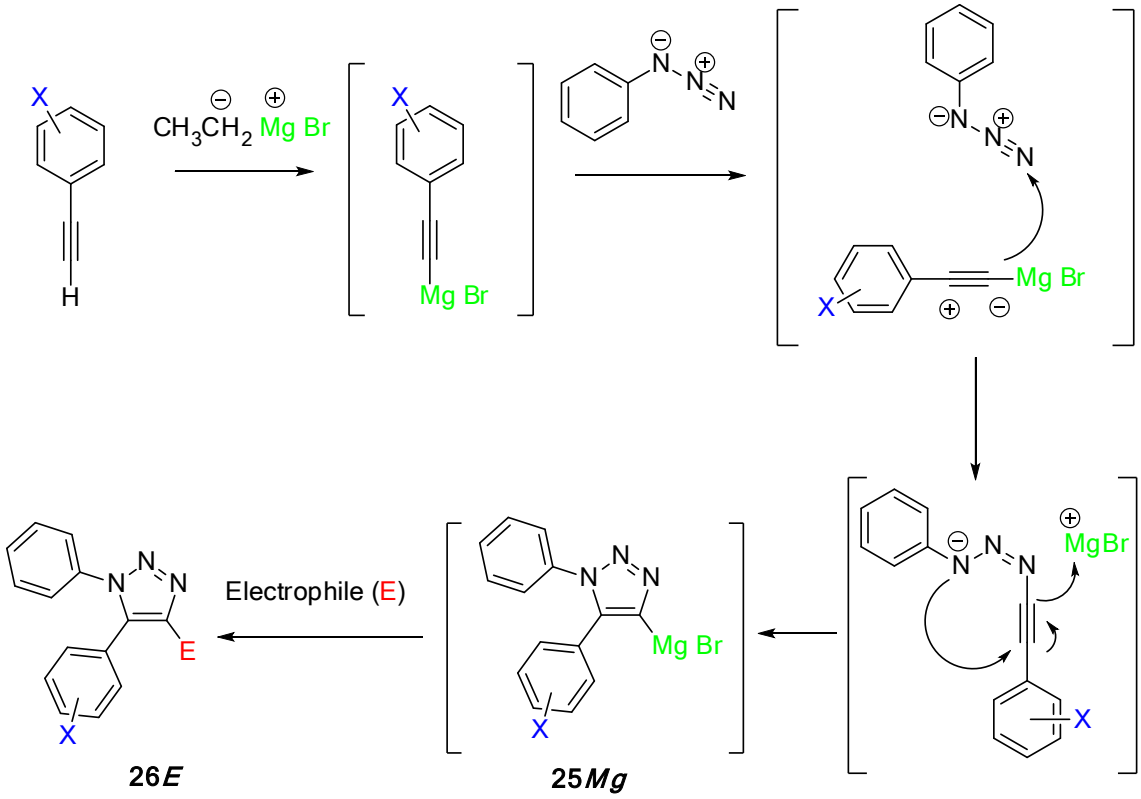

26*E* **25*Mg***

The reaction of the bromomagnesium acetylides with a suitable electrophile (E) gave, preferentially the 1,4,5-trisubstituted triazoles **26*E***. Electron poor azides reacted faster than electron rich ones, an observation consistent with the proposed nucleophilic attack

of the acetylide on the azide.

An interesting point to observe is that compared to all the other methodologies that we tried to synthesize the desired regioselective 1,5-diaryl-4-substituted-1,2,3-triazole, these one pot reactions resulting in 3 to 4 new bonds are generating modest to good yields. We are getting several reactions done at once and hence, these reactions are quite efficient in terms of utility of these click reactions. The yields reported here are not optimized because our main aim was to synthesize these regioselective 1,2,3-triazoles. Once we got a triazole analog, we wanted to try and identify it first in terms of binding affinity values and then we wanted to decide whether or not it's worth going back to that reaction.

As has been studied in our laboratories, substituent on the 3-position on the aryl of the carbon-5 of triazole (**30h, 30i, 30j, 31j, 31k, 31l**) gave much better yields (60-90%) as compared to triazoles with substituent on the 3-position on the aryl. It may be attributed to the fact that the substituent on the 3rd position of the aryl of aryl acetylene is draining electrons from the triple bond to a lesser extent. This is making the electrons

of the acetylene more available for the nucleophilic attack of the acetylide.

Scheme 9. Proposed mechanisms of side products during 1,2,3-triazole formation where M= Li or MgBr.

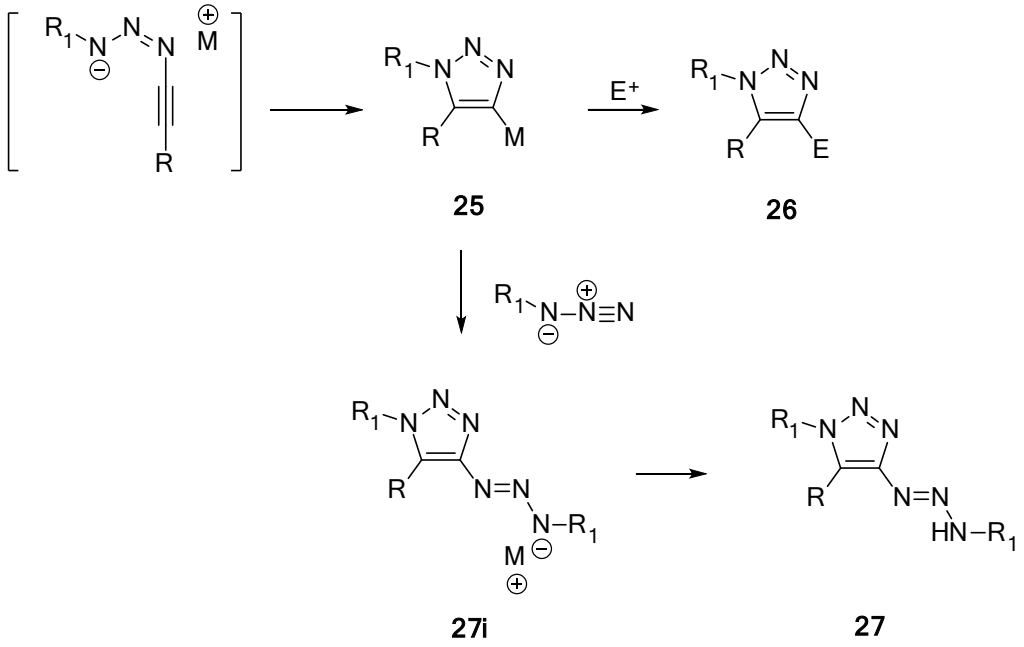

Although the reaction is usually fast and clean, several traces of by products can be observed leading to low yields of the desired **26*E*** triazoles (Scheme 8). Without strict exclusion of oxygen, these reactions can result in oxidative couplings. In the presence of excess azide over the acetylide as well as extended reaction times, the intermediate 4-metallotriazole **25** reacts with the second azide and gives the side product **27**

(Scheme 9).

Formation of byproduct was reported in some cases along with unreacted starting materials. On the other hand, the use of lithium acetylides favored further attack by intermediate **25** on a second molecule of azide, resulting upon hydrolysis, in the 4-triazene-substituted triazoles **27**, often in high yields.

Scheme 10. General synthesis scheme of triazole compounds via click chemistry.

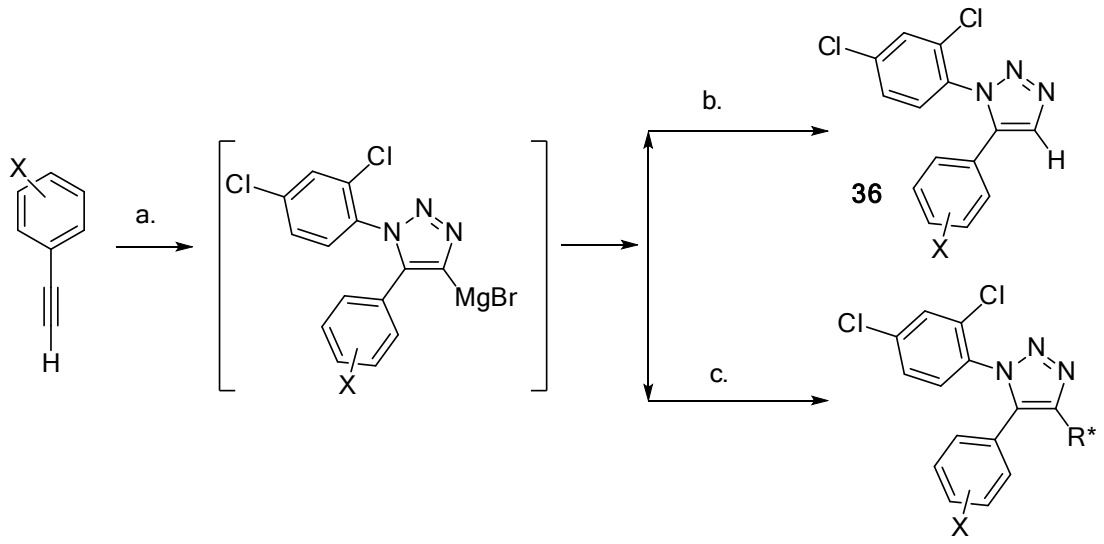

Reagents and conditions: a) EtMgBr, THF, rt-addition, 50 °C, 1 h; Azide **24**, THF, 50 °C, 2 h; b) 1 N NH_4Cl; 0 °C, 1 h c) ClR* (R*= Carbonyl, Alkyl group), THF, -20 °C, 3h;

To monitor the process of the one-pot three-step reaction and to optimize the yield for this reaction, the cycloaddition adduct was first directly treated with aqueous NH_4Cl solution. The evaluation of the resulting 4-unsubstituted analogs provided important

SAR information about the effects of substitution at this position on the binding of 1,2,3-triazoles to CB1 receptors.

The best yield of 1,2,3-triazole ring (85%) was obtained when freshly made azide in THF was added to the acetylide and was heated for a maximum of 2 hours at 50°C with a small amount of acetylene remaining unreacted. Excessive azide or extended reaction times led to decreased yields due to the addition of a second molecule of azide to the 4-magnesio-1,2,3-triazole.

This result validated the previous hypothesis that 1,2,3-triazole ring was suitable replacement for pyrazole ring in **SR141716A**. It also indicated that an amide moiety at C4-position was not essential for high binding at CB1 receptors, which updated the SAR information based on previous studies on other bioisosteric **SR141716A** analogs. More important for the future studies, it provided a very promising compound as a new lead compound.

Compared with the target analog (**22**) and even **SR141716A**, methyl ester **30a** had a few desirable pharmacological features (Table 2). First of all, it is near one order of

magnitude more potent than the target compound and its K_i value was already in the same range with that of **SR141716A**. It also has a significantly smaller molecular weight than those of **22** and **SR141716A**.

Scheme 11. Synthesis of triazole esters.

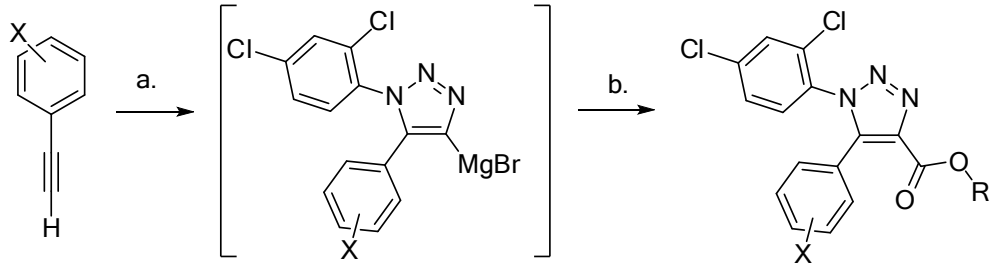

30, R = Me
31, R = Pr
32, R = Ph

Reagents and conditions: a) EtMgBr, THF, rt-addition, 50 °C, 1 h; Azide, THF, 50 °C, 2 h, 98% yield; b) $ClCO_2R$, THF, -20 °C, 3 h,

It has a much lower *C*log*P value* than that of **SR141716A.** Although the measurement of ligand half-lives is not part of this study, the development of an ester-based ligand would be an important step toward the development of shorter acting cannabinoids with better safety profiles.

Therefore methyl ester **30a** was identified as a new lead compound for further studies in the development of 1,2,3-triazoles as CB1 antagonists. Since alkyl chains longer than

three carbons were not showing conclusive results we decided to stick to a maximum of five carbons on the electrophile.

More importantly, the ester moiety may lead to a significant increase in compound metabolism since esters are typically more readily hydrolyzed than amides *in vivo*. This is extremely important in lieu of the long half-lives typically observed for cannabinoids. Ester derivatives will undoubtedly be more susceptible to metabolism and have shorter duration of action than amide or hydrazide analogs.

As illustrated in Scheme 10, a series of 1,2,3-triazole analogs with varying groups were prepared to investigate how lipophilicity and steric effects affect the binding of the ester to CB1 receptors. They were synthesized using the procedures described earlier for the methyl esters. The 4-magnesio-1,2,3-triazole intermediate was captured with a number of electrophiles. Since alkyl chains longer than three carbons were not showing conclusive results we decided to stick to a maximum of five carbons on the alkyl chloroformates and alkonyl chlorides.

Each of the analogs could be synthesized in gram-scale. But since only a small

quantity of product was required for the binding assay studies, only the cycloaddition reaction was conducted in a gram-scale.

Scheme 12. Synthesis of triazole ketones.

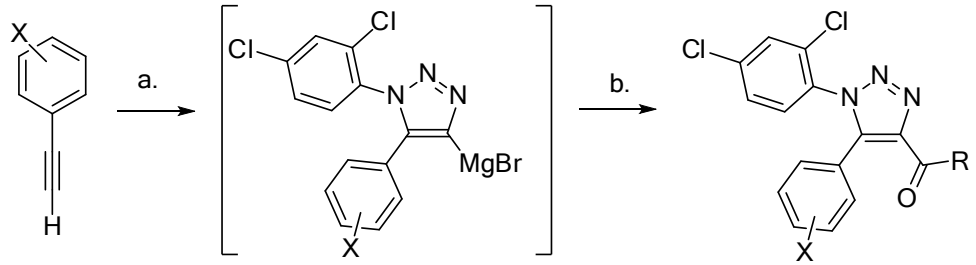

33, R = Et
34, R = Pr
35, R = Et

Reagents and conditions: a) EtMgBr, THF, rt-addition, 50 °C, 1 h; Azide, THF, 50 °C, 2 h; b) ClCOR, THF, -20 °C, 3 h;

The the solution of cycloaddition adduct in THF was separated into a number of portions and each portion was treated with a different commercially available chloroformates to provide the corresponding 4-alkoxycarbonyl-1,5-diaryl-1,2,3-triazole. Since our yields were not as high as expected, we tried to solve the problem by characterizing all the side products.

For example, when we attempted to synthesize 1,5-diaryl-1,2,3-triazole-4-propyl ester (**31b**) in high yields under rigorous inert conditions, we observed compound **39** was one

of the most prevalent side product in that 4-propyl ester derivative 1,2,3-triazole formation reaction (Scheme 13) along with the 4-unsubstituted triazole **36** which is inevitable to form along these reactions.

Scheme 13. Early attempt to synthesis of 1,5-diaryl-1,2,3-triazole-4-propyl ester

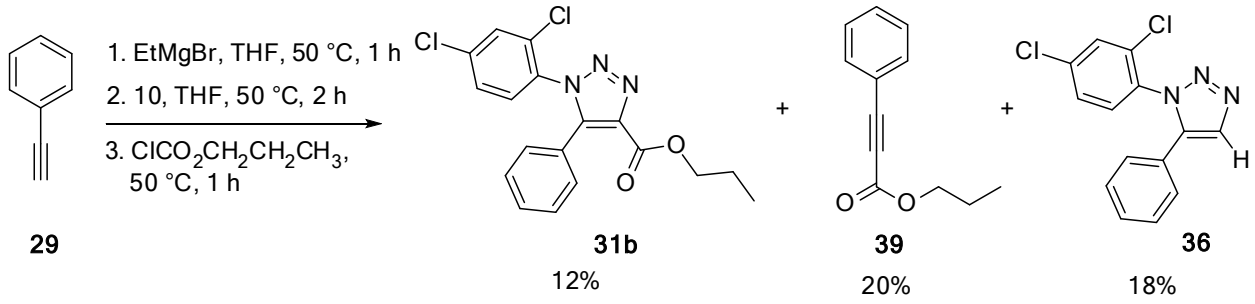

During our initial attempts to synthesize triazole rings, we came across a publication by Hlasta and Coats[54] where in they had described a solid-phase synthesis of 1,2,3-triazoles as shown in Scheme 14 in reasonably good yields.

Scheme 14. Solid phase synthesis of 1,2,3-triazoles.

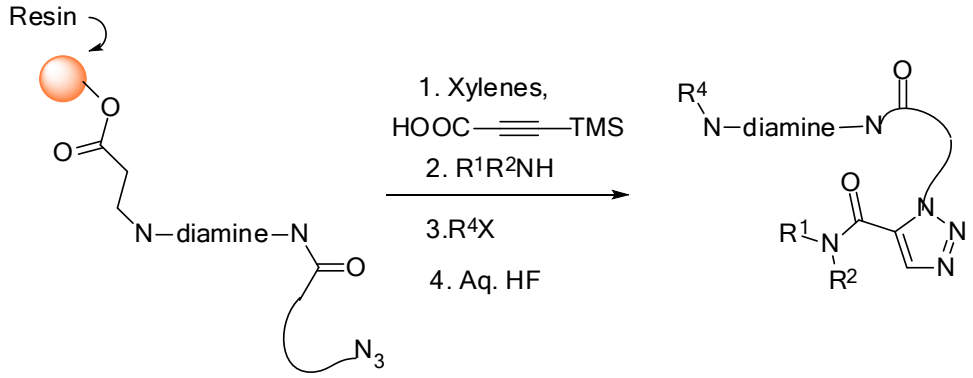

Taking advantage of the formation of side product **39** in Scheme3, it occurred to us that even this reaction mentioned in Scheme 14. would be regioselectively forming the 1,5-diaryl-1,2,3-triazole systems as shown in Figure 24 because of the umplong effect of **40** similar to that of **41**.

Figure 24. Similarity of umplongs.

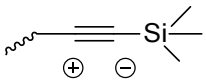

40

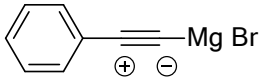

41

We also tried to synthesize triazole derivatives with trimethylsilyl groups on carbon-4 to explore these systems (Scheme 15).

Scheme 15. Synthesis of trimethyl silanes.

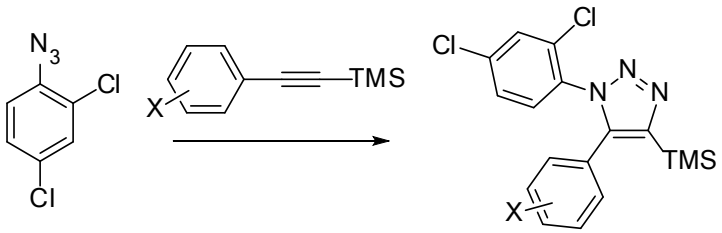

24 **37**

Reagents and conditions: a) Toluene, 110 °C, 19 h;

Based on a publication by Kim *et al*. we tried a coupling method for the synthesis of

ester as is shown in Scheme 16 to develop another method of formation of triazole ring derivatives and if possible, in high yields.[54]

Scheme 16. Synthesis of triazole ring by coupling methods.

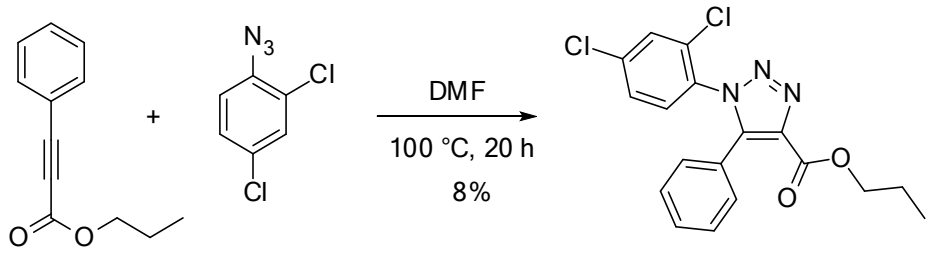

39 **24** **31b**

Even though the proton and carbon NMR peaks of both the propyl esters synthesized by Scheme 11 and Scheme 16 matched, we did not have the crystallographic data to prove the correct regiochemistry. Moreover, our original click chemistry method for the formation of 1,2,3-triazoles, still generated more yields and so we decided to abandon this coupling technique altogether.

We also incorporated an iodo atom on the carbon-4 position of the triazole system. It can not only be used as a handle for replacement of other bulky groups as is shown in Scheme 17, it was very stable also. It could be stored in the refrigerator and was not necessary to prepare fresh as was the case with phenyl azide (**24**). The 1,3-dipolar

cycloadditon reaction of azide **24** and the desired phenyl alkyne gave a 4-magnesio-1,2,3-triazole intermediate which was treated with elemental iodine giving **38.**

Scheme 17. Synthesis of triazole iodides.

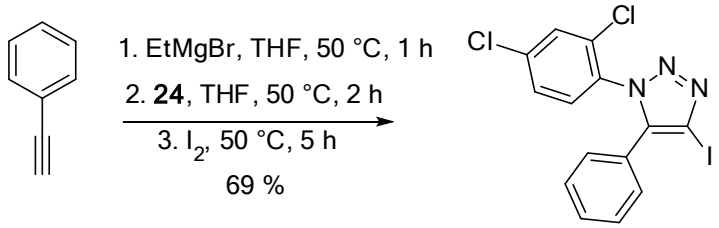

29 **38**

Even though we obtained good yields for **38**, our multiple attempts to replace the iodo group with desired electrophiles using *n*-butyl lithium as well as *t*-butyl lithium reagent either did not afford good yields (Scheme 16) or did not generate the required substitution on the triazole system (Scheme 18).

Scheme 18. Synthesis of **31b** by replacing the iodo group on carbon-4 of the triazole.

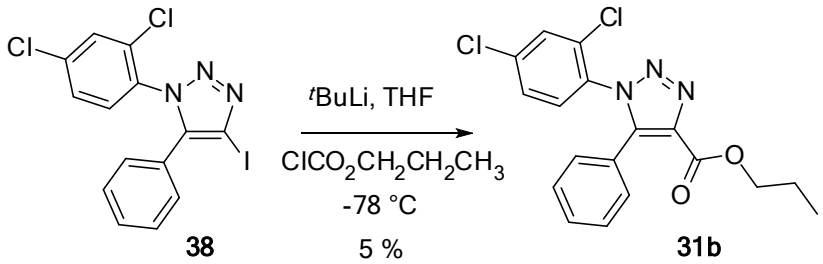

38 **31b**

Another method we tried, to increase the yields of the 1,5-diaryl-1,2,3-triazole was

lithiation of the iodo group followed by the nucleophilic addition to desired alkyl chloroformates as is shown in Scheme 19.

Scheme 19. Synthesis of triazole derivatives by replacing the iodo-group.

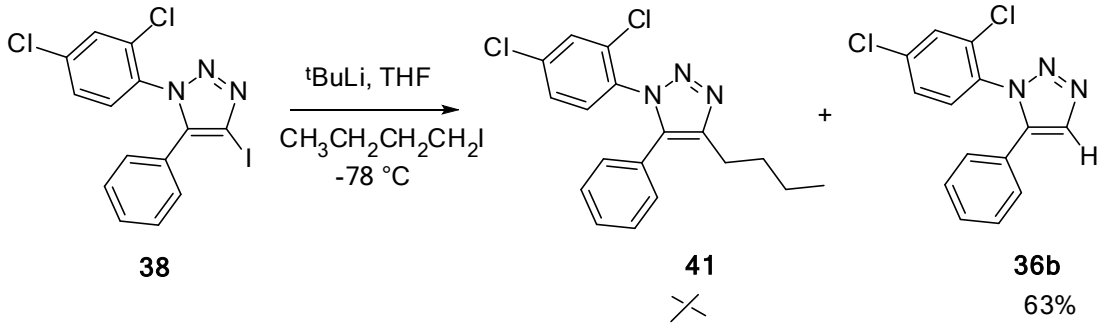

38 **41** **36b** 63%

However the yields observed were even lower than our original method of Scheme 10. Characterization of compound **31b** synthesized by the lithiation method in Scheme 19 was done by ^{1}H-NMR, ^{13}C-NMR as well as by thin layer chromatography and comparing the results with the same compound synthesized via the Scheme 10 whose regiochemistry we had confirmed with crystallographic methods.

Our low yields were also confirmed by the extensive studies performed by Akimova *et al*, in which a wide variety of azides and lithium acetylides were employed.[52] Formation of byproduct **27** (Scheme 9) was reported in some cases along with unreacted starting

materials. The reaction of the bromomagnesium acetylides with azides gave, after hydrolysis, preferentially the 1,5-disubstituted triazoles **36** (Scheme 10); however, the yields were low. On the other hand, the use of lithium acetylides favored further attack by intermediate **25** on a second molecule of azide, resulting upon hydrolysis, in the 4-triazene-substituted triazoles **27**, often in high yields.

In an attempt to improve yield of propyl ester **31b**, transesterification method as employed in our laboratories previously[58] was also employed by the procedure as reported by Shu *et al*, we tried to replace the methyl group of the methyl ester of compound **30b** by 1-prapanol.

Scheme 20. Transesterification of methyl ester **30b** to **31b**.

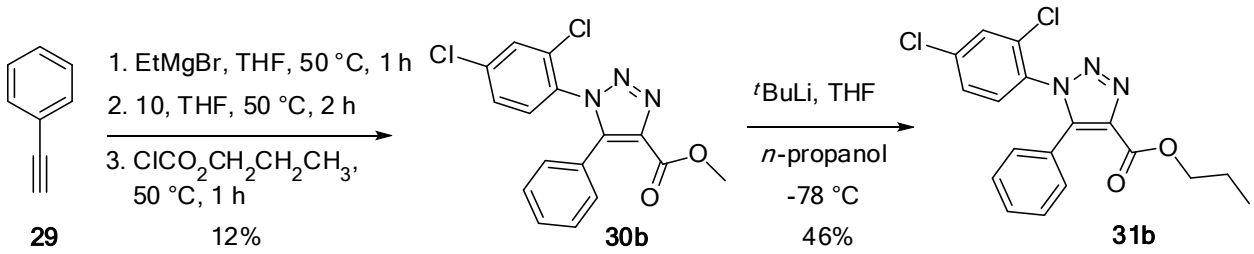

Even though the transesterification method (Scheme 20) gives fairly decent yields, the overall yield of 6% was much less than the ones we are getting by the usual 1,3-dipolar cycloaddition method for the direct synthesis of **31b** from **29**.

Another class of derivatives that we wanted to synthesize and do structure activity relationship studies were sulfonyl substituents at the carbon-4 position of the 1,2,3-triazoles (Scheme 21).

Scheme 21. Attempt to synthesize sulfonyl derivatives.

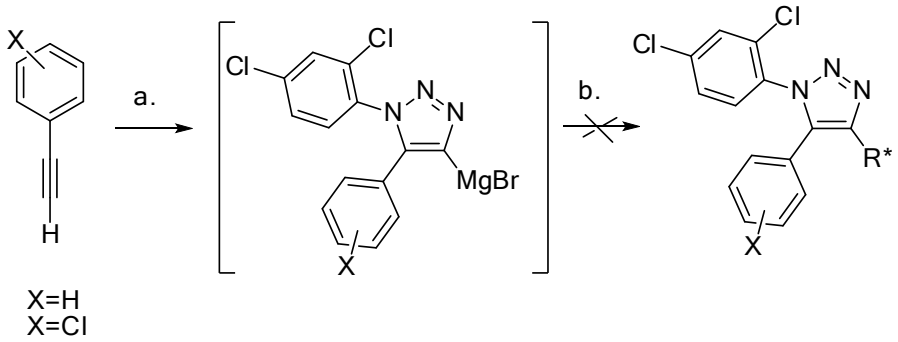

Reagents and conditions: a) EtMgBr, THF, rt-addition, 50 °C, 1 h; Azide **24**, THF, 50 °C, 2 h; b) 1-propane sulfonyl chloride (R* = $SO_2CH_2CH_2CH_3$), THF, -20 °C, 3h;

With this aim, we started with the desired arylacetylene derivative dissolved in anhydrous tetrahydrofuran and ethyl magnesium bromide was added to it dropwise under inert conditions. After heating this mixture for 1 hour, the 2,4-dichlorophenyl azide (**24**) dissolved in THF was added to it and heating was continued for another hour. Followed by this, our reaction mixture was added to 1-propane sulfonyl chloride which was cooled to below zero temperature.

Nonetheless, we faced failure to synthesize these sulfonyl derivatives which was also

validated by a study done by Sharpless *et al* [52] where it was found that the use of sulfamoyl and sulfonyl chlorides results in partial chlorination of the triazole ring at C-4. Hence the sulfonyl derivatives are not suitable for these electrophilic capture processes.

Another type of electrophile that we wanted to trap at the C-4 position of the triazole ring was an amide (Scheme 22). Though, it was not conclusive at our hands, nonetheless, intermediates like **39n** were found. However, except a proton and carbon NMR, **39n** and other byproducts were not characterized further.

Scheme 22. Reactions with isocyanates as electrophiles.

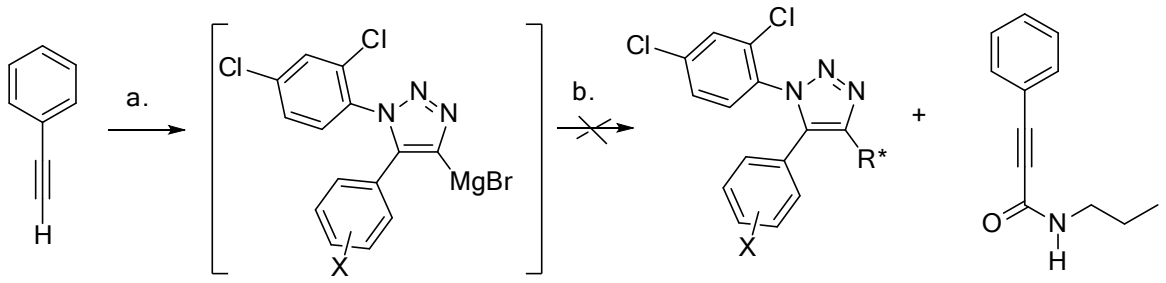

Reagents and conditions: a) EtMgBr, THF, rt-addition, 50 °C, 1 h; Azide **24**, THF, 50 °C, 2 h; b) Propyl isocyanate (R*= $CONHCH_2CH_2CH_3$), THF, -20 °C, 3h;

We also wanted to try using elecrophiles other than alkyl chloroformates and alkyl chlorides to be used for substituting the C-4 position of the triazole ring. For this purpose we tried 2,2,3,3,4,4,4-heptafluorobutanoic anhydride. This anhydride would

also help place a 4-carbon fluorinated alkyl chain at the 4th position of triazole which would make an interesting analog for structure relationship study as compared to other compounds (Scheme 23). Nonetheless, it was formed in a very small amount with 4-chloro phenyl acetylene and in trace amounts with phenyl acetylene. It was very difficult to purify because of its acidic nature and high polarity, due to which we were not able to characterize it.

Scheme 23. Synthesis of triazole derivatives using anhydride as electrophile.

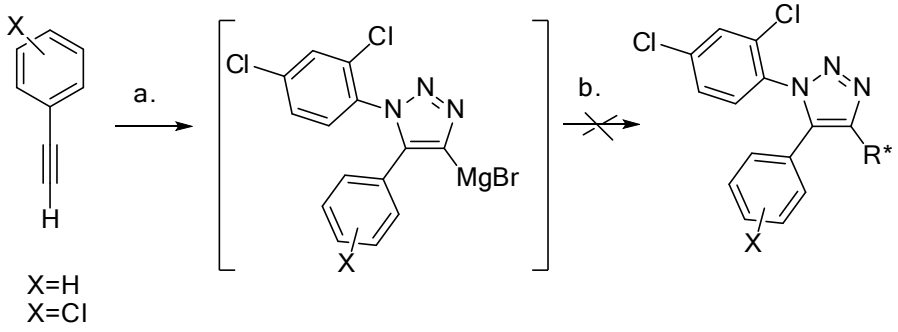

Reagents and conditions: a) EtMgBr, THF, rt-addition, 50 °C, 1 h; Azide **24**, THF, 50 °C, 2 h; b) 2,2,3,3,4,4,4-heptafluorobutanoic anhydride (R*= $COCF_2CF_2CF_3$), THF, -20 °C, 3h;

Inspired from the structure of AM251, we also wanted to synthesize the analogs with the iodo group on the aryl on carbon-5 of the triazole ring (Scheme 24). Since compound **43** was not easily available commercially, we decided to prepare it by using

Holmes *et al* method.[54] This method gave us very good yields for compound **43** which we would prepare fresh for its use in triazole ring formation of compound **31i** as is shown in Scheme 11.

Scheme 24. Attempt to synthesize **31i**.

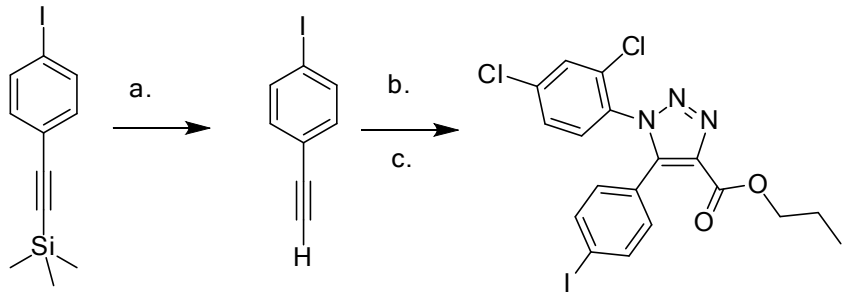

42 **43** **31i**

Reagents and conditions: a) KOH, CH_3OH/CH_2Cl_2, rt, 2h; b) EtMgBr, THF, rt-addition, 50 °C, 1 h; Azide **24**, THF, 50 °C, 2 h; c) Propyl chloroformate, THF, -20 °C, 3h;

However, this propyl ester triazole **31i** kept degrading with time and with every consequent column as well as preparative purification. Only a decent ^{1}H-NMR could be done for characterization since due to large quadrupole moment of iodine (^{127}I) high-resolution spectra could not be obtained.

It was initially envisaged, that by maintaining the diaryltriazole core scaffold we could achieve compounds with high potency at the CB1 receptor. However, by shifting the position of the ester moiety relative to the carboxamide linkage of **1** interaction at the

binding site would be weakened to furnish compounds with diminished efficacy. This strategy has been successful in several recent studies, providing neutral CB1 antagonists.[56,57]

The heterocyclic aromatic iodide **38** was attempted to convert into the 1,4,5-triphenyl-1,2,3-triazole through Suzuki cross coupling reaction with 2,4-dichlorophenylboronic acid by the methodology developed by Fu and coworkers (Scheme 25) and as reported in our laboratories by Murali *et al*.[72]

Scheme 25. Attempt to synthesize 1,4,5-triphenyl-1,2,3-triazole.

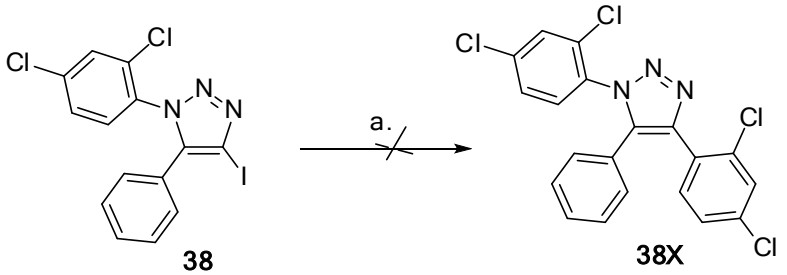

38 **38X**

Reagents and conditions: a) 2,4-Dichlorophenylboronicacid, $Pd_2(dba)_3$ (5%mol), PCy_3 (12%mol), K_3PO4 (1.7 equiv), THF/H_2O, 110 ºC, 16 h;

However, compound **38X** could not be characterized fully since it was sparingly soluble in chloroform, DMSO, benzene, water and even acetone.

11.2. Evaluation of regioselectively synthesized 1,5-diaryl-1,2,3-triazoles at the CB1-receptor.

In terms of evaluating the compounds, we look at the affinity of the compounds for the receptor by measuring the inhibition of the known drug by the synthetic drug. Before subjecting our synthesized molecules to animal models, we treat these molecules on tissue samples (Figure 25) to determine the binding affinity of our molecules to the protein receptor. Known ligands, here radiolabeled rimonabant and our ligands, the 1,2,3-triazole derivatives, compete for the same receptors and their strengths are determined in terms of binding affinities by how well our molecule displaces that compound. The better it competes, the smaller the number will be, the more potent that molecule is.

The binding affinities of the triazole derivatives (Table 3, Table 4 and Table 5) were determined by the inhibition of [^{3}H]**SR141716A** binding in homogenates of rat cerebellum.[62] Initially, each compound was evaluated at concentration of 10 μM for its ability to inhibit bound [^{3}H]SR141716. If less than 50% percent inhibition was observed,

further evaluation was not pursued.

Figure 25. Binding Affinity (K_i) - Measuring inhibition by competition. (Modified from reference 69)

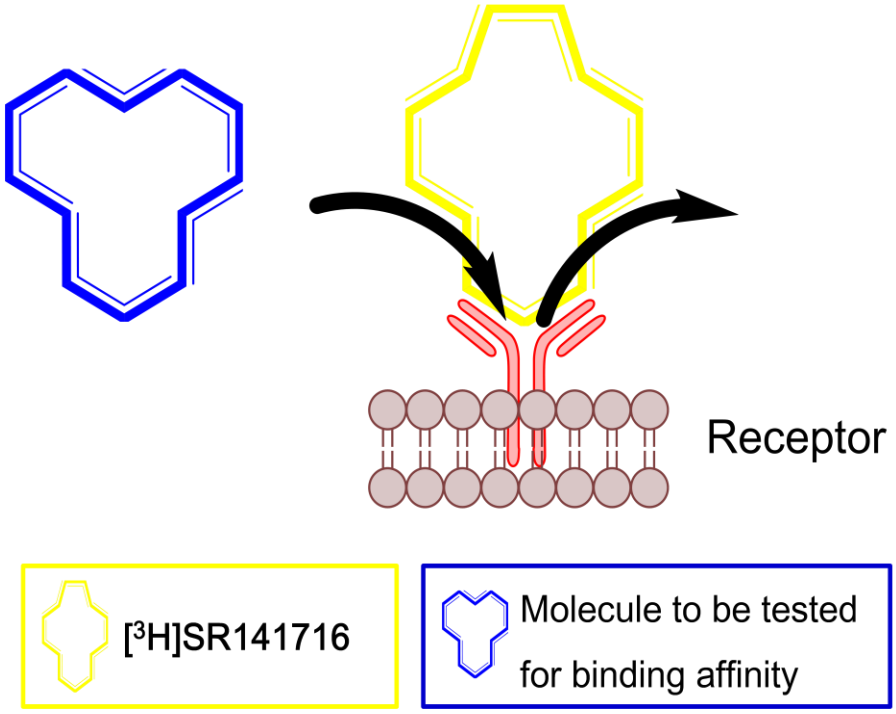

If greater than 50% inhibition at 10 μM was observed, only then a full concentration curve was measured and a K_i value was determined for the compound. Each concentration was tested in triplicate and each experiment was replicated three times. The binding data were analyzed using the non-linear regression analysis program of GraphPad Prism®.

On comparing our library among each other we see a broad range of affinity values.

These values of the triazole derivatives were determined at CB1-receptor by the inhibition of [^{3}H]SR141716 binding in rat cerebellum. The smaller this value, the stronger our ligand binds. On doing structure activity relationship study we determined that, the optimum values were obtained when the aryl at carbon-5 position had a chloro substituent and the carbon-4 of the triazole position had a chain length of approximately 4 carbons.

The esters were evaluated *in vitro* for binding affinity at CB1 receptors (Table 3). The *n*-propyl ester **31a**, with a K_i value slightly higher than **SR141716A**, was the most potent derivative of the series. We noticed that it exhibited similar lipophilicity to that of **SR141716A**. The phenyl ester **32a** also exhibited high affinity for CB1 receptors, but the affinity of the benzyl ester was somehow diminished, even though they share very similar lipophilicity.

Table 3. Inhibition of [^{3}H]**SR141716A** at CB1 Receptors in comparison to esters.

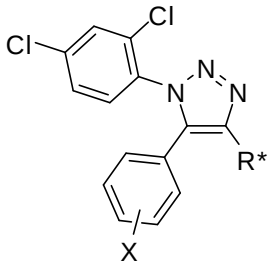

Cpd[a]	Code	R*	X	*C*log*P*	K_i (nM)[b]
30 a	AVG122M	CO_2CH_3	4-Cl	5.32	66 ± 7.0
30 b	AVG132M	CO_2CH_3	4-H	4.64	25[c]
30 c	AVG142M	CO_2CH_3	4-F	4.79	19[c]
30 d	AVG138M	CO_2CH_3	4-CH_3	5.16	143 ± 82
30 e	AVG157M	CO_2CH_3	4-OPh	6.14	51[c]
30 f	AVG131M	CO_2CH_3	2-CH_3, 4-OCH_3	5.68	910 ± 310
30 g	AVG146M	CO_2CH_3	3-CH_3, 4-F	5.3	20[c]
30 h	AVG 365M	CO_2CH_3	3-Cl	6.26	
30 i	AVG 366M	CO_2CH_3	3-CF_3	6.43	
30 j	AVG 382M	CO_2CH_3	3-CH_3	6.05	
31 a	AVG 276	$CO_2nC_3H_7$	4-Cl	6.21	4.6 ± 0.12
31 b	AVG 200	$CO_2nC_3H_7$	4-H	5.52	640 ± 360
31 c	AVG 342	$CO_2nC_3H_7$	4-F	5.66	394 ± 83
31 d	AVG 260P	$CO_2nC_3H_7$	4-Br	6.29	85 ± 5.1
31 e	AVG 267P	$CO_2nC_3H_7$	4-CH_3	6.04	NA
31 f	AVG 343	$CO_2nC_3H_7$	4-OCH_3	5.36	154 ± 38
31 g	AVG 338P3	$CO_2nC_3H_7$	4-CF_3	6.4	168 ± 19
31 h	AVG183P	$CO_2nC_3H_7$	2-CH_3, 4-OCH_3	5.88	620 ± 240
31 i	AVG 336P	$CO_2nC_3H_7$	4-I	7.73	N.T.
31 j	AVG 365P	$CO_2nC_3H_7$	3-Cl	7.32	
31 k	AVG 366P	$CO_2nC_3H_7$	3-CF_3	7.49	

Table 3 Contd.

Cpd[a]	Code	R*	X	*ClogP	K_i (nM)[b]
32 a	AVG 220Ph	CO_2Ph	4-Cl	6.83	11 ± 3.4
32 b	AVG 314Ph	CO_2Ph	4-H	6.3	2[d]
32 c	AVG 229Ph	CO_2Ph	4-F	6.44	1,900 ± 760
32 d	AVG 260Ph	CO_2Ph	4-Br	7.07	NA
32 e	AVG 267Ph	CO_2Ph	4-CH_3	6.81	52[d]
32 f	AVG 259Ph	CO_2Ph	4-OPh	7.8	350 ± 97

[a]All compounds were tested as the freebase. [b]All values are the mean ±SEM of three experiments performed in triplicate. Inhibition of [^{3}H]SR141716 binding in rat cerebellum.*The *C*log*P* values were calculated using CS ChemDrawOffice2010.[c]Percent inhibition at 10 μM. [d]Percent inhibition at 100 μM. NA-Not available. Compound decomposed in solution. N.T.-Not Tested.

The esters **30a**, **31a** and **32a** are the most potent analogs of the series. In general, replacement of the 4-chloro substituent on the 5-aryl moiety to give the series of congeners **30**, **31** and **32** did not improve binding affinity. In the methyl ester series **30**, only the 4-methyl congener **30d** (K_i = 143 nM) exhibited modest potency similar to **30a**.

The other substituted congeners were significantly less potent at CB1 receptors. Among the propyl ester congeners **31**, the 4-bromo (**31d**, K_i = 85 nM), 4-methoxy (**31f**, K_i = 154 nM) and 4-trifluoromethyl (**31g**, K_i = 168 nM) derivatives exhibited good potency but were less potent than the 4-chloro analogue **31a**.

None of the phenyl esters **32** exhibited even modestly potent affinity compared to

32a. The high binding affinities observed exclusively for 4-chloro derivatives **30a**, **31a** and **32a** was unexpected. The fact that the 4-fluoro substituted derivatives (e.g. **30c**, **31c**, **32c**) and the 4-methyl substituted derivatives (e.g. **30d**, **31e** and **32e**) were significantly less potent reinforces the idea that the 4-chloro substituent contributes favorably to both the electronic and the steric requirements for binding at CB1 receptors.

The importance of chloro substituent at the aryl of carbon-5 of triazole is quite evident on comparing the binding affinities of compounds **31a** and **31b**. Whereas, on one hand **31a** had high potency, on the other hand removing that chloro substituent dropped the potency to approximately 130 times. Similarly comparing compounds **32a** and **32b**, the removal of 4-chloro substituent from the aryl group on the carbon-5 of the **32a** triazole caused drop in activity so much so that compound **32b** only had 2% inhibition at 100 μM concentration.

Thus, presence of the 4-chloro substituent for the molecular recognition at the CB1-receptor was confirmed in our research. The larger alkyl esters exhibited high

lipophilicity and were difficult to handle in the binding assay. Preliminary binding studies indicated diminished binding affinity relative to propyl ester. In general, analogs with either decreased or increased lipophilicity relative to **SR141716A** exhibited diminished affinity. It seems to suggest that a narrow window of lipophilic character may exist for binding of these triazoles at CB1 receptors.

The second class of compounds prepared were based on the 1,5-diaryl-4-keto triazole ring system (Table 4). They were prepared to investigate the effects of the orientation of carboxyl group in triazole system on CB1 receptor affinity.

On moving from esters to ketones, we observe that a similar structure activity relationship still applied to ketones as was with esters. The ketone **34a**, with 4-chloro substituent at the aryl of carbon-5 was the most potent among the series. The presence of carbonyl group was observed to be essential and the optimum values were obtained when the aryl at carbon-5 position had a chloro substituent and the carbon-4 of the triazole position had a chain length of 4 carbons.

Table 4. Inhibition of [^{3}H]**SR141716A** at CB1 Receptors in comparison to ketones.

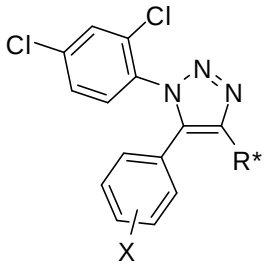

Cpd[a]	Code	R*	X	*C*log*P*	K_i (nM)[b]
33 a	AVG 194	-$COCH_2CH_3$	4-Cl	6.38	I.P.
33 b	AVG 226E	-$COCH_2CH_3$	4-F	5.81	500 ±105
33 c	AVG 260E	-$COCH_2CH_3$	4-Br	6.53	-
33 d	AVG 267E	-$COCH_2CH_3$	4-CH_3	6.17	-
34 a	AVG 165B	-$COCH_2CH_2CH_3$	4-Cl	6.9	105.3 ± 7.1
34 b	AVG 226B	-$COCH_2CH_2CH_3$	4-F	6.34	I.P.
34 c	AVG 209	-$COCH_2CH_2CH_3$	4-Br	7.06	-
34 d	AVG 249B	-$COCH_2CH_2CH_3$	4-OPh	8.29	N.T.
34 e	AVG 353B	-$COCH_2CH_2CH_3$	4-CF_3	7.1	
34 f	AVG 356B	-$COCH_2CH_2CH_3$	4-CH_3	6.69	-
35 a	AVG 359V	-$COCH_2CH_2CH_2CH_3$	4-Cl	7.44	-
35 b	AVG 229V	-$COCH_2CH_2CH_2CH_3$	4-F	6.87	165 ± 32
35 c	AVG 242V	-$COCH_2CH_2CH_2CH_3$	4-Br	7.59	-
35 d	AVG 267V	-$COCH_2CH_2CH_2CH_3$	4-CH_3	7.22	-
35 e	AVG 249V	-$COCH_2CH_2CH_2CH_3$	4-OPh	8.82	N.T.
35 f	AVG 346V	-$COCH_2CH_2CH_2CH_3$	4-CF_3	7.61	

[a]All compounds were tested as the freebase. [b]All values are the mean ±SEM of three experiments performed in triplicate. Inhibition of [^{3}H]SR141716 binding in rat cerebellum.*The *C*log*P* values were calculated using CS ChemDrawOffice2010.[c]Percent inhibition at 10 μM. [d]Percent inhibition at 100 μM. NA-Not available. Compound decomposed in solution. N.T.-Not Tested.

Compound **35b** with 4-fluoro substituent at the aryl of carbon-5 and 5 carbon chain at carbon-4 of the triazole also exhibited fairly decent potency.

As can be seen in case of 3-carbon chain length substituents at carbon-4 of the triazole as in compound **33b**, binding affinity (K_i) value are higher and thus indicating a decrease in potency as compared to compounds with 4-carbon chain length substituents at carbon-4 of the triazole.

In addition, these keto triazoles typically had higher lipophilicity the corresponding 1,5-diaryl-4-alkoxy triazoles. Since the presence of the carbonyl appeared to be an important factor, we tried to place substituents without carbonyl groups. Moreover we thought that lack of carbonyl will also help our design of compounds to avoid any inverse agonist behavior as was indicated by Hurst *et al.*[42]

However, the removal of the carbonyl altogether lead to a drop in activity as can be seen in Table 5, where we have substituted the carbon-4 position with just a hydrogen atom, a iodine atom or the trimethyl silyl group.

Table 5. Inhibition of [^{3}H]**SR141716A** at CB1 Receptors.

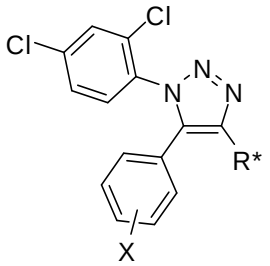

Cpd[a]	Code	R*	X	*ClogP	K_i (nM)[b]
36 a	AVG122H	H	4-Cl	5.01	1,400 ± 270
36 b	AVG 132H	H	H	4.46	4[c]
36 c	AVG 142H	H	4-F	4.60	17[c]
36 d	AVG 136	H	4-Br	5.22	1,300 ± 210
36 e	AVG 138H	H	4-CH_3	4.97	24[c]
36 f	AVG 152H	H	4-OCH_3	4.3	7[c]
36 g	AVG 140H	H	4-CF_3	5.33	39[c]
36 h	AVG 157H	H	4-OPh	5.95	3[c]
36 i	AVG 161H	H	4-$N(CH_3)_2$	4.56	43[c]
36 j	AVG 131H	H	2-CH_3, 4-OCH_3	4.81	7[c]
36 k	AVG 146H	H	3-CH_3, 4-F	5.11	10[d]
36 l	AVG 365H	H	3-Cl	5.01	
36 m	AVG 366H	H	3-CF_3	5.18	
36 n	AVG 382H	H	3-CH_3	4.79	
38	AVG 202	-I	H	6.05	
37 a	AVG 126	-$SiMe_3$	4-Cl	8.74	I.P.
37 b	AVG 148	-$SiMe_3$	4-Br	8.88	I.P.
37 c	AVG 150	-$SiMe_3$	4-OCH_3	7.98	-
37 d	AVG 156	- $SiMe_3$	-CH(OH)Ph	6.23	NT

[a]All compounds were tested as the freebase. [b]All values are the mean ±SEM of three experiments performed in triplicate. Inhibition of [^{3}H]SR141716 binding in rat cerebellum.*The *C*log*P* values were calculated using CS ChemDrawOffice2010.[c]Percent inhibition at 10 μM. [d]Percent inhibition at 100 μM. NA-Not available. Compound decomposed in solution. N.T.-Not Tested.

Attempts to synthesize triazoles with alkyl groups at carbon-4 position were not successful, either by method used in Scheme 10 or even by the lithiation methods used in Scheme 19.

As we can see, the unsubstituted triazoles have drastically low potency as compared to their ester and ketone analogs. The triazoles with trimethyl silyl substituents have more lipophilicity and surprisingly their percent inhibition values at 10 micromolar as well as at 100 micro molar gave good results.

From preliminary structure-activity studies, the esters **30a**, **31a** and **32a** were identified as potent CB1 receptor ligands.[58] It was subsequently determined that the propyl ester **31a** was highly selective for CB1 receptors over CB2 receptors (CB2 K_i = 1,920 ± 250 nM).[59] The high potency and selectivity of **6** at CB1 receptors prompted us to compare the structure of **31a** to that of **1**.

As illustrated in Figure 26, the alignment of predicted favorable solvated conformers of **1** and **31a** revealed several similarities between the two structures. The 1,5-diaryl triazole moiety of **31a** aligned well with the 1,5-diaryl pyrazole ring of **1**. Likewise, the

lipophilic propyl chain of the ester moiety of **31a** occupied a similar region to that of the methylene units of piperidine ring of **1**. However, as anticipated the superimposed structures clearly indicated that the ester moiety of **31a** was removed from the proximity of the carboxamide linkage of **1**.[60]

The triazole ring does not necessarily co-relate with the pyrazole ring system. This prompted us to go on and study the SAR of the system to understand better the binding motifs of these drugs at CB receptor. Proximity of the functional groups is same in terms of aryl rings but the substituents on the triazole ring are different and that's what we hope will lead to the difference in the activity of the molecule **31a** from being an inverse agonist as is Rimonabant (**1**).

The computational molecular studies (Figure 26) suggested that the interactions between the ester moiety and receptor-binding site would be weakened relative to the carboxamide-receptor interactions of **SR141716A (1)** and thus lead to diminished efficacy. This result encouraged us to move ahead with the triazole **31a** as our lead compound toward the development of a neutral antagonist.

Figure 26. Superimposed predicted favorable solvated conformers of **SR141716A** (**1**) (yellow) and **31a** (blue). [60]

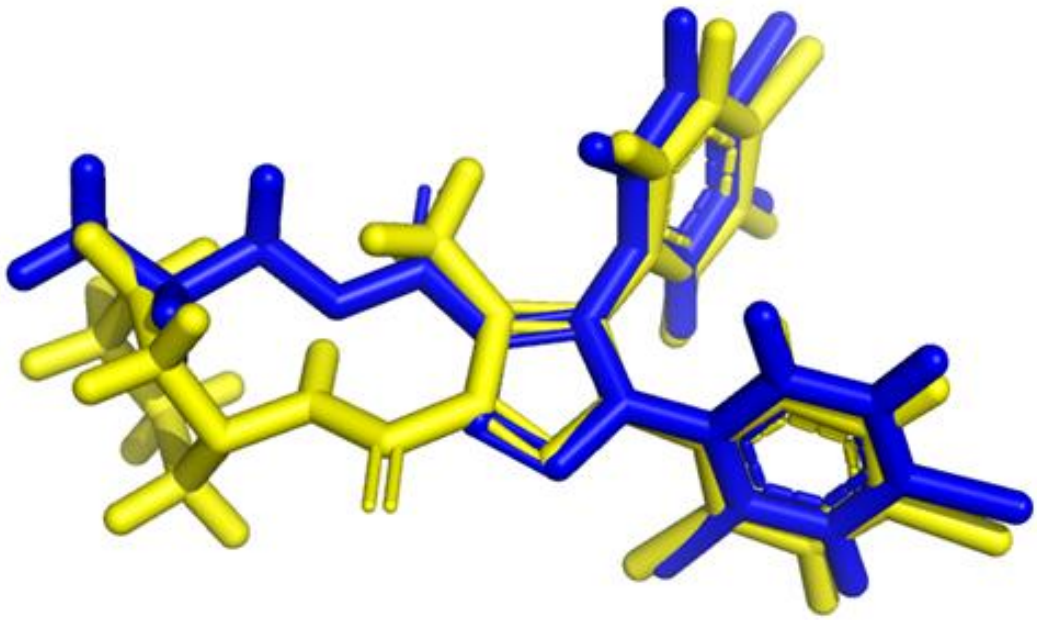

Since it had been shown in the pyrazole system that modification of the aryl substituents led to compounds with favorable pharmacological profiles, in this second phase of study our focus was on the evaluation of the structure-activity relationships of 5-aryl substitution. As illustrated in Scheme 10, we synthesized a number of triazole derivatives using a one-pot click/acylation reaction sequence previously established for this system.[52] Based upon the structure-activity relationships of our earlier study, the methyl, propyl and phenyl esters were identified as lead compounds for further

structural studies.[58] The required 2,4-dichlorphenylazide (**24**) was prepared in straightforward fashion from 2,4-dichloroaniline.[54]

The azide **24** was found to be somewhat unstable even when stored at subzero temperatures and away from light, so it was typically used immediately in the click reaction sequence with a series of commercially available aryl acetylenes. Treatment of these substituted aryl acetylenes with ethylmagnesium bromide in THF at room temperature and concomitant addition of **24** afforded an intermediate triazolyl magnesium bromide. This intermediate triazole was treated with the corresponding chloroformate reagent to give the triazole esters analogs in modest yields (10-50%).

The unacylated compounds were typical by-products of the reaction sequence. The formation of **36** presumably occurred during the work-up procedure by quenching the unreacted triazole intermediate. Alternatively, compounds **36** could be prepared directly in high yields (70-80%) by quenching the intermediate with ammonium chloride solution. Attempts to optimize the acylation reaction conditions using longer reaction times and higher concentrations of the various chloroformates did not significantly improved the

reaction yields. Despite the modest yields of the esters, sufficient quantities could be obtained for subsequent biological testing from a single run owing to the ease of the chromatographic separation of the esters from the corresponding unacylated triazoles. Although we were confident of the regiochemistry of the click reaction/acylation sequence, we unequivocally confirmed the structure of two congeners by X-ray crystallography.[61]

As evident from the structures of **36a** and **36a** in Figure 29 and Figure 30 respectively (see appendix), the 1,5-diaryl-1,2,3-triazole ring system was formed exclusively and none of the 1,4-diaryltriazole regioisomer was observed. It also confirmed the 1,3-dipolar cyloaddition method we were using gave us the desired regioselective results.

As summarized in Table 3, the esters **30a**, **31a** and **32a** remained the most potent analogs of the series. In general, replacement of the 4-chloro substituent on the 5-aryl moiety to give the series of congeners **30**, **31** and **32** did not improve binding affinity. In the methyl ester series **30**, only the 4-methyl congener **30d** (K_i = 143 nM) exhibited modest potency similar to **30a**. The other substituted congeners were significantly less

potent at CB1 receptors. Among the propyl ester congeners **31**, the 4-bromo (**31d**, K_i = 85 nM), 4-methoxy (**31f**, K_i = 154 nM) and 4-trifluoromethyl (**31g**, K_i = 168 nM) derivatives exhibited good potency but were less potent than the 4-chloro analogue **31a**. None of the phenyl esters **32** exhibited even modestly potent affinity compared to **32a**. The high binding affinities observed exclusively for 4-chloro derivatives **30a**, **31a** and **32a** was unexpected. The fact that the 4-fluoro substituted derivatives (e.g. **30c**, **31c**, **32c**) and the 4-methyl substituted derivatives (e.g. **30d**, **31e** and **32e**) were significantly less potent reinforces the idea that the 4-chloro substituent contributes favorably to both the electronic and the steric requirements for binding at CB1 receptors. Based upon these structure-activity relationships it was clear that the 4-chloro substituent on the 5-aryl moiety was optimal for molecular recognition at CB1 receptors for the triazole scaffold.

In general, the unacylated triazoles exhibited poor affinity for the CB1 receptors. Presumably, the steric and electronic effects of the acyl side-chain contribute significantly toward molecular recognition at CB1 receptors. Although we were unable to

improve potency relative to our lead compounds, the SAR results were somewhat gratifying in that they supported our initial design rationale that identified the 1-(2,4-dichlorophenyl)-5-(4-chlorophenyl)-1,2,3-triazole moiety as a key molecular scaffold for high affinity ligands.

Our final step as outlined in Figure 21 flowscheme of CB1 receptor drug discovery was to advance compounds exhibiting good blood-brain barrier permeability and meeting the goals of high *in vitro* efficacy to *in vivo* evaluation of antagonist efficacy.

To provide a pharmacological profile that can be used to guide future behavioral studies that is, dosing and efficacy, *in vivo* locomotor studies were done. The compounds along with vehicle were administered to rats via intraperitoneal injection 15 min before the start of locomotor activity testing (Figure 27). Data represent total distance traveled (cm) in 30 minutes.

Based on the SAR of the triazole ester series, the propyl ester **31a** and phenyl ester **32a** were deemed optimal ligands for advancement. However, the phenyl ester

presented significant solubility issues (*C*log*P* = 6.83)[62], thus our attention focused solely on the evaluation of the *in vivo* efficacy of **31a**.

Figure 27. A rat's response to ligand is measured by the distance it travels inside a locomotion chamber in which its movement is recorded and quantified.

A locomotor activity assay in rats was used to establish agonist, antagonist or inverse agonist efficacy. As illustrated in, the agonist **4** (WIN55,212-2 dissolved in 20% DMSO, 30% ethylene glycol and 50% sterile water) significantly diminished locomotor activity at a dose of 3.0 mg/kg as would be expected from the sedating effects of an agonist.

Locomotor activity was measured over a period of 30 mins. Rats were injected 15 mins before session began with either vehicle + vehicle (VEH), vehicle + 3 mg/kg WIN55,212-2 (WIN), 3 mg/kg **31a** + vehicle, 3 mg/kg **31a** + WIN (57-4/WIN), 1 mg/kg Rimonabant + vehicle (RIM), or Rimonabant + WIN55,212-2 (RIM/WIN). WIN55,212-2 decreased activity significantly compared to vehicle and this was blocked by both **31a** and by Rimonabant.

Figure 28. Locomotor activity studies.

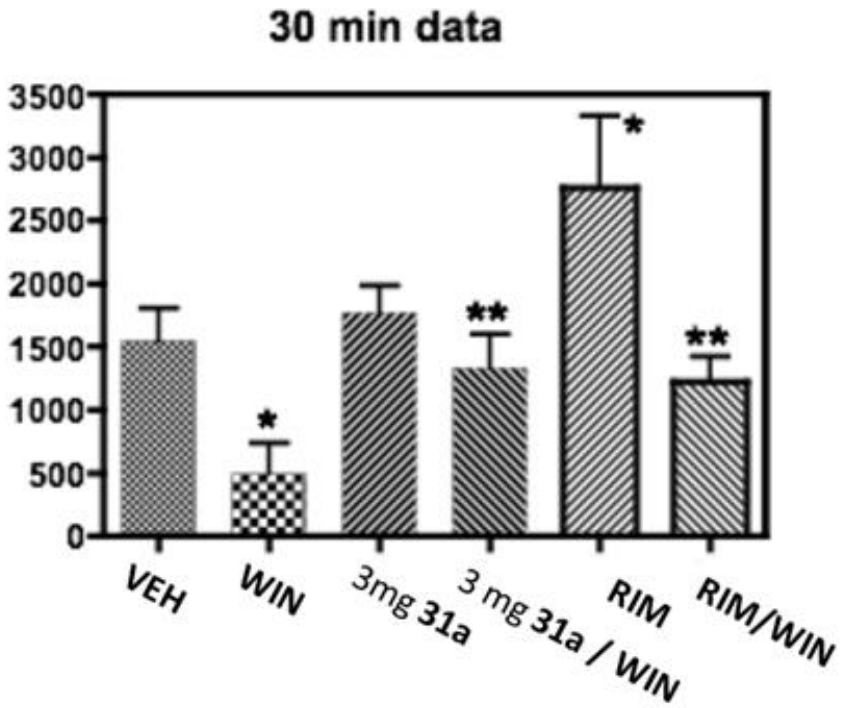

*p ≤ 0.05 compared to VEH

**p ≤ 0.05 compared to WIN

With agonist WIN we see the decrease in the locomotor activity as you will expect essentially because of the sedating effect of the cannabinoid agonist. When you treat it with a known antagonist you block the effects of the agonist. And so the agonist and the antagonist administered together we see basically normal locomotor activity.

Now if you look at our compound **31a**, we see that on its own it really does not have much activity of its own so we would access this as an antagonist. To prove that it blocks the effects of an agonist we gave our compound along with the agonist WIN and we saw the antagonized results in form of normal locomotor activity.

We believe our compound to be a neutral antagonist, at least at these doses, because if you look at dosing of the rimonobant by itself, which is an inverse agonist there is a stimulation in the locomotor activity which is the opposite to the effect of the agonist activity, whereas our compound looks pretty good next to it.

Based on this preliminary data, we believe that our compound is a neutral antagonist with no pharmacological profile of its own and its agonist blocking ability. The prototypical antagonist/inverse agonist **Rimonabant (1)** (1.0 mg/kg rimonabant dissolved

in 5% tween 80 and 95% sterile water), significantly stimulated activity relative to vehicle when given alone. However, when rats were pretreated with **Rimonabant (1)** together with the agonist **4**, the pyrazole **Rimonabant (1)** significantly antagonized the locomotor-reducing effects of **4**.

To determine the efficacy of **31a** (dissolved in 10% tween, 10% DMSO and 80% saline), initially a dose of 3.0 mg/kg was administered alone. At this dose, triazole **31a** exhibited no significant effect on locomotor activity compared to vehicle. Concomitantly, to establish that **31a** was penetrating into the brain, the ability of **6** to block the effects of the cannabinoid agonist WIN55,212-2 was measured. Initially, rats were pretreated with 3.0 mg/kg of triazole **31a** together with 3 mg/kg of the agonist **4**.

We were concerned about the pharmacological behavior of triazole **31a** and since locomotor activity is a good test for assessing the ability of the drug as agonist will diminish activity while inverse agonist will stimulate locomotor activity, the triazole **31a** fully antagonized the locomotor-reducing effects of the agonist **4** and triazole **31a** had no pharmacological profile of its own.

Thus, at these dose, triazole **31a** exhibited good penetration into the brain and a functional antagonist profile with statistically similar potency to that of **1**. However important to our goals, unlike antagonist/inverse agonist **1**, the triazole **31a** did not stimulate locomotor activity. Thus it appears that, at least at these dosing, triazole **31a** exhibits antagonist efficacy with no inverse agonist effects. Based upon the findings of these comparative locomotor-activity studies, it appears that triazole **31a** elicits a neutral cannabinoid antagonist profile at a dose that blocks agonist effects. Rimonabant alone significantly increased activity, whereas **31a** alone had no significant effect on activity.

12. CONLUSIONS

We designed and developed chemical synthesis to prepare several CB1-antagonists. Our preliminary binding assay results revealed the ester **30a** was 10-fold more potent than **22**. Better potency, together with other more optimal drug-like properties, ester **30a** was chosen to be our lead compound. With this lead compound, a series of esters (**30**, **31** and **32**) and ketones (**33**, **34** and **35**) were synthesized. The compounds exhibiting good potency binding to CB1 receptors are **30a**, **30d**, **31a**, **31f**, **31g**, **32a**, **34b** and **35a** and they are currently being evaluated to determine efficacy. Based on these results, an extensive study is undergoing in our research laboratory searching for novel selective CB1 receptor antagonists.

In the context of identifying new cannabinoid receptor ligands as potential leads for medication development for psychostimulant addiction, we have shown that the 1,5-diaryl-1,2,3-triazole ring system is clearly a novel molecular scaffold that exhibits potent and selective CB1 receptor affinity. A series of 4-alkoxycarbonyl-1-(2,4-dichlorophenyl)-5-(aryl)-1,2,3-triazole derivatives were synthesized via a one-pot regiospecific

click/acylation reaction sequence from commercially available arylacetylenes and the readily available 1-azido-2,4-dichlorobenzene. From the structure-activity studies the 5-(4-chlorophenyl) congeners exhibited the most potent CB1 receptor affinities relative to other 5-(substituted-phenyl) moieties.

The 1-(2,4-dichlorophenyl)-5-(4-chlorophenyl)-4-propylcarbonyl-1,2,3-triazole (**31a**) was found to be the optimal structure for this class of triazole esters. The ester **31a** exhibited both high binding affinity and high selectivity for CB1 receptors.

The triazole ester **31a** further was characterized as a cannabinoid antagonist in locomotor-activity studies by blocking the locomotor-reducing effects of a cannabinoid agonist. In addition, unlike the prototypical cannabinoid antagonist **SR141716A**, the triazole ester **31a** did not exhibit inverse agonist activity in the locomotor activity studies.

Therefore, it appears that the triazole ester **31a** possesses a neutral antagonist pharmacological profile. The availability of a high affinity CB1 selective neutral antagonist will undoubtedly be useful for the further studies in a variety of cannabinergic

pathologies and diseases. The potential of the triazole ester **31a** to be used as a treatment for psychostimulant abuse is under investigation.

After exhibiting good *in vivo* antagonist efficacy, **31a** has been submitted to the National Institute of Drug Abuse (NIDA) for:

- **Δ^9-THC** Drug Discrimination Studies to understand if **31a** is infact different from **Δ^9-THC** and other psychostimulants and not an addictive compound.

- Metabolic Stability Studies and other ADME pharmacokinetic studies to determine how long compound **31a** stays before getting eliminated from the system.

- Off-Target Binding Studies to see if compound **31a** interferes with other receptors or channels, by screening it for a wide variety of receptors and ion-channels.

Moreover, as can be seen in Table 2, our compound **31a** is approximately 417 times more selective for CB1-receptor (K_i =4.6 ± 0.012 nM) when compared with CB2-receptor (K_i =1916 ± 247 nM) which is towards the **Rimonabant's** end of spectrum

which is also quite selective. This is as opposed to other cannabinoid ligands like **THC** which is basically not selective at all for CB1 or CB2 receptors.

One of the things that we may be looking at is how it affects cocaine self-administration, how does it affects METHamphetamine self-administration as well as Cannabis cessation. Thus, we believe that compound **31a** which is derived from novel 1,2,3-triazole core frame, will serve as lead compound in future studies aimed at developing them further as drug abuse medications.

13. EXPERIMENTAL SECTION

All chemicals were purchased form Aldrich Chemical Co., Milwaukee, WI, unless otherwise noted. Anhydrous THF was purchased from VWR International Co. and used under argon without any further purification. Chromatography refers to flash column chromatography on silica gel (Silica Gel 60, 230-400 mesh, Sorbent Technologies). Preparative TLC was performed on 20 × 20 cm, 500· m Silica Gel GF plates (Analtech). Reported melting points are uncorrected. NMR spectra were recorded in $CDCl_3$ on a Varian-Gemini 400 MHz spectrometer. Chemical shifts are reported as values with teteramethylsilane (TMS), employed as the internal standard. ORTEP drawings of the X-ray crystal structures for **31a**, **36a** and **32c** are given in Figure 29, Figure 30 and Figure 31 respectively in Appendix section, with thermal ellipsoids at 30% (**31a**) and 25% (**36a**) probability for non-H atoms and open circles for H-atoms. Full crystallographic data have been deposited to the Cambridge CrystallographicDataCenter (CCDC 820556 and 820557). Copies of the data can be obtained free of charge via the Internet at http://www.ccdc.cam.ac.uk. Purity of all

compounds was determined to be >95% by combustion analysis as listed. Combustion analyses were obtained from Atlantic Microlabs, Inc., Norcross, GA.

13.1. General Experimental Methods

1-Azido-2,4-dichlorobenzene (24). 2,4-Dichloroaniline (320 mg, 2.0 mmol) was suspended in a mixture of water (2.2 mL) and conc. HCl (4.4 mL) under a nitrogen atmosphere. The solution was cooled to 0 °C and a solution of sodium nitrite (166 mg, 2.4 mmol) in water (1 mL) was added. After stirring for 1 h at 0 °C, a solution of sodium azide (170 mg, 2.6 mmol) in water (1 mL) was added to this mixture and stirring was continued for another 2 h at 0 °C. The resulting reaction mixture was diluted with brine (25 mL) and extracted using ethyl acetate (3 × 25 mL). The combined organic fractions were dried over Na_2SO_4 and the solvent was removed under reduced pressure. The residue was triturated with Et_2O to furnish the azide as light yellow solid (336 mg, 90%) in sufficiently pure form to be used in subsequent steps without additional purification. mp 51-52 °C [lit. mp 52.8-53.4 °C]. ^{1}H NMR (400 MHz, $CDCl_3$): δ 7.39 (s, 1H), 7.27-7.28 (m, 1H), 7.09 (d, *J* = 8.6 Hz, 1H).^{13}C NMR (400 MHz, $CDCl_3$): 136.0, 130.6, 130.4,

128.1, 120.4. Anal. ($C_6H_3Cl_2N_3$): C, 38.33; H, 1.61; N, 22.35. Found: C, 38.43; H, 1.72; N, 21.54.

General procedure for synthesis of 4-alkoxycarbonyl-5-(substituted phenyl)-1-(2,4-dichlorophenyl)-1H-1,2,3-triazoles. (**30-32**) Under a nitrogen atmosphere, a solution of ethyl magnesium bromide (1.5 mL, 1.0 M in THF) was added dropwise to neat aryl-acetylene (1.05 mmol) or in anhydrous THF (1 mL) at rt. The mixture was heated to 50 °C and stirring was continued for 1 h. A solution of freshly made 2,4-dichlorophenyl azide (**24**, 1 mmol) in 1 mL THF was added dropwise and the mixture was heated to 50 ºC for 1 h. The solution was allowed to cool to room temperature and added dropwise to a solution of alkyl chloroformate (1.5 mmol) in THF (3 mL) at -20ºC under inert conditions. After stirring for 3 h, or until the tentative product spot on thin layer chromatography was not changing, the reaction was quenched with sat. NH_4Cl (5 mL) and diluted with EtOAc (30 mL). The organic fraction was separated. The aqueous fraction was extracted with EtOAc (2×30 mL). The combined organic fractions were washed with brine (30 mL), dried over anhydrous $MgSO_4$, filtered, and concentrated

under reduced pressure. The residue was purified by chromatography (SiO_2, EtOAc/hexanes; 1/5) or by preparative TLC (SiO_2, EtOAc/hexanes/CH_2Cl_2; 1/3/1) to afford the corresponding 4-alkoxycarbonyl-1-(2,4-dichlorophenyl)-5-(substituted phenyl)-1H-1,2,3-triazole.

1-(2,4-dichlorophenyl)-5-(4-chlorophenyl)-4-methoxycarbonyl-1H-1,2,3-triazoles. (**30a**). Yield, 61%, as a white crystalline solid; mp 158-160 °C. ^{1}H NMR (400 MHz, $CDCl_3$) δ 7.93-7.40 (m, 7H), 3.78 (s, 3H). ^{13}C NMR (400 MHz, $CDCl_3$) δ 142.0, 137.9, 136.9, 136.3, 132.8, 132.1, 131.4, 130.8, 130.4, 129.0, 128.5, 123.3, 52.5. Anal. ($C_{16}H_{10}Cl_3N_3O_2$) : C, 50.22; H, 2.63; N, 10.98. Found: C, 49.95; H, 2.68; N, 10.70.

1-(2,4-Dichlorophenyl)-4-methoxycarbonyl-5-phenyl-1H-1,2,3-triazole (30b). Yield 12% as white crystalline solid; mp 140-140.5 °C. ^{1}H NMR (400 MHz, $CDCl_3$) δ 7.48 (s, 1H), 7.27-7.43 (m, 7H), 3.92 (s, 3H); ^{13}C NMR (400 MHz, $CDCl_3$) δ 160.2, 132.8, 137.4, 132.7, 132.2, 130.5, 130.3, 130.2, 129.7, 128.3, 128.1, 127.8, 124.5, 52.4, Anal. ($C_{16}H_{11}Cl_2N_3O_2$): C, 55.19; H, 3.18; N, 12.07. Found: C, 54.93; H, 3.21; N, 12.01.

1-(2,4-Dichlorophenyl)-5-(4-fluorophenyl)-4-methoxycarbonyl-1H-1,2,3-triazole (30c). Yield 14%, as a white waxy solid. ^{1}H NMR (400 MHz, $CDCl_3$) δ 7.50 (s, 1H), 7.28-7.39 (m, 4H), 7.04-7.09 (m, 2H), 3.95 (s, 3H); ^{13}C NMR (400 MHz, $CDCl_3$) δ 164.9, 161.2, 142.0, 137.6, 132.7, 132.0, 131.9, 130.6, 130.2, 128.2, 120.6, 115.9, 115.7, 52.3; Anal. ($C_{16}H_{10}FCl_2N_3O_2$) : C, 52.48; H, 2.75; N, 11.48. Found: C, 52.55; H, 2.92; N, 11.25.

1-(2,4-Dichlorophenyl)-4-methoxycarbonyl-5-(4-methylphenyl)-1H-1,2,3-triazole (30d). Yield 25%, as a white solid; mp 136-137 °C. ^{1}H NMR (400 MHz, $CDCl_3$) δ 7.49 (s, 1H), 7.33-7.34 (m, 2H), 7.15-7.18 (m, 4H), 3.94 (s, 3H), 2.36 (s, 3H); ^{13}C NMR (400 MHz, $CDCl_3$) δ 161.3, 144.1, 140.6, 137.3, 135.9, 132.8, 132.3, 130.5, 130.2, 129.6, 129.1, 128.1, 121.6, 52.2, 21.4; Anal. ($C_{17}H_{13}Cl_2N_3O_2$•0.33 H_2O) : C, 56.37; H, 3.62; N, 11.60. Found: C, 55.65; H, 3.64; N, 11.29.

1-(2,4-Dichlorophenyl)-4-methoxycarbonyl-5-(4-phenoxyphenyl)-1H-1,2,3-triazole (30e). Yield 18%, as yellow oil. ^{1}H NMR (400 MHz, $CDCl_3$) δ 7.51 (s, 1H), 7.34-7.39 (m, 4H), 7.25 (d, *J* = 8.4Hz, 2H), 7.16-7.19 (m, 1H), 7.05 (d, *J* = 8.4Hz, 2H), 6.92 (d, *J* = 8.4Hz, 2H), 3.95 (s, 3H); ^{13}C NMR (400 MHz, $CDCl_3$) δ 159.6, 155.1, 132.8, 132.3, 131.5,

130.6, 130.2, 130.0, 128.2, 124.6, 120.2, 118.4, 117.4, 52.6; Anal. ($C_{22}H_{15}Cl_2N_3O_3$) : C, 60.02; H, 3.43; N, 9.54. Found: C, 60.00; H, 3.50; N, 9.35.

1-(2,4-Dichlorophenyl)-4-methoxycarbonyl-5-(4-methoxy-2-methylphenyl)-1H-1,2,3triazole (30f). Yield 22%, yellow oil. ^{1}H NMR (400 MHz, $CDCl_3$) δ 7.48 (d, *J* = 2 Hz, 1H), 7.22 - 7.32 (m, 2H), 6.95 (d, *J* = 8.4 Hz, 1H), 6.76 (s, 1H), 6.66 (d, *J* = 8.4 Hz, 1H), 3.89 (s, 3H), 3.77 (s, 3H), 2.13 (s, 3H); ^{13}C NMR (400 MHz, $CDCl_3$) δ 161.0, 160.8, 153.6, 147.7, 139.6, 131.0, 130.6,129.9,127.9, 115.7, 111.4, 55.1, 52.2, 20.1; Anal. ($C_{18}H_{15}Cl_2N_3O$• 0.5 H_2O): C, 53.88; H, 4.02; N, 10.47. Found: C, 53.87; H, 3.93; N, 10.05.

1-(2,4-Dichlorophenyl)-5-(4-fluoro-3-methylphenyl)-4-methoxycarbonyl-1H-1,2,3-triazole (30g). Yield 14%, as white powder; mp 149-150 °C. ^{1}H NMR (400 MHz, $CDCl_3$) δ 7.51(s, 1H), 7.35 (m, 2H), 7.16 (br s, 1H), 7.05 (m, 1H), 6.96 (t, *J* = 8.8 Hz, 1H), 3.93 (s, 3H), 2.22 (s, 3H); ^{13}C NMR (400 MHz, $CDCl_3$) δ 163. 5, 161.2, 137.5, 133.2, 133.1, 132.8, 130.5, 130.2, 129.1, 129.0, 128.1, 125.5, 120.3, 115.4, 52.2, 14.2; Anal.

($C_{17}H_{12}Cl_2N_3O_2F$• 0.25 H_2O): C, 53.08; H, 3.27; N, 10.92. Found: C, 53.07; H, 3.17; N, 10.80.

1-(2,4-Dichlorophenyl)-5-(3-chlorophenyl)-4-methoxycarbonyl-1H-1,2,3-triazole (30h). Yield 93%, as a white powder; mp 127 °C. ^{1}H NMR (400 MHz, $CDCl_3$)δ 7.50(d, *J* = 2 Hz 1H), 7.39-7.28 (m, 5H), 7.14(d, *J* = 7.6 Hz, 1H), 3.93 (s, 3H); ^{13}C NMR (400 MHz, $CDCl_3$) δ 161, 141.4, 137.7, 136.3, 134.6, 132.7, 131.8, 130.6, 130.5, 130.1, 129.9, 129.6, 128.2, 127.9, 126.5, 52.4; Anal. ($C_{16}H_{10}Cl_3N_3O_2$): C, 50.22; H, 2.63; N, 10.98. Found: C, 50.74; H, 2.90; N, 10.48.

1-(2,4-Dichlorophenyl)-5-(3-(trifluoromethyl)phenyl)-4-methoxycarbonyl-1H-1,2,3-triazole (30i). Yield 36%, as white solid; mp 125-128 °C. ^{1}H NMR (400 MHz, $CDCl_3$) δ 7.67(bd, *J* = 5.2 Hz 1H), 7.58 (s, 1H), 7.52-7.47 (m, 3H), 7.42-7.37 (m, 2H), 3.93 (s, 3H); ^{13}C NMR (400 MHz, $CDCl_3$) δ 161, 141.3, 137.9, 136.4, 133.1, 132.6, 131.7, 131.1, 130.6, 130.1, 128.9, 128.3, 127.0 (t, *J* = 12, 12.4 Hz,), 126.99,126.95), 125.7, 124.7, 52.4; Anal. ($C_{17}H_{10}Cl_2F_3N_3O_2$): C, 49.06; H, 2.42; N, 10.10. Found: C, 49.10; H, 2.69; N, 9.38.

1-(2,4-Dichlorophenyl)-5-(3-methylphenyl)-4-methoxycarbonyl-1H-1,2,3-triazole (30j). Yield 64%, as a pale white powder; mp 105-105.5 °C. ^{1}H NMR (400 MHz, $CDCl_3$) δ 7.50(d, *J* = 2 Hz 1H), 7.39-7.28 (m, 5H), 7.14(d, *J* = 7.6 Hz, 1H), 3.91 (s, 3H), 2.29 (s, 3H); ^{13}C NMR (400 MHz, $CDCl_3$) δ 161.5, 143.3, 138.4, 137.6, 133.1, 132.5, 133.1, 132.5, 131.3, 130.9, 130.7,130.5, 130.2, 128.5, 128.2, 127.0, 124.8, 52.4, 21.5; Anal. ($C_{17}H_{13}Cl_2N_3O_2$• 0.25 C_7H_8): C, 58.37; H, 3.92; N, 10.91. Found: C, 58.43; H, 3.68; N, 13.41.

1-(2,4-dichlorophenyl)-5-(4-chlorophenyl)-4-propoxycarbonyl-1H-1,2,3-triazole (**31a**). Yield 17%, as a white solid; mp 117-118 °C. ^{1}H NMR (400 MHz, $CDCl_3$) δ 7.92-7.39 (m, 7H), 4.15 (t, *J* = 7.4 Hz, 2H), 1.54 (sextet, *J* = 7.5 Hz, 2H), 0.75 (t, *J* = 7.5 Hz, 3H). ^{13}C NMR (400 MHz, $CDCl_3$) δ 160.9, 141.8, 137.8, 136.7, 136.6, 132.8, 132.1, 131.4 130.7, 130.4, 128.9, 128.4, 123.6, 67.2, 22.0, 10.4. Anal. ($C_{18}H_{14}Cl_3N_3O_2$): C, 52.62; H, 3.44; N, 10.23. Found: C, 52.90; H, 3.47; N, 10.25.

1-(2,4-Dichlorophenyl)-5-phenyl-4-propoxycarbonyl-1H-1,2,3-triazole (31b). Yield 18%, as a yellow oil. ^{1}H NMR (400 MHz, $CDCl_3$) δ 7.45 (s, 1H), 7.29-7.39 (m, 5H), 7.25-

7.29 (m, 2H), 4.24 (t, *J* = 6.8 Hz, 2H), 1.67 (sextet, *J* = 6.8 Hz, 2H), 0.85 (t, *J* = 6.8 Hz, 3H); ^{13}C NMR (400 MHz, $CDCl_3$) δ 160.8, 142.6, 137.3, 136.4, 132.7, 132.1, 130.4, 130.2, 130.1, 129.8, 128.2, 128.0, 124.9, 66.8, 21.8, 10.3; Anal. ($C_{18}H_{15}Cl_2N_3O_2$): C, 57.46; H, 4.02; N, 11.17. Found: C, 57.76; H, 4.13; N, 10.50.

Procedure for conversion of compound 30b to 31b: A flame dried 50-mL round bottomed flask was vacuumed and backfilled with nitrogen gas. The flask was charged with 1-propanol (1 eq) in 10 mL of anhydrous THF. The solution was cooled to -78 ºC and *t*-butyl lithium (2.5 M in hexanes, 2.5 eq) was added slowly. After stirring for 10 minutes, compound **30b** (1 eq) dissolved in 2 mL of anhydrous THF was added drop wise. The resultant solution was stirred for 1 hour and poured into 30 mL ice water in a separatory funnel and extracted with EtOAc (2 x 30 mL). The combined organic fractions were washed by sat. NaCl, dried on anhydrous MgSO4, filtered, and purified by running through a thin pad of silica gel. After, the solution was concentrated *in vacuuo*, followed by column purification, compound **31b** in 46% yield.

Procedure for conversion of compound 39 to 31b: Under a nitrogen atmosphere, into a 25 mL round-bottomed flask equipped with a condensor was added benzyl azide **24** (1.0 mmol) and compound **39** (1.1 mmol), and DMF (4 mL). The mixture was stirred at reflux for 20 h and concentrated *in vacuo*. The residue was purified by chromatography (SiO_2, EtOAc/hexanes; 1/5) or by preparative TLC (SiO_2, EtOAc/hexanes/CH_2Cl_2; 1/3/1) to afford the compound **31b** in 8% yield.

Procedure for conversion of compound 38 to 31b: Under a nitrogen atmosphere, compound **38** (1 mmol) was dissolved in THF (2 mL), cooled to -78 °C and *t* – BuLi (1.6 M in hexanes, 1.5 mmol) was added drop wise. After 2 h, neat propyl chloroformate (1.5 mmol) was added dropwise. The temperature was maintained at -78 °C for another two hours, before allowing it to rt, after which the solution was stirred for another 4 h. After, the solution was concentrated *in vacuuo*, it was partitioned with water and ethyl acetate (3 X 20 mL). The combined organic fractions were washed with brine (30 mL), dried over anhydrous $MgSO_4$, filtered, and concentrated under reduced pressure. The residue

was purified by chromatography (SiO_2, EtOAc/hexanes; 1/5) or by preparative TLC (SiO_2, EtOAc/hexanes/CH_2Cl_2; 1/3/1) to afford the compound **31b** in 5.43% yield.

1-(2,4-Dichlorophenyl)-5-(4-fluorophenyl)-4-propoxycarbonyl-1H-1,2,3-triazole (31c). Yield 25%, as a yellow oil. ^{1}H NMR (400 MHz, $CDCl_3$) δ 7.48 (s, 1H), 7.32-7.38 (m, 2H), 7.26-7.32 (m, 2H), 7.04 (t, *J* = 8.0 Hz, 2H), 4.27 (t, *J* = 6.8 Hz, 2H), 1.71 (m, 2H), 0.90 (t, *J* = 7.6 Hz, 3H); ^{13}C NMR (400 MHz, $CDCl_3$) δ 164.8, 162.3, 160.8, 141.7, 137.5, 132.0, 131.9, 130.5, 130.2, 128.2, 120.9, 115.8, 115.5, 66.9, 21.8, 10.3; Anal. ($C_{18}H_{14}Cl_2N_3O_2F$): C, 54.84; H, 3.58; N, 10.66. Found: C, 55.12; H, 3.58; N, 10.39.

5-(4-Bromophenyl)-1-(2,4-dichlorophenyl)-4-propoxycarbonyl-1H-1,2,3-triazole (31d). Yield 21%, as a white crystalline solid; mp 122-123 °C. ^{1}H NMR (400 MHz, $CDCl_3$) δ 7.48-7.51 (m, 3H), 7.33-7.40 (m, 2H), 7.17 (d, *J* = 6.6Hz, 2H), 4.29 (t, *J* = 6.6 Hz, 2H), 1.74 (sextet, *J* = 7.4 Hz, 2H), 0.93 (t, *J* = 7.6 Hz, 3H); ^{13}C NMR (400 MHz, $CDCl_3$) δ 160.8, 141.6, 137.6, 136.5, 132.7, 131.9, 131.7, 131.4, 130.6, 130.2, 128.2, 124.9, 123.9, 67.0, 21.8, 10.3; Anal. ($C_{18}H_{14}Cl_2N_3O_2Br$): C, 47.50; H, 3.10; N, 9.23. Found: C, 47.74; H, 3.10; N, 9.11.

1-(2,4-Dichlorophenyl)-5-(4-methylphenyl)-4-propoxycarbonyl-1H-1,2,3-triazole (31e). Yield 40%, as a light yellow oil. ^{1}H NMR (400 MHz, $CDCl_3$) δ 7.43 (s, 1H), 7.31 (s, 2H), 7.09-7.15 (m, 4H), 4.23 (t, *J* = 6.8 Hz, 2H), 2.29 (s, 3H), 1.68 (sextet, *J* = 7.3 Hz, 2H), 0.86 (t, *J* = 7.4 Hz, 3H); ^{13}C NMR (400 MHz, $CDCl_3$) δ 160.8, 142.7, 140.3, 137.1, 136.1, 132.7, 132.2, 130.3, 130.2, 129.6, 128.9, 127.9, 121.7, 66.7, 21.7, 21.2, 10.1; Anal. ($C_{19}H_{17}Cl_2N_3O_2$): C, 58.47; H, 4.39; N, 10.77. Found: C, 58.22; H, 4.38; N, 10.60.

1-(2,4-Dichlorophenyl)-5-(4-methoxyphenyl)-4-propoxycarbonyl-1H-1,2,3-triazole (31f). Yield 20%, as a tan oil. ^{1}H NMR (400 MHz, $CDCl_3$) δ 7.47(s, 1H), 7.30-7.36 (m, 2H), 7.21 (d, *J* = 8.4Hz, 2H), 6.84 (d, *J* = 6.8 Hz, 2H), 4.27 (t, *J* = 6.8Hz, 2H), 3.79 (s, 3H), 1.73(sextet, *J* = 7.2 Hz, 2H), 0.92 (t, *J* = 7.6 Hz, 3H); ^{13}C NMR (400 MHz, $CDCl_3$) δ 161.3, 161.1, 142.9, 137.5, 136.3, 133.1, 132.6, 131.6, 130.7, 130.5, 128.3, 116.9, 114.7, 114.6, 114.1, 67.1, 55.5, 22.1, 10.6; Anal. ($C_{19}H_{17}Cl_2N_3O_3$) : C, 56.17; H, 4.22; N, 10.34. Found: C, 56.44; H, 4.06; N, 10.09.

1-(2,4-Dichlorophenyl)-5-(4-trifluoromethylphenyl)-4-propoxycarbonyl-1H-1,2,3-triazole (31g). Yield 16%, as a tan solid; mp 127-129 °C. ^{1}H NMR (400 MHz, $CDCl_3$)δ

7.62 (d, J = 8.2 Hz, 2H), 7.49 (s, 1H), 7.43 (d, J = 8.4 Hz, 2H), 7.35-7.40 (m, 2H), 4.27 (t, J = 6.8 Hz, 2H), 1.71 (sextet, J = 7.2 Hz, 2H), 0.89 (t, J = 7.2 Hz, 3H); ^{13}C NMR (400 MHz, $CDCl_3$) δ 160.7, 141.3, 137.9, 136.9, 132.6, 131.8, 130.7, 130.4, 130.1, 128.8, 128.3,125.4, 125.3, 115.3, 67.1, 21.8, 10.2; Anal. ($C_{19}H_{14}Cl_2N_3O_2$): C, 51.37; H, 3.18; N, 9.46. Found: C, 51.18; H, 3.22; N, 9.23.

1-(2,4-Dichlorophenyl)-5-(4-methoxy-2-methylphenyl)-4-propoxycarbonyl-1H-1,2,3-triazole (31h). Yield 12%, as a colorless oil. ^{1}H NMR (400 MHz, $CDCl_3$) δ 7.49 (s, 1H), 7.22-7.32 (m, 2H), 6.97 (d, J = 8.4 Hz, 1H), 6.76 (s, 1H), 6.67 (d, J = 8.4 Hz, 1H), 4.25 (t, J = 6.4 Hz, 2H), 3.78 (s, 3H), 2.14 (s, 3H), 1.68 (sextet, J = 6.8 Hz, 2H), 0.87 (t, J = 7.6 Hz, 3H); ^{13}C NMR (400 MHz, $CDCl_3$) δ 160.7, 142.3, 139.5, 137.3, 137.1, 132.7, 132.1, 131.2, 130.9, 130.4, 129.9, 127.8,116.6, 115.6, 111.3, 66.7, 55.1, 21.8, 20.0, 10.1; Anal. ($C_{20}H_{19}Cl_2N_3O_3$). C, 57.52; H, 4.60; N, 9.89. Found: C, 57.76; H, 4.59; N, 9.93.

1-(2,4-Dichlorophenyl)-5-(4-iodophenyl)-4-propoxycarbonyl-1H-1,2,3-triazole (31i). Yield >2%, as a tan oil. ^{1}H NMR (400 MHz, $CDCl_3$) δ 7.58-7.46 (m, 2H), 7.41 (d, J = 8.2

Hz, 1H), 7.36-7.30 (m, 3H), 7.16 (d, J = 8 Hz, 1H), 4.30-4.25 (m, 2H), 1.70 (td, J = 6.6, 7.4 Hz, 2H), 0.95-0.87 (m, 3H); ^{13}C NMR (400 MHz, $CDCl_3$) δ 160.7, 153.1, 149.2, 143.2, 141.9, 137.6, 135.4, 131.6, 130.7, 130.5, 130.2, 128.9, 128.2, 127.7, 125.8, 66.9, 21.9, 10.2.

1-(2,4-Dichlorophenyl)-5-(3-chlorophenyl)-4-propoxycarbonyl-1H-1,2,3-triazole (31j). Yield 60%, as a white solid; mp 105-106 °C. ^{1}H NMR (400 MHz, $CDCl_3$) δ 7.49 (d, J = 1.6 Hz, 1H), 7.39-7.32 (m, 3H), 7.29-7.25 (m, 2H), 7.12 (d, J = 8 Hz, 1H), 4.27(t, J = 6.8 Hz, 2H)1.71 (sextet, J = 7.6, 6.8, 7.2, 7.2, 6.8 Hz, 2H), 0.89 (t, J = 7.6, 7.2 Hz, 3H); ^{13}C NMR (400 MHz, $CDCl_3$) δ 160.8, 141.4, 137.9, 137, 134.5, 132.9, 132.1, 130.8, 130.6, 130.4, 130.3, 129.8, 128.5, 128.1, 127, 67.3, 22.1, 10.5; Anal. ($C_{18}H_{14}Cl_3N_3O_2$). C, 52.64; H, 3.44; N, 10.23. Found: C, 52.73; H, 3.38; N, 10.05.

1-(2,4-Dichlorophenyl)-5-(3-chlorophenyl)-4-propoxycarbonyl-1H-1,2,3-triazole (31k). Yield 54%, as a white solid; mp 110-110.5 °C. ^{1}H NMR (400 MHz, $CDCl_3$) δ 7.66 (d, J = 5.6 Hz, 1H), 7.58 (s, 1H), 7.51-7.45 (m, 3H), 7.40-7.35 (m, 2H), 4.26 (t, J = 6.4,6.8 Hz, 2H),1.68 (sextet, J = 7.2 Hz, 2H), 0.86 (t, J = 7.6, 7.2 Hz, 3H); ^{13}C NMR (400 MHz,

$CDCl_3$) δ 160.5, 141.0, 137.8, 136.8, 133.1, 132.6, 131.7, 131.0, 130.7, 130.6, 130.2, 128.9, 128.3, 126.9, 126.0, 67.1, 21.8, 10.2; Anal. ($C_{19}H_{14}Cl_2N_3F_3O_2$). C, 51.37; H, 3.18; N, 9.46. Found: C, 51.22; H, 3.06; N, 9.40.

1-(2,4-Dichlorophenyl)-5-(3-methylphenyl)-4-propoxycarbonyl-1H-1,2,3-triazole (31l). Yield 43%, as a white solid; mp 101-102 °C. ^{1}H NMR (400 MHz, $CDCl_3$) δ 7.48 (d, *J* = 2 Hz, 1H), 7.35-7.28 (m, 2H), 7.23-7.18 (m, 2H), 7.11 (s, 1H), 7.05-7.02 (m,1H), 4.26 (t, *J* = 6.4,6.8 Hz, 2H), 2.30 (s, 3H), 1.69 (sextet, *J* = 7.2 Hz, 2H), 0.88 (t, *J* = 7.6, 7.2 Hz, 3H); ^{13}C NMR (400 MHz, $CDCl_3$) δ 160.9, 142.8, 142.5, 138,0, 137.3, 136.4, 132.9, 132.3, 130.9, 130.5, 130.2, 128.2, 127.9, 126.8, 124.9, 115.4, 66.9, 21.8, 21.3, 10.3; Anal. ($C_{19}H_{17}Cl_2N_3O_2$• 0.15 C_7H_8). C, 59.60; H, 4.54; N, 10.40. Found: C, 59.36; H, 4.81; N, 10.33.

1-(2,4-Dichlorophenyl)-5-(4-chlorophenyl)-phenoxycarbonyl-1H-1,2,3-triazole (32a). Yield, 13% as a white solid; mp 205-208 °C. ^{1}H NMR (400 MHz, $CDCl_3$) δ 7.96-7.21 (m, 12H). ^{13}C NMR (400 MHz, $CDCl_3$) δ 169.4, 150.4, 142.9, 138.0, 137.0, 135.9, 132.8,

132.0, 131.4, 130.8, 130.4, 129.7, 129.0, 128.6, 126.4, 123.1, 121.7. Anal. ($C_{21}H_{12}Cl_3N_3O_2$): C, 57.64; H, 3.08; N, 9.16. Found: C, 57.84; H, 3.21; N, 9.08.

1-(2,4-Dichlorophenyl)-4-phenoxycarbonyl-5-phenyl-1H-1,2,3-triazole (32b). Yield 11%, as a white solid; mp 209-211 °C. ^{1}H NMR (400 MHz, $CDCl_3$) δ 7.50 (s, 1H), 7.33-7.40 (m, 8H), 7.19-7.26 (m, 4H); ^{13}C NMR (400 MHz, $CDCl_3$) δ 159.3, 150.3, 143.7, 137.5, 135.6, 132.8, 132.1, 130.5, 130.4, 130.2, 129.8, 129.4, 128.4, 128.2, 126.1, 124.5, 121.6; Anal. ($C_{21}H_{13}Cl_2N_3O_2$• $0.33H_2O$): C, 60.60; H, 3.31; N, 10.10. Found: C, 60.30; H, 3.05; N, 10.16.

1-(2,4-dichlorophenyl)-5-(4-fluorophenyl)-4-phenoxycarbonyl-1H-1,2,3-triazole (32c). Yield 30%, as a white solid; mp 230-231 °C. ^{1}H NMR (400 MHz, $CDCl_3$) δ 7.52 (s, 1H), 7.32-7.42 (m, 7H), 7.19-7.26 (m, 3H), 7.04 (t, J = 8.6 Hz, 2H) ; ^{13}C NMR (400 MHz, $CDCl_3$) δ 164.9, 162.5, 159.3, 150.2, 142.9, 137.8, 135.6, 132.7, 132.1, 132.0, 130.7, 130.2, 129.5, 128.3, 126.2, 121.6, 120.5, 120.4, 115.9, 115.7; Anal. ($C_{21}H_{12}Cl_2N_3O_2F$): C, 58.90; H, 2.82; N, 9.81. Found: C, 58.63; H, 2.66; N, 9.80.

5-(4-Bromophenyl)-1-(2,4-dichlorophenyl)-4-phenoxycarbonyl-1H-1,2,3-triazole (32d). Yield 9%, as a white solid; mp 191-192 °C. ^{1}H NMR (400 MHz, $CDCl_3$) δ 7.52 (s, 1H), 7.48 (d, *J* = 7.0 Hz, 2H), 7.37-7.42 (m, 5H), 7.19-7.26(m, 4H); ^{13}C NMR (400 MHz, $CDCl_3$) δ 159.3, 150.2, 142.7, 137.8, 135.7, 132.6, 131.9, 131.8, 131.4, 130.7, 130.2, 129.5, 128.4, 126.2, 125.2, 123.4, 121.6; Anal. ($C_{21}H_{12}Cl_2N_3O_2Br$): C, 51.56; H, 2.47; N, 8.59. Found: C, 51.67; H, 2.64; N, 8.39.

1-(2,4-Dichlorophenyl)-5-(4-methylphenyl)-4-phenoxycarbonyl-1H-1,2,3-triazole (32e). Yield 24%, as a white solid; 203-204 °C. ^{1}H NMR (400 MHz, $CDCl_3$) δ 7.51 (s, 1H), 7.35-7.41 (m, 4H), 7.26 (s, 1H), 7.20-7.24 (m, 4H), 7.13 (d, *J* = 8.0 Hz, 2H), 2.32 (s, 3H); ^{13}C NMR (400 MHz, $CDCl_3$) δ 159.4, 150.3, 143.9, 140.7, 137.4, 135.2, 132.8, 132.3, 130.6, 130.2, 129.7, 129.4, 129.1, 128.1, 126.0, 121.7, 121.4, 21.4; Anal. ($C_{22}H_{15}Cl_2N_3O_2$): C, 62.28; H, 3.56; N, 9.90. Found: C, 62.00; H, 3.39; N, 9.90.

1-(2,4-Dichlorophenyl)-5-(4-phenoxyphenyl)-4-phenoxycarbonyl-1H-1,2,3-triazole (32f). Yield 10%, as an orange solid; mp 159-161 °C. ^{1}H NMR (400 MHz, $CDCl_3$) δ 7.53(s, 1H), 7.38-7.42 (m, 3H), 7.35 (t, *J* = 8.0 Hz, 2H), 7.27-7.30 (m, 2H), 7.24 (t, *J* =

8.2 Hz, 3H), 7.16 (t, *J* = 7.6 Hz, 2H), 7.01(d, *J* = 8.2 Hz, 2H), 6.91(d, *J* = 6.8 Hz, 2H); ^{13}C NMR (400 MHz, $CDCl_3$) δ 159.6, 159.4, 155.3, 150.3, 143.4, 137.5, 135.3, 132.7, 132.2, 131.6, 130.6, 130.2, 129.9, 129.4, 128.2, 126.1, 124.5, 121.6, 120.1, 118.2, 117.4; Anal. ($C_{27}H_{17}Cl_2N_3O_3$): C, 64.55; H, 3.41; N, 8.36. Found: C, 64.23; H, 3.45; N, 8.04.

General procedure for synthesis of 4-ketocarbonyl-5-(substituted phenyl)-1-(2,4-dichlorophenyl)-1H-1,2,3-triazoles.(**33-35**) Under a nitrogen atmosphere, a solution of ethyl magnesium bromide (1.5 mL, 1.0 M in THF) was added dropwise to neat aryl-acetylene (1.05 mmol) or in anhydrous THF (1 mL) at rt. The mixture was heated to 50 °C and stirring was continued for 1 h. A solution of freshly made 2,4-dichlorophenyl azide (**24**, 1 mmol) in 1 mL THF was added dropwise and the mixture was heated to 50 ºC for 1 h. The solution was allowed to cool to room temperature and added dropwise to a solution of alkanoyl chloride (1.5 mmol) in THF (3 mL) at -20ºC under inert conditions. After stirring for 3 h, or until the tentative product spot on thin layer chromatography was not changing, the reaction was quenched with sat. NH_4Cl (5 mL) and diluted with EtOAc

(30 mL). The organic fraction was separated. The aqueous fraction was extracted with EtOAc (2×30 mL). The combined organic fractions were washed with brine (30 mL), dried over anhydrous $MgSO_4$, filtered, and concentrated under reduced pressure. The residue was purified by chromatography (SiO_2, EtOAc/hexanes; 1/5) or by preparative TLC (SiO_2, EtOAc/hexanes/CH_2Cl_2; 1/3/1) to afford the corresponding 4-ketocarbonyl-1-(2,4-dichlorophenyl)- 5-(substituted phenyl)-1H-1,2,3-triazole.

1-(5-(4-chlorophenyl)-1-(2,4-dichlorophenyl)-1H-1,2,3-triazol-4-yl)propan-1-one (33a)

Yield 18%, as a white powder; mp 153-153.5 °C. ^{1}H NMR (400 MHz, $CDCl_3$) δ 7.50(s, 1H), 7.30-7.37(m, 4H), 7.21-7.23(m, 2H); ^{13}C NMR (400 MHz, CDCl3) δ 195.8, 142.5, 139.8, 137.6, 136.5, 132.6, 132.0, 131.2, 130.6, 130.1, 128.7, 128.3, 123.4, 33.7, 7.6; Anal. Calcd for $C_{17}H_{12}Cl_3N_3O$• 0.33 H_2O: C, 52.81; H, 3.30; N, 10.87. Found: C, 52.83; H, 3.01; N, 10.56.

1-(1-(2,4-dichlorophenyl)-5-(4-fluorophenyl)-1H-1,2,3-triazol-4-yl)propan-1-one (33b)

Yield 30%, as a white powder; mp 115-116 °C. ^{1}H NMR (400 MHz, $CDCl_3$) δ 7.51(s, 1H), 7.27-7.40(m, 4H), 7.04(t, J=8.6Hz, 2H), 3.29(q, J=11Hz, 2H), 1.23(J=7.4Hz, 3H);

^{13}C NMR (400 MHz, $CDCl_3$) δ 196.1, 165.1, 162.6, 142.7, 140.3, 137.7, 132.9, 132.3, 132.2, 130.9, 130.3, 128.5, 121.2, 121.1, 116.0, 115.8, 33.9, 7.8; Anal. Calcd for $C_{17}H_{12}Cl_2N_3OF$: C, 56.06; H, 3.32; N, 11.54. Found: C, 56.13; H, 3.23; N, 11.34.

1-(5-(4-bromophenyl)-1-(2,4-dichlorophenyl)-1H-1,2,3-triazol-4-yl)propan-1-one (33c) Yield 11%, as a yellow powder; mp 157-160 °C. ^1H NMR (400 MHz, $CDCl_3$) δ 7.50(s, 1H), 7.47(d, J=6.8Hz, 2H), 7.38(d, J=8.4Hz, 1H), 7.32(d, J=8.4Hz, 1H), 7.15(d, d, J=6.6Hz, 2H), 3.29(q, J=7.6, 7.2, 7.2Hz, 2H), 1.22(t, J=7.6, 7.2Hz, 3H); ^{13}C NMR (400 MHz, $CDCl_3$) δ 195.9, 142.5, 139.9, 137.6, 132.6, 132.0, 131.7, 131.4, 130.7, 130.1, 128.3, 124.9, 123.9, 33.7, 7.6; Anal. Calcd for $C_{17}H_{12}Cl_2N_3OBr$ •0.7 H_2O: C, 46.65; H, 3.09; N, 9.60. Found: C, 46.95; H, 2.66; N, 9.26.

1-(1-(2,4-dichlorophenyl)-5-(p-tolyl)-1H-1,2,3-triazol-4-yl)propan-1-one (33d) Yield 15%, as a pale yellow powder; mp 123-125 °C. ^1H NMR (400 MHz, $CDCl_3$) δ 7.48(s, 1H), 7.29-7.36(m, 2H), 7.16(d, J=7.2Hz, 2H), 7.12(d, J=8.4Hz, 2H), 3.27(q, J=7.2, 7.6, 7.2Hz, 2H), 2.33(s, 3H), 1.21(t, J=7.2, 7.6Hz, 3H); ^{13}C NMR (400 MHz, $CDCl_3$) δ 195.8, 142.4, 141.1, 140.4, 137.2, 132.8, 132.4, 130.5, 130.2, 129.7, 129.0, 128.1, 121.8,

115.3, 33.6, 21.4, 7.6; Anal. Calcd for $C_{18}H_{15}Cl_2N_3O$: C, 60.01; H, 4.20; N, 11.66. Found: C, 59.77; H, 4.24; N, 11.44.

1-(5-(4-chlorophenyl)-1-(2,4-dichlorophenyl)-1H-1,2,3-triazol-4-yl)butan-1-one (34a)

Yield 5%, as a pale white solid; mp 133-134 °C. ^{1}H NMR (400 MHz, $CDCl_3$) δ 7.52(s, 1H), 7.32-7.34(m, 4H), 7.23,(d, J=7.6 Hz, 2 H), 3.25(t, J=7.2Hz, 2H), 1.79(sextet, J=7.6Hz, 2H),1.03(t, J=7.6Hz, 3H); ^{13}C NMR (400 MHz, $CDCl_3$) δ 139.9, 137.6, 136.6, 135.2, 131.2, 130.7, 130.1, 128.7, 128.3, 123.4, 42.3, 17.2, 13.8 ; Anal. Calcd for $C_{18}H_{14}Cl_3N_3O•H_2O$: C, 52.39; H, 3.91; N, 10.18. Found: C, 52.59; H, 3.51; N, 9.44.

1-(1-(2,4-dichlorophenyl)-5-(4-fluorophenyl)-1H-1,2,3-triazol-4-yl)butan-1-one (34b)

Yield 40%, as a white powder; mp 98-100 °C. ^{1}H NMR (400 MHz, $CDCl_3$) δ 7.50(s, 1H), 7.26-7.39(m, 4H), 7.00-7.05(m, 2H), 3.24(t, J=7.2Hz, 2H), 1.78(sextet, J=7.6Hz, 2H), 1.02(t, J=7.6Hz, 3H); ^{13}C NMR (400 MHz, $CDCl_3$) δ 195.7, 165.1, 162.6, 142.8, 137.8, 132.9, 132.4, 132.3, 132.2, 130.9, 130.4, 128.5, 121.2, 121.2, 116.1, 115.8, 42.5, 17.4, 14.0; Anal. Calcd for $C_{18}H_{14}Cl_2N_3OF$: C, 57.16; H, 3.73; N, 11.11. Found: C, 57.08; H, 3.54; N, 10.84.

1-(5-(4-bromophenyl)-1-(2,4-dichlorophenyl)-1H-1,2,3-triazol-4-yl)butan-1-one (34c)

Yield 7%, as a white waxy solid. ^{1}H NMR (400 MHz, $CDCl_3$) δ 7.47-7.51(m, 2H), 7.32-7.41(m, 3H), 7.16(d, J=8Hz, 2H), 3.25(t, J=7.2Hz, 2H), 1.79(sextet, J=7.2Hz, 2H), 1.03(t, J=7.2Hz, 3H) ; ^{13}C NMR (400 MHz, $CDCl_3$) δ 195.4, 155.1, 142.6, 137.6, 132.6, 132.0, 131.7, 131.4, 130.7, 130.1, 128.3, 124.9, 123.9, 42.3, 17.2, 13.8; Anal. Calcd for $C_{18}H_{14}Cl_2N_3OBr$• 0.25 H_2O: C, 51.3; H, 3.48; N, 9.09. Found: C, 50.91; H, 3.69; N, 8.74.

1-(1-(2,4-dichlorophenyl)-5-(4-phenoxyphenyl)-1H-1,2,3-triazol-4-yl)butan-1-one (34d) Yield 30%, as an oil. ^{1}H NMR (400 MHz, $CDCl_3$) δ 7.50(s, 1H), 7.30-7.374(m, 3H), 7.23(d, J=8.4Hz, 2H), 7.16(t, J=7.2Hz, 2H), 7.03(d, J=8Hz, 2H), 6.89(d, J=8.8Hz, 2H), 3.24(t, J=7.2Hz, 2H), 1.78(sextet, J=7.2Hz, 2H), 1.02(t, J=7.2, 7.6Hz, 3H); ^{13}C NMR (400 MHz, $CDCl_3$) δ 195.4, 159.4, 155.5, 142.4, 140.6, 137.3, 132.7, 132.4, 131.5, 130.6, 130.1, 129.9, 128.2, 124.4, 120.1,118.8, 117.3, 42.3, 17.2, 13.8; Anal. Calcd for $C_{24}H_{19}Cl_2N_3O_2$: C, 63.73; H, 4.23; N, 9.29. Found: C, 63.85; H, 4.24; N, 9.11.

1-(1-(2,4-dichlorophenyl)-5-(4-(trifluoromethyl)phenyl)-1H-1,2,3-triazol-4-yl)butan-1-one (34e) Yield 9%, as a white powder; mp 102-104 °C. ^{1}H NMR (400 MHz, $CDCl_3$) δ

7.59(d, J=8Hz, 2H), 7.49(s, 1H), 7.41(d, J=8Hz, 2H), 7.33-7.37(m, 1H), 3.24(t, J=7.2Hz, 2H), 1.78(sextet, J=7.2Hz, 2H), 1.02(t, J=7.2, 7.6Hz, 3H); ^{13}C NMR (400 MHz, $CDCl_3$) δ 195.3, 142.9, 139.5, 137.7, 132.5, 132.2, 131.8, 130.7, 130.3, 130, 129.3, 128.8, 128.4, 128.3, 125.298, 125.2, 124.9, 122.2, 42.2, 17.1, 13.8 ; Anal. Calcd for $C_{19}H_{14}Cl_2N_3OF_3$• 0.05 C_7H_8: C, 53.69; H, 3.35; N, 9.71. Found: C, 53.65; H, 3.40; N, 9.32.

1-(1-(2,4-dichlorophenyl)-5-p-tolyl-1H-1,2,3-triazol-4-yl)butan-1-one (34f) Yield 15%, as a white powder; mp 94-96 °C. ^{1}H NMR (400 MHz, $CDCl_3$) δ 7.47(d, J=2Hz, 1H), 7.26-7.36(m, 2H), 7.13(q, J=8,10,8 Hz, 4H), 3.21(t, J=7.2 Hz, 2H), 2.31(s, 3H), 1.77(sextet, J=7.2, 7.6, 7.2Hz, 2H), 1.00(t, J=7.6, 7.4Hz, 3H) ; ^{13}C NMR (400 MHz, $CDCl_3$) δ 195.2, 142.4, 141.1, 140.3, 137.1, 132.7, 132.4, 130.4, 130.1, 129.6, 128.9, 128, 121.8, 42.2, 21.4, 17.2, 13.8; Anal. Calcd for $C_{19}H_{17}Cl_2N_3O$•0.1 C_7H_8: C, 61.70; H, 4.68; N, 10.96. Found: C, 61.76; H, 4.70; N, 11.02.

1-(5-(4-chlorophenyl)-1-(2,4-dichlorophenyl)-1H-1,2,3-triazol-4-yl)pentan-1-one (35a) Yield 11%, as a white powder; mp 123-124 °C. ^{1}H NMR (400 MHz, $CDCl_3$) δ 7.48(d, J=2 Hz, 1H), 7.28-7.39(m, 4H), 7.21(d, J=8.8Hz, 2H), 3.24(t, J= 7.2, 7.6Hz, 2H),

1.72(quintet, J=7.2, 7.6, 8Hz, 2H), 1.42(sextet, J=7.6, 7.2 Hz, 2H), 0.94(t, J=7.2Hz, 3H); ^{13}C NMR (400 MHz, $CDCl_3$) δ 195.4, 142.6, 139.8, 137.5, 136.4, 132.5, 132.3, 131.9, 131.4, 131.1, 130.6, 130.1, 130, 128.6, 128.4, 128.3,128.2,123.4, 40, 25.7, 22.3, 13.9; Anal. Calcd for $C_{19}H_{16}Cl_2N_3O$•0.05 C_7H_8: C, 56.23; H, 4.00; N, 10.17. Found: C, 56.10; H, 3.85; N, 9.79.

1-(1-(2,4-dichlorophenyl)-5-(4-fluorophenyl)-1H-1,2,3-triazol-4-yl)pentan-1-one (35b)

Yield 4%, as an off white powder; mp 96.5-99 °C. ^{1}H NMR (400 MHz, $CDCl_3$) δ 7.49(s, 1 H), 7.26-7.39(m, 4H), 7.02(t, J=8.6Hz, 2H), 3.25(t, J=7.4Hz, 2H), 1.73(quintet, J=7.2Hz, 2H), 1.43(sextet, J=6.8, 6.4, 7.2Hz, 2H), 0.95(t, J=7.4Hz, 3H); ^{13}C NMR (400 MHz, $CDCl_3$) δ 195.6, 164.9, 163.3, 143.1, 142.6, 140.0, 137.5, 132.6,132.0, 131.9, 130.6, 130.1,128.6, 128.2, 127.9, 122.2, 120.96, 120.93, 40.1, 25.8, 22.3, 13.9; Anal. Calcd for $C_{19}H_{16}Cl_2N_3OF$: C, 58.18; H, 4.11; N, 10.71. Found: C, 58.05; H, 4.06; N, 10.50.

1-(5-(4-bromophenyl)-1-(2,4-dichlorophenyl)-1H-1,2,3-triazol-4-yl)pentan-1-one (35c)

*Yield 18%, as a yellow powder; mp 156-158 °C. ^{1}H NMR (400 MHz, $CDCl_3$) δ 7.49(s, 1H), 7.46(d, J=7.6Hz, 2H), 7.37(d, J=8.4Hz, 1H), 7.32(d, J=8.4Hz, 1H), 7.14(d, J=7.6Hz,

2H), 3.25(t, J=7.6, 7.2Hz, 2H), 1.72(quintet, J=8, 7.6Hz, 2H), 1.42(sextet, J=7.6Hz, 2H), 0.95(t, J=7.6Hz, 3H); ^{13}C NMR (400 MHz, CDCl3) δ 195.4, 142.6, 139.8, 137.5, 132.5, 132.2, 131.9, 131.6, 131.3, 130.6, 130.0, 128.6, 128.2, 127.8, 124.9, 123.9, 40.0, 25.8, 22.3, 13.9; Anal. Calcd for $C_{19}H_{16}Cl_2N_3OBr$ • 0.45 H_2O : C, 49.47; H, 3.69; N, 9.11. Found: C, 49.82; H, 3.45; N, 8.72.

1-(1-(2,4-dichlorophenyl)-5-p-tolyl-1H-1,2,3-triazol-4-yl)pentan-1-one (35d) Yield 27%, as a white powder; mp 99-100 °C. ^{1}H NMR (400 MHz, $CDCl_3$) δ 7.45(s, 1H), 7.28-7.33(m, 2H), 7.15(d, J=8Hz, 2H), 3.22(t, J=7.6, 2H), 2.29(s, 3H), 1.71(quintet, J=7.6Hz, 2H), 1.40(sextet, J=7.6Hz, 2H), 0.92(t, J=7.2Hz, 3H); ^{13}C NMR (400 MHz, $CDCl_3$) δ 195.2, 142.3, 141, 140.2, 137, 132.6, 132.3, 130.3, 130.1, 129.6, 128.9, 128, 121.8, 39.9, 25.7, 22.3, 21.3, 13.8; Anal. Calcd for $C_{20}H_{19}Cl_2N_3O$: C, 61.86; H, 4.93; N, 10.82. Found: C, 62.05; H, 5.00; N, 10.63.

1-(1-(2,4-dichlorophenyl)-5-(4-phenoxyphenyl)-1H-1,2,3-triazol-4-yl)pentan-1-one (35e) Yield 50%, as a tan oil. ^{1}H NMR (400 MHz, $CDCl_3$) δ 7.51(s, 1H), 7.30-7.39(m, 3H), 7.23(d, J=6.8Hz, 2H), 7.14-7.18(m, 2H), 7.04(d, J=8Hz, 2H), 6.89(d, J=6.8Hz, 2H),

3.26(t, J=7.2,7.6Hz, 2H), 1.74(quintet, J=7.6, 7.2Hz, 2H), 1.43(sextet, J=7.6, 7.2Hz, 2H), 0.96(t, J=6.4, 7.2Hz, 3H); ^{13}C NMR (400 MHz, $CDCl_3$) δ 195.5, 159.3, 155.4, 142.3, 140.5, 137.2, 132.6, 132.3, 131.5, 130.5, 130.1, 129.9, 128.1, 124.4, 120.1, 118.7, 117.3, 40.0, 25.8, 22.3, 13.8; Anal. Calcd for $C_{25}H_{21}C_{l2}N_3O_2$•0.1 C_7H_8: C, 64.91; H, 4.62; N, 8.84. Found: C, 64.77; H, 4.54; N, 8.84.

1-(1-(2,4-dichlorophenyl)-5-(4-(trifluoromethyl)phenyl)-1H-1,2,3-triazol-4-yl)pentan-1-one (35f) Yield 11%, as a white powder; mp 107.5-110 °C. ^1H NMR (400 MHz, $CDCl_3$) δ 7.6 (d, J=8.4Hz, 2H), 7.51 (d, J=2Hz, 1H), 7.41 (d, J=7.6 Hz, 2H), 7.38 (d, J=2 Hz, 1H), 7.35 (s, 1H), 3.27 (t, J=7.2, 2H), 1.73 (quintet, J=7.6, 2H), 1.44 (sextet, J=7.6 Hz, 2H), 0.96 (J=7.2, 7.6 Hz, 3H); ^{13}C NMR (400 MHz, $CDCl_3$) δ 195.5, 142.9, 139.5, 137.8,, 132.6, 131.8, 130.7, 130.3, 130, 129.3, 128.8, 128.3, 125.3, 125.3, 122.2, 40.1, 25.8, 22.4, 13.9; Anal. Calcd for ($C_{20}H_{16}Cl_2N_3OF_3$• 0.05 C_7H_8): C, 54.70; H, 3.70; N, 9.40. Found: C, 54.31; H, 3.84; N, 8.78.

General Procedure for synthesis of 5-(substituted phenyl)-1-(2,4-dichlorophenyl)-1H-[1,2,3]triazoles (36). Under a nitrogen atmosphere, a solution of ethyl magnesium

bromide (1.5 mL, 1.0 M in THF) was added dropwise to neat aryl-acetylene (1.05 mmol) or in anhydrous THF (1 mL) at rt. The mixture was heated to 50 °C and stirring was continued for 1 h. A solution of freshly made 2,4-dichlorophenyl azide (**24**, 1 mmol) in 1 mL THF was added dropwise and the mixture was heated to 50 ºC for 1 h. The solution was allowed to cool to room temperature was quenched with sat. NH_4Cl (20 mL) and diluted with EtOAc (30 mL). The organic fraction was separated. The aqueous fraction was extracted with EtOAc (2×30 mL). The combined organic fractions were washed with brine (30 mL), dried over anhydrous $MgSO_4$, filtered, and concentrated under reduced pressure. The residue was purified by chromatography (SiO_2, EtOAc/hexanes; 1/5) to afford the corresponding 1-(2,4-dichlorophenyl)- 5-(substituted phenyl)-1,2,3-triazole.

5-(4-Chlorophenyl)-1-(2,4-dichlorophenyl)-1H-1,2,3-triazole (36a). Yield, 85%, as a light yellow solid; mp 140-141 °C. ^1H NMR (400 MHz, $CDCl_3$) δ 8.28 (s, 1H), 7.96-7.28 (m, 7H). ^{13}C NMR (400 MHz, $CDCl_3$) δ 138.6, 135.8, 137.4, 136.0, 133.2, 132.7, 132.6, 130.9, 130.3, 129.6, 129.2, 128.6, 124.9. Anal. ($C_{14}H_8Cl_3N_3$): C, 51.80; H, 2.48; N, 12.95. Found: C, 51.80; H, 2.48; N, 12.79.

1-(2,4-Dichlorophenyl)-5-phenyl-1H-1,2,3-triazole (36b). Yield 68%, as a brown solid; mp 75-76 °C. ^{1}H NMR (400 MHz, $CDCl_3$) δ 7.91(s, 1H), 7.52v(s, 1H), 7.32-7.42 (m, 5H), 7.19 (d, *J* = 8.0 Hz, 2H); ^{13}C NMR (400 MHz, $CDCl_3$) δ 139.4, 136.9, 133.3, 132.7, 132.4, 130.6, 130.1, 129.5, 129.0, 128.2, 127.7, 126.2; Anal. ($C_{14}H_9Cl_2N_3$): C, 57.95; H,3.13; N, 14.48. Found: C, 57.67; H, 3.21; N, 13.79.

1-(2,4-Dichlorophenyl)-5-(4-fluorophenyl)-1H-1,2,3-triazole (36c). Yield 57%, as a white solid; mp 130-131 °C. ^{1}H NMR (400 MHz, $CDCl_3$) δ 7.89 (s, 1H), 7.53 (s, 1H), 7.74 (s, 2H), 7.15-7.23 (m, 2H), 7.01-7.09 (m, 2H) ; ^{13}C NMR (400 MHz, $CDCl_3$)δ 164.5, 138.6, 137.1, 132.4, 130.6, 130.1, 129.8, 129.7, 128.3, 122.3, 116.4, 116.2; Anal. ($C_{14}H_8Cl_2N_3F$): C, 54.57; H, 2.62; N, 13.64. Found: C, 54.51; H, 2.62; N, 13.53.

5-(4-Bromophenyl)-1-(2,4-dichlorophenyl)-1H-1,2,3-triazole (36d). Yield 60%, as a white crystalline solid; mp 157-157 °C. ^{1}H NMR (400 MHz, $CDCl_3$) δ 7.91 (s, 1H), 7.53 (s, 1H), 7.42-7.48 (m, 4H), 7.06 (d, *J* = 8.8 Hz, 2H); ^{13}C NMR (400 MHz, $CDCl_3$) δ 138.7, 137.5, 13.2, 132.8, 132.7, 132.6, 130.9, 130.3, 129.4, 128.6, 125.4, 124.3; Anal. ($C_{14}H_8Cl_2N_3Br$): C, 45.56; H, 2.18; N, 11.39. Found: C, 45.46; H, 2.11; N, 11.32.

1-(2,4-Dichlorophenyl)-5-(4-methylphenyl)-1H-1,2,3-triazole (36e). Yield 66%, as a yellow crystalline solid; mp 118-121 °C. ^{1}H NMR (400 MHz, $CDCl_3$) δ 7.89 (s, 1H), 7.54 (s, 1H), 7.42 (s, 2 H), 7.08-7.16 (m, 4H), 2.35 (3, H); ^{13}C NMR (400 MHz, $CDCl_3$) δ 139.5, 136.99, 132.97, 132.2, 130.6, 130.2, 129.8, 129.7, 128.2, 127.997, 127.6, 123.3, 21.3; Anal. ($C_{15}H_{11}Cl_2N_3$): C, 59.23; H, 3.65; N, 13.81. Found: C, 59.24; H, 3.94; N, 12.63.

1-(2,4-Dichlorophenyl)-5-(4-methoxyphenyl)-1H-1,2,3-triazole (36f). Yield 73%, as a yellow solid; mp 120-121.5 °C. ^{1}H NMR (400 MHz, $CDCl_3$) δ 7.84(s, 1H), 7.52 (s, 1H), 7.41 (s, 2H), 7.42 (d, *J* = 8.0 Hz, 2H), 6.85 (d, *J* =8.0 Hz, 2H), 3.81(s, 3H); ^{13}C NMR (400 MHz, $CDCl_3$) δ 160.4, 139.3, 136.8, 133.4, 132.7, 131.8, 130.5, 130.1, 129.1, 128.2, 118.4, 114.4, 55.3. Anal. ($C_{15}H_{11}Cl_2N_3O$): C, 56.27; H, 3.46; N, 13.12. Found: C, 56.24; H, 3.52; N, 12.83.

1-(2,4-Dichlorophenyl)-5-(4-trifluoromethylphenyl)-1H-1,2,3-triazole (36g). Yield 66%, as a white solid; mp 123-123.5 °C. ^{1}H NMR (400 MHz, $CDCl_3$) δ 7.98 (s, 1H), 7.61 (d, *J* = 8.4 Hz, 2 H), 7.55 (s, 1H), 7.46 (s, 2H), 7.33 (d, *J* = 8.0 Hz, 2H); ^{13}C NMR (400 MHz,

$CDCl_3$) δ 138.1, 137.4, 132.9, 132.8, 132.5 130.8. 130.0, 128.5, 128.0, 126.1, 126.0; Anal. ($C_{15}H_8Cl_2N_3F_3$): C, 50.30; H, 2.25; N, 11.73. Found: C, 50.35; H, 2.03; N, 11.73.

1-(2,4-Dichlorophenyl)-5-(4-phenoxyphenyl)-1H-1,2,3-triazole (36h). Yield 77%, as a yellow oil. ^{1}H NMR (400 MHz, $CDCl_3$) δ 7.89 (s, 1H), 7.55 (s, 1H), 7.43 (s, 2H), 7.38 (t, *J* = 8.0 Hz, 2H), 7.13-7.19(m, 3H), 7.03 (d, *J* = 8.6Hz, 2H), 6.93 (d, *J* = 6.6 Hz, 2H); ^{13}C NMR (400 MHz, $CDCl_3$) δ 158.8, 155.7, 139.0, 137.0, 133.3, 132.7, 132.2, 130.6, 130.1, 129.9, 129.3, 128.3, 124.3, 120.5, 119.9, 118.3; Anal. ($C_{20}H_{13}Cl_2N_3O$): C, 62.84; H, 3.43; N, 10.99. Found: C, 63.13; H, 3.39; N, 10.81.

1-(2,4-Dichlorophenyl)-5-(4-dimethylaminophenyl)-1H-1,2,3-triazole (36i). Yield 55%, as a yellow crystalline solid; mp 139.5-140.5 °C. ^{1}H NMR (400 MHz, $CDCl_3$) δ 7.82(s, 1H), 7.55 (s, 1H), 7.41 (s, 2H), 7.04 (d, *J* = 8.0 Hz, 2H), 6.59 (d, *J* =7.8 Hz, 2H), 2.93 (s, 6H); ^{13}C NMR (400 MHz, $CDCl_3$) δ 150.6, 139.9, 136.6, 135.2, 133.8, 132.9, 131.2, 130.5, 130.2, 128.5, 128.1, 111.9, 40.1; Anal. ($C_{16}H_{14}Cl_2N_4$): C, 57.67; H, 4.23; N, 16.81. Found: C, 57.69; H, 4.20; N, 16.71.

1-(2,4-Dichlorophenyl)-5-(4-methoxy-2-methylphenyl)-1H-1,2,3-triazole (36j). Yield 61%, as a colorless oil. ^{1}H NMR (400 MHz, $CDCl_3$) δ 7.78 (s, 1H), 7.48 (s, 1H), 7.32-7.33 (m, 2H), 6.90 (d, *J* = 8.4 Hz, 1H), 6.77 (s, 1H), 6.64 (d, *J* = 8.4 Hz, 1H), 3.79 (s, 3H), 2.22 (s, 3H); ^{13}C NMR (400 MHz, $CDCl_3$) δ 160.4, 138.9, 138.3, 136.5, 133.7, 131.3, 130.5, 130.0, 127.9, 117.4, 116.0, 111.5, 55.2, 20.4; Anal. ($C_{16}H_{13}Cl_2N_3O$): C, 57.50 ; H, 3.92; N, 12.57. Found: C, 57.51; H, 3.77; N, 12.44.

1-(2,4-Dichlorophenyl)-5-(4-fluoro-3-methylphenyl)-1H-1,2,3-triazole (36k). Yield 58%, as a white solid; mp 136-137 °C. ^{1}H NMR (400 MHz, $CDCl_3$) δ 7.87 (s, 1H), 7.54 (s, 1H), 7.42 (s, 2H), 7.97 (d, *J* = 7.2Hz, 1H), 6.89-6.98 (m, 2H), 2.23 (s, 3H); ^{13}C NMR (400 MHz, $CDCl_3$) δ 163.1, 160.6, 138.8, 137.0, 132.3, 131.3, 131.2, 130.6, 130.1, 128.2, 126.9, 126.8, 115.8, 115.6, 14.5. Anal. ($C_{15}H_{10}Cl_2N_3F$): C, 55.92; H, 3.13; N, 13.04. Found: C, 56.06; H, 2.92; N, 12.99.

1-(2,4-Dichlorophenyl)-5-(3-chlorophenyl)-1H-1,2,3-triazole (36l). Yield 66%, as a waxy solid. ^{1}H NMR (400 MHz, $CDCl_3$) δ 7.92 (s, 1H), 7.54 (t, *J* = 1.2, 1.6 Hz, 1H), 7.44 (d, *J* = 1.2 Hz, 2H), 7.35 (dq, *J* = 7.3 Hz, 1H), 7.28-7.24 (m, 2H), 7.02(dt, *J* = 7.7 Hz,

3H); ^{13}C NMR (400 MHz, $CDCl_3$) δ 138.4, 137.5, 135.2, 133.1, 132.9, 132.8, 130.9, 130.5, 130.3, 129.9, 128.6, 128.2, 128.1, 125.9. Anal. ($C_{14}H_8Cl_2N_3$•0.05 C_7H_8): C, 52.36; H, 2.57; N, 12.76. Found: C, 52.22; H, 2.54; N, 12.37.

General Procedure for synthesis of 5-(substituted phenyl)-1-(2,4-dichlorophenyl)-4-(trimethylsilyl)-[1,2,3]triazoles (37) Under a nitrogen atmosphere, into a 25 mL round-bottomed flask equipped with a condensor was added benzyl azide **24** (1.0 mmol) and (4-substituted)ethynyl trimethylsilane (2.0 mmol), and toluene (7 mL). The mixture was stirred at reflux for 19 h and concentrated *in vacuo*. The residue was purified by chromatography (SiO_2, EtOAc/hexanes; 1/5) to afford the corresponding 4-trimethylsilyl-1-(2,4-dichlorophenyl)-5-(substituted phenyl)-1H-1,2,3-triazole (**37**).

5-(4-chlorophenyl)-1-(2,4-dichlorophenyl)-4-(trimethylsilyl)-1H-1,2,3-triazole (37a) Yield 15%, as a brown powder; mp 139-139.5 °C. ^{1}H NMR (400 MHz, $CDCl_3$) δ 7.47 (s, 1H), 7.28-7.35 (m, 3H), 7.11 (d, J=10 Hz, 2H), 0.21 (s, 9H); ^{13}C NMR (400 MHz, $CDCl_3$) δ 144.6, 143.96, 136.8, 135.7, 135.2, 132.8, 133.8, 130.9, 130.4, 130.2, 128.8, 127.9,

126.3, 0.3; Anal. Calcd for $C_{17}H_{16}Cl_3N_3Si$: C, 51.46; H, 4.06; N, 10.59. Found: C, 51.93; H, 4.21; N, 10.17.

5-(4-bromophenyl)-1-(2,4-dichlorophenyl)-4-(trimethylsilyl)-1H-1,2,3-triazole (37b)

Yield 7%, as a brown flaky solid; mp 148-149 °C. ^{1}H NMR (400 MHz, $CDCl_3$) δ 7.43-7.48(m, 3H), 7.26-7.33(m, 2H), 7.01-7.06(m, 2H), 0.25(s, 9H); ^{13}C NMR (400 MHz, $CDCl_3$) δ 144.5, 143.9, 136.7, 132.8, 132.7, 131.7, 131.1, 130.3, 130.1, 127.9, 126.7, 123.9, -0.7; Anal. Calcd for $C_{17}H_{16}Cl_2N_3BrSi$: C, 46.28; H, 3.66; N, 9.52. Found: C, 46.44; H, 3.55; N, 9.27.

1-(2,4-dichlorophenyl)-5-(4-methoxyphenyl)-4-(trimethylsilyl)-1H-1,2,3-triazole (37c)

Yield 6%, as a dark brown oil. ^{1}H NMR (400 MHz, $CDCl_3$) δ 7.43(s, 1H), 7.254-7.283(m, 2H), 7.06(d, J=8.4Hz, 2H), 6.819 (d, J=8.4 Hz, 2H), 3.78(s, 3H), 0.23(s, 9H) ; ^{13}C NMR (400 MHz, $CDCl_3$) δ 160.3, 145.0, 144.1, 136.4, 133.3, 132.9,130.9,130.3,119.6, 113.8, 55.2, -0.773; Anal. Calcd for $C_{18}H_{19}Cl_2N_3OSi•0.1C_7H_8$: C, 55.93; H,4.97; N, 10.46. Found: C, 55.68; H, 5.22; N, 10.20.

1-(2,4-dichlorophenyl)-4-(trimethylsilyl)-1H-1,2,3-triazol-5-yl)(phenyl)methanol (37d)

Yield 9%, as a white crystalline solid; mp 189.5-190 °C. ^{1}H NMR (400 MHz, $CDCl_3$) δ 7.39(s, 1H), 7.15-7.26(m, 3H), 7.13(d, J=7.6Hz, 1H), 6.96(d, J=6.96Hz, 2H), 6.82(bs, 1H), 6.03(d, J=3.2Hz, 1H), 0.42(s, 9H); ^{13}C NMR (400 MHz, $CDCl_3$) δ 145.8, 144.4, 139.7, 136.6, 135.2, 132.953, 130.4, 129.8, 128.4, 128.2, 127.3, 126.1, -0.3; Anal. Calcd for $C_{18}H_{19}Cl_2N_3OSi$: C, 55.10; H, 4.88; N, 10.71. Found: C, 54.90; H, 4.72; N, 10.62.

1-(2,4-dichlorophenyl)-4-iodo-5-phenyl-1H-1,2,3-triazole (38) Under a nitrogen atmosphere, a solution of ethyl magnesium bromide (1.5 mL, 1.0 M in THF) was added dropwise to neat **29** (1.05 mmol) or in anhydrous THF (1 mL) at rt. The mixture was heated to 50 °C and stirring was continued for 1 h. A solution of freshly made 2,4-dichlorophenyl azide (**24**, 1 mmol) in 1 mL THF was added dropwise and the mixture was heated to 50 ºC for 1 h. The solution was allowed to cool to room temperature and 1.5mmol iodine dissolved in 3ml of THF was added to it. This reaction mixture was heated at 50 ºC for 15h.The reaction was then quenched with 2ml of 1M $Na_2S_2O_3$ and

diluted with EtOAc (30 mL). The organic fraction was separated. The aqueous fraction was extracted with EtOAc (2×30 mL). The combined organic fractions were washed with brine (30 mL), dried over anhydrous $MgSO_4$, filtered, and concentrated under reduced pressure. The residue was purified by chromatography (SiO_2, EtOAc/hexanes; 1/9). Yield 69%, as a pale yellow powder; mp 142-143 °C. ^1H NMR (400 MHz, $CDCl_3$) δ 7.49(s, 1H), 7.36-7.40(m, 6H), 7.25-7.27(m, 1H); ^{13}C NMR (400 MHz, $CDCl_3$) δ 139.0, 137.5, 132.8, 130.8, 130.3, 130.2, 129.5, 129.0, 128.4, 125.6, 110.7, 108.1, 89.9; Anal. Calcd for $C_{14}H_8Cl_2N_3I$: C, 40.02; H, 1.94; N, 10.10. Found: C, 40.21; H, 1.80; N, 9.91.

Procedure for conversion of 38 to 38x: Compound **38** (0.5 mmol), 2,4-dichlorophenyl boronic acid (0.55 mmol), $Pd_2(dba)_3$ (0.025 mmol), tricyclohexylphosphine (0.06 mmol), and K_3PO_4 (0.85 mmol)were suspended in 8 mL THF + 2 mL H_2O in a 30 mL pressure tube. The reaction vessel was purged with N2, sealed, and heated to 120 ºC for 16 hours in an oil bath. The reaction mixture was partitioned between water (40 mL) and EtOAc (40 mL). The organic layer was separated and the aqueous layer was extracted with EtOAc (2 x 40 mL). Combined organic fractions were washed by sat. NaCl, dried

on anhydrous MgSO4, filtered, and concentrated *in vacuo* followed by column purification.

Propyl 3-phenylpropiolate (39) Yield 19%, as a white powder; mp 328-329 °C. ^{1}H NMR (400 MHz, $CDCl_3$) δ 7.59(d, J=7.6Hz, 2H), 7.43-7.47(m, 1H), 7.36-7.39(m, 2H); ^{13}C NMR (400 MHz, $CDCl_3$) δ 154.2, 132.9, 130.6, 128.5, 119.7, 118.5, 86.0, 80.7, 67.6, 21.8, 10.3; Anal. Calcd for $C_{12}H_{12}O_2$: C, 76.57; H, 6.43. Found: C, 76.04; H, 6.45.

1-ethynyl-4-iodobenzene (43) In a nitrogen flushed three neck round bottom flask, potassium hydroxide (0.37 g, 6.6 mmol) was added to methanol (10 mL), dichloromethane (5mL) and 1-[2-(trimethylsilyl)ethynyl]-4-iodobenzene (1.00 g, 3.3 mmol). After stirring for 2 h, the reaction mixture was quenched with water; extracted with dichloromethane, dried with magnesium sulfate and filtered. The solvent was removed under reduced pressure and the pure product was isolated by column chromatography (silica gel, 4:1 hexane/dichloromethane) and recrystallized from hexane. Yield 90%, as a pale white powder; mp 220-222 °C. ^{1}H NMR (400 MHz, CDCl3) δ 7.66 (d, J= 8.4 Hz, 2H), 7.21 (d, J=8.4 Hz, 2H), 3.126 (s, 1H); ^{13}C NMR (400

MHz, $CDCl_3$) δ 155.3, 137.5, 135.2, 133.6, 78.6; Anal. Calcd for $C_8H_5I \cdot 0.25H_2O$: C, 41.32; H, 2.32. Found: C, 41.45; H, 2.32.

13.2. CB1 Binding Assay.

Binding of [^{3}H]SR 141716A was carried out as previously described.[63] Cerebellum were dissected on ice and suspended in 10 volumes of ice-cold buffer (50 mM Tris-HCl, 3 mM $MgCl_2$, 0.1 M EDTA, pH 7.4) and homogenized for 20 sec with a polytron (setting 6). The homogenates were centrifuged at 31000 x *g* for 10 min at 4 °C, the supernatants discarded and the tissue resuspended in buffer and centrifuged again. The final pellet was resuspended at a concentration of 5 mg wet weight/mL. Triplicate samples of membranes were incubated in buffer for 2 h at 30 °C in a final volume of 1 mL buffer (50 mM Tris-HCl, 3 mM $MgCl_2$, 0.1 mM EDTA, 100 mM NaCl, pH 7.7 with NaOH) in the presence of 0.5 nM [^{3}H]SR 141716A and 30 μM GDP. Non-specific binding was determined as binding in the presence of 1 μM CP 55,940. The incubation was terminated by rapid filtration through Whatman GF/B glass fiber filter paper (presoaked in cold Tris buffer). The filters were rinsed 3 times, each with 5 mL Tris

buffer containing 0.1% BSA and transferred to scintillation vials. Beckman Ready Value Scintillation Cocktail was added to the vials, which were counted the next day at an efficiency of approximately 40%.

13.3. Locomotor Activity Studies.

Male Sprague-Dawley rats (Charles River, Wilmington, MA) were used for all studies. Rats were housed two per cage in a temperature and humidity-controlled environment under a 12 h light/dark cycle. Food and water were available ad libitum. Rats were placed in 40.4 x 40.5 x 30.3 cm Plexiglas enclosures placed in Digiscan locomotor activity monitors (Omnitech Electronics, Columbus, OH).

Panels of infrared beams (16 beams per side) with corresponding photodetectors are located on the sides of the chambers, and distance traveled, in centimeters, and horizontal activity (expressed as number of beam breaks) were measured in 5 min intervals for 60 min post-injection, as described previously.[64, 65] Each dose was administered in a volume of 1 mL/kg.

14. REFERENCES AND NOTES

(1) (a) Substance Abuse and Mental Health Services Administration. (2010). *Results from the 2009 National Survey on Drug Use and Health: Volume I. Summary of National Findings* (Office of Applied Studies, NSDUH Series H-38A, HHS Publication No. SMA 10-4586 Findings) Rockville, MD. (b) National Institute on Drug Abuse, NIDA Infofacts: Cocaine http://www.nida.nih.gov/DrugPages/Cocaine.html (c) Trudell, M. L.; Izenwasser, S. (eds). *Dopamine Transporters: Chemistry, Biology and Pharmacology*. Wiley Interscience: New York, 2008. (d) National Institute on Drug Abuse, NIDA Infofacts: Marijuana http://www.nida.nih.gov/infofacts/marijuana.html (e) http://www.nida.nih.gov/pubs/teaching/teaching5.html. (f) http://www.drugabuse.gov/publications/infofacts/marijuana

(2) Vocci, F.; Ling, W. Medications development: Success and challenges. *Pharmacol.Ther*. **2005**, *108*, 94-108.

(3) LeFoll, B.; Goldberg, S. R. Cannabinoid CB1 receptor antagonists as promising new medications for drug dependence. *J. Pharmacol. Exp. Ther.* **2005**, *312*, 875-883.

(4) Beardsley, P. M.; Thomas, B. F.; Current evidence supporting a role of cannabinoid CB1 receptor (CB1R) antagonists as potential pharmacotherapies for drug abuse disorders. *Behavior. Pharm*. **2005**, *16*, 275-296.

(5) Janerao, D. R.; Makriyannis, A. Cannabinoid receptor antagonists: pharmacological opportunities, clinical experience, and translational prognosis. *Expert Opin. Emerging Drugs* **2009**, *14*, 43-65.

(6) (a) Rinaldi-Carmona, M.; Barth, F.; Héaulme, M.; Shire, D.; Calandra, B.; Congy, C.; Martinez, S.; Maruani, J.; Néliat, G.; Caput, D.; Ferrara, P.; Soubrié, P.; Brelière, J. C.; Fur, G. L. SR141716A, a potent and selective antagonist of the brain cannabinoid

receptor. *FEBS Lett*. **1994**, *350*, 240-244. (b) Stewart, J.; McMahon, L. R. Rimonabant-induced Tetrahydrocannabinol withdrawal in Rhesus Monkeys: Discriminative stimulus effects and other signs. *J. Phramacol. Exp Ther.* **2010**, *334*, 347-356.

(7) Huestis, M. A.; Boyd, S. J.; Heishman, S. J.; Preston, K. L.; Bonnet, D.; LeFur, G.; Gorlick, D. A. Single and multiple doses of rimonabant antagonize acute effects of smoked cannabis in male cannabis users. *Psychopharmacology* **2007**, *194*, 505-515.

(8) Wiley, J. L.; Lowe, J. A.; Balster, R. L.; Martin, B. R. Antagonism of the discriminative stimulus effects of delta-9-tetrahydrocannabinal in rats and rhesus monkeys. *J. Pharamcol. Exp. Ther* **1995**, *275*, 1-6.

(9) Beardsley, P. M.; Dance, M. E.; Balster, R. L; Munzar, P. Evaluation of the reinforcing effects of the cannabinoid CB1 receptor antagonist, **SR141716A**, in rhesus monkeys. *Eur. J. Pharmacol*. **2002**, *435*, 209-216.

(10) (a) Meschler, J. P.; Kraichely, D. M.; Wilken, G. H.; Hewlett, A. C. Inverse agonist properties of N(piperidin-1-yl)-5-(4-chlorophenyl)-1-(2, 4-dichlorophenyl)-4-methyl-1H-pyrazole-3-carboxamide HCl (**SR141716A**) and 1-(2-chlorophenyl)-4-cyano-5-(4-methoxyphenyl)-1H-pyrazole-3-carboxylic acid phenylamide (CP-272871) for the CB1 cannabinoid receptor. *Biochem. Pharmacol*. **2000**, *60*, 1315-1323. (b) Bouaboula, M.; Perrachon , S.; Milligan, L.; Canat, X.; Rinaldi-Carmona, M.; Portier, M.; Barth, F.; Calandra, B.; Pecceu, F.; Lupker, J.; Maffrand, J-P.; Fur, G. L.; Casellas, P. A Selective Inverse Agonist for Central Cannabinoid Receptor Inhibits Mitogen-activated Protein Kinase Activation Stimulated by Insulin or Insulin-like Growth Factor 1: EVIDENCE FOR A NEW MODEL OF RECEPTOR/LIGAND INTERACTIONS. *J. Biol. Chem.* **1997**, *272*, 22330-22339. (c) Pan, X.; Ikeda, S. R.; Lewis, D. L. SR 141716A Acts as an Inverse Agonist to Increase Neuronal Voltage-Dependent Ca^{2+} Currents by Reversal of Tonic CB1 Cannabinoid Receptor Activity. *Mol. Pharmacol.* **1998**, *54*, 1064-1072.

(11) Childers, S. R. Activation of G-proteins in brain by endogenous and exogenous cannabinoids. *AAPS J.* **2006**, *8*, E112-E117.

(12) Aceto, M. D.; Scates, S. M.; Lowe, J. A.; Martin, B. R. Cannabinoid precipitated withdrawal by the selective cannabinoid receptor antagonist, SR 141716A. *Eur J Pharmacol* **1995**, *282*, R1–R2.

(13) Tsou, K.; Patrick, S. L.; Walker, J. M. Physical withdrawal in rats tolerant to delta9-tetrahydrocannabinol precipitated by a cannabinoid receptor antagonist. *Eur. J. Pharmacol.* **1995**, *280*, R13–R15.

(14) Wikerke, J.; Pattij, T.; Schoffelmeer, A. N.; DeVries, J. T. The role of CB1 receptors in psychostimulant addiction. *Addict. Biol*. **2008**, *13*, 225-38.

(15) (a) Koob, GF. Dopamine addiction and reward. *Semin. Neurosci* **1992**, 4, 139-148 (b) Koob, GF. Drugs of abuse: anatomy, pharmacology and function of award pathways. *Trends Pharmacol Sci*. **1992**, *13*, 177-184.

(16) Tanda G, Goldberg SR. Cannabinoids: reward, dependence and underlying neurochemical mechanisms. *Psychopharmacol.* **2003**, *169*, 115-134.

(17) Wise RA. Dopamine, learning and motivation. *Nat. Rev. Neurosci*. **2004**, *5*, 483-494.

(18) Herkenham, M. Cannabinoid receptor localization in brain: relationship to motor and reward systems. *Ann NY Acad Sci* **1992**, *654*, 19–32.

(19) De Vries, T. J.; Shaham, Y.; Homberg, J. R.; Crombag, H.; Schuurman, K.; Dieben, J. A. Cannabinoid mechanism in relapse to cocaine seeking. *Nat. Med.* **2001**, *7*, 1151–1154.

(20) Vinklerova, J.; Novakova, J.; Sulcova, A. Inhibition of methamphetamine administration in rats by cannabinoid receptor antagonists AM251. *J. Pyschopharmacol*. **2002**, *16*, 139 -143.

(21) Anggadredja, K.; Nakamichi, M.; Hiranita, T.; Tanaka, H.; Shoyama, Y.; Waranabe, S.; Yamamota, T. Endocannabinoid system modulates relapse to methamphetamine seeking. *Neuropsychopharmacol.* **2005**, *29*, 1470-1478.

(22) Mclaughlin, P. J.; Winston, K.; Swezey, L.; Wisniecki, A.; Aberman, J.; Tardif, D. J.; Betz, A. J.; Ishiwari, K.; Makriyannis, A.; Salamone, J. D. The cannabinoid CB1 antagonists SR 141716And AM 251 suppress food intake and food-reinforced behavior in a variety of tasks in rats. *Behav. Pharmacol*. **2003**, *14*, 583-588.

(23) Jarbe, T. U.; DiPatrizio, N. V.; Li, C.; Makriyannis, A. The cannabinoid receptor antagonist SR-141716 does not readily antagonize open-field effects induced by the cannabinoid receptor agonist (R)methanandamide in rats. *Pharmacol. Biochem. Behav*. **2003**, **75**, 809-821.

(24) Vivian, J. A.; Kishioka, S.; Butelman, E. R.; Broadbear, J.; Lee, K. O.; Woods, J. H. Analgesic, respiratory and heart rate effects of cannabinoid and opioid agonists in rhesus monkeys: antagonist effects of **SR141716A**. *J. Pharmacol. Exp. Ther.* **1998**, *286*, 697-703.

(25) Winsauer, P. J.; Lambert, P.; Moerschbaecher, J. M. Cannabinoid ligands and their effects on learning and performance in rhesus monkeys. *Behav. Pharmacol*. **1999**, *10*, 497-511.

(26) Christensen, R.; Kristensen, P. K.; Bartels, E. M.; Bliddal, H.; Astrup, A. Efficacy and safety of the weight-loss drug rimonabant: A meta-analysis of randomised trials. *Lancet*. **2007**, *370*, 1671-1672.

(27) (a) Pavon, F. J.; Bilbao, A.; Hernandez-Folgado, L.; Cippitelli, A.; Jagerovic, N.; Abellan, G.; Rodriguez-Franco M. I.; Serrano, A.; Macias, M.; Gomez, R.; Navarro, M.; Goya, P.; deFonsica, F. R. Antiobesity effects of the novel in vivo neutral cannabinoid antagonist LH21. *Neuropharmacology,* **2006**, *51*, 358-366. (b) Alonso, M.; Antonia Serrano, A.; Margarita Vida, M.; Ana Crespillo, A.; Hernandez-Folgado, L.; Jagerovic, N.; Goya, P.; Reyes-Cabello, C.; Perez-Valero, V. ;Juan Decara, J.; Macías-González, M.; Bermúdez-Silva, F. J.; Suárez, J.; de Fonseca, F. R.; Pavón, F. J. Anti-obesity efficacy of LH-21, a cannabinoid CB1 receptor antagonist with poor brain penetration, in diet-induced obese rats. *Bri. J. Pharmacol.* **2012**, *7*, 2274–2291.

(28) Traynor, K. Panel advises against rimonabant approval. *Am. J. Health Syst. Pharm*. **2007**, *65*, 1460-1461.

(29) Taylor, D. Withdrawal of rimonabant-Walking the tightrope of 21st century pharmaceutical regulation? *Curr. Drug Safety*, **2009**, *4*, 2-4.

(30) (a) Piomelli, D. The endocannabinoid system: a drug discovery perspective *Curr. Opin. Invest. Drugs* **2005**, *6*, 672-679. (b) Piomelli, D. The molecular logic of endocannabinoid signaling *Nat. Rev. Neurosci*. **2003**, *4*, 873-874.

(31) (a) Kim, J.; Isokawa, M.; Ledent, C.; Alger, B. E. Activation of Muscarinic Acetylcholine Receptors Enhances the Release of Endogenous Cannabinoids in the Hippocampus. *J. Neurosci*. **2002**, *22*, 10182-10191. (b) Butler, H.; Korbonits, M. Cannabinoids for clinicians: the rise and fall of the cannabinoid antagonists. *Eur. J. Endocrinol.* **2009**, *161*, 655-662.

(32) (a) Howlett, A. C.; Barth, F.; Bonner, T. I.; Cabral, G.; Casellas, P.; Devane, W. A.; Felder, C.; Herkenham, M.; Mackie, K.; Martin, B. R.; Mechoulam, R.; Pertwee, R. G. Nonpsychotropic Cannabinoid Receptors Regulate Microglial Cell Migration *Pharmacol. Rev.* **2002**, *54*, 161-202. (b) Howlett, A. C. Cannabinoid inhibition of adenylate cyclase: Relative activity of constituents and metabolites of marihuana *Neuropharmacol*. **1987**, *26*, 507-512. (c) Onaivi, E. S.; Ishiguro, H.; Gong, J. P.; Patel, S.; Perchuk, A.; meozzi, P. A.; Myers, L.; Mora, Z.; Tagliaferro, P.; Gardner, E.; Brusco, A.; Akinshola, B. E.; Liu, Q. R.; Hope, B.; Iwasaki, S.; Arinami, T.; Teasenfitz, L.; Uhl, G. R. Discovery of the Presence and Functional Expression of Cannabinoid CB2 Receptors in Brain *Ann. N. Y. Acad. Sci.* **2006**, *1070*, 514-536.

(33) Di Marzo, V; Petrosino, S. Endocannabinoids and the regulation of their levels in health and disease *Curr. Opin. Lipidol*. **2007**, *18*, 129-140.

(34) Felder, C. C. Comparison of the pharmacology and signal transduction of the human cannabinoid CB1 and CB2 receptors *Mol. Pharmacol.* **1995**, *48*, 443-450.

(35) Herkenham, M.; Lynn, A. B.; Johnson, M. R.; Melvin, L.S.; De Costa, B.R.; Rice, K.C. Characterization and localization of cannabinoid receptors in rat brain: a quantitative in vitro autoradiographic study *J. Neurosci*. **1991**, *11*, 563-583.

(36) Jansen, E. M; Haycock, D. A.; Ward, S.J.; Seybold, V.S. Distribution of cannabinoid receptors in rat brain determined with aminoalkylindoles *Brain Res*. **1992**, *575*, 93-102.

(37) (a) Matsuda, L.A.; Lolait, S.J.; Brownstein, M.J.; Young, A.C.; Bonner, T.I. Structure of a cannabinoid receptor and functional expression of the cloned cDNA *Nature*, **1990**, *346*, 561-564. (b) Gerard, C. M.; Mollereau, C.; Vassart, G.; Parmentier, M. Molecular cloning of a human cannabinoid receptor which is also expressed in testis *Biochem. J.* **1991**, *279*, 129-134. (c) Pertwee, R. G. Phamacological, physiological and

clinical implications of the discovery of cannabinoid receptors: an overview. In *Cannabinoid Receptors*; Pertwee, R. G., Ed.; Academic Press: London, 1995: pp 1-29. (d) Pertwee, R. G. Pharmacology of cannabinoid CB1 and CB2 receptors *Pharmacol. Ther.* **1997**, *74*, 129-180. (e) Huffman, J. W.; Lainton, J. A. H. Recent developments in the **medicinal** chemistry of cannabinoids *Current Med. Chem.* **1996**, *3*, 101-116.

(38) (a) Munro, S.; Thomas, K.L.; Abu-Shaar, M. Molecular characterization of a peripheral receptor for cannabinoids *Nature*, **1993**, *365*, 61-65. (b) Thomas, G. Fundamentals of medicinal chemistry. John Wiley & Sons, Inc. New York, NY. **2003**. (c) Steffens, S.; Veillard, N.R.; Arnaud, C.; Pelli, G.; Burger, F.; Staub, C.; Karsak, M.; Zimmer, A.; Frossard, J.L.; Mach, F. Low dose oral cannabinoid therapy reduces progression of atherosclerosis in mice, *Nature* **2005**, *434*, 782–786. (d) Zhao, Y.; Yuan, Z.; Liu, Y.; Xue, J.; Tian, Y.; Liu, W.; Zhang, W.; Shen, Y.; Xu, W.; Liang, X.; Chen, T. Activation of cannabinoid CB2 receptor ameliorates atherosclerosis associated with suppression of adhesion molecules, *J. Cardiovasc. Pharmacol.,* **2010**, *55*, 292–298.

(39) (a) Mackie, K. Distribution of cannabinoid receptors in the central and peripheral nervous system *Handb. Exp. Pharmacol.* **2005**, *168*, 299-325. (b) Mackie, K. Cannabinoid receptors: where they are and what they do *J. Neuroendocrinol.* **2008**, *20*,10-14. (c) Mackie, K. Hille, B. Cannabinoids inhibit N-type calcium channels in neuroblastoma-glioma cells *Proc. Nat. Acad. Sci.* **1992**, *89*, 3825-3829.

(40) Di Marzo, V.; Bifulco, M.; De Petrocellis, L. The endocannabinoid system and its therapeutic exploitation *Nat. Rev. Drug. Discov*. **2004**, *3*, 771-784.

(41) Cervino, C.; Pasquali, R.; Pagotto, U. Cannabinoid Receptor Antagonists and the Metabolic Syndrome: Novel Promising Therapeutical Approaches *Mini-Reviews in Medicinal Chemistry,* **2007***, 1*, 21-30.

(42) (a) Hurst, D.; Umejiego, U.; Lynch, D.; Seltzman, H.; Hyatt, S.; Roche, M.;

Mcallister, S.; Fleischer, D.; Kapur, A.; Abood, M.; Shi, S.; Jones, J.; Lewis, D.; Reggio, P. Biarylpyrazole Inverse Agonists at the Cannabinoid CB1 Receptor: Importance of the C-3 Carboxamide Oxygen/Lysine3.28(192) Interaction. *J. Med. Chem.* **2006**, *49*, 5969-5987. (b) Hurst, D. P.; Lynch, D. L.; Barnett-Norris, J.; Hyatt, S. M.; Seltzman, H. H.; Zhong, M.; Song, Z. H.; Nie, J. et al. N-(piperidin-1-yl)-5-(4-chlorophenyl)-1-(2,4-dichlorophenyl)-4-methyl-1H-pyrazole-3-carboxamide (**SR141716A**) interaction with LYS 3.28(192) is crucial for its inverse agonism at the cannabinoid CB1 receptor. *Mol. Pharmacology* **2002**, *62*, 1274–1287.

(43) Thomas, B. F.; Francisco, F. E.; Seltzman, H. H.; Thomas, J. B.; Fix, S. E.; Schulz, A. K.; Gilliam, A. F.; Pertwee, R. G.; Stevenson, L. A. Conformational Characteristics of the Interaction of SR141716A with the CB1 Cannabinoid Receptor as Determined Through the Use of Conformationally Constrained Analogs Bioorg. Med. Chem. 2005, 13, 5463-5474.

(44) (a) Alekseeva, O. O.; Mahadevan, A.; Wiley, J. L.; Martin B. B.; Razdan, R. K. Synthesis of novel 5-substituted pyrazole derivatives as cannabinoid antagonists Tetrahedron Lett. 2005, 46, 2159-2161. (b) Netherland,C.; Thewke, D. P. Rimonabant is a dual inhibitor of acyl CoA:cholesterol acyltransferases 1 and 2. Biochemic. & Biophysic. Res. Comm. 2010, 398, 671-676. (c) Chang, T. Y.; Li, B. L.; Chang, C. C.; Urano, Y. Acyl-coenzyme A: cholesterol acyltransferases, Am. J. Physiol. Endocrinol. Metab. **2009**, *297*, E1-E9. (d) Stary, H.C.; Chandler, A.B.; Glagov, S.; Guyton, J.R.; Insull Jr., W.; Rosenfeld, M.E.; Schaffer, S.A. ; Schwartz, C.J.; Wagner, W.D.; Wissler, R.W. A definition of initial, fatty streak, and intermediate lesions of atherosclerosis. A report from the Committee on Vascular Lesions of the Council on Arteriosclerosis, American Heart Association. *Arterioscler. Thromb.* **1994**, *14*, 840–856. (e) Rudel, L.L. ; Lee, R.G.; Cockman, T.L. Acyl coenzyme A: cholesterol acyltransferase types 1 and 2: structure and function in atherosclerosis, Curr. Opin. Lipidol. 2001, *12,* 121–127. (f) Miyazaki, A.; Sakai, M.; Sakamoto, Y.; Horiuchi, S. Acyl-coenzyme A:cholesterolacyltransferase inhibitors for controlling hypercholesterolemia and

atherosclerosis. *Curr. Opin. Investig. Drugs* **2003**, *4*, 1095–1099. (g) Fujiwara, Y.; Kiyota, N.; Hori, M.; Matsushita, S.; Iijima, Y.; Aoki, K.; Shibata, D.; Takeya, M.; Ikeda, T.; Nohara, T.; Nagai, R. Esculeogenin A, a new tomato sapogenol, ameliorates hyperlipidemia and atherosclerosis in ApoE-deficient mice by inhibiting ACAT. *Arterioscler. Thromb. Vasc. Biol.* **2007**, *27*, 2400–2406. (h) Terasaka, N.; Miyazaki, A.; Kasanuki, N.; Ito, K.; Ubukata, N.; Koieyama, T.; Kitayama, K.; Tanimoto, T.; Maeda, N.; Inaba, T. ACAT inhibitor pactimibe sulfate (CS-505) reduces and stabilizes atherosclerotic lesions by cholesterol-lowering and direct effects in apolipoprotein E-deficient mice, *Atherosclerosis* **2007**, *190*, 239–247. (i) Pi-Sunyer, F.X.; Aronne, L.J.; Heshmati, H.M.; Devin, J.; Rosenstock, J. Effect of rimonabant, a cannabinoid-1 receptor blocker, on weight and cardiometabolic risk factors in overweight or obese patients: RIO-North America: a randomized controlled trial. *Jama* **2006**, *295*, 761–775. (j) Van Gaal, L.F.; Rissanen, A.M.; Scheen, A.J.; Ziegler, O.; Rossner, S. Effects of the cannabinoid-1 receptor blocker rimonabant on weight reduction and cardiovascular risk factors in overweight patients: 1-year experience from the RIO-Europe study. *Lancet* **2005**, *365*, 1389–1397. (k) Nissen, S.E. Nicholls, S.J.; Wolski, K.; Rodes-Cabau, J.; Cannon, C.P.; Deanfield, J.E.; Despres, J.P.; Kastelein, J.J.; Steinhubl, S.R.; Kapadia, S.; Yasin, M.; Ruzyllo, W.; Gaudin, C.; Job, B.; Hu, B.; Bhatt, D.L.; Lincoff, A.M.; Tuzcu, E.M.; Effect of rimonabant on progression of atherosclerosis in patients with abdominal obesity and coronary artery disease: the STRADIVARIUS randomized controlled trial, *Jama* **2008**, *299*, 1547–1560. (l) Dol-Gleizes, F. ; Paumelle, R.; Visentin, V.; Mares, A.M.; Desitter, P.; Hennuyer, N. ; Gilde, A.; Staels, B.; Schaeffer, P.; Bono, F.; Rimonabant, a selective cannabinoid CB1 receptor antagonist Inhibits atherosclerosis in LDL receptor-deficient mice, *Arterioscler. Thromb. Vasc. Biol.* **2009**, *29*, 12–18. (m) Sugamura, K.; Sugiyama, S.; Fujiwara, Y.; Matsubara, J.; Akiyama, E.; Maeda, H.; Ohba, K.; Matsuzawa, Y.; Konishi, M.; Nozaki, T.; Horibata, Y.; Kaikita, K.; Sumida, H.; Takeya, M.; Ogawa, H. Cannabinoid 1 receptor blockade reduces atherosclerosis with enhances reverse cholesterol transport, *J. Atheroscler. Thromb.* **2010**, *17*, 141–147.

(45) (a) Schindler, C. W.; Panlilio, L. V.; Gilman, J. P.; Justinova, Z.; Vemuri, V. K.; Makriyannis, A.; Goldberg, S. R. Effects of cannabinoid receptor antagonists on maintenance and reinstatement of methamphetamine self-administration in rhesus monkeys *Eur. J. Pharmacol.* **2010**, *633*, 44-49.) (b) Jagerovic, N.; Fernandez-Fernandez, C.; Goya, P. CB1 Cannabinoid Antagonists: Structure-Activity Relationships and Potential Therapeutic Applications *Curr. Top. Med. Chem*. **2008**, *8*, 205-230.

(46) (a)Trudell, M. L.; Izenwasser, S. (eds). *Dopamine Transporters: Chemistry, Biology and Pharmacology*. Wiley Interscience: New York, 2008. (b) Lange, Jos H.M.; Kruse, Chris G. Medicinal chemistry strategies to CB1 cannabinoid receptor antagonists. *Drug Discovery Today* **2005**, *10*, 693. (c) Foloppe, N.; Allen, N.H.; Bentley, C.H.; Brooks, T.D.; Kennett, G.; Knight, A.R.; Leonardi, S.; Misra, A. Discovery of a novel class of selective human CB_1 inverse agonists*. Bioorg. Med. Chem. Lett.* **2008**, *18,* 1199-1206. (d) Jonathon, C. A. The role of endocannabinoid transmission in cocaine addiction. *Pharmacol. Biochem. Behavior* **2005**, *81*, 396-406. (e) Elphick, M. R.; Egertova, M. The neurobiology and evolution of cannabinoid signalling *Phil. Trans. R. Soc. Lond.* B **2001**, *356*, 381-408. (g) http://lalaleigha.wordpress.com/2009/08/10/the-pharmacology-of-marijuana/

(47) Plummer C. W.; Finke, P. E.; Mills, S. G.; Wang, J.; Tong, X.; Doss, G. A.; Fong, T. M.; Lao, J. Z.; Schaeffer, M. T.; Chen, J.; Shen, C. P.; Stribling, D. S.; Shearman, L. P.; Strack, A. M.; Van der Ploeg, L. H. Synthesis and activity of 4,5-diarylimidazoles as human CB1 receptor inverse agonists. *Bioorg. Med. Chem. Lett*. **2005**, *15*, 1441-1446.

(48) Dyck, B.; Goodfellow, V. S.; Phillips, T.; Grey, J.; Haddach, M.; Rowbottom, M.; Naeve, G. S.; Brown, B.; Saunders, J. Potent imidazole and triazole CB_1 receptor antagonists related to SR141716. *Bioorg. Med. Chem. Lett*. **2004**, *14*, 1151-1154.

(49) Pavon, F. J.; Bilbao, A.; Hernandes-Folgado, L.; Cippitelli, A.; Jagerovic, N.; Abellan, G.; Rodriguez-Franco, M. A.; Serrano, A.; Macias, M.; Gomez, R.; Navarro, M.;

Goya, P.; Rodriguez de Fonseca, F. Antiobesity effects of the novel in vivo neutral cannabinoid receptor antagonist 5-(4-chlorophenyl)-1-(2,4-dichlorophenyl)-3-hexyl-1*H*-1,2,4-triazole – LH 21. *Neuropharmacol.* **2006**, *51*, 358-366.

(50) Smith, R. A.; Fathi, Z.; Brown, S. E.; Choi, S.; Fan, J.; Jenkins, S.; Kluender, H. C.; Konkar, A.; Lavoie, R.; Mays, R.; Natoli, J.; O'Connor, S. J.; Ortiz, A. A.; Podlogar, B.; Taing, C.; Tomlinson, S.; Tritto, T.; Zhang, Z. Constrained analogs of CB-1 antagonists: 1,5,6,7-Tetrahydro-4H-pyrrolo[3,2-c]pyridine-4-one derivatives. *Bioorg. Med. Chem. Lett*. 2007, *17*, 673-678.

(51) (a) Barth, F. CB1 Cannabinoid Receptor Antagonists. *Ann. Reports Med. Chem.* **2005**, *40*, 103-117. (b) Lange, J. H. M.; VanStuivenberg, H. H.; Coolen, H. K. A. C.; Kruse, C. G. *et al.* Bioisosteric Replacements of the Pyrazole Moiety of Rimonabant: Synthesis, Biological Properties, and Molecular Modeling Investigations of Thiazoles, Triazoles, and Imidazoles as Potent and Selective CB_1 Cannabinoid Receptor Antagonists. *J. Med. Chem.* **2005**, *48*, 1823-1838. (c) Meurer, L.C.; Finke, P. E.; Mills, S. G.; Walsh, T. F.; Toupence, R. B.; Goulet, M. T.; Wang, J.; Tong, X.; Fong, T. M.; Lao, J.; Schaeffer, M.-T.; Chen, J.; Shen, C-P.; Stribling, D. S; Shearman, L. P.; Strack, A. M.; Van der Ploeg, L. H. T. Synthesis and SAR of 5,6-diarylpyridines as human CB1 inverse agonists. *Bioorg. Med. Chem. Lett.* **2005**, *15*, 645-651. (d) Debenham, J. S.; Madsen-Duggan, C. B.; Walsh,T. F.; Wang, J.;Tong, X.; Doss, G. A.; Lao, J.; Fong, T. M.; Schaeffer, M.-T.; Xiao,J. C.; Huang, C. R.-R. C.; Shen, C.-P.; Feng, Y.; Marsh, D. J.; Stribling, D. S.; Shearman, L. P.; Strack, A. M.; MacIntyre, D. E.; Van der Ploeg, L. H. T. ; Goulet, M. T. Synthesis of functionalized 1,8-naphthyridinones and their evaluation as novel, orally active CB1 receptor inverse agonists. *Bioorg. Med. Chem. Lett.* **2006**, *16*, 681-685. (e) Debenham, J. S.; Madsen-Duggan, C.B.; Wang, V; Tong, X.; Lao, J.; Fong, T. M. Schaeffer, M.-T.; Xiao, J. C.; Huang, C. C.R.-R.; Shen, C.-P.; Stribling, D. S.; Shearman, L. P.; Strack, A. M.; MacIntyre, D. E.; Hale, J. J.; Walsh, T. F. Pyridopyrimidine based cannabinoid-1 receptor inverse agonists: Synthesis and biological evaluation. *Bioorg. Med. Chem. Lett.* **2009**, *19*, 2591-2594.

(52) (a) Krasinski, A.; Fokin, V. V.; Sharpless, K. B. Direct synthesis of 1,5-disubstituted-4-magnesio-1,2,3-triazoles, revisited. *Org. Lett.* **2004**, 6, 1237-1240. (b) Bourne, Y.; Kolb, H. C.; Radic´, Z.; Sharpless, K. B.; Taylor, P.; Marchot, P. Freeze-frame inhibitor captures acetylcholinesterase in a unique conformation *Proc. Natl. Acad. Sci. U.S.A.* **2004**, *101*, 1449-1454. (c) Lewis, W. G.; Green, L. G.; Grynszpan, F.; Radic´, Z.; Carlier, P. R.; Taylor, P.; Finn, M. G.; Sharpless, K. B. Click Chemistry In Situ: Acetylcholinesterase as a Reaction Vessel for the Selective Assembly of a Femtomolar Inhibitor from an Array of Building Blocks *Angew. Chem., Int. Ed.* **2002**, *41*, 1053-1057. (d) Huisgen, R. In *1,3-Dipolar Cycloadditon Chemistry*; Padwa, A., Ed.; Wiley: New York, 1984; pp1-176. (e) Padwa, A. In *ComprehensNe Organic Synthesis*; Trost, B. M., Ed.; Pergamon: Oxford, 1991; Vol. 4, pp 1069-1109. (f) Fan, W.-Q.; Katritzky, A. R. In *ComprehensNe Heterocyclic Chemistry II*; Katritzky, A. R., Rees, C. W., Scriven, E. F. V., Eds.; Pergamon: Oxford, 1996; Vol. 4, pp 101-126. (g) http://en.wikipedia.org/wiki/Azide_alkyne_Huisgen_cycloaddition.

(53) (a) Bass, C. E.; Griffin, G.; Grier, M.; Mahadevan, A.; Razdan, R. K.; Martin, B. R. SR-141716A-induced stimulation of locomotor activity: a structure-activity relationship study. *Pharmacol. Biochem. Behav*. **2002**, *74*, 31-40. (b) Wu, Y.-M.; Deng, J.; Li, Y.; Chen, Q.-Y. Regiospecific Synthesis of 1,4,5-Trisubstituted-1,2,3-triazole via One-Pot Reaction Promoted by Copper(I) Sal*t. Synthesis* **2005**, *8*, 1314-1318. (c) Rostovtsev, V. V.; Green, L. G.; Fokin V. V.; Sharpless, K. B. A Stepwise Huisgen Cycloaddition Process: Copper(I)-Catalyzed Regioselective "Ligation" of Azides and Terminal Alkynes *Angew. Chem., Int. Ed.* **2002**, *41*, 2596-2599. (d) Himo, F.; Lovell, T.; Hilgraf,R.; Rostovtsev, V. V.; Noodleman, L.; Sharpless, K.B.; Fokin, V. V. Copper(I)-Catalyzed Synthesis of Azoles. DFT Study Predicts Unprecedented Reactivity and Intermediates. *J. Am. Chem. Soc.*, **2005**, *127*, 210–216.

(54) (a) Amenta, D. S.; Mallory, F. B. Evidence against the intramolecular cyclllizations of o-azidobenzendiazonium ions. *J. Org. Chem.* **1980**, *45*, 5236-5238. (b) Coats, S. J.; Link, J. S.; Gauthier, D., Hlasta, D. J. Trimethylsilyl-Directed 1,3-Dipolar

Cycloaddition Reactions in the Solid-Phase Synthesis of 1,2,3-Triazoles *Org. Lett.* **2005**, *7*, 1469- 1472. (c) Kim, D.; Kim, J.; Park, H. Synthesis and biological evaluation of novel 2-pyridinyl-[1,2,3]triazoles as inhibitors of transforming growth factor β1 type 1 receptor *Bioorg. Med. Chem. Lett.* **2004**, *14*, 2401-2405. (d) Holmes, B. T.; Pennington, W. T.; Hanks, T. W. Efficient synthesis of a complete donor/acceptor bis(aryl)diyne family *Synthetic Commun.* **2003**, *33* (14), 2447-2461.

(55) (a) Thakur, G.A.; Nikas, S. P.; Li, C.; Makriyannis, A. Structural Requirements for Cannabinoid Receptor Probes *Hand. Exp. Pharm*. **2005**, *768*, 209-246. (b) Ritchie, C. D.; Wright, D. J. Anion-cation combination reactions. III. Reaction of diazonium ions with azide ion in aqueous solution. *J. Am. Chem. Soc*.**1971**, *93*, 2429-2432. (c) Markies,P. R.; Akkerman, O. S.; Bickelhaupt, F.; Smeets, W. J. J.; Spek, A. L. X-Ray Structural Analyses of Organomagnesium Compounds. *Adv. Orgmet. Chem.* **1991,** *32*, 147-226.

(56) Reggio, P. H. Pharmacophores for ligand recognition and activation/inactivation of the cannabinoid receptors. *Curr. Pharm. Des.* **2003**, *9*, 1607-33.

(57) Boström, J.; Olsson,R. I.; Tholander, J.; Greasley P. J.; Ryberg, E.; Nordberg, H.; Hjorth, S.; Cheng, L. Novel thioamide derivatives as neutral CB1 receptor antagonists. *Bioorg. Med. Chem. Lett*. **2010**, *20*, 479-482.

(58) (a) Shu, H.; Izenwasser, S.; Wade, D.; Stevens, E. D.; Trudell, M. L. Synthesis and CB1 cannabinoid affinity of 4-alkoxycarbonyl-1,5-diaryl-1,2,3-triazoles. *Bioorg. Med. Chem. Lett.* 2009, *19*, 891-893. (b) Liu, Q.; Tor, Y. Simple Conversion of Aromatic Amines into Azides *Org. Lett*. **2003**, *5*, 2571-2572.

(59) CB2 K_i determination was generously provided by the National Institute of Mental Health's Psychoactive Drug Screening Program, Contract # HHSN-271-2008-00025-C (NIMH PDSP). The NIMH PDSP is directed by Bryan L. Roth MD, PhD at the

University of North Carolina at Chapel Hill and Project Officer Jamie Driscol at NIMH, Bethesda MD, USA. For experimental details please refer to the PDSP web site http://pdsp.med.unc.edu/ and click on "Binding Assay" menu bar.

(60) Structures in Figure 26 were generated using OpenEye Scientific Software's Omega for conformers and OEChem for shape overlays, and the images were generated with PyMol (Delano Scientific LLC).

(61) The authors have deposited the crystallographic data for structures **31a** and **36a** with the Cambridge Crystallographic Data Centre (http://www.ccdc.cam.ac.uk/); Deposition numbers: CCDC 820556 and CCDC 820557.

(62) Breivogel, C.; Sim, L.; Childers, S. Regional differences in cannabinoid receptor/G-protein coupling in rat brain. *J. Pharmacol. Exp. Ther*. **1997**, *282*, 1632-42.

(63) (a) Onaivi, E. S. An endocannabinoid hypothesis of drug reward. *Cannabinoids* **2007**, *2*, 22-26. (b) Baker, D.; Pryce, G.; Giovannoni, G.; Thompson, A. J. The therapeutic potential of cannabis *Lancet Neurol*. **2003**, *2*, 291-298. (c) Carlson, Neil R. Physiology of Behavior: Pearson Education, Inc: Boston, 2004; pp 673-700.

(64) Izenwasser S, French D, Carroll FI and Kunko PM. Continuous infusion of selective dopamine uptake inhibitors or cocaine produces time-dependent changes in rat locomotor activity. *Behav Brain Res* **1999** *99*, 201-208.

(65) Kunko P, French D and Izenwasser S. Alterations in locomotor activity during chronic cocaine administration: effect on dopamine receptors and interaction with opioids. *J Pharmacol Exp Ther* **1998**, *285*, 277-84.

(66) (a) Lambert, D. M. Medical use of cannabis through history. *J. Pharm. Belg.* **2001**, *56*, 111-118. (b) Adams, I. B.; Martin, B. R. Cannabis: pharmacology and toxicology in animals and humans. *Addiction* **1996**, *91*, 1585-1614. (c) Lane, M.; Vogel, C. L.; Ferguson, J.; Krasnow, S.; Saiers, J. L.; Hamm, J.; Salva, K.; Wiernik, P. H.; Holroyde, C. P.; Hammill, S.; Shepard, K.; Plasse, T. Dronabinol and prochlorperazine in combination for treatment of cancer chemotherapy-induced nausea and vomiting *J. Pain & Symptom Management* **1991**, *6*, 352-359. (d) Beal, J.E.; Olson, R.; Lefkowitz, L.; Laubenstein, L.; Bellman, P.; Yangco, B.; Morales, J. O.; Murphy, R.; Powderly, W.; Plasse, T. F. Mosdell, K. W.; Shepard, K. V. Long-term efficacy and safety of dronabinol for acquired immunodeficiency syndrome-associated anorexia. *J. Pain & Symptom Management* **1997**, *14*, 7-14. (e) Lambert, D. M.; Fowler, C. J. The Endocannabinoid System: Drug Targets, Lead Compounds, and Potential Therapeutic Applications. *J. Med. Chem.* **2005**, *48*, 5059-5087. (f) http://www.druglibrary.org/schaffer/hemp/history/first12000/1.htm.

(67) (a) Gaoni, Y.; Mechoulam, R. Isolation, structure, and partial synthesis of an active constituent of hashish. *J. Am. Chem. Soc.* **1964**, *86*, 1646-1647. (b) Mechoulam, R; Shvo, Y. Hashish—I: The structure of Cannabidiol. *Tetrahedron*. **1993**, *19*, 2073-2078. (c) Ilan, A. B.; Gevins, A.; Coleman, M.; ElSohly, M. A.; de Wit, H. Neurophysiological and subjective profile of marijuana with varying concentrations of cannabinoids. *Behavioural Pharmacology*. **2005**, *16*, 487-496. (d) Burns, T. L.; Ineck, J. R. Novel Cannabinol Probes for CB1 and CB2 Cannabinoid Receptors. *J. Med. Chem.* **2000**, *43*, 3778-3785.

(68) (a) Ng Cheong Ton, J. M.; Gerhardt, G. A.; Friedemann, M.; Etgen, A. M; Rose, G. M.; Sharpless, N. S. The effects of Δ^9-tetrahydrocannabinol on potassium-evoked release of dopamine in the rat caudate nucleus: an in vivo electrochemical and in vivo microdialysis study. *Brain Res.* 1988, *451*, 59-68. (b) Chen, J.; Paredes, W.; Lowinson, J. H.; Gardner, E. L. Δ^9-Tetrahydroeannabinol enhances presynaptic dopamine efflux in medial prefrontal cortex. *Eur. J. Pharmacol.* 1990, *190*, 259-262. (c) Chen, J.; Paredes,

W.; Li, J.; Smith, D.; Lowinson, J. H.; Gardner, E. L. Δ^9-Tetrahydrocannabinol produces naloxone-blockable enhancement of presynaptic basal dopamine efflux in nucleus accumbens of conscious, freely-moving rats as measured by intracerebral microdialysis. *Psychopharmacol.* **1990**, *102*, 156-162. (d) Chen, J.; Marmur, R. Pulles, A.; Paredes, W.; Gardner, E. L. Ventral tegmental microinjection of Δ^9-tetrahydrocannabinol enhances ventral tegmental somatodendritic dopamine levels but not forebrain dopamine levels: evidence for local neural action by marijuana's psychoactive ingredient *Brain Res.* **1993**, *621*, 65-70.

(69) (a) Grotenhermen, F. Cannabinoids. *CNS & Neurological Disorders*. **2005**, *4(5)*, 507-530. (b) Stella, N.; Schweitzer, P.; Piomelli, D. A second endogenous cannabinoid that modulates long-term potentiation. *Nature* **1997**, *388*, 773-778. (c) Joss, R. A.; Galeazzi, R. L.; Bischoff, A.; Do, D. D.; Goldhirsch, A.; Brunner, K. W. Levonantradol, a new antiemetic with a high rate of side-effects for the prevention of nausea and vomiting in patients receiving cancer chemotherapy. *Cancer Chemother.Pharmacol*. **1982**, *9*, 61-64. (d) Meng, I. D.; Manning, B. H.; Martin, W. J.; Fields, H. L. An analgesia circuit activated by cannabinoids. *Nature* **1998**, *395*, 381-383. (e) Herzberg, U.; Eliav, E.; Bennett, G. J.; Kopin, I. The analgesic effects of R (+)-WIN 55,212-2 mesylate, a high affinity cannabinoid agonist, in a rat model of neuropathic pain. J. *Neurosci. Lett*. **1997**, *221*, 157-160. (f) Marchalant, Y.; Rosi, S.; Wenk, G. L. Anti-inflammatory property of the cannabinoid agonist WIN-55212-2 in a rodent model of chronic brain inflammation. *Neurosci.* **2007**, *144*, 1516-1522. (g) Kuster, J. E.; Stevenson, J. I.; Ward, S. J.; D'Ambra, T. E.; Haycock, D. A. Aminoalkylindole binding in rat cerebellum: selective displacement by natural and synthetic cannabinoids. *J. Pharmacol. Exp. Ther*. **1993**, *264*, 1352-1363. (h) Voet, D.; Voet, J. G. Fundamentals of biochemistry upgrade. John Wiley & Sons, Inc.: New York, 2002.

(70) (a) Cheng, Y. C.; Prusoff, W. H. Relationship between the Inhibition Constant (K_i) and the Concentration of inhibitor Which Causes 50 percent Inhibition (IC50) of an Enzymatic reaction. *Biochem. Pharmacol.* **1973**, *22*, 3099-3108. (b) Kenakin T

Principles: receptor theory in pharmacology. *Trends Pharmacol. Sci.* **2004**, *25*, 186–92. (c) eds, David E. Golan, ed.-in-chief ; Armen H. Tashjian, Jr., deputy ed. ; Ehrin J. Armstrong, April W. Armstrong, associate (2008). *Principles of pharmacology : the pathophysiologic basis of drug therapy* (2nd ed.). Philadelphia, Pa., : Lippincott Williams & Wilkins. p. 25. ISBN 978-0-7817-8355-2. http://books.google.com/books?id=az8uSDkB0mgC&pg=PA23&lpg=PA23&dq=noncompetitive+active+site+antagonist#v=onepage&q&f=false.

(71) (a) Appendino, G.; Gibbons, S.; Giana, A.; Pagani, A.; Grassi, G.; Smith , S. E. ; Rahman , M. M. Antibacterial Cannabinoids from *Cannabis sativa*: A Structure−Activity Study *J. Nat. Prod.*, **2008**, *71*, 1427–1430. (b) http://www.theweedblog.com/cannabis-science-presents-photographic-evidence-showing-cannabis-shrinking-cancer-tumors/ (c)http://www.cbsnews.com/8300-504763_162-10391704-3.html?contributor=10470103.

(72) Papudippu, M.; Shu, H.; Izenwasser, S.; Wade, D.; Gulasey, G.; Fournet, S.; Stevens, E. D.; Lomenzo, S. A.; Trudell, M. L. Regioselective synthesis and cannabinoid receptor binding affinity of N-alkylated 4,5-diaryl-1,2,3-triazoles. *Med. Chem. Res.* Ahead of Print. DOI: 10.1007/s00044-012-9991-3

APPENDIX

All esds (except the esd in the dihedral angle between two l.s. planes) are estimated using the full covariance matrix. The cell esds are taken into account individually in the estimation of esds in distances, angles and torsion angles; correlations between esds in cell parameters are only used when they are defined by crystal symmetry. An approximate (isotropic) treatment of cell esds is used for estimating esds involving l.s. planes.

1. Data_HS-57-4 (Compound **31a**) (Figure 28)

Table 1. Crystal data and structure refinement for **31a**.

Identification code	HSP574	
Empirical formula	$C_{18}H_{14}Cl_3N_3O_2$	
Formula weight	410.67	
Temperature	120(2) K	
Wavelength	0.71073 Å	
Crystal system	Monoclinic	
Space group	$P2_1/n$	
Unit cell dimensions	a = 16.6316(8) Å	· = 90°.
	b = 19.5734(9) Å	· = 104.2960(10)°.
	c = 23.7372(11) Å	· = 90°.
Volume	7488.0(6) $Å^3$	
Z	16	
Density (calculated)	1.457 Mg/m^3	
Absorption coefficient	0.507 mm^{-1}	
F(000)	3360	
Crystal size	0.60 x 0.60 x 0.20 mm^3	
Theta range for data collection	1.71 to 27.50°.	
Index ranges	-21<=h<=21, -25<=k<=25, -30<=l<=30	
Reflections collected	226453	
Independent reflections	17128 [R(int) = 0.0222]	
Completeness to theta = 27.50°	99.6 %	
Absorption correction	Enpirical multi-scan	
Max. and min. transmission	0.9054 and 0.7506	
Refinement method	Full-matrix least-squares on F^2	
Data / restraints / parameters	17128 / 0 / 1161	

Goodness-of-fit on F^2	1.165
Final R indices [I>2sigma(I)]	R_1 = 0.0295, wR_2 = 0.0881
R indices (all data)	R_1 = 0.0342, wR_2 = 0.0933
Largest diff. peak and hole	0.986 and -0.669 e.Å^{-3}

Table 2. Atomic coordinates (x 10^4) and equivalent isotropic displacement parameters (Å^{2}x 10^3) for **31a**. U(eq) is defined as one third of the trace of the orthogonalized U^{ij} tensor.

	x	y	z	U(eq)
O(1D)	-1417(1)	4865(1)	9222(1)	20(1)
Cl(1C)	236(1)	729(1)	1964(1)	32(1)
O(1C)	-1446(1)	229(1)	4153(1)	21(1)
Cl(1D)	-90(1)	4410(1)	6931(1)	36(1)
Cl(1A)	-8511(1)	2780(1)	2261(1)	46(1)
Cl(1B)	-3398(1)	2603(1)	2501(1)	56(1)
O(1A)	-6342(1)	1842(1)	671(1)	28(1)
N(1B)	-1577(1)	-68(1)	462(1)	22(1)
N(1C)	-13(1)	1005(1)	5360(1)	20(1)
O(1B)	-1221(1)	1699(1)	818(1)	28(1)
N(1D)	-76(1)	3902(1)	10359(1)	19(1)
N(1A)	-6410(1)	32(1)	460(1)	22(1)
C(1A)	-6068(1)	2853(1)	1613(1)	38(1)
C(1D)	-2645(1)	4770(1)	8150(1)	34(1)
C(1C)	-2723(1)	467(1)	3089(1)	38(1)
C(1B)	-1700(2)	3073(1)	1060(1)	56(1)
O(2D)	-1357(1)	4885(1)	10178(1)	23(1)
Cl(2D)	3361(1)	2225(1)	9018(1)	30(1)
O(2A)	-5384(1)	1200(1)	389(1)	30(1)
O(2C)	-1386(1)	110(1)	5106(1)	24(1)
Cl(2A)	-9924(1)	-1359(1)	1877(1)	32(1)
N(2C)	616(1)	1392(1)	5347(1)	20(1)
Cl(2B)	-4826(1)	-1521(1)	2054(1)	35(1)
N(2D)	518(1)	3492(1)	10312(1)	20(1)
Cl(2C)	3446(1)	2788(1)	4106(1)	39(1)

O(2B)	-443(1)	1006(1)	405(1)	32(1)
N(2A)	-6930(1)	-384(1)	614(1)	22(1)
N(2B)	-2146(1)	-451(1)	590(1)	22(1)
C(2C)	-2488(1)	-227(1)	3362(1)	31(1)
C(2A)	-6267(1)	3005(1)	963(1)	29(1)
C(2D)	-2390(1)	5442(1)	8465(1)	30(1)
C(2B)	-831(1)	2781(1)	1248(1)	38(1)
Cl(3D)	497(1)	1971(1)	9667(1)	24(1)
Cl(3C)	630(1)	2955(1)	4819(1)	27(1)
Cl(3A)	-6733(1)	-721(1)	2021(1)	31(1)
N(3A)	-7386(1)	-5(1)	906(1)	19(1)
Cl(3B)	-1771(1)	-629(1)	2048(1)	28(1)
N(3C)	662(1)	1422(1)	4781(1)	18(1)
N(3D)	562(1)	3510(1)	9745(1)	17(1)
N(3B)	-2558(1)	-59(1)	904(1)	19(1)
C(3A)	-5902(1)	2475(1)	634(1)	26(1)
C(3C)	-2175(1)	-218(1)	4014(1)	23(1)
C(3D)	-2098(1)	5358(1)	9114(1)	22(1)
C(3B)	-648(1)	2264(1)	828(1)	34(1)
C(4D)	-1110(1)	4681(1)	9772(1)	17(1)
C(4C)	-1116(1)	337(1)	4716(1)	18(1)
C(4B)	-1021(1)	1104(1)	615(1)	22(1)
C(4A)	-6012(1)	1254(1)	549(1)	21(1)
C(5D)	-419(1)	4190(1)	9830(1)	17(1)
C(5C)	-379(1)	783(1)	4810(1)	18(1)
C(5A)	-6532(1)	674(1)	646(1)	20(1)
C(5B)	-1612(1)	566(1)	695(1)	20(1)
C(6A)	-7154(1)	658(1)	939(1)	18(1)
C(6B)	-2234(1)	580(1)	986(1)	19(1)
C(6D)	-12(1)	3944(1)	9428(1)	16(1)
C(6C)	54(1)	1044(1)	4429(1)	17(1)
C(7A)	-7507(1)	1173(1)	1264(1)	19(1)
C(7D)	-78(1)	4065(1)	8806(1)	18(1)
C(7B)	-2530(1)	1089(1)	1347(1)	19(1)
C(7C)	13(1)	965(1)	3806(1)	18(1)
C(8C)	16(1)	1542(1)	3459(1)	22(1)

C(8B)	-1973(1)	1362(1)	1834(1)	23(1)
C(8A)	-7351(1)	1133(1)	1866(1)	25(1)
C(8D)	-7(1)	4727(1)	8603(1)	21(1)
C(9B)	-2238(1)	1831(1)	2188(1)	27(1)
C(9C)	74(1)	1470(1)	2888(1)	24(1)
C(9D)	-19(1)	4832(1)	8022(1)	24(1)
C(9A)	-7666(1)	1627(1)	2174(1)	30(1)
C(10C)	121(1)	820(1)	2668(1)	24(1)
C(10D)	-101(1)	4275(1)	7652(1)	25(1)
C(10B)	-3063(1)	2021(1)	2052(1)	32(1)
C(10A)	-8135(1)	2154(1)	1871(1)	28(1)
C(11C)	91(1)	239(1)	2999(1)	24(1)
C(11D)	-182(1)	3617(1)	7843(1)	27(1)
C(11A)	-8302(1)	2203(1)	1274(1)	29(1)
C(11B)	-3626(1)	1756(1)	1576(1)	34(1)
C(12A)	-7983(1)	1707(1)	971(1)	24(1)
C(12D)	-169(1)	3512(1)	8425(1)	23(1)
C(12C)	39(1)	313(1)	3572(1)	22(1)
C(12B)	-3359(1)	1287(1)	1220(1)	28(1)
C(13D)	1234(1)	3184(1)	9573(1)	17(1)
C(13C)	1341(1)	1762(1)	4630(1)	18(1)
C(13B)	-3131(1)	-381(1)	1182(1)	19(1)
C(13A)	-8007(1)	-320(1)	1142(1)	19(1)
C(14C)	1938(1)	1370(1)	4463(1)	23(1)
C(14B)	-3968(1)	-423(1)	907(1)	23(1)
C(14A)	-8838(1)	-265(1)	852(1)	21(1)
C(14D)	1856(1)	3592(1)	9457(1)	22(1)
C(15D)	2510(1)	3297(1)	9278(1)	23(1)
C(15B)	-4503(1)	-767(1)	1179(1)	25(1)
C(15A)	-9439(1)	-580(1)	1080(1)	22(1)
C(15C)	2583(1)	1685(1)	4291(1)	25(1)
C(16B)	-4177(1)	-1064(1)	1717(1)	24(1)
C(16A)	-9187(1)	-944(1)	1595(1)	22(1)
C(16C)	2627(1)	2395(1)	4305(1)	24(1)
C(16D)	2533(1)	2591(1)	9228(1)	20(1)
C(17B)	-3342(1)	-1026(1)	2000(1)	23(1)

C(17D)	1923(1)	2173(1)	9347(1)	20(1)
C(17C)	2042(1)	2797(1)	4474(1)	24(1)
C(17A)	-8359(1)	-997(1)	1896(1)	23(1)
C(18D)	1265(1)	2477(1)	9518(1)	17(1)
C(18C)	1389(1)	2472(1)	4632(1)	19(1)
C(18A)	-7771(1)	-678(1)	1662(1)	21(1)
C(18B)	-2821(1)	-678(1)	1724(1)	20(1)

Table 3. Bond lengths [Å] and angles [°] for **31a**.

O(1D)-C(4D)	1.3297(14)
O(1D)-C(3D)	1.4612(13)
Cl(1C)-C(10C)	1.7389(12)
O(1C)-C(4C)	1.3306(14)
O(1C)-C(3C)	1.4649(13)
Cl(1D)-C(10D)	1.7362(12)
Cl(1A)-C(10A)	1.7422(13)
Cl(1B)-C(10B)	1.7432(13)
O(1A)-C(4A)	1.3369(15)
O(1A)-C(3A)	1.4541(14)
N(1B)-N(2B)	1.3014(14)
N(1B)-C(5B)	1.3656(15)
N(1C)-N(2C)	1.2990(14)
N(1C)-C(5C)	1.3687(15)
O(1B)-C(4B)	1.3336(15)
O(1B)-C(3B)	1.4572(15)
N(1D)-N(2D)	1.3001(14)
N(1D)-C(5D)	1.3668(15)
N(1A)-N(2A)	1.3036(14)
N(1A)-C(5A)	1.3636(15)
C(1A)-C(2A)	1.524(2)
C(1D)-C(2D)	1.522(2)
C(1C)-C(2C)	1.515(2)
C(1B)-C(2B)	1.516(3)

O(2D)-C(4D)	1.2067(14)
Cl(2D)-C(16D)	1.7311(11)
O(2A)-C(4A)	1.2012(15)
O(2C)-C(4C)	1.2087(14)
Cl(2A)-C(16A)	1.7377(12)
N(2C)-N(3C)	1.3642(13)
Cl(2B)-C(16B)	1.7423(12)
N(2D)-N(3D)	1.3669(13)
Cl(2C)-C(16C)	1.7295(12)
O(2B)-C(4B)	1.2021(16)
N(2A)-N(3A)	1.3664(14)
N(2B)-N(3B)	1.3667(13)
C(2C)-C(3C)	1.5059(18)
C(2A)-C(3A)	1.5128(18)
C(2D)-C(3D)	1.5070(18)
C(2B)-C(3B)	1.503(2)
Cl(3D)-C(18D)	1.7215(11)
Cl(3C)-C(18C)	1.7210(11)
Cl(3A)-C(18A)	1.7275(12)
N(3A)-C(6A)	1.3522(14)
N(3A)-C(13A)	1.4308(14)
Cl(3B)-C(18B)	1.7284(12)
N(3C)-C(6C)	1.3605(14)
N(3C)-C(13C)	1.4308(14)
N(3D)-C(6D)	1.3575(14)
N(3D)-C(13D)	1.4315(14)
N(3B)-C(6B)	1.3568(14)
N(3B)-C(13B)	1.4329(14)
C(4D)-C(5D)	1.4778(15)
C(4C)-C(5C)	1.4769(15)
C(4B)-C(5B)	1.4831(16)
C(4A)-C(5A)	1.4802(16)
C(5D)-C(6D)	1.3857(15)
C(5C)-C(6C)	1.3841(15)
C(5A)-C(6A)	1.3811(16)
C(5B)-C(6B)	1.3797(16)

C(6A)-C(7A)	1.4753(15)
C(6B)-C(7B)	1.4755(15)
C(6D)-C(7D)	1.4733(15)
C(6C)-C(7C)	1.4718(15)
C(7A)-C(12A)	1.3902(16)
C(7A)-C(8A)	1.3909(16)
C(7D)-C(12D)	1.3940(16)
C(7D)-C(8D)	1.3970(16)
C(7B)-C(12B)	1.3923(17)
C(7B)-C(8B)	1.3957(16)
C(7C)-C(12C)	1.3970(16)
C(7C)-C(8C)	1.3983(16)
C(8C)-C(9C)	1.3903(17)
C(8B)-C(9B)	1.3881(17)
C(8A)-C(9A)	1.3907(17)
C(8D)-C(9D)	1.3898(16)
C(9B)-C(10B)	1.3805(19)
C(9C)-C(10C)	1.3851(18)
C(9D)-C(10D)	1.3857(18)
C(9A)-C(10A)	1.3826(19)
C(10C)-C(11C)	1.3886(18)
C(10D)-C(11D)	1.3827(19)
C(10B)-C(11B)	1.378(2)
C(10A)-C(11A)	1.380(2)
C(11C)-C(12C)	1.3912(17)
C(11D)-C(12D)	1.3911(17)
C(11A)-C(12A)	1.3891(18)
C(11B)-C(12B)	1.3921(19)
C(13D)-C(14D)	1.3874(16)
C(13D)-C(18D)	1.3923(15)
C(13C)-C(14C)	1.3870(16)
C(13C)-C(18C)	1.3907(15)
C(13B)-C(14B)	1.3866(17)
C(13B)-C(18B)	1.3891(16)
C(13A)-C(14A)	1.3884(16)
C(13A)-C(18A)	1.3896(16)

C(14C)-C(15C)	1.3849(16)
C(14B)-C(15B)	1.3949(18)
C(14A)-C(15A)	1.3931(16)
C(14D)-C(15D)	1.3866(16)
C(15D)-C(16D)	1.3877(16)
C(15B)-C(16B)	1.3859(19)
C(15A)-C(16A)	1.3863(18)
C(15C)-C(16C)	1.3907(17)
C(16B)-C(17B)	1.3869(18)
C(16A)-C(17A)	1.3889(17)
C(16C)-C(17C)	1.3853(17)
C(16D)-C(17D)	1.3852(16)
C(17B)-C(18B)	1.3862(16)
C(17D)-C(18D)	1.3914(16)
C(17C)-C(18C)	1.3880(16)
C(17A)-C(18A)	1.3863(16)

C(4D)-O(1D)-C(3D)	116.36(9)
C(4C)-O(1C)-C(3C)	115.73(9)
C(4A)-O(1A)-C(3A)	118.68(10)
N(2B)-N(1B)-C(5B)	108.88(10)
N(2C)-N(1C)-C(5C)	109.36(9)
C(4B)-O(1B)-C(3B)	116.71(10)
N(2D)-N(1D)-C(5D)	109.19(9)
N(2A)-N(1A)-C(5A)	108.92(10)
N(1C)-N(2C)-N(3C)	106.96(9)
N(1D)-N(2D)-N(3D)	107.15(9)
N(1A)-N(2A)-N(3A)	106.95(9)
N(1B)-N(2B)-N(3B)	107.14(9)
C(3C)-C(2C)-C(1C)	114.55(12)
C(3A)-C(2A)-C(1A)	112.01(12)
C(3D)-C(2D)-C(1D)	112.89(11)
C(3B)-C(2B)-C(1B)	113.17(15)
C(6A)-N(3A)-N(2A)	111.39(9)
C(6A)-N(3A)-C(13A)	127.96(10)
N(2A)-N(3A)-C(13A)	120.63(9)

C(6C)-N(3C)-N(2C)	111.49(9)
C(6C)-N(3C)-C(13C)	127.72(10)
N(2C)-N(3C)-C(13C)	120.46(9)
C(6D)-N(3D)-N(2D)	111.22(9)
C(6D)-N(3D)-C(13D)	127.76(9)
N(2D)-N(3D)-C(13D)	120.25(9)
C(6B)-N(3B)-N(2B)	111.20(9)
C(6B)-N(3B)-C(13B)	128.73(10)
N(2B)-N(3B)-C(13B)	118.94(9)
O(1A)-C(3A)-C(2A)	106.29(10)
O(1C)-C(3C)-C(2C)	107.19(10)
O(1D)-C(3D)-C(2D)	106.84(10)
O(1B)-C(3B)-C(2B)	106.52(11)
O(2D)-C(4D)-O(1D)	124.81(10)
O(2D)-C(4D)-C(5D)	123.48(11)
O(1D)-C(4D)-C(5D)	111.72(9)
O(2C)-C(4C)-O(1C)	124.93(11)
O(2C)-C(4C)-C(5C)	123.57(11)
O(1C)-C(4C)-C(5C)	111.49(9)
O(2B)-C(4B)-O(1B)	125.79(11)
O(2B)-C(4B)-C(5B)	124.24(11)
O(1B)-C(4B)-C(5B)	109.96(10)
O(2A)-C(4A)-O(1A)	125.55(11)
O(2A)-C(4A)-C(5A)	124.70(11)
O(1A)-C(4A)-C(5A)	109.75(10)
N(1D)-C(5D)-C(6D)	109.06(10)
N(1D)-C(5D)-C(4D)	119.44(10)
C(6D)-C(5D)-C(4D)	131.50(10)
N(1C)-C(5C)-C(6C)	109.03(10)
N(1C)-C(5C)-C(4C)	119.21(10)
C(6C)-C(5C)-C(4C)	131.76(11)
N(1A)-C(5A)-C(6A)	109.38(10)
N(1A)-C(5A)-C(4A)	121.16(10)
C(6A)-C(5A)-C(4A)	129.39(11)
N(1B)-C(5B)-C(6B)	109.45(10)
N(1B)-C(5B)-C(4B)	119.83(10)

C(6B)-C(5B)-C(4B)	130.71(11)
N(3A)-C(6A)-C(5A)	103.35(10)
N(3A)-C(6A)-C(7A)	122.75(10)
C(5A)-C(6A)-C(7A)	133.79(10)
N(3B)-C(6B)-C(5B)	103.31(10)
N(3B)-C(6B)-C(7B)	121.90(10)
C(5B)-C(6B)-C(7B)	134.70(11)
N(3D)-C(6D)-C(5D)	103.37(9)
N(3D)-C(6D)-C(7D)	121.66(10)
C(5D)-C(6D)-C(7D)	134.96(10)
N(3C)-C(6C)-C(5C)	103.17(10)
N(3C)-C(6C)-C(7C)	121.12(10)
C(5C)-C(6C)-C(7C)	135.60(10)
C(12A)-C(7A)-C(8A)	119.69(11)
C(12A)-C(7A)-C(6A)	120.20(11)
C(8A)-C(7A)-C(6A)	120.10(10)
C(12D)-C(7D)-C(8D)	120.08(11)
C(12D)-C(7D)-C(6D)	119.65(10)
C(8D)-C(7D)-C(6D)	120.19(10)
C(12B)-C(7B)-C(8B)	119.40(11)
C(12B)-C(7B)-C(6B)	121.15(11)
C(8B)-C(7B)-C(6B)	119.43(10)
C(12C)-C(7C)-C(8C)	119.88(11)
C(12C)-C(7C)-C(6C)	119.85(10)
C(8C)-C(7C)-C(6C)	120.07(10)
C(9C)-C(8C)-C(7C)	120.29(11)
C(9B)-C(8B)-C(7B)	120.70(11)
C(9A)-C(8A)-C(7A)	120.16(12)
C(9D)-C(8D)-C(7D)	119.83(11)
C(10B)-C(9B)-C(8B)	118.78(12)
C(10C)-C(9C)-C(8C)	118.93(11)
C(10D)-C(9D)-C(8D)	119.15(12)
C(10A)-C(9A)-C(8A)	118.88(12)
C(9C)-C(10C)-C(11C)	121.73(11)
C(9C)-C(10C)-Cl(1C)	119.08(10)
C(11C)-C(10C)-Cl(1C)	119.18(10)

C(11D)-C(10D)-C(9D)	121.88(11)
C(11D)-C(10D)-Cl(1D)	119.40(10)
C(9D)-C(10D)-Cl(1D)	118.71(10)
C(11B)-C(10B)-C(9B)	121.69(12)
C(11B)-C(10B)-Cl(1B)	119.49(11)
C(9B)-C(10B)-Cl(1B)	118.82(11)
C(11A)-C(10A)-C(9A)	122.08(12)
C(11A)-C(10A)-Cl(1A)	119.32(10)
C(9A)-C(10A)-Cl(1A)	118.60(11)
C(10C)-C(11C)-C(12C)	119.17(11)
C(10D)-C(11D)-C(12D)	118.90(12)
C(10A)-C(11A)-C(12A)	118.53(12)
C(10B)-C(11B)-C(12B)	119.44(12)
C(11A)-C(12A)-C(7A)	120.66(12)
C(11D)-C(12D)-C(7D)	120.16(11)
C(11C)-C(12C)-C(7C)	119.95(11)
C(11B)-C(12B)-C(7B)	119.99(12)
C(14D)-C(13D)-C(18D)	120.43(10)
C(14D)-C(13D)-N(3D)	118.26(10)
C(18D)-C(13D)-N(3D)	121.30(10)
C(14C)-C(13C)-C(18C)	120.62(10)
C(14C)-C(13C)-N(3C)	118.59(10)
C(18C)-C(13C)-N(3C)	120.76(10)
C(14B)-C(13B)-C(18B)	120.79(11)
C(14B)-C(13B)-N(3B)	120.87(11)
C(18B)-C(13B)-N(3B)	118.28(10)
C(14A)-C(13A)-C(18A)	120.57(11)
C(14A)-C(13A)-N(3A)	119.96(10)
C(18A)-C(13A)-N(3A)	119.47(10)
C(15C)-C(14C)-C(13C)	119.89(11)
C(13B)-C(14B)-C(15B)	119.39(12)
C(13A)-C(14A)-C(15A)	119.65(11)
C(15D)-C(14D)-C(13D)	120.01(11)
C(14D)-C(15D)-C(16D)	118.79(11)
C(16B)-C(15B)-C(14B)	118.65(11)
C(16A)-C(15A)-C(14A)	118.68(11)

C(14C)-C(15C)-C(16C)	118.58(11)
C(15B)-C(16B)-C(17B)	122.78(11)
C(15B)-C(16B)-Cl(2B)	119.49(10)
C(17B)-C(16B)-Cl(2B)	117.72(10)
C(15A)-C(16A)-C(17A)	122.53(11)
C(15A)-C(16A)-Cl(2A)	119.39(9)
C(17A)-C(16A)-Cl(2A)	118.08(10)
C(17C)-C(16C)-C(15C)	122.52(11)
C(17C)-C(16C)-Cl(2C)	118.92(9)
C(15C)-C(16C)-Cl(2C)	118.56(9)
C(17D)-C(16D)-C(15D)	122.24(10)
C(17D)-C(16D)-Cl(2D)	119.27(9)
C(15D)-C(16D)-Cl(2D)	118.48(9)
C(18B)-C(17B)-C(16B)	117.70(11)
C(16D)-C(17D)-C(18D)	118.33(10)
C(16C)-C(17C)-C(18C)	118.02(11)
C(18A)-C(17A)-C(16A)	117.93(11)
C(17D)-C(18D)-C(13D)	120.19(10)
C(17D)-C(18D)-Cl(3D)	119.37(9)
C(13D)-C(18D)-Cl(3D)	120.43(9)
C(17C)-C(18C)-C(13C)	120.34(10)
C(17C)-C(18C)-Cl(3C)	119.32(9)
C(13C)-C(18C)-Cl(3C)	120.33(9)
C(17A)-C(18A)-C(13A)	120.63(11)
C(17A)-C(18A)-Cl(3A)	119.93(9)
C(13A)-C(18A)-Cl(3A)	119.43(9)
C(17B)-C(18B)-C(13B)	120.69(11)
C(17B)-C(18B)-Cl(3B)	119.89(9)
C(13B)-C(18B)-Cl(3B)	119.40(9)

Table 4. Anisotropic displacement parameters ($Å^2 x\ 10^3$) for **31a**. The anisotropic displacement factor exponent takes the form: $-2\cdot^2[\ h^2\ a^{*2}U^{11} + ... + 2\ h\ k\ a^*\ b^*\ U^{12}\ ]$

	U^{11}	U^{22}	U^{33}	U^{23}	U^{13}	U^{12}
O(1D)	20(1)	21(1)	21(1)	0(1)	7(1)	6(1)
Cl(1C)	34(1)	44(1)	20(1)	-2(1)	8(1)	7(1)
O(1C)	20(1)	20(1)	25(1)	0(1)	8(1)	-4(1)
Cl(1D)	42(1)	50(1)	17(1)	3(1)	9(1)	2(1)
Cl(1A)	61(1)	28(1)	60(1)	-11(1)	33(1)	7(1)
Cl(1B)	44(1)	53(1)	74(1)	-39(1)	20(1)	4(1)
O(1A)	28(1)	20(1)	40(1)	-1(1)	17(1)	-5(1)
N(1B)	25(1)	20(1)	21(1)	1(1)	8(1)	1(1)
N(1C)	22(1)	17(1)	23(1)	1(1)	9(1)	1(1)
O(1B)	31(1)	19(1)	41(1)	-3(1)	18(1)	-5(1)
N(1D)	22(1)	17(1)	20(1)	-1(1)	7(1)	0(1)
N(1A)	22(1)	20(1)	23(1)	1(1)	8(1)	1(1)
C(1A)	49(1)	35(1)	32(1)	-4(1)	15(1)	0(1)
C(1D)	34(1)	41(1)	25(1)	-3(1)	0(1)	4(1)
C(1C)	45(1)	37(1)	28(1)	3(1)	0(1)	-9(1)
C(1B)	82(2)	31(1)	61(1)	2(1)	30(1)	16(1)
O(2D)	24(1)	25(1)	23(1)	-4(1)	9(1)	4(1)
Cl(2D)	24(1)	27(1)	42(1)	-9(1)	16(1)	3(1)
O(2A)	27(1)	29(1)	40(1)	-2(1)	17(1)	-4(1)
O(2C)	23(1)	25(1)	28(1)	4(1)	11(1)	-2(1)
Cl(2A)	28(1)	39(1)	35(1)	1(1)	17(1)	-8(1)
N(2C)	24(1)	19(1)	21(1)	0(1)	10(1)	0(1)
Cl(2B)	32(1)	31(1)	51(1)	0(1)	25(1)	-5(1)
N(2D)	24(1)	19(1)	18(1)	1(1)	8(1)	2(1)
Cl(2C)	26(1)	30(1)	69(1)	13(1)	24(1)	-3(1)
O(2B)	33(1)	31(1)	38(1)	-5(1)	20(1)	-6(1)
N(2A)	24(1)	20(1)	25(1)	0(1)	10(1)	1(1)
N(2B)	27(1)	19(1)	22(1)	-2(1)	9(1)	2(1)
C(2C)	34(1)	29(1)	30(1)	-6(1)	8(1)	-8(1)
C(2A)	35(1)	21(1)	35(1)	3(1)	15(1)	-2(1)

C(2D)	32(1)	29(1)	28(1)	6(1)	6(1)	9(1)
C(2B)	61(1)	25(1)	31(1)	-3(1)	16(1)	-12(1)
Cl(3D)	22(1)	19(1)	32(1)	-1(1)	9(1)	-4(1)
Cl(3C)	28(1)	17(1)	41(1)	-1(1)	18(1)	3(1)
Cl(3A)	21(1)	32(1)	36(1)	14(1)	2(1)	-1(1)
N(3A)	22(1)	16(1)	21(1)	0(1)	7(1)	0(1)
Cl(3B)	20(1)	35(1)	28(1)	7(1)	3(1)	-2(1)
N(3C)	19(1)	15(1)	20(1)	0(1)	7(1)	-1(1)
N(3D)	19(1)	15(1)	18(1)	1(1)	6(1)	2(1)
N(3B)	22(1)	16(1)	20(1)	-2(1)	6(1)	-1(1)
C(3A)	29(1)	20(1)	30(1)	1(1)	12(1)	-6(1)
C(3C)	21(1)	20(1)	30(1)	-1(1)	8(1)	-6(1)
C(3D)	21(1)	19(1)	26(1)	0(1)	6(1)	5(1)
C(3B)	40(1)	24(1)	42(1)	-4(1)	19(1)	-13(1)
C(4D)	16(1)	14(1)	22(1)	-3(1)	6(1)	-3(1)
C(4C)	18(1)	14(1)	25(1)	2(1)	9(1)	3(1)
C(4B)	24(1)	22(1)	22(1)	1(1)	8(1)	-2(1)
C(4A)	22(1)	22(1)	18(1)	0(1)	5(1)	-2(1)
C(5D)	18(1)	14(1)	20(1)	-2(1)	6(1)	-1(1)
C(5C)	19(1)	15(1)	23(1)	2(1)	8(1)	2(1)
C(5A)	20(1)	20(1)	18(1)	0(1)	5(1)	0(1)
C(5B)	22(1)	19(1)	20(1)	0(1)	6(1)	1(1)
C(6A)	18(1)	18(1)	18(1)	2(1)	4(1)	-1(1)
C(6B)	20(1)	16(1)	19(1)	1(1)	3(1)	0(1)
C(6D)	17(1)	13(1)	20(1)	-1(1)	5(1)	0(1)
C(6C)	17(1)	13(1)	22(1)	0(1)	6(1)	1(1)
C(7A)	19(1)	17(1)	22(1)	0(1)	7(1)	-2(1)
C(7D)	17(1)	20(1)	17(1)	0(1)	5(1)	2(1)
C(7B)	22(1)	15(1)	21(1)	0(1)	7(1)	0(1)
C(7C)	16(1)	19(1)	21(1)	0(1)	6(1)	0(1)
C(8C)	23(1)	19(1)	22(1)	0(1)	5(1)	0(1)
C(8B)	20(1)	24(1)	25(1)	-1(1)	5(1)	1(1)
C(8A)	32(1)	20(1)	23(1)	1(1)	8(1)	2(1)
C(8D)	21(1)	20(1)	21(1)	0(1)	6(1)	2(1)
C(9B)	29(1)	26(1)	27(1)	-6(1)	6(1)	-2(1)
C(9C)	26(1)	25(1)	22(1)	4(1)	5(1)	0(1)

C(9D)	23(1)	25(1)	23(1)	5(1)	6(1)	2(1)
C(9A)	42(1)	25(1)	24(1)	-2(1)	13(1)	1(1)
C(10C)	20(1)	32(1)	18(1)	-2(1)	5(1)	2(1)
C(10D)	22(1)	36(1)	16(1)	2(1)	4(1)	2(1)
C(10B)	32(1)	24(1)	42(1)	-12(1)	15(1)	2(1)
C(10A)	31(1)	18(1)	39(1)	-6(1)	18(1)	0(1)
C(11C)	24(1)	23(1)	26(1)	-5(1)	7(1)	0(1)
C(11D)	30(1)	29(1)	20(1)	-5(1)	5(1)	1(1)
C(11A)	26(1)	22(1)	39(1)	4(1)	11(1)	5(1)
C(11B)	23(1)	30(1)	49(1)	-10(1)	7(1)	5(1)
C(12A)	23(1)	26(1)	25(1)	4(1)	6(1)	3(1)
C(12D)	26(1)	21(1)	22(1)	-2(1)	5(1)	0(1)
C(12C)	23(1)	19(1)	25(1)	-1(1)	8(1)	-1(1)
C(12B)	23(1)	23(1)	34(1)	-5(1)	2(1)	2(1)
C(13D)	18(1)	15(1)	18(1)	0(1)	5(1)	3(1)
C(13C)	17(1)	16(1)	21(1)	2(1)	6(1)	-2(1)
C(13B)	22(1)	15(1)	22(1)	-3(1)	8(1)	-1(1)
C(13A)	22(1)	15(1)	22(1)	-1(1)	9(1)	-2(1)
C(14C)	23(1)	15(1)	31(1)	3(1)	11(1)	2(1)
C(14B)	24(1)	20(1)	25(1)	-4(1)	5(1)	0(1)
C(14A)	24(1)	19(1)	20(1)	-2(1)	6(1)	0(1)
C(14D)	25(1)	14(1)	28(1)	-1(1)	11(1)	0(1)
C(15D)	23(1)	18(1)	29(1)	-3(1)	11(1)	-3(1)
C(15B)	20(1)	22(1)	33(1)	-6(1)	7(1)	0(1)
C(15A)	20(1)	22(1)	26(1)	-5(1)	7(1)	-1(1)
C(15C)	21(1)	21(1)	36(1)	6(1)	12(1)	5(1)
C(16B)	25(1)	18(1)	33(1)	-5(1)	16(1)	-3(1)
C(16A)	24(1)	21(1)	26(1)	-4(1)	12(1)	-3(1)
C(16C)	17(1)	22(1)	34(1)	8(1)	8(1)	-2(1)
C(16D)	19(1)	20(1)	24(1)	-4(1)	7(1)	3(1)
C(17B)	27(1)	20(1)	24(1)	-2(1)	10(1)	0(1)
C(17D)	22(1)	14(1)	24(1)	-3(1)	5(1)	2(1)
C(17C)	22(1)	15(1)	33(1)	3(1)	7(1)	-2(1)
C(17A)	27(1)	20(1)	24(1)	1(1)	9(1)	-2(1)
C(18D)	18(1)	15(1)	18(1)	0(1)	3(1)	-1(1)
C(18C)	18(1)	15(1)	23(1)	0(1)	5(1)	1(1)

C(18A)	20(1)	18(1)	24(1)	1(1)	4(1)	-1(1)
C(18B)	20(1)	19(1)	23(1)	-3(1)	6(1)	-1(1)

Table 5. Hydrogen coordinates (x 10^4) and isotropic displacement parameters (Å^{2}x 10^3) for **31a**.

	x	y	z	U(eq)
H(1AC)	-6266(14)	2400(12)	1696(9)	57(6)
H(1AB)	-6305(13)	3200(11)	1834(9)	58(6)
H(1AA)	-5478(13)	2855(10)	1771(9)	44(5)
H(1DC)	-2892(13)	4853(11)	7747(9)	51(6)
H(1DB)	-2155(13)	4486(10)	8184(9)	48(5)
H(1DA)	-3070(13)	4521(10)	8314(9)	48(5)
H(1CC)	-2269(14)	760(11)	3141(9)	48(5)
H(1CB)	-3159(13)	685(10)	3250(9)	47(5)
H(1CA)	-2936(13)	431(10)	2676(9)	50(6)
H(1BC)	-2105(16)	2708(13)	1017(11)	72(7)
H(1BB)	-1727(14)	3321(12)	712(10)	63(7)
H(1BA)	-1814(18)	3408(15)	1352(12)	92(9)
H(2CB)	-2056(12)	-446(10)	3203(8)	44(5)
H(2CA)	-2981(13)	-532(10)	3264(8)	44(5)
H(2AB)	-6848(11)	3017(9)	802(7)	31(4)
H(2AA)	-6062(11)	3441(9)	899(8)	37(5)
H(2DB)	-1936(12)	5667(9)	8324(8)	37(5)
H(2DA)	-2852(12)	5747(10)	8401(8)	42(5)
H(2BB)	-756(11)	2593(10)	1628(8)	38(5)
H(2BA)	-431(12)	3139(10)	1281(8)	46(5)
H(3AB)	-5965(10)	2591(9)	230(8)	31(4)
H(3AA)	-5292(10)	2416(8)	808(7)	27(4)
H(3CB)	-2599(10)	-51(8)	4193(7)	26(4)
H(3CA)	-2016(10)	-660(8)	4168(7)	24(4)
H(3DB)	-2535(10)	5189(8)	9283(7)	25(4)
H(3DA)	-1902(10)	5768(8)	9302(7)	25(4)

H(3BB)	-743(11)	2448(9)	442(8)	38(5)
H(3BA)	-66(13)	2102(10)	943(9)	46(5)
H(8C)	-34(10)	1983(9)	3617(7)	29(4)
H(8B)	-1417(11)	1222(9)	1929(7)	32(4)
H(8A)	-7020(10)	772(8)	2062(7)	27(4)
H(8D)	59(10)	5108(9)	8857(7)	29(4)
H(9B)	-1842(12)	2030(10)	2517(9)	46(5)
H(9C)	93(11)	1876(9)	2652(8)	33(4)
H(9D)	46(11)	5286(9)	7885(8)	33(4)
H(9A)	-7566(11)	1603(9)	2587(8)	40(5)
H(11C)	140(11)	-208(9)	2835(8)	33(4)
H(11D)	-231(11)	3229(9)	7583(8)	36(4)
H(11A)	-8615(11)	2569(9)	1071(7)	34(4)
H(11B)	-4180(11)	1896(9)	1494(8)	36(4)
H(12A)	-8080(10)	1733(9)	566(7)	31(4)
H(12D)	-222(10)	3062(8)	8572(7)	23(4)
H(12C)	53(11)	-81(9)	3806(8)	32(4)
H(12B)	-3740(11)	1119(9)	895(7)	31(4)
H(14C)	1902(10)	899(9)	4471(7)	27(4)
H(14B)	-4174(10)	-217(8)	531(7)	28(4)
H(14A)	-8991(10)	-22(8)	505(7)	24(4)
H(14D)	1826(11)	4066(9)	9495(7)	30(4)
H(15D)	2928(11)	3573(9)	9182(8)	35(4)
H(15B)	-5060(11)	-800(8)	1000(7)	28(4)
H(15A)	-10001(11)	-552(8)	885(7)	28(4)
H(15C)	2989(12)	1434(10)	4158(8)	41(5)
H(17B)	-3150(10)	-1248(9)	2363(7)	29(4)
H(17D)	1957(10)	1695(8)	9312(7)	24(4)
H(17C)	2095(10)	3283(9)	4477(7)	29(4)
H(17A)	-8219(11)	-1255(9)	2249(8)	30(4)

Table 6. Torsion angles [°] for **31a**.

C(5C)-N(1C)-N(2C)-N(3C)	-0.05(12)
C(5D)-N(1D)-N(2D)-N(3D)	-0.17(12)
C(5A)-N(1A)-N(2A)-N(3A)	-0.63(13)
C(5B)-N(1B)-N(2B)-N(3B)	0.56(13)
N(1A)-N(2A)-N(3A)-C(6A)	0.07(13)
N(1A)-N(2A)-N(3A)-C(13A)	-178.90(10)
N(1C)-N(2C)-N(3C)-C(6C)	-0.45(12)
N(1C)-N(2C)-N(3C)-C(13C)	-174.30(9)
N(1D)-N(2D)-N(3D)-C(6D)	0.44(12)
N(1D)-N(2D)-N(3D)-C(13D)	171.17(9)
N(1B)-N(2B)-N(3B)-C(6B)	-1.22(13)
N(1B)-N(2B)-N(3B)-C(13B)	-170.12(10)
C(4A)-O(1A)-C(3A)-C(2A)	-163.14(11)
C(1A)-C(2A)-C(3A)-O(1A)	67.05(15)
C(4C)-O(1C)-C(3C)-C(2C)	175.51(10)
C(1C)-C(2C)-C(3C)-O(1C)	-58.86(15)
C(4D)-O(1D)-C(3D)-C(2D)	-175.25(10)
C(1D)-C(2D)-C(3D)-O(1D)	56.44(14)
C(4B)-O(1B)-C(3B)-C(2B)	-160.86(12)
C(1B)-C(2B)-C(3B)-O(1B)	-62.80(17)
C(3D)-O(1D)-C(4D)-O(2D)	0.67(16)
C(3D)-O(1D)-C(4D)-C(5D)	-179.23(9)
C(3C)-O(1C)-C(4C)-O(2C)	-1.73(16)
C(3C)-O(1C)-C(4C)-C(5C)	179.05(9)
C(3B)-O(1B)-C(4B)-O(2B)	-5.4(2)
C(3B)-O(1B)-C(4B)-C(5B)	173.65(11)
C(3A)-O(1A)-C(4A)-O(2A)	-2.62(19)
C(3A)-O(1A)-C(4A)-C(5A)	176.87(10)
N(2D)-N(1D)-C(5D)-C(6D)	-0.14(13)
N(2D)-N(1D)-C(5D)-C(4D)	-179.80(9)
O(2D)-C(4D)-C(5D)-N(1D)	5.57(17)
O(1D)-C(4D)-C(5D)-N(1D)	-174.53(10)
O(2D)-C(4D)-C(5D)-C(6D)	-174.00(12)
O(1D)-C(4D)-C(5D)-C(6D)	5.90(16)

N(2C)-N(1C)-C(5C)-C(6C)	0.51(13)
N(2C)-N(1C)-C(5C)-C(4C)	-179.48(10)
O(2C)-C(4C)-C(5C)-N(1C)	-5.89(17)
O(1C)-C(4C)-C(5C)-N(1C)	173.33(9)
O(2C)-C(4C)-C(5C)-C(6C)	174.12(12)
O(1C)-C(4C)-C(5C)-C(6C)	-6.66(17)
N(2A)-N(1A)-C(5A)-C(6A)	0.97(13)
N(2A)-N(1A)-C(5A)-C(4A)	178.20(10)
O(2A)-C(4A)-C(5A)-N(1A)	-11.71(19)
O(1A)-C(4A)-C(5A)-N(1A)	168.80(11)
O(2A)-C(4A)-C(5A)-C(6A)	164.90(13)
O(1A)-C(4A)-C(5A)-C(6A)	-14.58(17)
N(2B)-N(1B)-C(5B)-C(6B)	0.26(13)
N(2B)-N(1B)-C(5B)-C(4B)	179.62(10)
O(2B)-C(4B)-C(5B)-N(1B)	-7.93(19)
O(1B)-C(4B)-C(5B)-N(1B)	173.03(11)
O(2B)-C(4B)-C(5B)-C(6B)	171.28(13)
O(1B)-C(4B)-C(5B)-C(6B)	-7.76(18)
N(2A)-N(3A)-C(6A)-C(5A)	0.50(13)
C(13A)-N(3A)-C(6A)-C(5A)	179.37(11)
N(2A)-N(3A)-C(6A)-C(7A)	-176.02(10)
C(13A)-N(3A)-C(6A)-C(7A)	2.85(18)
N(1A)-C(5A)-C(6A)-N(3A)	-0.87(13)
C(4A)-C(5A)-C(6A)-N(3A)	-177.81(11)
N(1A)-C(5A)-C(6A)-C(7A)	175.07(12)
C(4A)-C(5A)-C(6A)-C(7A)	-1.9(2)
N(2B)-N(3B)-C(6B)-C(5B)	1.32(12)
C(13B)-N(3B)-C(6B)-C(5B)	168.85(11)
N(2B)-N(3B)-C(6B)-C(7B)	-175.68(10)
C(13B)-N(3B)-C(6B)-C(7B)	-8.16(18)
N(1B)-C(5B)-C(6B)-N(3B)	-0.96(13)
C(4B)-C(5B)-C(6B)-N(3B)	179.77(12)
N(1B)-C(5B)-C(6B)-C(7B)	175.47(12)
C(4B)-C(5B)-C(6B)-C(7B)	-3.8(2)
N(2D)-N(3D)-C(6D)-C(5D)	-0.50(12)
C(13D)-N(3D)-C(6D)-C(5D)	-170.36(10)

N(2D)-N(3D)-C(6D)-C(7D)	178.66(10)
C(13D)-N(3D)-C(6D)-C(7D)	8.80(17)
N(1D)-C(5D)-C(6D)-N(3D)	0.39(12)
C(4D)-C(5D)-C(6D)-N(3D)	179.99(11)
N(1D)-C(5D)-C(6D)-C(7D)	-178.61(12)
C(4D)-C(5D)-C(6D)-C(7D)	1.0(2)
N(2C)-N(3C)-C(6C)-C(5C)	0.74(12)
C(13C)-N(3C)-C(6C)-C(5C)	174.03(10)
N(2C)-N(3C)-C(6C)-C(7C)	-176.06(9)
C(13C)-N(3C)-C(6C)-C(7C)	-2.77(17)
N(1C)-C(5C)-C(6C)-N(3C)	-0.74(12)
C(4C)-C(5C)-C(6C)-N(3C)	179.25(11)
N(1C)-C(5C)-C(6C)-C(7C)	175.34(12)
C(4C)-C(5C)-C(6C)-C(7C)	-4.7(2)
N(3A)-C(6A)-C(7A)-C(12A)	-114.57(13)
C(5A)-C(6A)-C(7A)-C(12A)	70.13(18)
N(3A)-C(6A)-C(7A)-C(8A)	66.66(16)
C(5A)-C(6A)-C(7A)-C(8A)	-108.64(15)
N(3D)-C(6D)-C(7D)-C(12D)	53.79(15)
C(5D)-C(6D)-C(7D)-C(12D)	-127.36(14)
N(3D)-C(6D)-C(7D)-C(8D)	-122.95(12)
C(5D)-C(6D)-C(7D)-C(8D)	55.90(18)
N(3B)-C(6B)-C(7B)-C(12B)	-58.01(16)
C(5B)-C(6B)-C(7B)-C(12B)	126.10(15)
N(3B)-C(6B)-C(7B)-C(8B)	120.16(13)
C(5B)-C(6B)-C(7B)-C(8B)	-55.74(19)
N(3C)-C(6C)-C(7C)-C(12C)	122.01(12)
C(5C)-C(6C)-C(7C)-C(12C)	-53.53(18)
N(3C)-C(6C)-C(7C)-C(8C)	-52.82(15)
C(5C)-C(6C)-C(7C)-C(8C)	131.64(14)
C(12C)-C(7C)-C(8C)-C(9C)	-2.22(17)
C(6C)-C(7C)-C(8C)-C(9C)	172.61(11)
C(12B)-C(7B)-C(8B)-C(9B)	-0.45(19)
C(6B)-C(7B)-C(8B)-C(9B)	-178.64(11)
C(12A)-C(7A)-C(8A)-C(9A)	-0.46(19)
C(6A)-C(7A)-C(8A)-C(9A)	178.32(12)

C(12D)-C(7D)-C(8D)-C(9D)	-0.67(17)
C(6D)-C(7D)-C(8D)-C(9D)	176.06(10)
C(7B)-C(8B)-C(9B)-C(10B)	0.3(2)
C(7C)-C(8C)-C(9C)-C(10C)	0.46(18)
C(7D)-C(8D)-C(9D)-C(10D)	0.00(18)
C(7A)-C(8A)-C(9A)-C(10A)	0.2(2)
C(8C)-C(9C)-C(10C)-C(11C)	1.75(19)
C(8C)-C(9C)-C(10C)-Cl(1C)	-177.36(9)
C(8D)-C(9D)-C(10D)-C(11D)	0.74(19)
C(8D)-C(9D)-C(10D)-Cl(1D)	-178.41(9)
C(8B)-C(9B)-C(10B)-C(11B)	0.1(2)
C(8B)-C(9B)-C(10B)-Cl(1B)	179.30(11)
C(8A)-C(9A)-C(10A)-C(11A)	0.2(2)
C(8A)-C(9A)-C(10A)-Cl(1A)	-178.89(10)
C(9C)-C(10C)-C(11C)-C(12C)	-2.16(18)
Cl(1C)-C(10C)-C(11C)-C(12C)	176.95(9)
C(9D)-C(10D)-C(11D)-C(12D)	-0.79(19)
Cl(1D)-C(10D)-C(11D)-C(12D)	178.34(10)
C(9A)-C(10A)-C(11A)-C(12A)	-0.3(2)
Cl(1A)-C(10A)-C(11A)-C(12A)	178.80(10)
C(9B)-C(10B)-C(11B)-C(12B)	-0.4(2)
Cl(1B)-C(10B)-C(11B)-C(12B)	-179.56(12)
C(10A)-C(11A)-C(12A)-C(7A)	-0.03(19)
C(8A)-C(7A)-C(12A)-C(11A)	0.38(18)
C(6A)-C(7A)-C(12A)-C(11A)	-178.39(11)
C(10D)-C(11D)-C(12D)-C(7D)	0.11(19)
C(8D)-C(7D)-C(12D)-C(11D)	0.61(18)
C(6D)-C(7D)-C(12D)-C(11D)	-176.13(11)
C(10C)-C(11C)-C(12C)-C(7C)	0.35(18)
C(8C)-C(7C)-C(12C)-C(11C)	1.80(17)
C(6C)-C(7C)-C(12C)-C(11C)	-173.04(11)
C(10B)-C(11B)-C(12B)-C(7B)	0.2(2)
C(8B)-C(7B)-C(12B)-C(11B)	0.2(2)
C(6B)-C(7B)-C(12B)-C(11B)	178.35(12)
C(6D)-N(3D)-C(13D)-C(14D)	64.04(16)
N(2D)-N(3D)-C(13D)-C(14D)	-105.01(12)

C(6D)-N(3D)-C(13D)-C(18D)	-115.33(13)
N(2D)-N(3D)-C(13D)-C(18D)	75.62(14)
C(6C)-N(3C)-C(13C)-C(14C)	-64.99(16)
N(2C)-N(3C)-C(13C)-C(14C)	107.76(13)
C(6C)-N(3C)-C(13C)-C(18C)	113.10(13)
N(2C)-N(3C)-C(13C)-C(18C)	-74.14(14)
C(6B)-N(3B)-C(13B)-C(14B)	100.14(14)
N(2B)-N(3B)-C(13B)-C(14B)	-93.16(13)
C(6B)-N(3B)-C(13B)-C(18B)	-82.66(15)
N(2B)-N(3B)-C(13B)-C(18B)	84.04(13)
C(6A)-N(3A)-C(13A)-C(14A)	80.03(15)
N(2A)-N(3A)-C(13A)-C(14A)	-101.19(13)
C(6A)-N(3A)-C(13A)-C(18A)	-99.77(14)
N(2A)-N(3A)-C(13A)-C(18A)	79.01(14)
C(18C)-C(13C)-C(14C)-C(15C)	-0.73(19)
N(3C)-C(13C)-C(14C)-C(15C)	177.36(11)
C(18B)-C(13B)-C(14B)-C(15B)	0.02(17)
N(3B)-C(13B)-C(14B)-C(15B)	177.14(10)
C(18A)-C(13A)-C(14A)-C(15A)	-0.93(17)
N(3A)-C(13A)-C(14A)-C(15A)	179.27(10)
C(18D)-C(13D)-C(14D)-C(15D)	0.60(18)
N(3D)-C(13D)-C(14D)-C(15D)	-178.78(11)
C(13D)-C(14D)-C(15D)-C(16D)	-0.86(19)
C(13B)-C(14B)-C(15B)-C(16B)	-0.61(18)
C(13A)-C(14A)-C(15A)-C(16A)	-0.21(17)
C(13C)-C(14C)-C(15C)-C(16C)	1.63(19)
C(14B)-C(15B)-C(16B)-C(17B)	0.80(18)
C(14B)-C(15B)-C(16B)-Cl(2B)	-177.81(9)
C(14A)-C(15A)-C(16A)-C(17A)	1.11(18)
C(14A)-C(15A)-C(16A)-Cl(2A)	-178.33(9)
C(14C)-C(15C)-C(16C)-C(17C)	-1.1(2)
C(14C)-C(15C)-C(16C)-Cl(2C)	178.54(10)
C(14D)-C(15D)-C(16D)-C(17D)	0.35(19)
C(14D)-C(15D)-C(16D)-Cl(2D)	-178.88(10)
C(15B)-C(16B)-C(17B)-C(18B)	-0.37(18)
Cl(2B)-C(16B)-C(17B)-C(18B)	178.27(9)

C(15D)-C(16D)-C(17D)-C(18D)	0.44(18)
Cl(2D)-C(16D)-C(17D)-C(18D)	179.66(9)
C(15C)-C(16C)-C(17C)-C(18C)	-0.4(2)
Cl(2C)-C(16C)-C(17C)-C(18C)	180.00(9)
C(15A)-C(16A)-C(17A)-C(18A)	-0.83(18)
Cl(2A)-C(16A)-C(17A)-C(18A)	178.61(9)
C(16D)-C(17D)-C(18D)-C(13D)	-0.71(17)
C(16D)-C(17D)-C(18D)-Cl(3D)	179.83(9)
C(14D)-C(13D)-C(18D)-C(17D)	0.20(17)
N(3D)-C(13D)-C(18D)-C(17D)	179.56(10)
C(14D)-C(13D)-C(18D)-Cl(3D)	179.66(9)
N(3D)-C(13D)-C(18D)-Cl(3D)	-0.98(15)
C(16C)-C(17C)-C(18C)-C(13C)	1.29(18)
C(16C)-C(17C)-C(18C)-Cl(3C)	-177.59(10)
C(14C)-C(13C)-C(18C)-C(17C)	-0.76(18)
N(3C)-C(13C)-C(18C)-C(17C)	-178.82(11)
C(14C)-C(13C)-C(18C)-Cl(3C)	178.11(9)
N(3C)-C(13C)-C(18C)-Cl(3C)	0.06(15)
C(16A)-C(17A)-C(18A)-C(13A)	-0.33(18)
C(16A)-C(17A)-C(18A)-Cl(3A)	179.36(9)
C(14A)-C(13A)-C(18A)-C(17A)	1.21(18)
N(3A)-C(13A)-C(18A)-C(17A)	-178.99(11)
C(14A)-C(13A)-C(18A)-Cl(3A)	-178.49(9)
N(3A)-C(13A)-C(18A)-Cl(3A)	1.32(15)
C(16B)-C(17B)-C(18B)-C(13B)	-0.25(17)
C(16B)-C(17B)-C(18B)-Cl(3B)	-178.66(9)
C(14B)-C(13B)-C(18B)-C(17B)	0.43(18)
N(3B)-C(13B)-C(18B)-C(17B)	-176.78(10)
C(14B)-C(13B)-C(18B)-Cl(3B)	178.85(9)
N(3B)-C(13B)-C(18B)-Cl(3B)	1.64(15)

Figure 28. ORTEP Drawing of 1,5-diaryl-1,2,3-triazoles **31a** .[61]

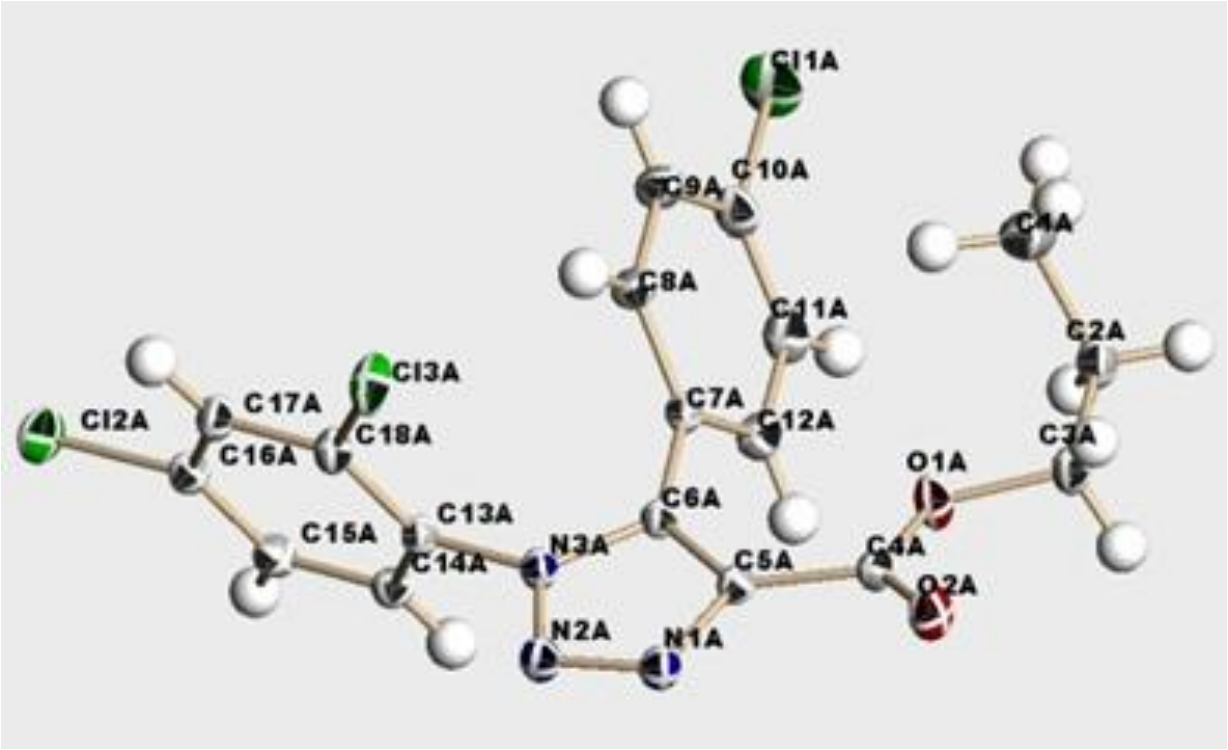

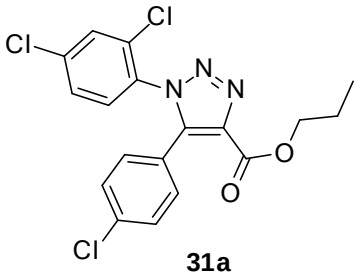

31a

2. Data_hsp572 (Compound **36a**) (Figure 27)

Table 1. Crystal data and structure refinement for **36a**.

Identification code	HSP572
Empirical formula	$C_{14}H_8Cl_3N_3$
Formula weight	324.58
Temperature	120(2) K
Wavelength	0.71073 Å
Crystal system	Monoclinic

Space group	$P2_1/c$	
Unit cell dimensions	a = 19.8341(7) Å	· = 90°.
	b = 5.5235(2) Å	· = 98.2660(10)°.
	c = 12.3196(4) Å	· = 90°.
Volume	1335.64(8) $Å^3$	
Z	4	
Density (calculated)	1.614 Mg/m^3	
Absorption coefficient	0.676 mm^{-1}	
F(000)	656	
Crystal size	0.65 x 0.50 x 0.25 mm^3	
Theta range for data collection	2.08 to 46.84°.	
Index ranges	-39<=h<=39, -9<=k<=9, -24<=l<=24	
Reflections collected	88047	
Independent reflections	10494 [R(int) = 0.0224]	
Completeness to theta = 46.84°	86.7 %	
Absorption correction	Empirical multi-scan	
Max. and min. transmission	0.8491 and 0.6675	
Refinement method	Full-matrix least-squares on F^2	
Data / restraints / parameters	10494 / 0 / 213	
Goodness-of-fit on F^2	1.116	
Final R indices [I>2sigma(I)]	R_1 = 0.0363, wR_2 = 0.0953	
R indices (all data)	R_1 = 0.0447, wR_2 = 0.1073	
Largest diff. peak and hole	0.769 and -0.439 e.$Å^{-3}$	

Table 2. Atomic coordinates (x 10^4) and equivalent isotropic displacement parameters ($Å^2$x 10^3) for **36a**. U(eq) is defined as one third of the trace of the orthogonalized U^{ij} tensor.

	x	y	z	U(eq)
Cl(1)	1988(1)	9551(1)	1679(1)	20(1)
N(1)	2544(1)	10470(1)	-1581(1)	22(1)
C(1)	3091(1)	9084(2)	-1194(1)	21(1)
Cl(2)	201(1)	2229(1)	1580(1)	26(1)
N(2)	2010(1)	9651(1)	-1186(1)	20(1)

C(2)	2895(1)	7301(1)	-518(1)	17(1)
N(3)	2215(1)	7730(1)	-536(1)	16(1)
Cl(3)	4617(1)	-511(1)	1842(1)	27(1)
C(3)	3302(1)	5384(1)	81(1)	16(1)
C(4)	3910(1)	4668(2)	-288(1)	20(1)
C(5)	4322(1)	2890(2)	257(1)	22(1)
C(6)	4121(1)	1790(1)	1174(1)	19(1)
C(7)	3528(1)	2475(2)	1565(1)	20(1)
C(8)	3122(1)	4280(2)	1020(1)	19(1)
C(9)	1712(1)	6465(1)	-39(1)	15(1)
C(10)	1556(1)	7179(1)	984(1)	16(1)
C(11)	1073(1)	5922(1)	1473(1)	18(1)
C(12)	754(1)	3943(1)	923(1)	18(1)
C(13)	890(1)	3233(1)	-105(1)	20(1)
C(14)	1371(1)	4519(1)	-585(1)	18(1)

Table 3. Bond lengths [Å] and angles [°] for **36a**.

Cl(1)-C(10)	1.7245(7)
N(1)-N(2)	1.3081(9)
N(1)-C(1)	1.3564(11)
C(1)-C(2)	1.3811(9)
Cl(2)-C(12)	1.7356(7)
N(2)-N(3)	1.3567(8)
C(2)-N(3)	1.3654(8)
C(2)-C(3)	1.4650(10)
N(3)-C(9)	1.4265(8)
Cl(3)-C(6)	1.7389(8)
C(3)-C(8)	1.3986(9)
C(3)-C(4)	1.4046(9)
C(4)-C(5)	1.3873(11)
C(5)-C(6)	1.3908(11)
C(6)-C(7)	1.3859(9)
C(7)-C(8)	1.3919(10)

C(9)-C(14)	1.3907(9)
C(9)-C(10)	1.3974(8)
C(10)-C(11)	1.3887(9)
C(11)-C(12)	1.3891(10)
C(12)-C(13)	1.3886(10)
C(13)-C(14)	1.3888(10)

N(2)-N(1)-C(1)	108.83(6)
N(1)-C(1)-C(2)	109.57(6)
N(1)-N(2)-N(3)	107.46(6)
N(3)-C(2)-C(1)	103.23(6)
N(3)-C(2)-C(3)	127.22(6)
C(1)-C(2)-C(3)	129.54(6)
N(2)-N(3)-C(2)	110.91(5)
N(2)-N(3)-C(9)	117.89(5)
C(2)-N(3)-C(9)	131.14(6)
C(8)-C(3)-C(4)	118.51(6)
C(8)-C(3)-C(2)	122.95(6)
C(4)-C(3)-C(2)	118.52(6)
C(5)-C(4)-C(3)	121.07(6)
C(4)-C(5)-C(6)	119.02(6)
C(7)-C(6)-C(5)	121.24(7)
C(7)-C(6)-Cl(3)	119.06(6)
C(5)-C(6)-Cl(3)	119.70(5)
C(6)-C(7)-C(8)	119.31(6)
C(7)-C(8)-C(3)	120.83(6)
C(14)-C(9)-C(10)	119.92(6)
C(14)-C(9)-N(3)	119.49(5)
C(10)-C(9)-N(3)	120.59(6)
C(11)-C(10)-C(9)	120.44(6)
C(11)-C(10)-Cl(1)	119.30(5)
C(9)-C(10)-Cl(1)	120.20(5)
C(10)-C(11)-C(12)	118.39(6)
C(13)-C(12)-C(11)	122.21(6)
C(13)-C(12)-Cl(2)	119.32(6)
C(11)-C(12)-Cl(2)	118.39(5)

C(12)-C(13)-C(14)	118.63(6)
C(13)-C(14)-C(9)	120.37(6)

Table 4. Anisotropic displacement parameters ($Å^2 x\ 10^3$) for **36a**. The anisotropic displacement factor exponent takes the form: $-2\pi^2[h^2 a^{*2} U^{11} + ... + 2 h k a^* b^* U^{12}]$

	U^{11}	U^{22}	U^{33}	U^{23}	U^{13}	U^{12}
Cl(1)	24(1)	22(1)	16(1)	-3(1)	4(1)	-5(1)
N(1)	29(1)	21(1)	19(1)	3(1)	7(1)	-2(1)
C(1)	23(1)	23(1)	18(1)	2(1)	6(1)	-4(1)
Cl(2)	23(1)	27(1)	30(1)	2(1)	11(1)	-6(1)
N(2)	25(1)	19(1)	16(1)	3(1)	5(1)	2(1)
C(2)	17(1)	20(1)	14(1)	0(1)	4(1)	-2(1)
N(3)	18(1)	18(1)	14(1)	1(1)	5(1)	0(1)
Cl(3)	25(1)	30(1)	25(1)	-1(1)	2(1)	10(1)
C(3)	15(1)	20(1)	14(1)	-1(1)	4(1)	-2(1)
C(4)	16(1)	26(1)	18(1)	-1(1)	6(1)	-2(1)
C(5)	16(1)	29(1)	21(1)	-3(1)	6(1)	2(1)
C(6)	16(1)	23(1)	18(1)	-3(1)	2(1)	2(1)
C(7)	18(1)	26(1)	17(1)	2(1)	4(1)	3(1)
C(8)	17(1)	26(1)	16(1)	3(1)	6(1)	3(1)
C(9)	16(1)	17(1)	13(1)	0(1)	4(1)	1(1)
C(10)	16(1)	18(1)	14(1)	-1(1)	3(1)	0(1)
C(11)	16(1)	22(1)	16(1)	-1(1)	5(1)	0(1)
C(12)	16(1)	20(1)	19(1)	1(1)	5(1)	-1(1)
C(13)	22(1)	20(1)	20(1)	-2(1)	5(1)	-3(1)
C(14)	22(1)	18(1)	15(1)	-2(1)	4(1)	-1(1)

Table 5. Hydrogen coordinates (x 10^4) and isotropic displacement parameters ($Å^2$x 10^3) for **36a**.

	x	y	z	U(eq)
H(1)	3541(9)	9340(30)	-1374(14)	31(4)
H(4)	4016(8)	5430(30)	-910(13)	28(4)
H(5)	4749(9)	2410(30)	2(14)	35(4)
H(7)	3405(9)	1740(30)	2216(14)	33(4)
H(8)	2726(8)	4700(30)	1315(12)	23(3)
H(11)	989(8)	6390(30)	2214(13)	27(3)
H(13)	667(8)	1910(30)	-464(14)	31(4)
H(14)	1476(8)	4040(30)	-1278(13)	27(4)

Table 6. Torsion angles [°] for **36a**.

N(2)-N(1)-C(1)-C(2)	-0.17(9)
C(1)-N(1)-N(2)-N(3)	0.29(8)
N(1)-C(1)-C(2)-N(3)	-0.03(8)
N(1)-C(1)-C(2)-C(3)	179.76(7)
N(1)-N(2)-N(3)-C(2)	-0.32(8)
N(1)-N(2)-N(3)-C(9)	-177.78(6)
C(1)-C(2)-N(3)-N(2)	0.21(7)
C(3)-C(2)-N(3)-N(2)	-179.58(6)
C(1)-C(2)-N(3)-C(9)	177.23(6)
C(3)-C(2)-N(3)-C(9)	-2.57(11)
N(3)-C(2)-C(3)-C(8)	-24.37(11)
C(1)-C(2)-C(3)-C(8)	155.89(8)
N(3)-C(2)-C(3)-C(4)	157.36(7)
C(1)-C(2)-C(3)-C(4)	-22.38(11)
C(8)-C(3)-C(4)-C(5)	0.61(11)
C(2)-C(3)-C(4)-C(5)	178.95(7)
C(3)-C(4)-C(5)-C(6)	0.78(11)

C(4)-C(5)-C(6)-C(7)	-1.47(12)
C(4)-C(5)-C(6)-Cl(3)	177.90(6)
C(5)-C(6)-C(7)-C(8)	0.73(12)
Cl(3)-C(6)-C(7)-C(8)	-178.64(6)
C(6)-C(7)-C(8)-C(3)	0.71(12)
C(4)-C(3)-C(8)-C(7)	-1.37(11)
C(2)-C(3)-C(8)-C(7)	-179.63(7)
N(2)-N(3)-C(9)-C(14)	90.35(8)
C(2)-N(3)-C(9)-C(14)	-86.50(9)
N(2)-N(3)-C(9)-C(10)	-89.04(7)
C(2)-N(3)-C(9)-C(10)	94.11(9)
C(14)-C(9)-C(10)-C(11)	1.55(10)
N(3)-C(9)-C(10)-C(11)	-179.06(6)
C(14)-C(9)-C(10)-Cl(1)	178.73(5)
N(3)-C(9)-C(10)-Cl(1)	-1.88(9)
C(9)-C(10)-C(11)-C(12)	0.29(10)
Cl(1)-C(10)-C(11)-C(12)	-176.91(5)
C(10)-C(11)-C(12)-C(13)	-1.83(11)
C(10)-C(11)-C(12)-Cl(2)	174.99(5)
C(11)-C(12)-C(13)-C(14)	1.47(11)
Cl(2)-C(12)-C(13)-C(14)	-175.32(6)
C(12)-C(13)-C(14)-C(9)	0.43(11)
C(10)-C(9)-C(14)-C(13)	-1.92(10)
N(3)-C(9)-C(14)-C(13)	178.68(6)

Figure 27. ORTEP Drawing of 1,5-diaryl-1,2,3-triazoles **36a** .[61]

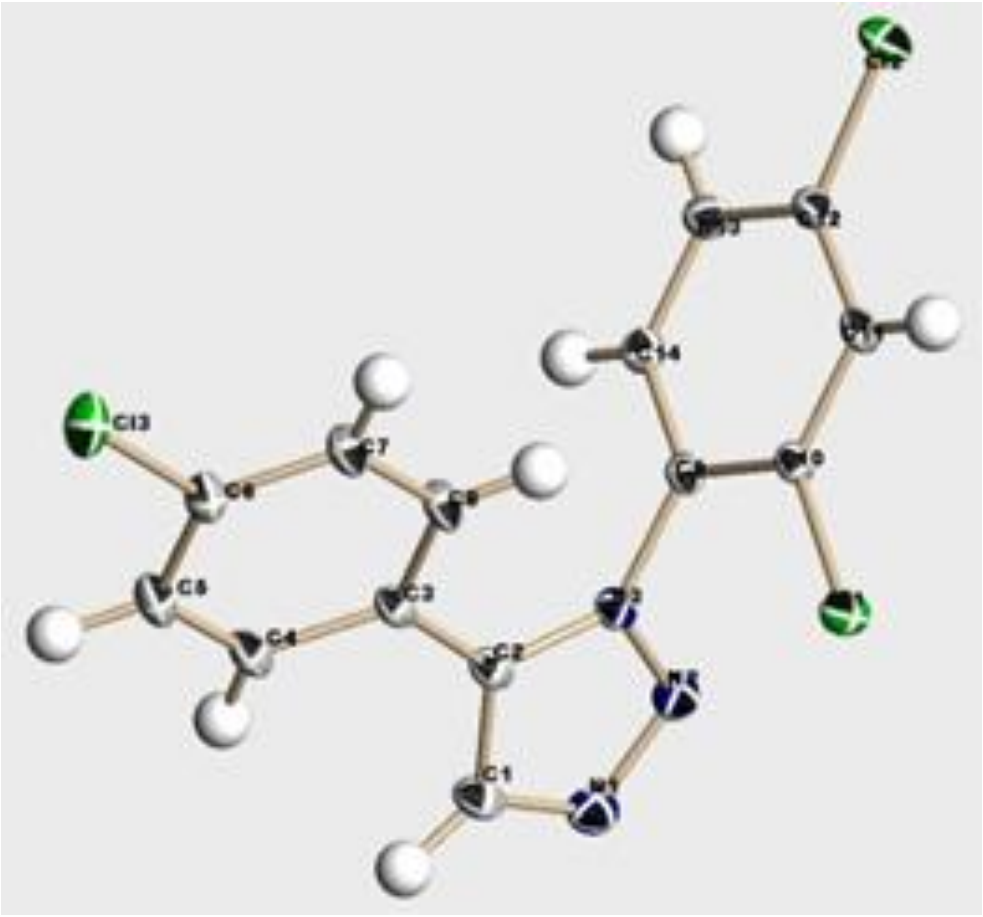

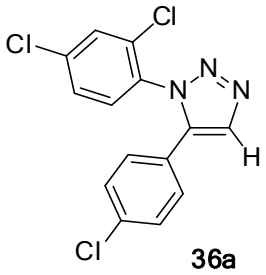

36a

3. Data_avg229ph_0m (Compound **32 c**) (Figure 31)

Table 1. Crystal data and structure refinement for **32c**.

Identification code	avg229ph_0m
Empirical formula	$C_{21}H_{12}Cl_2F\ N_3O_2$
Formula weight	428.24

Temperature	120(2) K
Wavelength	0.71073 Å
Crystal system	Orthorhombic
Space group	Pbca
Unit cell dimensions	a = 8.9553(5) Å · = 90°.
	b = 20.5764(11) Å · = 90°.
	c = 20.8197(11) Å · = 90°.
Volume	3836.4(4) $Å^3$
Z	8
Density (calculated)	1.483 Mg/m^3
Absorption coefficient	0.371 mm^{-1}
F(000)	1744
Crystal size	0.70 x 0.50 x 0.40 mm^3
Theta range for data collection	2.21 to 45.32°.
Index ranges	-17<=h<=17, -41<=k<=41, -39<=l<=40
Reflections collected	210038
Independent reflections	15821 [R(int) = 0.0183]
Completeness to theta = 45.32°	98.3 %
Absorption correction	empirical mult-scan
Max. and min. transmission	0.8657 and 0.7811
Refinement method	Full-matrix least-squares on F^2
Data / restraints / parameters	15821 / 0 / 310
Goodness-of-fit on F^2	0.839
Final R indices [I>2sigma(I)]	R1 = 0.0398, wR2 = 0.0979
R indices (all data)	R1 = 0.0464, wR2 = 0.1046
Largest diff. peak and hole	1.123 and -0.924 $e.Å^{-3}$

Table 2. Atomic coordinates (x 10^4) and equivalent isotropic displacement parameters ($Å^2$x 10^3) for **32c**. U(eq) is defined as one third of the trace of the orthogonalized U^{ij} tensor.

	x	y	z	U(eq)
Cl(1)	5874(1)	4596(1)	7347(1)	33(1)
F(1)	11297(1)	6118(1)	8452(1)	32(1)
N(1)	3423(1)	4718(1)	9228(1)	18(1)
O(1)	4866(1)	6333(1)	9160(1)	26(1)
C(1)	5472(1)	7176(1)	9914(1)	24(1)
Cl(2)	9038(1)	2393(1)	7427(1)	33(1)
O(2)	3032(1)	5972(1)	9814(1)	23(1)
N(2)	4024(1)	4204(1)	8976(1)	18(1)
C(2)	5390(1)	7827(1)	10095(1)	28(1)
N(3)	5416(1)	4373(1)	8768(1)	15(1)
C(3)	4542(1)	8259(1)	9742(1)	28(1)
C(4)	3770(1)	8046(1)	9205(1)	29(1)
C(5)	3830(1)	7397(1)	9017(1)	24(1)
C(6)	4685(1)	6975(1)	9378(1)	19(1)
C(7)	4004(1)	5869(1)	9428(1)	16(1)
C(8)	4403(1)	5225(1)	9175(1)	16(1)
C(9)	5704(1)	5009(1)	8884(1)	15(1)
C(10)	7172(1)	5307(1)	8762(1)	16(1)
C(11)	8415(1)	5078(1)	9098(1)	18(1)
C(12)	9818(1)	5353(1)	8999(1)	21(1)
C(13)	9933(1)	5853(1)	8559(1)	22(1)
C(14)	8728(1)	6089(1)	8215(1)	26(1)
C(15)	7331(1)	5814(1)	8321(1)	22(1)
C(16)	6314(1)	3904(1)	8445(1)	15(1)
C(17)	6835(1)	3368(1)	8782(1)	18(1)
C(18)	7665(1)	2894(1)	8470(1)	21(1)
C(19)	7999(1)	2977(1)	7825(1)	20(1)
C(20)	7502(1)	3510(1)	7479(1)	23(1)
C(21)	6620(1)	3969(1)	7790(1)	19(1)

Table 3. Bond lengths [Å] and angles [°] for **32c**.

Cl(1)-C(21)	1.7215(6)
F(1)-C(13)	1.3563(7)
N(1)-N(2)	1.2988(7)
N(1)-C(8)	1.3664(7)
O(1)-C(7)	1.3491(7)
O(1)-C(6)	1.4067(7)
C(1)-C(6)	1.3828(10)
C(1)-C(2)	1.3925(10)
Cl(2)-C(19)	1.7319(6)
O(2)-C(7)	1.2028(7)
N(2)-N(3)	1.3637(6)
C(2)-C(3)	1.3821(11)
N(3)-C(9)	1.3570(7)
N(3)-C(16)	1.4242(7)
C(3)-C(4)	1.3852(12)
C(4)-C(5)	1.3927(10)
C(5)-C(6)	1.3815(9)
C(7)-C(8)	1.4701(7)
C(8)-C(9)	1.3860(7)
C(9)-C(10)	1.4726(7)
C(10)-C(11)	1.3968(8)
C(10)-C(15)	1.3960(8)
C(11)-C(12)	1.3931(8)
C(12)-C(13)	1.3816(9)
C(13)-C(14)	1.3834(10)
C(14)-C(15)	1.3909(9)
C(16)-C(17)	1.3886(7)
C(16)-C(21)	1.3961(8)
C(17)-C(18)	1.3879(8)
C(18)-C(19)	1.3868(9)
C(19)-C(20)	1.3853(9)
C(20)-C(21)	1.3903(9)
N(2)-N(1)-C(8)	108.82(4)

C(7)-O(1)-C(6)	117.70(5)
C(6)-C(1)-C(2)	118.68(6)
N(1)-N(2)-N(3)	107.43(4)
C(3)-C(2)-C(1)	120.22(7)
C(9)-N(3)-N(2)	111.29(4)
C(9)-N(3)-C(16)	129.04(4)
N(2)-N(3)-C(16)	119.59(4)
C(2)-C(3)-C(4)	120.03(6)
C(3)-C(4)-C(5)	120.72(7)
C(6)-C(5)-C(4)	118.13(6)
C(5)-C(6)-C(1)	122.22(6)
C(5)-C(6)-O(1)	118.60(6)
C(1)-C(6)-O(1)	118.92(6)
O(2)-C(7)-O(1)	124.39(5)
O(2)-C(7)-C(8)	125.09(5)
O(1)-C(7)-C(8)	110.51(4)
N(1)-C(8)-C(9)	109.35(4)
N(1)-C(8)-C(7)	120.13(4)
C(9)-C(8)-C(7)	130.50(5)
N(3)-C(9)-C(8)	103.10(4)
N(3)-C(9)-C(10)	122.76(4)
C(8)-C(9)-C(10)	133.84(5)
C(11)-C(10)-C(15)	120.03(5)
C(11)-C(10)-C(9)	118.97(5)
C(15)-C(10)-C(9)	121.00(5)
C(10)-C(11)-C(12)	120.50(5)
C(13)-C(12)-C(11)	117.87(6)
F(1)-C(13)-C(12)	118.35(6)
F(1)-C(13)-C(14)	118.49(6)
C(12)-C(13)-C(14)	123.15(5)
C(13)-C(14)-C(15)	118.46(6)
C(14)-C(15)-C(10)	119.99(6)
C(17)-C(16)-C(21)	120.20(5)
C(17)-C(16)-N(3)	119.22(5)
C(21)-C(16)-N(3)	120.53(5)
C(16)-C(17)-C(18)	120.16(5)

C(19)-C(18)-C(17)	118.77(5)
C(20)-C(19)-C(18)	122.14(5)
C(20)-C(19)-Cl(2)	118.27(5)
C(18)-C(19)-Cl(2)	119.58(5)
C(19)-C(20)-C(21)	118.54(5)
C(20)-C(21)-C(16)	120.10(5)
C(20)-C(21)-Cl(1)	118.67(5)
C(16)-C(21)-Cl(1)	121.20(4)

Table 4. Anisotropic displacement parameters ($Å^2 x\ 10^3$) for **32c**. The anisotropic displacement factor exponent takes the form: $-2\cdot^2[\ h^2\ a^{*2}U^{11} + ... + 2\ h\ k\ a^*\ b^*\ U^{12}\ ]$

	U^{11}	U^{22}	U^{33}	U^{23}	U^{13}	U^{12}
Cl(1)	53(1)	24(1)	23(1)	8(1)	-4(1)	8(1)
F(1)	19(1)	32(1)	46(1)	4(1)	6(1)	-11(1)
N(1)	14(1)	15(1)	25(1)	-1(1)	3(1)	-1(1)
O(1)	26(1)	14(1)	38(1)	-4(1)	17(1)	-3(1)
C(1)	24(1)	20(1)	28(1)	3(1)	-2(1)	0(1)
Cl(2)	33(1)	33(1)	34(1)	-13(1)	5(1)	11(1)
O(2)	24(1)	18(1)	26(1)	-2(1)	11(1)	0(1)
N(2)	14(1)	15(1)	25(1)	-1(1)	2(1)	-2(1)
C(2)	30(1)	24(1)	29(1)	-4(1)	-3(1)	-5(1)
N(3)	14(1)	12(1)	20(1)	0(1)	2(1)	0(1)
C(3)	34(1)	16(1)	34(1)	-3(1)	4(1)	0(1)
C(4)	31(1)	23(1)	31(1)	0(1)	-1(1)	11(1)
C(5)	21(1)	26(1)	26(1)	-5(1)	-2(1)	4(1)
C(6)	17(1)	14(1)	26(1)	-1(1)	5(1)	-1(1)
C(7)	15(1)	14(1)	20(1)	-1(1)	3(1)	0(1)
C(8)	13(1)	14(1)	21(1)	0(1)	3(1)	0(1)
C(9)	13(1)	12(1)	19(1)	1(1)	2(1)	0(1)
C(10)	13(1)	13(1)	20(1)	0(1)	3(1)	-1(1)
C(11)	15(1)	19(1)	22(1)	1(1)	2(1)	-2(1)
C(12)	14(1)	23(1)	25(1)	-1(1)	2(1)	-3(1)

C(13)	16(1)	19(1)	30(1)	-1(1)	6(1)	-5(1)
C(14)	21(1)	20(1)	37(1)	8(1)	5(1)	-4(1)
C(15)	17(1)	18(1)	31(1)	7(1)	3(1)	-1(1)
C(16)	15(1)	13(1)	17(1)	0(1)	0(1)	1(1)
C(17)	22(1)	17(1)	17(1)	1(1)	0(1)	5(1)
C(18)	23(1)	19(1)	20(1)	-1(1)	-2(1)	7(1)
C(19)	19(1)	20(1)	22(1)	-6(1)	1(1)	3(1)
C(20)	28(1)	22(1)	17(1)	-2(1)	4(1)	1(1)
C(21)	25(1)	17(1)	17(1)	2(1)	0(1)	1(1)

Table 5. Hydrogen coordinates (x 10^4) and isotropic displacement parameters ($Å^2$x 10^3) for **32c**.

	x	y	z	U(eq)
H(1)	6048(15)	6880(7)	10158(7)	35(3)
H(2)	5926(16)	7970(7)	10491(7)	41(4)
H(3)	4508(18)	8712(8)	9861(7)	46(4)
H(4)	3182(17)	8352(7)	8948(7)	45(4)
H(5)	3289(16)	7228(7)	8652(7)	37(3)
H(11)	8294(13)	4725(6)	9406(6)	25(3)
H(12)	10673(15)	5209(7)	9209(7)	33(3)
H(14)	8874(17)	6436(7)	7916(7)	42(4)
H(15)	6452(15)	5986(6)	8094(6)	29(3)
H(17)	6620(14)	3327(6)	9239(6)	27(3)
H(18)	8011(14)	2519(6)	8686(6)	29(3)
H(20)	7747(16)	3552(7)	7034(7)	37(3)

Table 6. Torsion angles [°] for **32c**.

C(8)-N(1)-N(2)-N(3)	1.11(7)
C(6)-C(1)-C(2)-C(3)	-0.33(11)
N(1)-N(2)-N(3)-C(9)	-0.60(6)
N(1)-N(2)-N(3)-C(16)	-177.46(5)
C(1)-C(2)-C(3)-C(4)	0.02(12)
C(2)-C(3)-C(4)-C(5)	0.27(13)
C(3)-C(4)-C(5)-C(6)	-0.25(12)
C(4)-C(5)-C(6)-C(1)	-0.08(10)
C(4)-C(5)-C(6)-O(1)	-174.21(6)
C(2)-C(1)-C(6)-C(5)	0.36(10)
C(2)-C(1)-C(6)-O(1)	174.48(6)
C(7)-O(1)-C(6)-C(5)	-99.77(7)
C(7)-O(1)-C(6)-C(1)	85.90(8)
C(6)-O(1)-C(7)-O(2)	4.68(10)
C(6)-O(1)-C(7)-C(8)	-176.38(6)
N(2)-N(1)-C(8)-C(9)	-1.24(7)
N(2)-N(1)-C(8)-C(7)	-179.61(5)
O(2)-C(7)-C(8)-N(1)	18.29(9)
O(1)-C(7)-C(8)-N(1)	-160.65(6)
O(2)-C(7)-C(8)-C(9)	-159.68(6)
O(1)-C(7)-C(8)-C(9)	21.38(9)
N(2)-N(3)-C(9)-C(8)	-0.15(6)
C(16)-N(3)-C(9)-C(8)	176.33(5)
N(2)-N(3)-C(9)-C(10)	174.36(5)
C(16)-N(3)-C(9)-C(10)	-9.16(9)
N(1)-C(8)-C(9)-N(3)	0.82(6)
C(7)-C(8)-C(9)-N(3)	178.96(6)
N(1)-C(8)-C(9)-C(10)	-172.77(6)
C(7)-C(8)-C(9)-C(10)	5.37(11)
N(3)-C(9)-C(10)-C(11)	-61.90(7)
C(8)-C(9)-C(10)-C(11)	110.68(7)
N(3)-C(9)-C(10)-C(15)	118.50(6)
C(8)-C(9)-C(10)-C(15)	-68.93(9)
C(15)-C(10)-C(11)-C(12)	0.19(9)

C(9)-C(10)-C(11)-C(12)	-179.42(5)
C(10)-C(11)-C(12)-C(13)	-0.19(9)
C(11)-C(12)-C(13)-F(1)	-179.13(6)
C(11)-C(12)-C(13)-C(14)	-0.16(10)
F(1)-C(13)-C(14)-C(15)	179.48(7)
C(12)-C(13)-C(14)-C(15)	0.52(11)
C(13)-C(14)-C(15)-C(10)	-0.51(11)
C(11)-C(10)-C(15)-C(14)	0.17(10)
C(9)-C(10)-C(15)-C(14)	179.78(6)
C(9)-N(3)-C(16)-C(17)	116.78(6)
N(2)-N(3)-C(16)-C(17)	-66.99(7)
C(9)-N(3)-C(16)-C(21)	-65.73(8)
N(2)-N(3)-C(16)-C(21)	110.50(6)
C(21)-C(16)-C(17)-C(18)	0.14(9)
N(3)-C(16)-C(17)-C(18)	177.64(5)
C(16)-C(17)-C(18)-C(19)	1.94(9)
C(17)-C(18)-C(19)-C(20)	-1.45(10)
C(17)-C(18)-C(19)-Cl(2)	179.83(5)
C(18)-C(19)-C(20)-C(21)	-1.13(10)
Cl(2)-C(19)-C(20)-C(21)	177.60(5)
C(19)-C(20)-C(21)-C(16)	3.23(10)
C(19)-C(20)-C(21)-Cl(1)	-174.76(5)
C(17)-C(16)-C(21)-C(20)	-2.77(9)
N(3)-C(16)-C(21)-C(20)	179.76(6)
C(17)-C(16)-C(21)-Cl(1)	175.16(5)
N(3)-C(16)-C(21)-Cl(1)	-2.30(8)

Figure 31. ORTEP Drawings of 1,5-diaryl-1,2,3-triazoles **32c**.

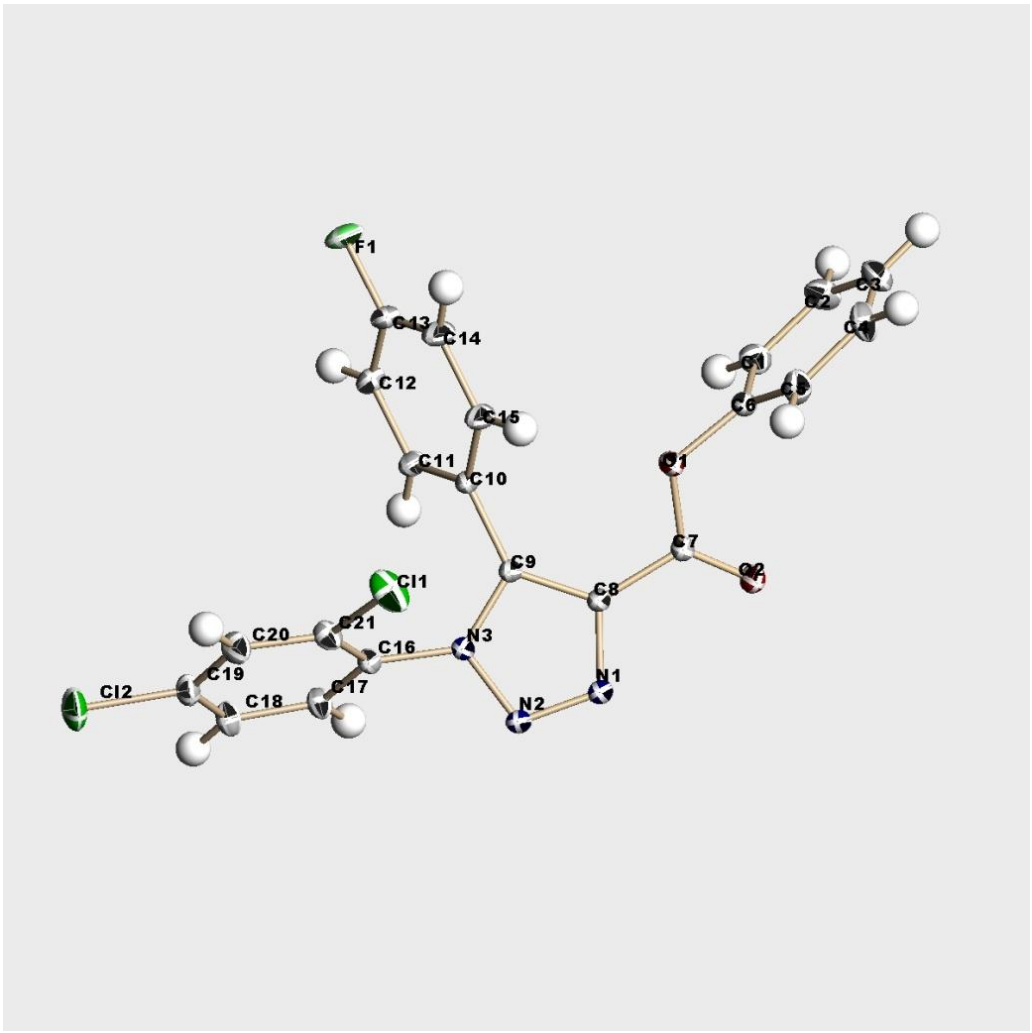

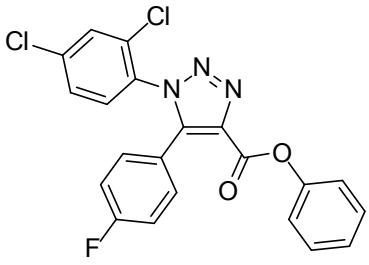

32c

Vita

Abha Verma was born in Chandigarh (Chandigarh U.T.), India. She obtained her B.Sc. (Honors) in Chemistry in 2002 and M.Sc. (Honors) in Chemistry in 2004 from Panjab University, Chandigarh (India). She worked at Dr. *Reddy's* Pharmaceutical Company, Hyderabad in India for a few months before joining Indian Institute of Science at Bangalore, India where she worked for a Chemical Biology program for two years. In August 2007, she joined the chemistry graduate program at the University of New Orleans as a graduate assistant to pursue a PhD in organic chemistry. In December, of year 2007 she joined the research group of Prof. Mark L. Trudell at University of New Orleans, New Orleans and obtained a M.S. degree in 2010. She was then promoted as a research assistant to work towards her Ph.D. degree under supervision of Prof. Trudell at University of New Orleans, New Orleans.